Characterisation of DRAM-1 *in vitro* and *in vivo*

Li Yen Mah

A thesis submitted to the University of Glasgow for the degree of Doctor of Philosophy

November 2012

Beatson Institute of Cancer Research
Garscube Estate
Switchback Road
Glasgow G61 1BD

Abstract

Autophagy is a cellular housekeeping process that drives the degradation of intracellular and extracellular components in the lysosomes. Defects in this process have been implicated with many diseases, among them cancer. *Damage-Regulated Autophagy Modulator (DRAM-1)* is a p53 target gene that has been shown to regulate autophagy, and it is believed to act as a tumour suppressor. In addition to the full-length transcript (splice variant 1) that has previously been characterised, multiple splice isoforms of *DRAM-1* have been identified.

The first part of this thesis focuses on the investigation of the properties of the DRAM-1 isoforms 1, 4 and 5. These isoforms are localised to different cellular compartments. DRAM-1 isoforms are highly specific regulators of autophagy. They neither mediate the turnover of long-lived proteins nor do they decrease enhanced intracellular reactive oxygen species (ROS). Although activation of DRAM-1 on its own does not promote cell death, it is required for effective p53-mediated cell death *in vitro.*

The next step was to proceed to the characterisation of the cellular function of DRAM-1 *in vivo.* Loss of *DRAM-1 in vivo* is not embryonic lethal and DRAM-1 knockout mice do not display any phenotypic changes. Additionally, genetic deletion of *DRAM-1* does not impede p53-dependent cell death in the intestine upon exposure to ionising radiation. However, DRAM-1 is required for effective intestinal crypt proliferation and mitosis post radiation-induced injury in the small intestine. DRAM-1 does not modulate p53-induced senescence in the liver, but the loss of *DRAM-1* increases apoptosis and possibly mitotic arrest in hepatocytes. Furthermore, the deletion of *DRAM-1* does not accelerate spontaneous and radiation-induced tumourigenesis. Preliminary results indicate that the loss of DRAM-1 does not predispose to inflammation-driven tumourigenesis. However, *DRAM-1*-null mice are sensitised to DSS-induced inflammation in the colon.

In the final part of the thesis, the role of DRAM-1 in mediating T cell activation was examined. Although *DRAM-1* is coregulated with the T cell activating molecule, *CD80,* the loss of DRAM-1 in the professional antigen presenting cells (APCs) do

not affect their ability to activate T cells. However, p53 activation in the APCs inhibits antigen processing, and consequently T cell activation.

In summary, these results contribute to the understanding of how autophagy is regulated by DRAM-1, and uncover novel roles for p53 and DRAM-1 beyond cell death and autophagy regulation. Still, these pathways necessitate further investigation and harness a great potential to be targeted therapeutically to enhance tumour cell death.

Table of Contents

Acknowledgement

Firstly, I would like to thank my supervisor Prof. Kevin Ryan for his guidance over the course of my PhD. I would like to thank my advisor, Prof. Laura Machesky for her encouragement and advice. I would also like to thank my collaborators, Prof. Owen Sansom and Dr. Simon Milling, as well as their team for the highly valued inputs and suggestions. Thanks to the past and present members of the Tumour Cell Death Laboratory (R5), and Dr. Karen Blyth for their help and motivation, as well as to Dr. Ayala King and Prof. Seamus Martin for helpful discussions. I would also like to extend my greatest gratitude to Colin Nixon and his team for their assistance and guidance in histology and tissue processing; and to Tom and Margaret for their help in flow cytometry and microscopy. Many thanks to all the friends and colleagues at the Beatson for making this place extremely educating. Special thanks goes to Tan Thuan Thung for his patience, support and great company, especially during the last phase of my PhD. Finally, I would like to thank Cancer Research UK for funding my four years of studies and research, without which I would not have been able to complete my research and this thesis. I'd like to dedicate this thesis to my parents, Mah Meng Kong and Mak Foon Hing for their love and endless support.

Author’s Declaration

I declare that all of the work and figures generated in this thesis was performed personally, except where indicated. No part of this work has been submitted for consideration as part of any other degree or award.

Publications

Publications arising from this work included in thesis:

Mah, L. Y., J. O'Prey, et al. (2012). "DRAM-1 encodes multiple isoforms that regulate autophagy." Autophagy **8**(1): 18-28.

Rosenfeldt, M., C. Nixon, et al. (2012). "Analysis of macroautophagy by immunohistochemistry." Autophagy **8**(6).

Mah, L. Y. and K. M. Ryan (2012). "Autophagy and cancer." Cold Spring Harb Perspect Biol **4**(1): a008821.

Abbreviations

2-Me	2-Mercaptoethanol
^{35}S	Sulfur-35
^{32}P	Phosphate-35
AOM	Azoxymethane
Asp	Aspartate
Bip	Binding immunoglobulin protein
Brdu	5-bromo-2'-deoxyuridin
BSA	Bovine serum albumin
CD	Cluster Differentiation
cDNA	DNA complementary to mRNA
CFSE	5-(and 6)-Carboxyfluorescein diacetate succinimidyl ester
Ci	Curie
CO_2	Carbon dioxide
$CuSo_4$	Copper sulfate
Cys	Cysteine
DAB	3, 3'-diaminobenzidine
DCFDA	2',7' –dichlorofluorescein diacetate
DFCP1	Double FYVE-containing protein 1
DMEM	Dulbecco's modified Eagle's medium
DMSO	Dimethylsulphoxide
DNA	Deoxyribonucleic acid
DNAse	Deoxyribonuclease
dNTP	deoxynucleotide
DSS	Dextran Sodium Sulfate
EBP	Enhancer binding protein
EBSS	Earl's Balance Salt Solution
ECL	Enhanced chemiluminesence
EDTA	Ethylene diamine triacetic acid
ERK	Extracellular signal-regulated kinases
EtBr	Ethidium Bromide
FCS	Fetal Calf Serum
Flt-3L	Fms-like tyrosine kinase 3 ligand
GAPDH	Glyceraldehyde-3-Phosphate Dehydrogenase

GFP	Green flourescent protein
GRP	Glucose-regulated protein
H & E	Haematoxylin and Eosin
H2O	Water
HBS	HEPES-buffered saline
HEPES	4-(2-hydroxyethyl)-1-piperazineethane-sulfonic acid
HRP	Horseradish Peroxidase
LB	Leuria-Bertani medium
LPS	Lipopolysacharride
M-CSF	Macrophage colony-stimulating factor
MEFs	Mouse Embryonic Fibroblast
MEM	Minimal Essential Medium
Met	Methionine
$MgCl_2$	Magnesium chloride
MPO	Myeloperoxidase
mRNA	Messenger RNA
mTOR	Mammalian Target of Rapamycin
NLR	Nuclear localisation signal
OCT	Optimal Cutting Temperature
OLFM4	Olfactomedin 4
OVA	Chicken ovalbumin
p	Phospho
PBS	Phosphate-Buffered Saline
PCR	Polymerase chain reaction
PFA	Paraformaldehyde
PMP70	Peroxisomal membrane protein 70
RBC	Red blood cells
Rnase	Ribonuclease
ROS	Reactive oxygen species
RPE	Retinal Pigment Epithelia
RPM	Revolutions per Minutes
rRNA	Ribosomal RNA
RT-PCR	Reverse transcription polymerase chain reaction
SA-β-gal	Senescence associated beta galactosidase
SDS	Sodium dodecyl sulphate

SDS-PAGE	SDS-polyacrylamide gel electrophoresis
Ser	Serine
SV	Splice variant
TAE	Tris-acetate-EDTA
TBS	Tris buffered saline
TBST	TBS-Tween
TCA	Tricholoacetic acid
TE	Tris-EDTA
TGN	Transgolgi network
Tris	Tris(hydroxymethyl)aminomethane
U	Unit
UV	Ultraviolet
X-gal	5-bromo-4-chloro-indolyl-β-D-galactopyranoside

List of Figures

List of Tables

Chapter 1: Introduction

1.1 The multiple flavours of autophagy

Cellular homeostasis is in part maintained by the degradation of cellular materials via the ubiquitin-proteasomal and lysosomal pathways (Codogno and Meijer 2005). Concerted efforts to study the lysosomal degradation of various cellular components like superfluous or damaged organelles, proteins and protein aggregates as well as extracellular materials like viruses and bacteria have led to the identification of a conserved cellular process termed autophagy (Ciechanover 2005) (Gozuacik and Kimchi 2004) (Cuervo 2004).

The term autophagy originates from the Greek roots “auto” (self) and “phagy” (eating), and is broadly defined as the transportation and lysosomal degradation of cytoplasmic material (Ravikumar, Sarkar et al. 2010). The emergence of autophagy research stems from the identification of lysosomes in 1955 by De Duve and colleagues (De Duve, Pressman et al. 1955). Shortly after this, the morphological process of autophagy was described in the 1960s by electron microscopy studies, revealing the sequestration of the cytoplasm and other cellular organelles into novel membrane-bound vesicles (Klionsky 2007) (De Duve and Wattiaux 1966).

Depending on the delivery route and cargo specificity, three different types of autophagy have been distinguished – macroautophagy, microautophagy and chaperone-mediated autophagy (CMA) (Eskelinen and Saftig 2009). Macroautophagy (herein referred to as autophagy), which resembles De Duve’s initial description of autophagy, is characterised by the engulfment and delivery of bulk cytoplasm and specific organelles by the autophagosome (a double-membrane organelle) to the lysosome whereas microautophagy is the direct uptake and degradation of the cytoplasm by the invagination of the lysosomal membrane (Mizushima, Levine et al. 2008). CMA is a cellular process whereby soluble proteins which are tagged with a specific pentapeptide, are shuttled into the lysosomal lumen across the lysosome membrane via the HSC70 chaperone protein, and the integral membrane receptor LAMP-2A (lysosome-associated membrane protein type 2A) (Cuervo 2004) (Ogier-

Denis and Codogno 2003). Of these three pathways, macroautophagy is the most characterized form and has been extensively researched in yeast and mammals (Chen and Klionsky 2011).

Autophagy is also frequently characterised into selective and non-selective autophagy. Non-selective autophagy involves the random engulfment and degradation of bulk cytosol to maintain the cytoplasmic volume and its contents in equilibrium (Liang and Jung 2010). On the other hand, selective autophagy is the highly specific recognition and digestion of specific cargoes (Liang and Jung 2010), ranging from nucleic acids, proteins, and lipids to organelle turnover (Munafo and Colombo 2001) (Tanida ; Sakai, Oku et al. 2006) (Bernales, Schuck et al. 2007) (Kraft, Deplazes et al. 2008) (Weidberg, Shvets et al. 2009). Some of these lysosomal degradation processes involve specific genes, such as *Pex* and *Parkin* which modulate the degradation of peroxisomes and mitochondria respectively (Sakai, Oku et al. 2006) (Xie and Klionsky 2007). Given this, selective autophagy has been proposed to evolve to specifically match the changing demands in different organisms, or even different tissues within the same organism to sustain cellular viability (Liang and Jung 2010).

Autophagy is a fundamental and indispensable process that is required to maintain cellular homeostasis and to regulate or respond to other cellular pathways. A deregulation in autophagy could lead to cellular demise, and other diseases, such as cancer, which is discussed later in this thesis.

1.2 The mammalian autophagy molecular machinery

Autophagy is initiated by the expansion of a membrane structure called autophagosomal structure, which expands into the isolation membrane, or phagophore where the cargoes are sequestered (Webber and Tooze 2010). The isolation membrane then closes to form double-membrane bound vesicles called autophagosomes, which fuse with lysosomes, where the inner autophagic vesicles and the contents are degraded by vacuolar or lysosomal hydrolases (Mizushima 2007). Autophagosomes occasionally fuse with endosomal vesicles, such as endosomes and multivesicular bodies to form the intermediate organelle amphisomes, and the fusion of autophagosomes to endosomes and/or lysosomes are collectively termed autophagosome maturation (Mizushima 2007).

The degraded products are released into the cytosol for recycling via lysosomal membrane permeases (Xie and Klionsky 2007). The morphological steps of autophagy are schematically shown in Fig. 1.1. Different names have been coined to describe autophagosomes or autophagosome-like structures, depending on the physiological conditions under which they are formed (Xie and Klionsky 2007). The origin of the isolation membrane has been researched extensively in yeast (Reggiori, Tucker et al. 2004; Reggiori, Shintani et al. 2005; He, Baba et al. 2008), and has facilitated the understanding of phagophore formation in eukaryotes. The isolation membrane is proposed to be formed from de novo lipid synthesis, or is derived from pre-existing organelles such as the ER, Golgi complex, plasma membrane and mitochondria (Webber and Tooze 2010) (Hailey, Rambold et al. 2010).

The identification of a panel of genes that regulate autophagy, termed ATG (AuTophaGy-related genes) in yeast and mammals has provided insights into the study of the molecular machinery of autophagy. To date, about 30 *ATG* genes have been identified in yeast, *Saccharomyces cerevisiae*, and most of these genes have known orthologues in other eukaryotes (Suzuki and Ohsumi 2007). Many researchers have studied the participation of these ATG proteins in the cellular and molecular network of autophagy.

The formation of the isolation membrane for the sequestration of cytoplasmic materials is termed vesicle nucleation and is regulated by the formation of two complexes, as illustrated in Fig.1.2. The first complex consists of ATG13, focal adhesion kinase family interacting protein of 200 kD (FIP200), ULK 1 and ATG101 (Hosokawa, Hara et al. 2009) (Itakura and Mizushima 2010). ULK1 and FIP200 are mammalian orthologues of ATG1 and ATG17, respectively, whereas ATG101 is a novel mammalian autophagy protein that is absent in yeast (Itakura and Mizushima 2010). Upon exposure to autophagic stimuli, ATG13 (triphosphorylated when inacitve), is phosphorylated and associates with ULK1 and FIP200 (Maiuri, Zalckvar et al. 2007) (Itakura, Kishi et al. 2008). ATG101 binds to human ATG13 and also interacts with ULK1 (Mercer, Kaliappan et al. 2009). ULK 1 and ATG14 are occasionally found in punctate structures that are tightly associated with the ER and the ER protein vacuole membrane protein 1 (VMP1) has been demonstrated to transiently associate with this early autophagic structure (Itakura and Mizushima 2010). ATG17 has been shown to recruit the integral transmembrane protein, ATG9 to the pre-autophagosomal site (PAS) in yeast (Sekito, Kawamata et al. 2009), and the trafficking of ATG9 to PAS is proposed to facilitate membrane flow for membrane formation (He, Baba et al. 2008). Albeit this, mammalian ATG9 has been observed to cycle between the transgolgi network (TGN) and LC3-II positive components, hypothesised to be phagophores during starvation (Young, Chan et al. 2006) (Webber and Tooze 2010). The cycling of ATG 9 is proposed to be regulated by p38IP (p38 interacting protein) and PI3K (Webber and Tooze 2010) (Young, Chan et al. 2006).

The second complex, which is known as the autophagy-specific class III PI3-kinase complex, comprises of Beclin 1 (Atg6/Vps30 homologue), Atg14, Vps34 and the myristylated kinase p150 (Vps15) (Itakura and Mizushima 2010). Beclin 1 is a Bcl-2-interacting protein that also interacts with ATG14 and activating molecule in Beclin 1-regulated autophagy (AMBRA-1) (Itakura and Mizushima 2010). Whereas AMBRA-1 positively regulates the Beclin 1-dependent programme of autophagy (Fimia, Stoykova et al. 2007), ultraviolet radiation resistance-associated gene (UVRAG) and ATG14 are thought to form distinct Beclin 1 complexes, which are involved in membrane trafficking and protein sorting, respectively (Itakura, Kishi et al. 2008).

Autophagosome elongation and completion involves two ubiquitin-like conjugation systems (Figure 1.3). This process involves the conjugation of Atg12 to Atg5 which is catalysed by Atg7 (E1-like enzyme) and Atg10 (E2-like enzyme) (Maiuri, Zalckvar et al. 2007). The conjugation of phosphatidylethanolamine (PE) to LC3 (one of the mammalian orthologues of yeast Atg8) is catalysed by the protease, Atg4 and the E1- and E2-like enzymes - Atg7 and Atg3 respectively (Maiuri, Zalckvar et al. 2007).

The fusion of autophagosomes to endosomal vesicles is mediated by the endosomal sorting complex required for transport (ESCRT) proteins, and the subsequent fusion of the amphisome and lysosome is facilitated by Fab 1 and Rab 7 (Rusten, Vaccari et al. 2007) (Fader and Colombo 2009). The final fusion of both autophagosomes and amphisomes to lysosomes is also thought to be mediated by Beclin 1, UVRAG, Vacuolar protein sorting 34 (Vps34), p150, and ESCRT (Matsunaga, Saitoh et al. 2009) (Fader and Colombo 2009) (Fig. 1.4).

There may well be other proteins that are involved in the step-wise formation of isolation membrane up to the degradation of autophagosomes that have yet to be identified. This is reflected in the robust discovery of new interactors of the core autophagic machinery. For instance, the recently characterised Bif-1 (also known as Endophilin B1) is reported to bind to UVRAG and Beclin 1 (Takahashi, Coppola et al. 2007). Additionally, Barkor, has been shown to form a complex with Beclin 1 to facilitate LC3 conjugation and autophagosome assembly (Sun, Fan et al. 2008). Likewise, a novel PI(3)P-binding protein termed double FYVE-containing protein 1 (DFCP1), translocates to a subdomain of the ER and generates the “omegasome” during starvation (Axe, Walker et al. 2008). Thus, the mapping of autophagy regulators to their role in the autophagy machinery requires the participation of different proteins at various steps.

Autophagy can also proceed in the absence of ATG5 and ATG7. This form of autophagy, which does not rely on the cascade of ATG signalling, has been termed non-canonical or alternative autophagy (Nishida, Arakawa et al. 2009). This form of autophagy might be triggered when canonical autophagy is inactivated due to mutations in the panel of *Atg* genes (Scarlatti, Maffei et al. 2008).

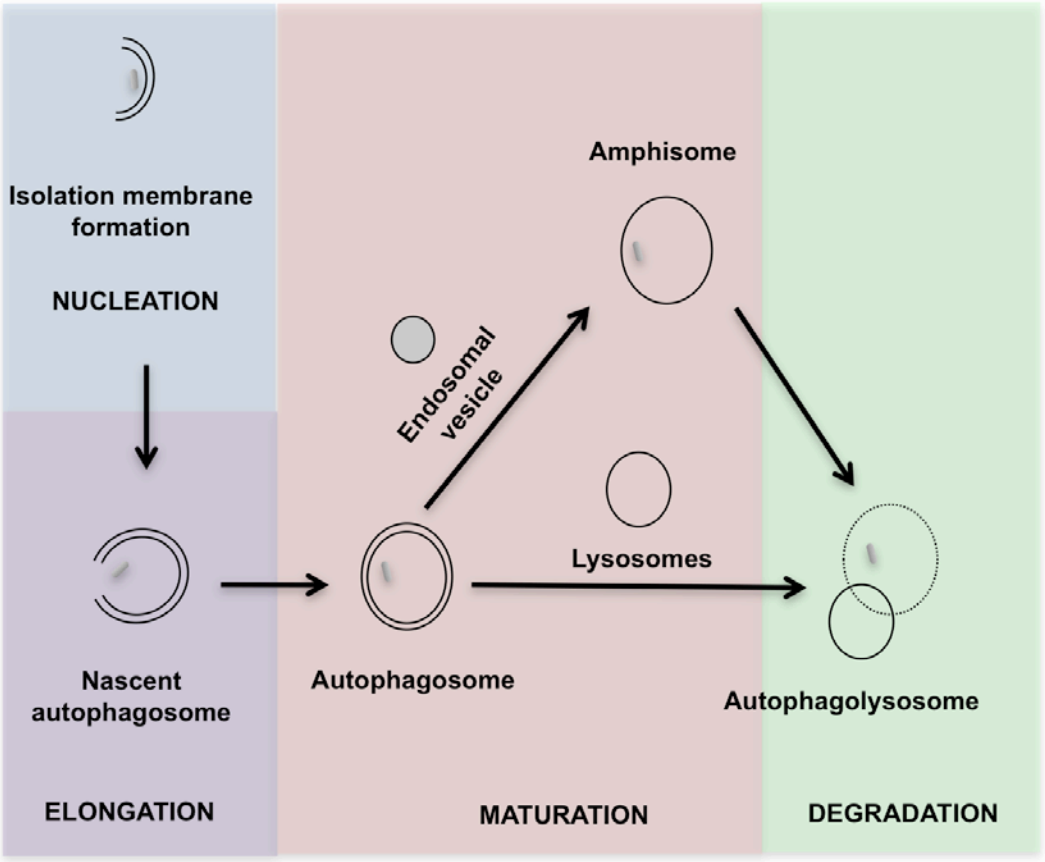

Figure 1.1: Schematic representation of autophagy
Nucleation: Autophagy begins with the formation of the isolation membrane from phagopohore.
Elongation: Autophagy cargoes are sequestered by the isolation membrane, which closes to form the autophagosome.
Maturation: Autophagosomes can either fuse with lysosomes or endosomal vesicles to form amphisomes, before docking with lysosomes.
Degradation: The inner membrane of the autophagosome and its cargoes are degraded by lysosomal hydrolases.

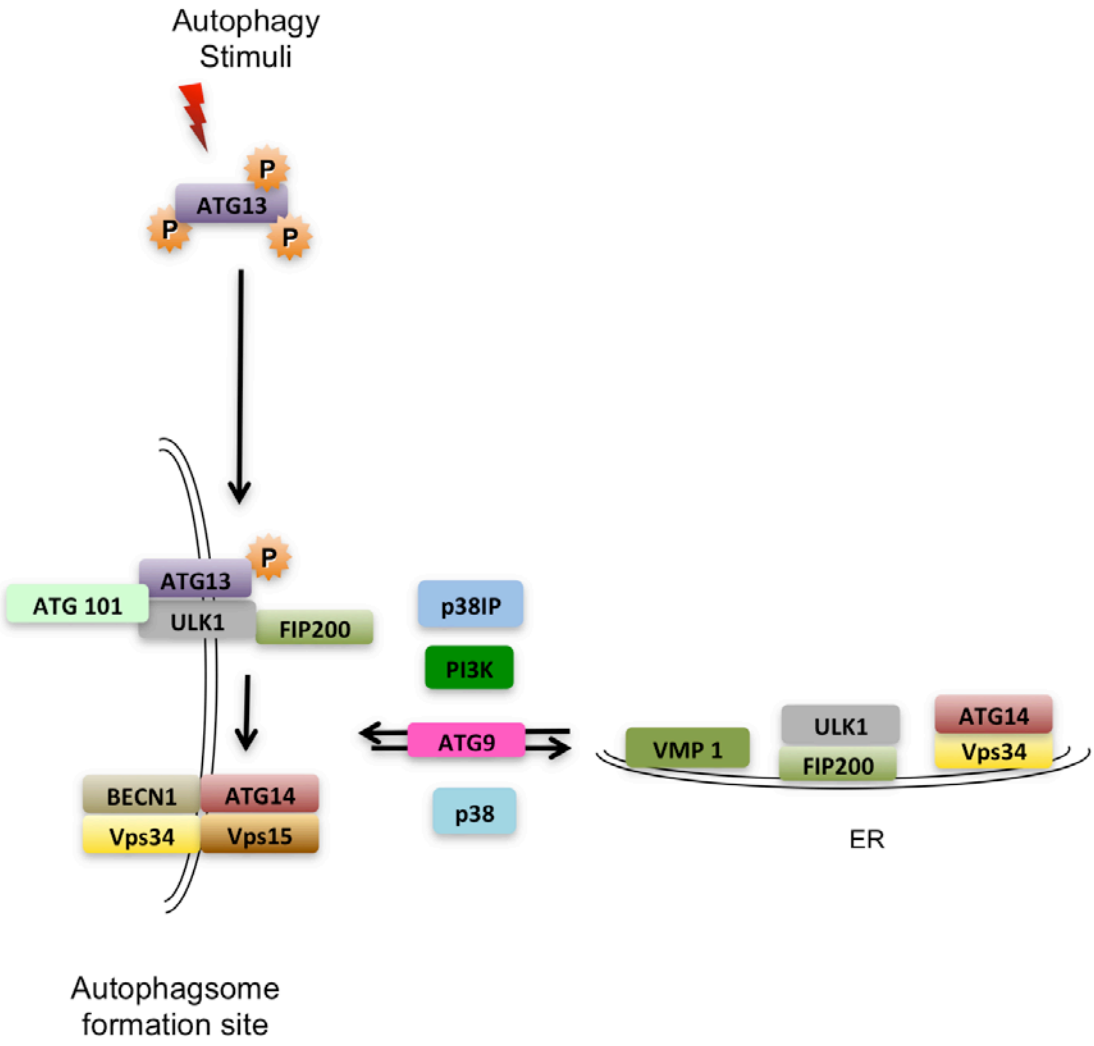

Figure 1.2: Vesicle nucleation in mammalian cells requires the formation of two complexes

The first complex consists of ULK1, ATG13, FIP200, and ATG101. ULK 1 and ATG14 are also found in putative early autophagic structures that are tightly associated with the ER, and VMP 1 is transiently localised to this site. The second complex comprises of UVRAG, Beclin1, AMBRA, Vps34 and p150. The cycling of ATG9, which is mediated by p38, p38IP and PI3K is proposed to facilitate membrane flow for the formation of the isolation membrane.

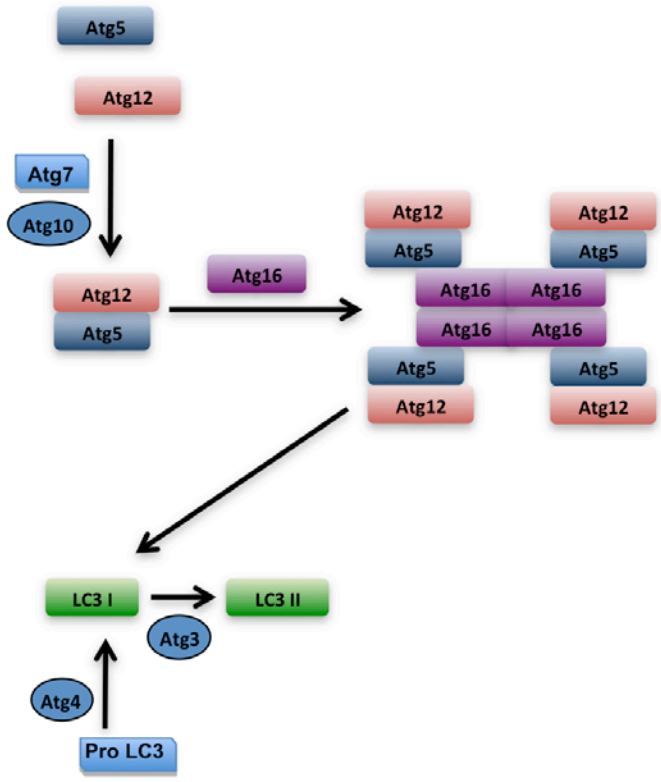

Figure 1.3: Elongation of the isolation membrane to form autophagsome
This involves the conjugation of Atg12 to Atg5 which is catalysed by Atg7 (E1-like enzyme) and Atg10 (E2-like enzyme). The conjugation of phosphatidylethanolamine (PE) to LC3 (one of the mammalian orthologues of yeast Atg8) is catalysed by Atg4 (a protease), Atg7 and Atg3 (E2-like enzyme).

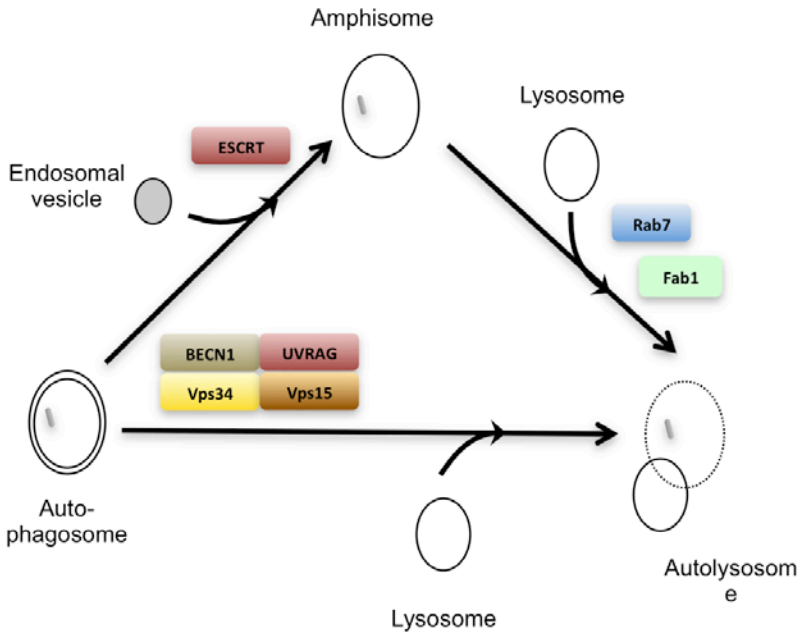

Figure 1.4: Autophagosome maturation
The fusion of autophagosomes to endosomes and/or lysosomes is mediated by Beclin 1, UVRAG, Vps 34and Vps15. Additionally, ESCRT, as well as Rab7 and Fab1 are also proposed to facilitate the fusion of autophagsome to endosomal vesicle, and the subsequent fusion lysosomes respectively.

Subsequent to the *in vitro* characterisation of these panels of autophagy regulators, elegant systemic and tissue-specific deletion of these genes in mice has greatly facilitated the involvement of autophagy in mammalian development (Section 1.3.1) and disease progression.

Beclin 1 knockout mice failed to survive post embryonic day 7.5 (Yue, Jin et al. 2003), while *Atg5* and *Atg7* knockout mice die of starvation soon after birth due to the inhibition of autophagy (Kuma, Hatano et al. 2004) (Komatsu, Waguri et al. 2005).
The difference in phenotype may suggest that Beclin 1 might have more complicated functions beyond autophagy. Indeed, it was later reported that Beclin 1 also regulates endocytosis (Ruck, Attonito et al. 2011).

The genetic ablation of autophagy has also been shown to contribute to tumourigenesis, with some autophagy regulators playing more significant roles than others, as discussed in section 1.6.

However, mice deficient for either of the Atg8 paralogues (Section 3.0), LC3B or GABARAP were able to develop normally and appear phenotypically normal. (Cann, Guignabert et al. 2008) (O'Sullivan, Kneussel et al. 2005). *LC3B*$^{-/-}$ embryonic fibroblasts were able to form autophagosomes normally under nutrient-limiting conditions (Cann, Guignabert et al. 2008). Additionally, *GABARAP*$^{-/-}$ do not show an upregulation of other GABARAP homologues (O'Sullivan, Kneussel et al. 2005). These scenarios probably reflect a biological redundancy in the regulation of autophagy, and that other autophagy regulators can compensate the functions of Atg8 paralogues.

In short, autophagy is a multi-step process that is regulated by a panel of genes, and the majority of these genes are conserved from yeast to mammals. Some of the autophagy regulators, such as Beclin 1 may have other functions beyond autophagy regulation. The identification of novel mammalian regulators such as ATG101 suggests that mammalian cells have evolved to sustain the escalating demand for autophagy regulation in a more complex environment. Thus, when there's a block in the signalling cascade, one can imagine that cells must have adopted alternative

routes to activate autophagy, or may even switch to activate other types of autophagy to respond to intracellular and extracellular changes. However, functional redundancy may occur, as observed by the deletion of the ATG8 paralogues, LC3B and GABARAP.

1.3 Autophagy: Life and breath of cells

Autophagy occurs constitutively at basal levels to maintain cellular homeostasis by regulating various cellular processes, some of which will be discussed in this section.

1.3.1 Autophagy is required for development and hematopoiesis

The investigation of the homeostatic role of autophagy in mammalian development and hematopoiesis has been greatly propelled by the genetic knockout studies of *ATG* genes. Mammalian embryogenesis begins with the fertilization of mature oocyte by sperm to form zygote, followed by early embryo development to form two-, four- and eight-cells structure (Al-Gubory, Fowler et al. 2010). Further cellular divisions result in the development of blastocyst in which the inner cell mass gives rise to the fetus, whereas the rest contribute to extra embryonic tissues such as the placenta (Surani and Tischler 2012). The importance of autophagy in embryogenesis is highlighted by the findings the conventional knockout of *BECN-1* and *AMBRA* is embryonic lethal due to the failure to develop structures that facilitate the stages of embryogenesis (Mizushima and Levine 2010).

Downstream of embryogenesis, autophagy is required to sustain neonatal survival. Prior to birth, fetuses obtain the essential nutrients from the placenta (Mizushima and Levine 2010). Upon birth, this flow of nutrient is terminated and neonates rely on autophagy for the synthesis of essential nutrients (Mizushima and Levine 2010). *Atg5*$^{-/-}$ and *Atg7*$^{-/-}$ neonates which are deficient for autophagy, despite being born at the expected Mendelian frequency, have decreased amino acid levels and succumbed to severe starvation-induced cell death soon after birth (Kuma, Hatano et al. 2004) (Komatsu, Waguri et al. 2005) (Mizushima and Levine 2010).

The production of mature and specialised cells, which are required for normal tissue functions, arose from stem cells, a population of pluripotent and self-renewing cells which can differentiate into multiple cell types. (Herberts, Kwa et al. 2011). In line with this, autophagy was found to be upregulated in human embryonic stem cells

(hESCs) induced to undergo differentiation by treatment with type I TGF-beta receptor inhibitor SB431542 or removal of MEF secreted maintenance factors (Tra, Gong et al. 2011). This suggests that autophagy might be required for cellular differentiation. Likewise, autophagy has been proposed to facilitate cellular reprogramming and the generation of the induced pluripotent stem (iPS) cells (Vessoni, Muotri et al. 2012). In this context, autophagy is hypothesized to provide ATP for chromatin remodelling and the subsequent induction or repression of genes involved for the maintenance of pluripotency and differentiation (Vessoni, Muotri et al. 2012).

Autophagy has also been implicated in the production of red blood cells, megakaryocytes, myeloid cells (monocyte/macrophage and neutrophil), and lymphocytes from hematopoietic stem cells – a process collectively termed hematopoiesis (Orkin and Zon 2008). The involvement of autophagy in hematopoiesis begins as early as maintaining the integrity of the HSC pool, where it is required to prevent the accumulation of mitochondria and reactive oxygen species (ROS) in the HSCs and progenitor cells (Mortensen, Soilleux et al. 2011). Upon genetic ablation of autophagy by *Atg7* deletion, the bone marrow-derived $Lin^{-}Sca\text{-}1^{+}c\text{-}Kit^{+}$ (LSK) cells, which are enriched for HSCs and early progenitors, exhibited an increase in DNA damage, proliferation and apoptosis, leading to reduced HSC cell count within this compartment (Mortensen, Soilleux et al. 2011). Thus, autophagy is critical to maintain a healthy pool of HSCs and progenitors for efficient production of blood cells.

The autophagic removal of mitochondria is also required for erythroid and lymphocyte differentiation (Mizushima and Levine 2010). Inhibition of autophagy in red blood cells by deleting *Atg7* causes pre-mature cell death (Mortensen, Ferguson et al. 2010). Likewise, the cell count of circulating T and B lymphocytes were significantly reduced upon *Atg5* and *Atg7* deletion (Pua, Dzhagalov et al. 2007) (Mortensen, Ferguson et al. 2010). Though this lymphopenia did not progress, *ex vivo* and *in vitro* cultures of $CD4^{+}$ and $CD8^{+}$ $Atg7^{-/-}$ T lymphocytes exhibited higher levels of mitochondrial number and mass, as well as increased mitochondrial superoxide and consequently more apoptosis (Mortensen, Ferguson et al. 2010). Although Atg5 is critical for the development of B cells in the bone marrow and the survival of certain types of

circulating B cells, the mechanism underlying autophagy and B cell defects is unknown and requires further investigation (Mizushima and Levine 2010). While studies from mouse models lacking the core *Atg* genes do not implicate a defect in the production of platelets from megakaryocytes (megakaryocytopoiesis), megakaryocytic differentiation and the production of pro-platelets involves drastic morphological changes, which is most likely facilitated by autophagy (Colosetti, Puissant et al. 2009). The involvement of autophagy in this process is further suggested by the findings whereby caspases, which also regulates autophagy (refer to section 1.4), are required in the late steps of megakaryocytic differentiation (De Botton, Sabri et al. 2002). Thus, it would be of great interest to determine if autophagy plays a significant role in platelet formation.

In summary, autophagy is required for cellular development and hematopoiesis. Thus, it is important to identify other autophagy regulators which contribute to these processes in order to reinforce our understanding between autophagy, cellular development and differentiation.

1.3.2 Stimulating Autophagy - Survival or death?

When cells are exposed to unfavourable conditions, autophagy is activated above basal levels to counteract ‘stress’ to achieve cellular equilibrium and to maintain a stable and favourable environment. This switch from its default housekeeping to a cytoprotective role is triggered by various stimuli, and will be discussed in this section.

Nutrient withdrawal has been long considered as a potent stimulus of autophagy. When cells are deprived of amino acids, mature autophagic vacuoles have been reported to occupy ~1% of the cytoplasm (Mizushima, Yamamoto et al. 2001). Indeed, markers of autophagy are rapidly detected within 10 minutes of starvation (Munafo and Colombo 2001). The dependence on autophagy for survival under nutrient-limiting conditions is conserved from yeast to higher eukaryotes. During nitrogen starvation, autophagy-defective yeast mutants were susceptible to cell death compared to the wild-type controls (Suzuki, Onodera et al. 2011). This is attributed to the inability of the mutants to prevent ROS accumulation, thus leading to the fatal loss

of mitochondria function (Suzuki, Onodera et al. 2011). Recently, another group of protein - ubiquilins (UBQLNs) - were shown to be upregulated upon nutrient starvation to activate autophagy to sustain survival (N'Diaye, Kajihara et al. 2009).

However, autophagy may have dual roles in survival during starvation. Excessive autophagy induced by starvation can cause irreversible cellular damage beyond rescue. It has been shown that physiological levels of autophagy promotes survival in *Caenorhabditis elegans* during starvation, but excessive levels of autophagy can lead to cell death (Kang, You et al. 2007). Occasionally, autophagy has also been demonstrated to potentiate cell death upon serum withdrawal (Steiger-Barraissoul and Rami 2009). Thus, autophagy may act as a double-edged sword in cellular survival upon nutrient withdrawal. The decision to invoke cell death or cellular processes could be affected by cell type and other reasons that have yet to be elucidated.

The link between vacuolization and autophagy, and corresponding cell death has led to the coinage of the term autophagic cell death. In fact, this process has been well-studied in the model organism *Dictyostelium discoideum* (Tresse, Giusti et al. 2008). This form of cell death accompanied by autophagy activation has also been reported in the Drosophilla midgut (Lee, Cooksey et al. 2002). It was later revealed that autophagic cell death is required for development. Elegant *in vivo* studies by Berry and Baehrecke (2007) reported that autophagy promotes cel death in Drosophila salivary glands upon growth arrest. They also demonstrated that the developmental degradation of salivary glands is inhibited when autophagy is blocked by mutating *atg* genes, despite the presence of caspases, and that autophagy induces cell death in a caspase-independent manner (Berry and Baehrecke 2007).

Autophagy is also implicated in cellular regeneration. The regenerative role of autophagy has been demonstrated in the simple metazoan, planarian (Gonzalez-Estevez, Felix et al. 2007). In planarian, autophagic degradation generates energy and the building blocks for cell proliferation and differentiation to facilitate organism remodeling and cellular regeneration (Gonzalez-Estevez, Felix et al. 2007).

Alternatively, autophagy is also required for the clearance of degenerated axons during the regeneration of rat striatic nerve (Piao, Wang et al. 2004).

Metabolic stress caused by oxygen limitation has also been shown to induce autophagy. During hypoxia, *platelet-derived growth factor receptors (PDGFR)*, an orthologue of the human *tyrosine kinase Poliovirus receptor* (*Pvr*) selectively induces HIF-1α- dependent hypoxia-induced autophagy, leading to cellular survival (Wilkinson, O'Prey et al. 2009). The pro-survival role of autophagy in this context is not attributed to the removal of defective mitochondria, but rather the degradation of cytosolic protein (Wilkinson, O'Prey et al. 2009).

Reactive oxygen species (ROS) are potent DNA damaging agents (Wiseman and Halliwell 1996), and have been shown to induce autophagy (Scherz-Shouval, Shvets et al. 2007) (Bensaad, Cheung et al. 2009). Other DNA damaging agents such as ionising radiation and cisplatin were also shown to induce autophagy in the paneth cells of the small intestine (Gorbunov and Kiang 2009) and the renal proximal tubular cells (Periyasamy-Thandavan, Jiang et al. 2008) respectively. In the renal cells, autophagy is required for sustaining cellular survival (Periyasamy-Thandavan, Jiang et al. 2008). Whether occurring at physiological levels or induced above the basal levels, the role of autophagy to maintain genome integrity for cellular survival has been well characterised. *In vitro* cultures of autophagy-defective tumour cells accumulate more DNA damage and exhibit an impaired survival when compared to the wild-type counterparts upon exposure to metabolic stress (Karantza-Wadsworth, Patel et al. 2007). This is attributed to the failure of autophagy-defective cells to adapt to metabolic stress, which leads to insufficient ATP generation and the built-up of damaged mitochondria with excessive ROS (Jin 2006). Direct DNA insult by ROS may cause replication stress and DNA damage response activation, which normally arrests cell cycle progression or triggers apoptosis (Karantza-Wadsworth, Patel et al. 2007).

Other known agents which activate autophagy include hormones (Deng, Feng et al. 2010), and certain chemicals or drugs (Kanzawa, Germano et al. 2004). The novel estrogen-induced gene *EIG121* which is associated with the endosome–lysosome

compartments, is speculated to induce autophagy and promote cell survival upon exposure to nutrient-limiting conditions and cytotoxic agents (Deng, Feng et al. 2010). Autophagy also facilitates cell death in sarcoma cell lines which were treated with the genotoxic chemotherapy agent doxorubicin and cyclin-dependent kinase inhibitors (Lambert, Qiao et al. 2008).

In addition, heat stress, osmotic and mechanical pressure have also been documented to induce autophagy (Swanlund, Kregel et al. 2008) (Han, Kim et al. 2010) (King, Veltman et al. 2011). The effect of autophagy in this context, whether to induce cell death or sustain cell survival requires further investigation.

In conclusion, autophagy is activated upon exposure to various forms of stress such as nutrient deprivation, metabolic stress, and DNA damage. Although most evidence demonstrate that autophagy in these contexts promotes cellular viability, it can also induce cell death. On the other hand, autophagy occurring at physiological levels facilitates cellular regeneration, which is critical for homeostasis.

1.4 Autophagy and apoptosis crosstalk

Apoptosis is characterized by cell shrinking, nuclear condensation and fragmentation, membrane blebbing and the engulfment of cellular components into apoptotic bodies (Kerr, Wyllie et al. 1972). This form of cell death requires the participation of caspases - a group of cysteine proteases that play important roles in regulating apoptosis (Degterev, Boyce et al. 2003). The interplay of both autophagy and apoptosis in cell death has been documented by many studies.

Both pathways have been demonstrated to occur in parallel for effective cell killing. This is evident in the p53 and DRAM-1 signalling network, whereby *DRAM-1*, a direct target of p53, promotes autophagy, and is required for effective p53-mediated apoptosis (Crighton, Wilkinson et al. 2006). Similarly, Yee et al. (2009) showed that the potent pro-apoptotic protein, Puma, activates Bax, thus resulting in mitochondrial outer membrane permeabilisation. Autophagy induction was also detected alongside

the release of cytochrome *c* into the cytoplasm, proposing the occurrence of mitophagy in response to mitochondrial perturbations (Yee, Wilkinson et al. 2009). The inhibition of autophagy by silencing *Atg5* diminishes the PUMA- and Bax-induced apoptotic response (Yee, Wilkinson et al. 2009). These lines of evidence suggest that the cross talk between autophagy and apoptosis is required for effective cell killing.

Other inhibitors of apoptosis that also inhibit autophagy are the well-characterised anti-apoptotic proteins of the Bcl-2 family, which primarily repress the activation of the pro-apoptotic Bax/Bak proteins (Pattingre, Tassa et al. 2005). In line with this, Bcl-X_L binds to the BH3-domain of Beclin 1, resulting in an inhibition of starvation-induced autophagy (Pattingre, Tassa et al. 2005). Additionally, Bcl-2, which is found in the mitochondria and ER inhibits apoptosis, but only ER-localised Bcl-2 functionally inhibits autophagy by preventing calcium release from the ER, resulting in the subsequent activation of mTOR and the repression of autophagy (Pattingre, Tassa et al. 2005). These studies suggest that autophagy and apoptosis are regulated in a similar manner.

Regulators of the extrinsic apoptotic pathway also interact with the conventional ATG proteins. For instance, the ATG5 protein has been documented to interact with Fas-associated protein with death domain (FADD) to induce apoptosis (Pyo, Jang et al. 2005). In an independent study, calpain-cleaved ATG5 has been documented to translocate from the cytosol to mitochondria and associate with the anti-apoptotic molecule Bcl-X_L to trigger cytochrome *c* release and caspase activation (Yousefi, Perozzo et al. 2006). The cleaved form of ATG5, however, does not modulate autophagy, but the fact that calpain activity is required for autophagy induction by rapamycin treatment and amino acid starvation (Demarchi, Bertoli et al. 2006) suggests that the cleavage of ATG5 only occurs below a certain threshold to ensure that there is enough uncleaved and cleaved ATG5 to modulate both autophagy and apoptosis. These lines of evidence indicate that apoptosis and autophagy share common regulators. Additionally, the specific processing or cellular localisation of the protein is the key factor which determines whether cells undergo apoptosis or autophagy, or both.

Nevertheless, apoptosis and autophagy occasionally occur in a mutually exclusive manner. Caspases, effectors of the apoptotic pathways, have been shown to cleave and inactivate Beclin 1, and the resulting suppression of Beclin 1 increases apoptosis in HeLa cervical cancer cells (Cho, Jo et al. 2009). In a less drastic scenario, Campthothecan (CPT) treatment in breast cancer cells results in autophagy activation and delayed apoptosis (Munoz-Gamez, Rodriguez-Vargas et al. 2009). These lines of evidence imply that apoptosis is either inhibited, or delayed when autophagy is activated. In this context, autophagy maybe activated to protect cells from dying.

Thus, autophagy and apoptosis share a common panel of regulators, and the decision to activate either or both of these cellular processes is governed by the specific post-translational modification and the cellular localisation of these proteins. Both autophagy and apoptosis can occur together to enhance cell killing, or in a mutually exclusive manner. The decision to activate either of these pathways is most likely governed by the health status of the cell, or perhaps the nature of the stimuli.

1.5 Autophagy and the regulation of the immune system

Immunity confers protection to the host by resisting and destroying pathogens or pathogenic materials, and is mainly classified into the innate and adaptive immune system. Innate immunity is the first line of defence and consists of the physical and chemical barriers such as skin, mucous membranes and stomach acids; phagocytic cells such as neutrophils and macrophages; the complement system and various cytokines which mediate inflammation and other non-specific responses which can in turn, activate the adaptive immune system (Rabb 2002). The adaptive immune system consists of T and B cells which function to invoke the cell mediated and humoral response for effective pathogen killing, in addition to establishing a long-lived immunological memory against reinfection (Dunkelberger and Song 2010). Autophagy and immunity is now considered as two inseparable entities, as autophagy has been demonstrated to modulate both the innate and adaptive immune responses, as discussed in this section.

1.5.1 Autophagy mediates innate immunity

When cells are attacked by pathogens such as viruses or bacteria, autophagy is often stimulated in parallel to the immune response. These integrated responses are coordinated by various players of the innate immunity including pathogen recognition receptors (PRRs) including the Toll like receptors (TLR), NOD-Like Receptors (NLR), RIG-1 like receptors, and C-type lectin receptors (Kroemer, Marino et al. 2010)

Members of the PRR family such as TLR and NLR have been demonstrated to be involved in the autophagic pathway upon pathogen invasion. Activation of TLR3 and TLR7 by viruses results in autophagy induction (Delgado, Elmaoued et al. 2008; Shi and Kehrl 2008). The tight cross talk between TLRs and autophagy regulators is reflected when the autophagic response is diminished upon acute silencing of TLR7 and myeloid differentiation factor 88 (MyD88), a component of the TLR7 signalling cascade (Shi and Kehrl 2008). Additionally, the recognition of bacterial peptidoglycans by NOD2 results in the activation of autophagy for bacterial clearance, and these processes are compromised in individuals harbouring mutations in either

NOD2 or ATG16L1 (Cooney, Baker et al. 2010). A more direct role of autophagy in innate immunity is by facilitating the delivery of pathogens to designated cellular compartments for lysosomal digestion or sensing by PRRs (Lee, Lund et al. 2007) (Jia, Thomas et al. 2009).

Autophagy also suppresses innate immune response by toning down the production of inflammatory cytokines. In conjunction with this, many autophagy proteins have been demonstrated to regulate innate immunity beyond autophagy. Atg5 and Atg12, down-regulate another group of PRRs, the cytoplasmic viral nucleic acid sensors to suppress type1 interferon (IFN) production (Jounai, Takeshita et al. 2007). Similarly, deletion of Atg16L1 in hematopoietic cells results in increased production of the pro-inflammatory cytokines, IFN-β and IL-18, following endotoxin stimulation (Saitoh, Fujita et al. 2008).

The influence of autophagy on innate immunity is not only limited to the immune cells. In fact, elegant *in vivo studies* done by Cadwell and colleague showed that the deletion of the *bona-fide* autophagy gene, *ATG16L1* drastically disrupts the function of paneth cells of the small intestine, leading to aberrant exocytosis, and increased expression of a subset of inflammatory cytokines (Cadwell, Liu et al. 2008). Elevated expression of adipocytokine and other inflammatory cytokines are often associated Crohn's disease, a complex inflammatory disease of the small intestine (Yamamoto, Kiyohara et al. 2005) (Cadwell, Liu et al. 2008). In this context, autophagy is most likely to be activated to limit the production of inflammatory cytokines above a certain threshold that would cause dire consequences to the cell.

Based on these lines of evidence, autophagy induction is required to trigger innate immune responses upon initial pathogen attack. However, autophagy also downregulates innate immunity by suppressing the production of inflammatory cytokines. This is mostly the case when the production of inflammatory cytokines reaches a certain threshold that would jeopardise the health status of the cells, or when innate immunity fails to contain or kill off the pathogen, autophagy then limits the magnitude of the innate immune response to switch on the more potent adaptive immune response for complete destruction of the pathogen.

1.5.2 Autophagy modulates adaptive immunity

The adaptive immune response is evoked when the innate immune response fails to contain or destroy the pathogenic attack. When this occurs, antigens are picked up by antigen presenting cells (APCs) and presented on either major histocompatibility complex (MHC) class I or class II molecules to CD8+ and CD4+ T cells (Munz 2010; Munz 2012) (Munz 2006) (Fig.1.5). MHC class I molecules are expressed by all nucleated cells whereas, the expression of MHC class II molecules is restricted to antigen presenting cells (APCs), like B cells, macrophages and dendritic cells (Neefjes, Jongsma et al. 2011) (Munz 2012). However, MHC class II expression can be induced by various stimuli such as the cytokine interferon gamma and other stimuli in non-APCs such as mesenchymal stromal cells, fibroblasts, endothelial cells, epithelial cells, and enteric glial cells (Neefjes, Jongsma et al. 2011). MHC class I molecule, which was conventionally thought to present endogenous antigens which are processed within the cytoplasm, has been demonstrated to also process exogenous peptides which are originally presented by MHC class II molecules by a pathway called cross presentation. (Amigorena and Savina 2010) (Fig. 1.5). Vice versa, intracellular antigens have also been found on MHC class II molecules (Nimmerjahn, Milosevic et al. 2003) (Fig.1.5).

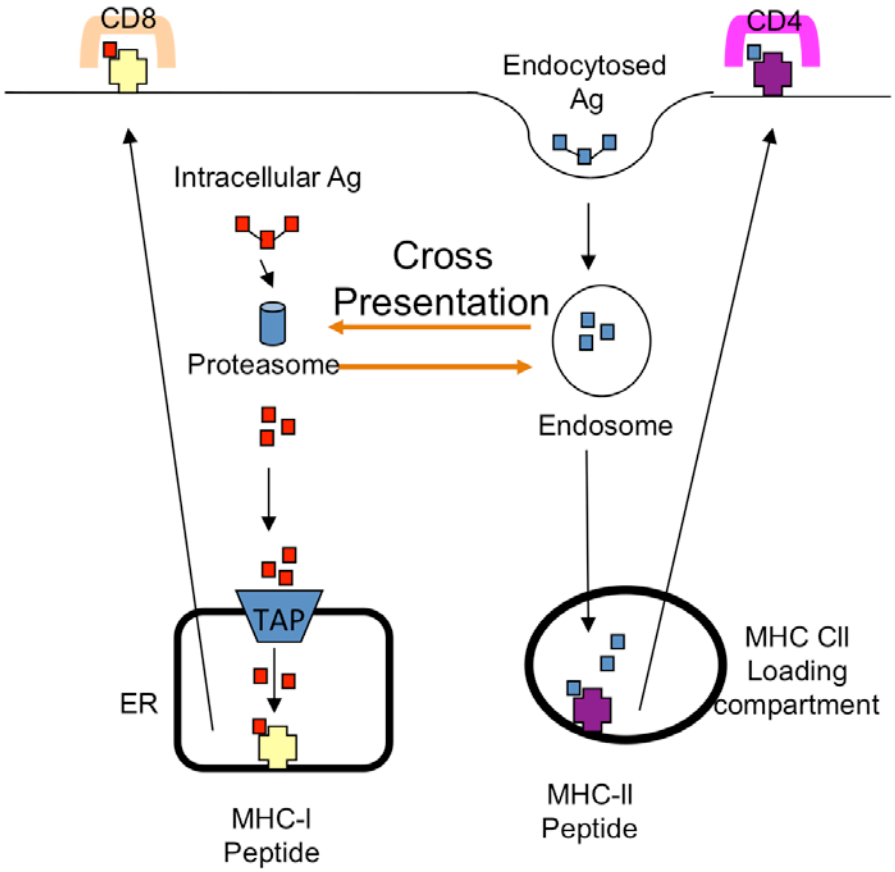

Figure 1.5: MHC class I and II antigen presentation
Intracellular antigen is processed in the cytoplasm by the proteasome, and shuttled into the ER via TAP, where the antigenic fragments are presented on MHC class I molecules. MHC class I/peptide complex is transported on the cell surface to mediate CD8+ T cell activation. Extracellular antigen is delivered into the MHC class II loading compartment by multivesicular bodies such as endosomes, where they are presented on MHC class II molecules. The MHC class II/peptide complex is translocated to the cell surface of the antigen presenting cells to mediate CD4+ T cell activation. Intracellular and extracellular peptide is also cross-presented on MHC class II and class I respectively.

The participation of the autophagic machinery in regulating antigen presentation on MHC molecules has been demonstrated in many studies. Acute silencing of Atg5 in apoptosis-deficient mouse embryonic fibroblasts (*Bax/Bak*$^{-/-}$) decreases antigen presentation on MHC class I molecules and subsequently diminishes the CD8+ T cell activation upon infection with the influenza virus A (Uhl, Kepp et al. 2009). Consistent with this, Li et. al (2008) showed that the priming of CD8+ T cells by melanocytes and epithelial cells presenting the tumour antigen gp100 and the model antigen ovalbumin was greatly reduced when *Atg6* and *Atg12* were silenced in these cell lines, or when the earlier stages of autophagy were pharmacologically blocked with 3-MA. The authors also found that inhibiting autophagy at later stages by blocking autophagosome turnover with the lysosomotropic agent, NH_4Cl strikingly augmented antigen presentation. This suggests that the presence of autophagosomes, regardless of autophagy status is crucial for CD8+ activation, and impinges a role for autophagosomes as efficient antigen transporters from endosomes to MHC class I molecules.

However, the late-stage inhibition of autophagy with another lysosomotropic agent, chloroquine, is reported to block antigen presentation of the tumour antigen mucin1 (MUC1) onto MHC class II molecules, but with no obvious effects on MHC class I machinery (Dorfel, Appel et al. 2005). The significance of autophagy in promoting efficient MHC class II processing is further highlighted when autophagy stimulation enhances, whereas siRNA knockdown of *Atg5* and *Atg8* in dendritic cells decreases HIV antigen presentation on MHC class II due to a defect in forming immunoamphisomes (Blanchet, Moris et al. 2010). The mechanism by which autophagy affects MHC class II presentation was further dissected by Lee and colleagues (2010) who observed that *Atg5*$^{-/-}$ dendritic cells displayed a reduced capacity to form phagolysosomes, leading to a decreased ability to prime CD4+ lymphocytes. However, they also discovered that autophagy induced by starvation and rapamycin treatment decreases class II presentation, thus proposing that a non-metabolic autophagy pathway mediates antigen presentation by DC on Class II. These lines of evidence emphasises that the induction and completion of autophagy is critical for efficient endosome cargo delivery to amphisomes and lysosomes for

degradation which results in increased antigen processing for MHC class II presentation to CD4+ cells.

Nonetheless, autophagy status does not seem to play a significant role in facilitating antigen processing on MHC class I molecules, as long as autophagosomes are present at a reasonable level to facilitate the transport of the cargoes for loading (Li, Wang et al. 2008). However, the presence of autophagsomes, as well as the completion of a 'non-metabolic' autophagic process is critical for proper regulation of antigen loading onto MHC class II molecules (Lee, Mattei et al. 2010) (Dorfel, Appel et al. 2005) (Blanchet, Moris et al. 2010). Despite these recent discoveries, there are many questions pertaining to autophagy and immunity that have yet to be answered. Given that these two pathways are tightly linked, pathogens have also evolved to avoid from being targeted, and in some circumstances sabotage autophagy components to 'multiply and prosper' (Mostowy and Cossart 2012). In this case is there any way to induce selective destruction of the hijacked compartments? Aside from autophagy, the role of chaperone-mediated autophagy in the regulation of the host defence system is slowly being revealed, particularly in the presentation of endogenous antigen of the cytoplasm origin (Deretic 2005). It is conceivable that more than one form of autophagy operates in innate and adaptive immunity, and the dissection of this network is an encouraging step towards understanding the interplay of autophagy and immunity.

To summarise this section, autophagy initiation is required for both MHC class I and II processing. Weighing the observations between Li et al (2008) and Dorfel (2005), the synthesis, but not degradation of autophagosomes, is the determining factor for class I, whereas for class II, both synthesis and degradation of autophagosomes are crucial. Pathogens have also evolved to evade being targeted, and in some circumstances sabotage autophagy components for their own benefit.

1.6 Autophagy from molecules to cancer.

The deregulation of autophagy has been associated with the pathogenesis of many diseases. In fact, a plethora of autophagic proteins which are targets for oncogenic transformation have been identified (Rosenfeldt and Ryan 2009). As such, the modulation of autophagy is perceived to be an alternative therapeutic target for these diseases. However, this strategy is very tricky, as autophagy activation can limit or exacerbate the amplitude of these diseases, especially cancer.

The pivotal discovery which links autophagy and cancer was initiated by the finding that *BECN1*, the gene which codes for Beclin 1 is mono-allelically deleted in breast and ovarian cancer, and that restoration of this gene in multiple human cancer cell lines results in autophagy activation and growth inhibition, overall limiting tumourigenesis (Liang, Jackson et al. 1999; Koneri, Goi et al. 2007; Kang, Kim et al. 2009). Following from this, mutations in the clusters of ATG genes - *Atg2B, Atg5, Atg9B* and *Atg12* are associated with the onset of gastric and colorectal cancers (Kang, Kim et al. 2009). The involvement of *Atg* genes in tumourigenesis is confirmed by *in vivo* models of cancer in genetically modified mouse models lacking these autophagy regulators. Mice harbouring hemizygous deletion of *beclin 1,* or lacking the *Atg4C* and *bif-1* have an increased predisposition to tumour formation (Qu, Yu et al. 2003) (Yue, Jin et al. 2003) (Marino, Salvador-Montoliu et al. 2007) (Takahashi et al. 2007). However, some autophagy regulators may be redundant with respect to tumour suppression in certain tissues. Takamura et al (2011) demonstrated that mosaic deletion of *Atg5* and liver-specific deletion of *Atg7* results only in benign lesions, with no obvious effect on tumour formation.

Clearly, autophagy is a double-edged sword in cancer. The overexpression of the receptor for advanced glycation end products (RAGE) – also known as MHC class III ligand, is prominent in many cancer cell type and tumours, and is associated with diminished apoptosis, enhanced autophagy and tumour survival (Kang, Tang et al. 2010). In fact, the role of autophagy in mediating resistance of cancer cells to anticancer therapy has been reviewed by many researchers (Vazquez-Martin, Oliveras-Ferraros et al. 2009).

Additionally, a variety of genes that are often mutated in cancer have been reported to promote and repress autophagy. The classical tumour suppressor p53 induces autophagy by upregulating a subset of autophagy promoters such as Sestrin-2 and damage-regulated autophagy modulator-1 (DRAM-1) (Maiuri, Malik et al. 2009) (Crighton, Wilkinson et al. 2006) and also by inhibiting mTOR (Feng, Zhang et al. 2005). Another example is the potent oncogene *Ras*, which induces the expression Beclin 1 and Noxa to promote autophagy and cell death (Elgendy, Sheridan et al. 2011). Ras also represses starvation-induced autophagy through the class I PI3-kinase signaling pathway (Furuta, Hidaka et al. 2004).

The significance of autophagy in limiting or accelerating cancer progression is emerging into the limelight. Some of the well-studied cellular pathways that are modulated by autophagy is this context have been studied by many researches, as reviewed by Mah and Ryan (2012). Autohagy may potentially act as a tumour suppressor during the early stages of cancer, by maintaining the integrity of the genome (Karantza-Wadsworth, Patel et al. 2007) and proteome (Mathew, Karp et al. 2009). However, autophagy may promote tumour immunity by facilitating tumour antigen presentation and mediating the clearance of immune cells. This is suggested by the finding that the core autophagy regulators, ATG6 and ATG12 are required for the presentation of the tumour antigen gp100 by melanocytes to CD8+ T cells (Li, Wang et al. 2008). Furthermore, autophagy has been shown to mediate the release of ATP from dying cells and the clearance of cancer cells by immune cells (Michaud, Martins et al. 2011). However, since autophagy can modulate cell death in both directions, its implication in cancer cell killing can be perceived as having both tumour suppressive and promoting effects. Furthermore, autophagy can be exploited by transformed cells at later stages to sustain their viability in less-favourable conditions and the development of drug resistance (Cuervo 2004) (Kondo, Kanzawa et al. 2005). These lines of evidence show that autophagy is a double-edged sword in cancer, as illustrated in Fig. 1.6. Given this, the key to the development of tumour therapies targeted at autophagy is encrypted in the identification of novel autophagy modulators and subsequently unravelling the effects of autophagy on cellular mechanisms which are involved during cancer development, progression or regression.

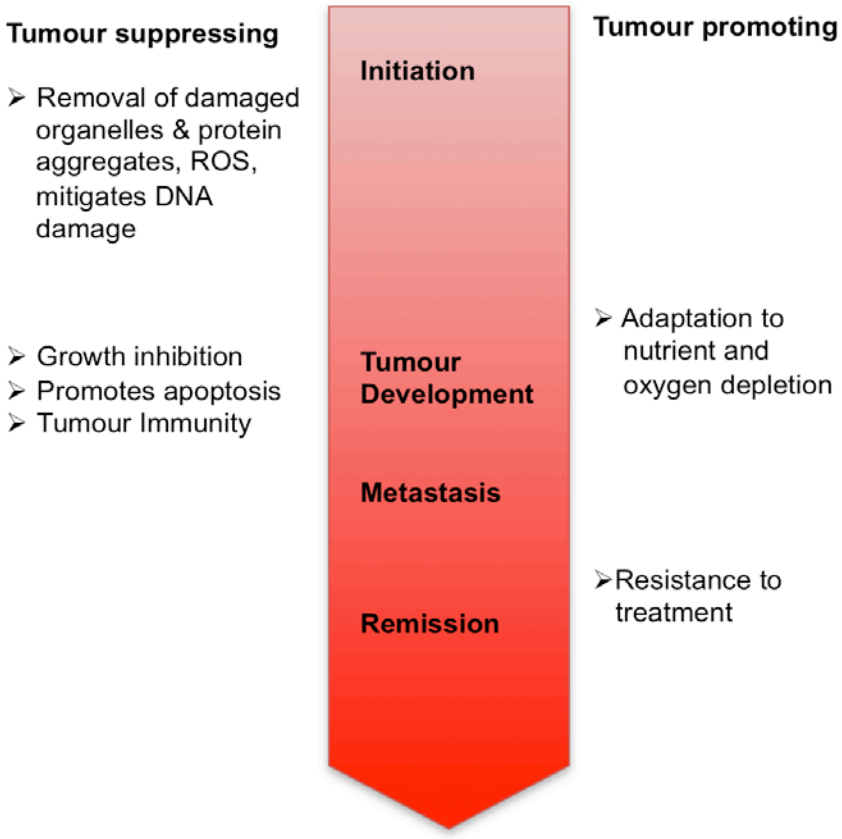

Figure 1.6: The dual roles of autophagy in cancer development
In the early stages of cancer development, autophagy facilitates the removal of molecules that can potentially compromise the integrity of the cellular genome. In the later stages, autophagy limits tumour progression by inhibiting the growth of cancer cells, mediating apoptosis and facilitating tumour immunity. Autophagy can be exploited by transformed cells at later stages to sustain their viability in less-favourable conditions and the development of drug resistance.

1.7 The tumour suppressor p53

1.7.1 Introduction to the biology of p53

The p53 protein is a transcription factor, which is often mutated, in human cancers (Dehay and Kennedy 2007; Vousden and Lane 2007). Consistent with this, many mouse models lacking the wild-type p53 function succumbed to tumourigenesis (Donehower and Lozano 2009). With these observations over the years, p53 eventually gained its rightful reputation as an important tumour suppressor. The regulation and functional roles of p53 have been studies extensively, and are reviewed in this section.

p53 is activated upon exposure to various types of stress, and modulates the transcription and repression of numerous target genes to bring about various cellular responses (Chene 2003). Given that p53 regulates multiple cellular functions, it is of critical importance that p53 is maintained at relatively low levels in unstressed cells (Kubbutat and Vousden 1998). Several tiers of p53 regulation have been described, ranging from transcriptional to translational and protein stability control (Kubbutat and Vousden 1998).

One of the well studied mechanism of p53 control is the proteasomal turnover, which is mediated by several E3 ubiquitin ligases, as illustrated in Figure 1.7 (Meek 2009) (Liu, Urbe et al. 2012). Of these ligases, the murine double minute 2, commonly known as MDM2 (termed HDM2 for its human equivalent) is proposed to be the main regulator of p53 levels (Meek 2009). Apart from directing p53 for proteasomal degradation, MDM2 has been shown to bind to N-terminal end of p53 to inhibit its transcriptional activity. (Oliner, Pietenpol et al. 1993) (Momand, Zambetti et al. 1992). A negative feedback loop exists between p53 and MDM2, as MDM2 itself is in turn activated by p53 (Manfredi 2010). The tight control between p53 and MDM2 is reflected in mouse models of *Mdm2* deletion, which results in aberrant apoptosis and lethality at the blastocyst stage (Jones, Roe et al. 1995). This phenotype can be rescued upon p53 deletion (Jones, Roe et al. 1995). MDM2 is frequently overexpressed in certain cancers (Momand, Jung et al. 1998), and may potentially

reduce the effectiveness of p53-dependent cancer therapies (Harris 2006). This led to the development of a class of small molecules, nultins, which bind to the p53-binding site in MDM2 (Vassilev 2005). The association of nutlins with MDM2 disrupts the interaction between p53 and MDM2, subsequently restoring the activity of p53 (Vassilev 2005).

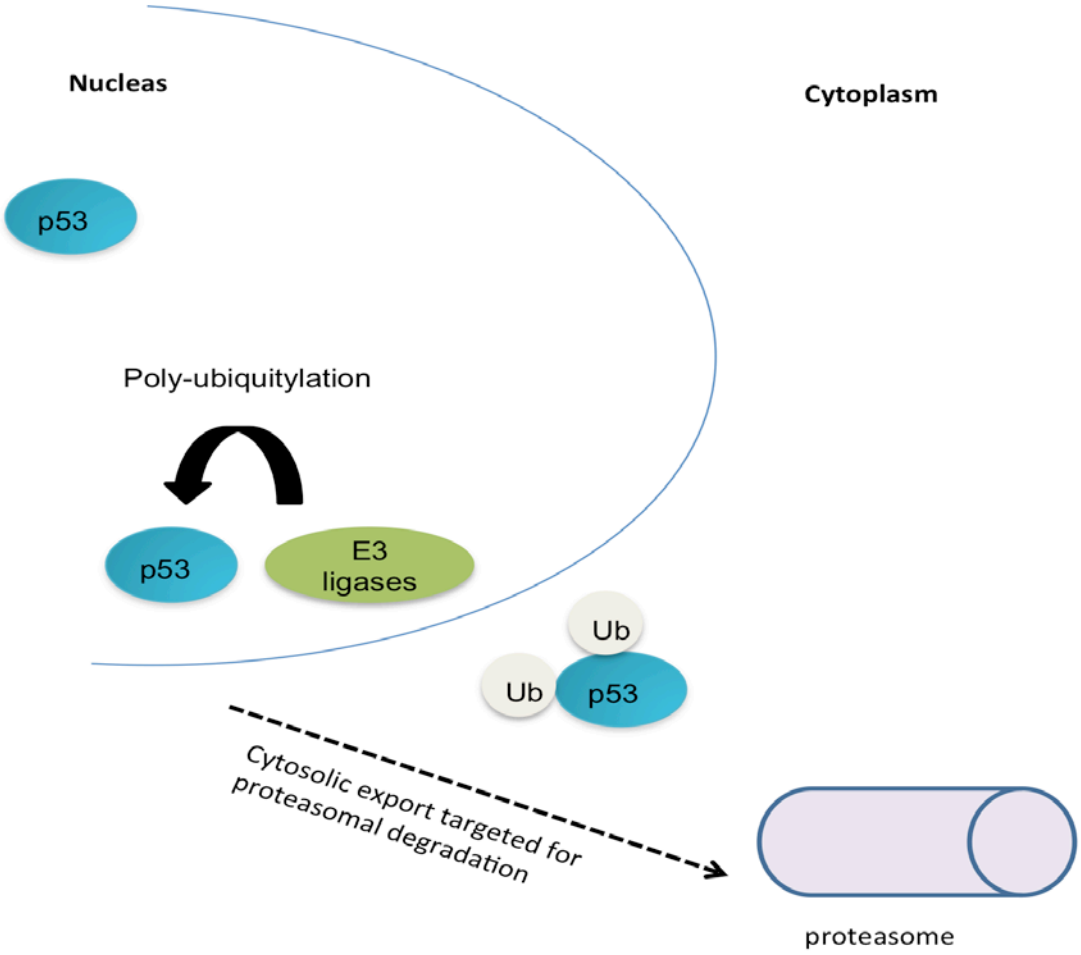

Figure 1.7: Mechanism of p53 turnover via proteasomal degradation
p53 is ubiquitylated and subjected to proteasomal degradation mediated by several E3-ubiquitin ligases. These ligases mediate p53 ubiquitylation and its subsequent export from the nucleas to the proteasome for degradation turnover. Ub, ubiquitin.

1.7.2 The many functional roles of p53

The role of p53 in mediating apoptosis has long been established. p53 transactivates many members of the pro-apoptotic family, such as Puma and Noxa (Yee, Wilkinson et al. 2009) (O'Prey, Crighton et al. 2010). However, the mechanism to bring about cellular demise could be slightly different in different cell types, and may have different therapeutic outcomes in cancer (Shibue, Suzuki et al. 2006). Recently, the pro-survival transcription factor NFκB, has been shown to be required for efficient activation of the p53 target genes, *Noxa* and *p53AIP1*, suggesting a complex interplay between p53 and pro-survival regulators to potentially invoke effective cell death (O'Prey, Crighton et al. 2010). However, not all p53 target genes promote apoptosis. The recently identified TP53-induced glycolysis and apoptosis regulator (TIGAR) protects cells from genomic instability by inhibiting glycolysis and reducing intracellular reactive oxygen species (ROS) (Bensaad, Tsuruta et al. 2006). As a result, this protects cells from ROS-induced apoptosis (Bensaad, Tsuruta et al. 2006). Decreased TIGAR expression sensitised cells to p53-induced death (Bensaad, Tsuruta et al. 2006). Thus, p53 activation can mediate the expression of pro-apoptotic and pro-survival genes. Perhaps the activation of pro-survival genes serves to rescue or limit the accumulation of cellular stress before cell killing begins, and the decision to live or die reflects the flexibility of p53 in the regulation of cellular functions.

p53 has also been shown to regulate autophagy. Various cellular stress stimuli that induce p53 activation also induce autophagy. Upon exposure to DNA damaging agents, p53 is activated and signals through the AMPK and the TSC1/TSC2 complex to inhibit mTOR and subsequently activate autophagy (Feng, Zhang et al. 2005). p53-induced autophagy can both have pro-survival and pro-death effects. For example, p53-driven autophagy via the autophagy modulator DRAM-1, is pro-apoptotic and this effect can be rescued by the silencing of *DRAM-1* (Crighton, Wilkinson et al. 2006). On the other hand, p53-mediated autophagy in *c-myc*-driven lymphomas increases cell survival (Levine and Abrams 2008). p53 has also been demonstrated to negatively regulate autophagy. The inhibition or genetic ablation of p53 induces autophagy in various human, mouse and nematode cells (Tasdemir, Maiuri et al. 2008). Additionally, forced autophagy activation in *p53*-deficient cancer cells has

been shown to sustain cellular viability under hypoxic and nutrient-limiting conditions, implying that autophagy activation in the absence of p53 promotes tumourigenesis (Tasdemir, Maiuri et al. 2008). This form of autophagy can be inhibited by the reinforcement of cytoplasmic or ER-targeted, but not nuclear-targeted p53 (Tasdemir, Maiuri et al. 2008). Thus, p53 plays dual roles in the regulation of autophagy, and the decision to activate or inhibit autophagy is largely governed by the localisation of p53 in the cell.

Cellular senescence is a process where cells enter a state of irreversible cell cycle arrest, and undergo significant changes in gene expression profile and cellular phenotypes (Zilfou and Lowe 2009). p53 has been indirectly implicated in senescence (Sugrue, Shin et al. 1997). For instance, near-senescent fibroblasts can prolong their proliferative life span when wild-type p53 activity is disrupted by the introduction of mutant p53 (Bond, Wyllie et al. 1994). Furthermore, p53 expression and the transcription of its target genes that are involved in inhibiting the cell cycle, were found to be elevated in fibroblasts which are approaching senescence. (Kulju and Lehman 1995) (Bond, Haughton et al. 1996) (Noda, Ning et al. 1994) Recently, it has also been found that the reactivation of p53 in p53-deficient human tumours results in the onset of rapid senescence (Sugrue, Shin et al. 1997). This finding is reinforced by the observation that p53 restoration in p53-knockdown murine liver carcinomas causes tumour regression, and that the primary response to this was the acquisition of the senescence-associated phenotype characterised by an upregulation of a panel of inflammatory cytokines (Xue, Zender et al. 2007). From these lines of evidence, the activation of p53 promotes cellular senescence, and subsequently promotes tumour regression.

p53 is also involved in regulating the progression of the cell cycle. The cell cycle of eukaryotes is comprised four successive phases: M phase/ mitosis (division of the nucleus and the cytoplasm); S phase (DNA synthesis), and two gap phases, G1 and G2, as illustrated in Fig. 1.8 (Dehay and Kennedy 2007).

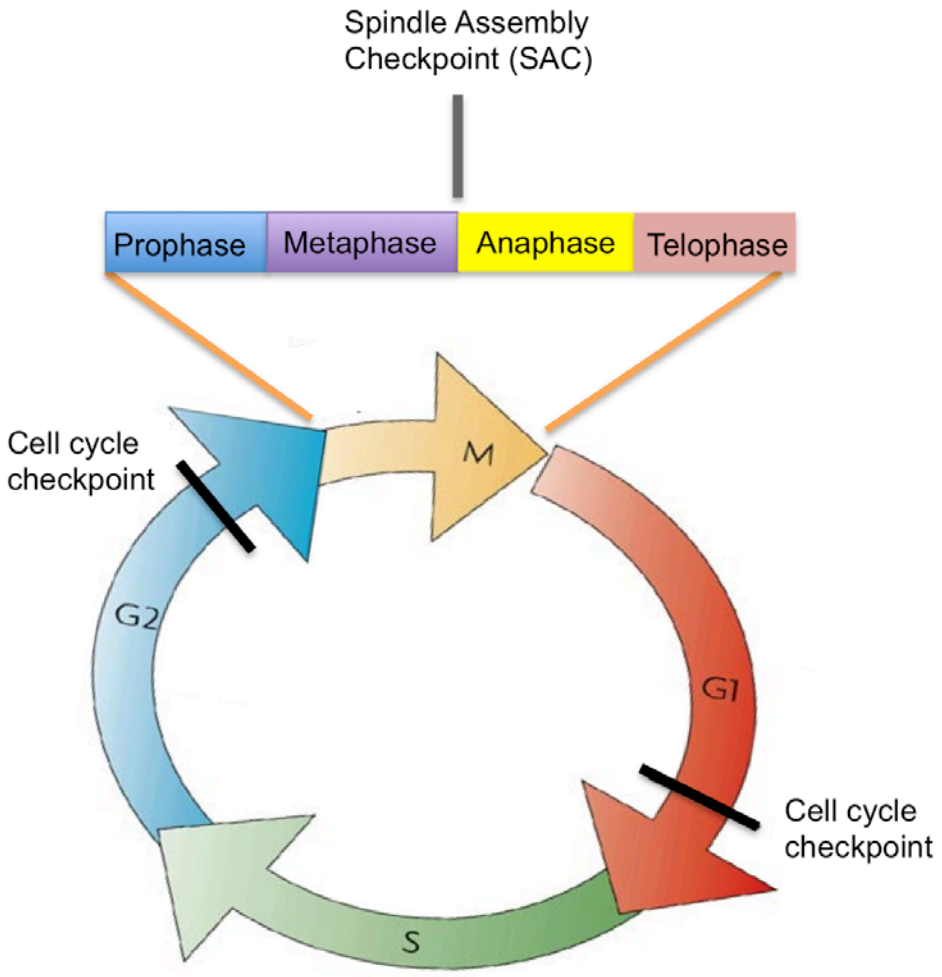

Adapted from Colette Dehay & Henry Kennedy (2007)

Figure 1.8: Cell cycle progression
The cell cycle consists of four stages – S phase (where DNA synthesis occurs); G2 ; M-phase (where cell division occurs) and G1. G1 and G2 are two important gap phases where the cell cycle checkpoints are activated to control DNA integrity. M-phase or mitosis is generally divided into prophase, metaphase, anaphase and telophase. The spindle assembly checkpoint (SAC) occurs at metaphase prior to the seperation of sister chromatids to opposit poles of the cells.

In response to genotoxic stress, cells which accumulate DNA damage undergo mitotic arrest at the cell cycle checkpoints to prevent the transmission of mutations in the DNA (Fig. 1.8) (Zilfou and Lowe 2009). p53 has been shown to regulate the activation of the G1/S (Deng, Zhang et al. 1995) and G2/M checkpoints (Hermeking, Lengauer et al. 1997) (Zilfou and Lowe 2009). It has also been documented that the enhanced activation of p53 can result in cell cycle arrest in the absence of DNA damage (Agarwal, Agarwal et al. 1995). Yet another well studied checkpoint is the spindle assembly checkpoint (SAC) which occurs in mitosis to constrain the transition from metaphase to anaphase until all sister chromatids are properly attached to the mitotic spindle and aligned at the metaphase plate (Huang, Chang et al. 2009). Although the direct regulation of SAC by p53 has yet to be shown, p53 has been shown to regulate BubR1, a key component of the mitotic spindle checkpoint machinery (Oikawa, Okuda et al. 2005). In this study, *p53*$^{-/-}$ cells have reduced levels of BubR1, resulting in a compromised spindle checkpoint that allows error-prone anaphase progression (Oikawa, Okuda et al. 2005). These lines of evidence reinforce the role of p53 as a critical regulator of the cell cycle checkpoints to maintain genome integrity.

The interplay of p53 in the regulation of the immune response has been established in animal models of inflammation and autoimmunity. *p53*-null mice exhibited an exacerbated inflammatory response and tissue destruction in mouse models of collagen-induced arthritis (a model of rheumatoid arthritis) (Yamanishi, Boyle et al. 2002) and experimental autoimmune encephalomyelitis (EAE) (Okuda, Okuda et al. 2003). Furthermore, p53 has been indicated to inhibit the transactivation activity of NFκB, which promotes the activation of major inflammatory regulators such as IL-6 (Santhanam, Ray et al. 1991). This implies that p53 negatively regulates the production of inflammatory cytokines. Apart from that, *p53*$^{-/-}$ macrophages which were treated with the inflammatory agents, lipopolysacharride (LPS) and interferon gamma□ produced more proinflammatory cytokines and exhibited higher levels of total and phosphorylated signal transducer and activator of transcription (STAT)-1, a transcription factor important for immunity and inflammation compared to wild-type macrophages (Zheng, Lamhamedi-Cherradi et al. 2005). This indicates that p53 also modulates innate immunity in addition to inflammation and autoimmunity.

Dendritic cells (DCs) that are transduced with wild-type p53 have been demonstrated to induce a CD8+ T cell response to mediate the specific killing of tumour cells that are overexpressing p53 (Tokunaga, Murakami et al. 2005). The involvement of DCs and T cells in this context suggests that p53 is involved in the regulation of the adaptive immune response as well. This is consistent with the finding that p53 induces the transporter associated with antigen processing (TAP) 1 to enhance the transport of MHC class I peptides and the activation of the MHC class I pathway. In fact, the targeted deletion of p53 in T cells predisposes to spontaneous autoimmunity, due to enhanced Th17 T cells responses (Zhang, Zheng et al. 2011). These lines of evidence imply that not only does p53 regulates innate and adaptive immunity, but it also bridges these two forms of immune responses.

In a nutshell, p53 coordinates a wide range of cellular processes in response to various forms of stress signals to maintain cellular integrity. Mutations or loss of p53 functions could provide many facets for tumourigenesis.

1.8 An overview of DRAM

1.8.1 Functions of DRAM-1 beyond autophagy

Damage Regulated Autophagy Modulator (DRAM), now known as *DRAM-1*, is a direct p53 target gene and was initially identified by Crighton et. al (2006) in the *p53*-null human osteosarcoma cell line, Saos-2. Human DRAM-1 consists of 238 amino acids, and domain prediction analysis suggested that it contains an ER targeting signal and six hydrophobic transmembrane regions, as illustrated in Fig. 1.9 (Crighton, Wilkinson et al. 2006). DRAM-1 is found primarily in lysosomes, although its presence in other secretory compartments have been documented (Park, Kim et al. 2009) (Mah, O'Prey et al. 2012). DRAM-1 is highly conserved across species (Crighton, Wilkinson et al. 2006), thus suggesting that it must have a very important function since it does not mutate very often.

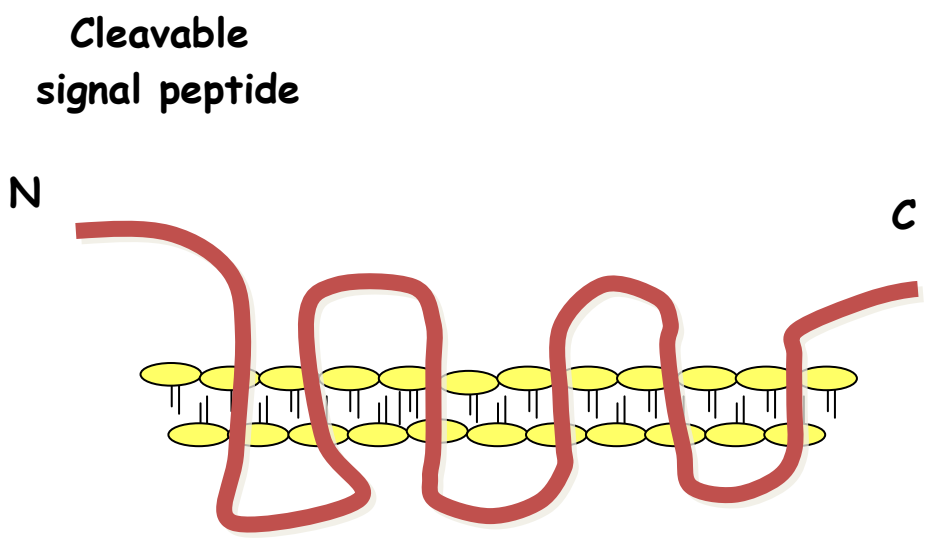

Figure 1.9: Schematic representation of DRAM-1

DRAM-1 is a six-transmembrane spanning protein that contains a putative ER-targeting signal.

DRAM-1 modulates autophagy and enhances p53-dependent cell death by mediating autophagosome accumulation and cytochrome *c* release, respectively (Crighton, Wilkinson et al. 2006). This suggests that the apoptotic and autophagic functions of DRAM act in parallel, and seemingly converge, in a p53-dependent manner. The participation of key regulators of cellular viability in the p53 and DRAM-1 dependent apoptotic and autophagic pathways are slowly emerging. In line with this, 2-methoxyestradiol (2-ME) has been demonstrated to induce autophagy and apoptosis in Ewings sarcoma cells via the activation of p53 and JNK (Lorin, Pierron et al. 2010). In this context, p53 regulates Jun N-terminal kinase (JNK), which in turn modulates autophagy through two distinct mechanisms, one of which is by up-regulating DRAM-1, and DRAM-1 is critical for effective induction of autophagy and apoptosis (Lorin, Borges et al. 2009). Additionally, the nuclear factor κB (NFκB) inhibitor, SN50, also induces the expression of the pro-apoptotic proteins, p53 and PUMA, as well as DRAM-1 in gastric cancer cell lines which exhibit morphological features of autophagy and eventually succumb to apoptosis in a p53 dependent manner (Zhu, Xing et al. 2011). This highlights the mechanism in which NFκB modulates apoptosis and autophagy via the p53 - DRAM-1 pathway. However, NFκB has been shown to promote both cell death and survival under different cellular conditions (Ryan, Ernst et al. 2000) (Griffiths, Grundl et al. 2011). Consistent with this, Wang et al (2009) showed that the overstimulation of NMDA receptors in rat striatum can induce NFκB - dependent expression of p53 and DRAM-1, and proposed that p53 triggers autophagy and apoptosis, which eventually contribute to excitotoxic neuronal death (Wang, Dong et al. 2009). These lines of evidence imply that DRAM-1 is required for effective killing upon treatment with anti-tumoural compounds in many cancer cell lines.

Apart from p53, DRAM-1 expression is also induced by p73, a protein that shares many functional similarities to p53 (Crighton, O'Prey et al. 2007). Like p53, p73 also promotes cell death and autophagy, but both of these cellular events are independent of DRAM-1 (Crighton, O'Prey et al. 2007). So far, the significance of p73-induced DRAM-1 expression has yet to be elucidated.

Another known regulator of DRAM-1 is E2F1, a member of the E2F family that is involved in modulating a variety of cellular functions, such as DNA repair, differentiation and development. Polager et al (2008) reported that in addition to mediating apoptosis, E2F1 also regulates autophagy at the transcriptional level by upregulating the expression of four autophagy genes—*LC3*, *ATG1*, *ATG5* and *DRAM-1*, eluding to the fact that E2F1 modulates autophagy via the DRAM-1 pathway (Polager, Ofir et al. 2008).

Recently, DRAM-1 has been shown to regulate p53 levels (Valbuena, Castro-Obregon et al. 2011). Upon genotoxic stress, p53 is stabilised via specific phosphorylation by VRK-1, and DRAM-1 is required for the lysosomal degradation of VRK-1 and the subsequent HDM2-mediated dephosphorylation and destabilisation of p53 (Valbuena, Castro-Obregon et al. 2011) This double regulatory loop is proposed to be required to modulate the block in cell cycle progression upon DNA damage (Valbuena, Castro-Obregon et al. 2011).

Because DRAM-1 regulates apoptosis and autophagy, two critical cellular processes that are closely associated to tumourigenesis, DRAM-1 is hypothesised to be a tumour suppressor downstream of p53 (Crighton, Wilkinson et al. 2006). Indeed, *DRAM-1* mRNA level is reduced in a panel of oral tumour cell lines and primary squamous tumours (Crighton, Wilkinson et al. 2006). Upon further analysis, it was found that the downregulation of *DRAM-1* is mediated by the direct hypermethylation within the CpG island of the *DRAM-1* promoter (Crighton, Wilkinson et al. 2006). However, DRAM levels remains unchanged in colorectal cancer (Chang, Tseng et al. 2011). These lines of evidence imply that the changes in *DRAM-1* expression is cancer-type specific.

Recent microarray analysis on the breast adenocarcinoma MCF-7 cell line revealed that several autophagy-core machinery genes including *DRAM*, *BECN1*, and *UVRAG* were upregulated in TNF-resistant cells (Moussay, Kaoma et al. 2011). The upregulation of these panels of autophagy regulators is postulated to activate

autophagy to sustain viability upon challenge with chemotherapeutic agents, eventually leading to drug resistance (Moussay, Kaoma et al. 2011).

In short, these studies suggest that the critical regulators of apoptosis, DNA repair, differentiation and development explicitly regulate autophagy and potentially cell cycle via the participation of DRAM-1, as illustrated in Fig. 1.10. This suggests that there are other functional roles of DRAM-1 beyond those that are discussed in this section, and are worth pursuing. DRAM-1 level is also altered in some cancer cells, and is suggested to be upregulated in cancer cells that are exposed to chemotherapeutic challenge to sustain cellular survival. These findings suggest that the modulation of *DRAM-1* expression could be important for developing therapeutic strategies.

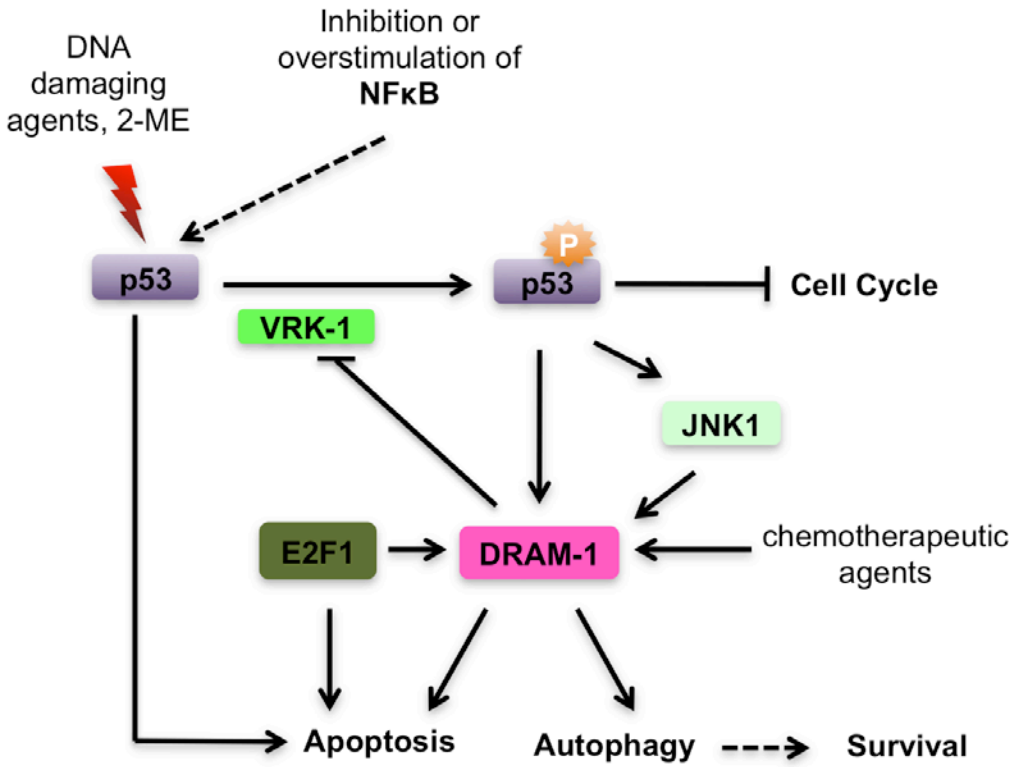

Figure 1.10: The role of DRAM-1 in the regulation of apoptosis, autophagy and cell cycle

Upon exposure to DNA damaging agents, p53 phosphorylation is mediated by VRK1 to inhibit cell cycle progression which is reversed by DRAM-1. DRAM-1 is also required for effective p53-mediated apoptosis. The anti-tumoural compound, 2-ME, also induces apoptosis and autophagy via the p53–JNK–DRAM-1 pathway. Additionally, the overstimulation or inhibition of NFκB also modulates apoptosis and autophagy, which involves the activation of p53 and DRAM-1. Another apoptosis regulator, E2F1, also promotes the expression of a panel of autophagy genes, including *DRAM-1*. *DRAM-1* expression in cancer cell lines is upregulated upon exposure to chemotherapeutic agents to mediate autophagy for survival.

1.8.2 DRAM family proteins

The evolutionary conservation and divergence of DRAM's functional roles in human is reflected by the identification of four other proteins that show significant homology to DRAM-1 which are nominally named as DRAM-2, DRAM-3, DRAM-4, DRAM-5 (which is comprises of two isoforms, DRAM-5a and DRAM-5b (O'Prey, Skommer et al. 2009). However, simpler organisms, such as drosophila, contains only one DRAM protein (O'Prey, Skommer et al. 2009).

DRAM-2 colocalises with DRAM-1 and is found primarily in the lysosomes (Park, Kim et al. 2009). Although the individual expression of DRAM-1 or DRAM-2 does not induce cell death, the co-expression of both homologues significantly induced cell death (Park, Kim et al. 2009). Additionally, DRAM-2 also induces autophagy upon nutrient starvation, and the silencing of *DRAM-2* abolishes this effect (Yoon, Her et al. 2012). These lines of evidence reveal that DRAM-1 and DRAM-2 share a high degree of functional similarity, and both homologues could be responsible for induction of a balance between apoptosis and autophagy. The functions of DRAM-3, -4, and -5 remain to be elucidated.

Moreover, DRAM-1 encodes not just one mRNA, but a series of splice variants in multiple human and mouse cell lines (which will be discussed in Chapter 3). Thus, it is tempting to believe that alternative splicing is also present in other DRAM family members, thus conferring functional versatility for a strong and powerful response upon activation.

The recent discovery and characterisation of DRAM-1 and other DRAM family members is certainly an exciting aspect in cancer biology. It remains possible that the members of the DRAM family work in synergy to invoke multiple cellular responses, mainly apoptosis and autophagy. In light of this, the generation of conditional DRAM knockout mice and flies—would indeed be very rewarding and would yield information with respect to both the functional and evolutionary nature of DRAM function, which could be targeted for the strategic development of cancer therapeutics

1.9 Project Aims

The aims of this project are:

1. To investigate the role of human DRAM-1 isoforms *in vitro* with respect to autophagy and cell death.
2. To characterise *DRAM-1* conditional knockout mice with respect to:
    a. Ability to survive post birth/ longevity
    b. Spontaneous development of autophagy-related diseases and cancer
    c. Irradiation induced p53-dependent and –independent cell death
    d. p53-induced liver senescence
    e. Irradiation- and inflammation-induced tumourigenesis
    f. Acute colitis (*in vivo* DSS model)
3. To determine if the p53 – DRAM-1 signalling pathway regulates adaptive immunity

Chapter 2: Materials and Methods

2.1 Materials

The commercial materials used for general cell culture are listed in this section.

Table 2.1: General tissue culture reagents and their suppliers.

Reagent	**Supplier**
2-Mercaptoethanol	GIBCO
Agarose	Sigma
Ampicillin	Sigma
Blasticidin	Invitrogen
Bovine Serum Albumin (BSA)	Sigma
CryoTube™ vials	Nunc
Cys/Met free medium	GIBCO
Dimethylsulphoxide (DMSO)	Fisher Scientific
DNase I	Roche
Doxycycline	Sigma
Dulbecco's modified Eagle's medium (DMEM)	GIBCO
Fetal Calf Serum (FCS)	PAA
Flt-3L	R&D Systems
Gentamycin	GIBCO
Hygromycin	Roche
Kanamycin	Sigma
L-Glutamine	Invitrogen
M-CSF	Peprotech Ltd
Opti-MEM®	GIBCO
Penicillin	GIBCO
Polybrene (hexadimethrine bromide)	Sigma
Puromycin	Sigma
RBC Lysis Buffer	Sigma
RPMI-1640	GIBCO
Streptomycin	GIBCO
Tet-On® Gene Expression Systems	Clontech
Trypsin	GIBCO
Virkon tablets	DuPont
Xfect polymer and reagent buffer	Clontech

Table 2.2: Reagents used for molecular, biological, and biochemical analyses.

Reagent	**Supplier**
35S	Perkin Elmer
30% (w/v) Acrylamide (bis-acrylamide ratio 37:5:1)	Severn Biotech Ltd
5U Calf Intestine Alkaline Phosphatase	New England Biolabs (NEB)
AdEasyTM Viral Titer Kit	Stratagene
Adeno-XTM Maxi purification kit	Clontech
Adriamycin	Sigma
Agarose	Sigma
BCA	Sigma
CFSE	Molecular Probes
DCFDA	Molecular Probes
DyNAmo™ Probe 2-Step qRT-PCR Kit	Finnzymes
Enhanced Chemiluminescence Reagent (ECL)	Amersham Biosciences
Enzymes used for restriction digest	New England Biolabs (NEB)
Etoposide	Sigma
Fluorescent Mounting Medium	Dako
Giemsa Stain	Sigma
Lipopolysaccharide (LPS)	Sigma
Low Fat Milk Powder	Marvel
Nitrocellulose membrane	Amersham Biosciences
Nutlin-3	Sigma
OVA peptide (257-264)	Abgent
OVA peptide (323-339)	Abgent
Ovalbumin	Sigma
Paraformaldehyde (PFA)	Electron Microscopy Sciences
Ponceau S	Sigma
ProofStartTM DNA polymerase	Qiagen
Propidium Iodide (PI)	Sigma
Rapid DNA Ligation Kit	Roche
RNase	Sigma
RNeasy® Mini Kit	Qiagen
Tamoxifen	Sigma
TEMED	Sigma
Trichloroacetic acid (TCA)	Fluka
X-ray film	Fuji

Table 2.3: Reagents used for *in vivo* experiments

Reagent	**Source**
Puregene DNA extraction Kit	Flowgen
Proteinase K	Roche
Protein Precipitation Solution	Flowgen
GoTaq® Flexi DNA Polymerase Kit	Promega
β-napthoflavone	Sigma
4-Hydroxytamoxifen (4-OHT) (active Z-isomer >98%)	Sigma
Autoclaved Sunfower Oil	Sigma
RNAlater	Sigma
Dextran Sodium Sulfate (DSS)	MP Biochemicals
Azoxymethane (AOM)	Sigma
Poly-L-lysine slides	Sigma
Citrate Buffer for Heat-Induced Epitope Retrieval (10X)	Thermo Scientific
Hydrogen Peroxide (30% w/v)	Sigma
X-Gal	Gold Biotechnology
Potassium ferricyanide(III) ($K_3Fe(CN)_6$)	Sigma
Potassium hexacyanoferrate(II) Trihydrate, ($C_6FeK_4N_6*3H_2O$)	Fluka
Dimethylformamide	Sigma
DAB complex	Thermo Scientific
Goat Serum	DAKO Ltd

Table 2.4: Composition of Buffers and Solutions

Reagent	**Composition**
2 x Western Sample Buffer	100mM Tris Base, pH 6.8; 2% (w/v) SDS; 5% (v/v) ß- mercaptoethanol; 15% (v/v) glycerol; bromophenol blue
20x Potassium cyanide (KC) solution	1 mM Potassium ferricyanide(III) ($K_3Fe(CN)_6$); 1 mM Potassium hexacyanoferrate(II) Trihydrate ($K_4Fe(CN)_6 \cdot 3H_2O$); diluted in PBS
4 x Western Sample Buffer	60mM Tris-HCl,pH 6.8; 2% (w/v) SDS; 14.4mM ß-mercaptoethanol; 20% (v/v) glycerol; 0.1% (w/v) bromophenol blue
5% BSA (in TBS-T)	5% (w/v) BSA; 0.01% (v/v) Sodium Azide; diluted in TBS-T
HBS	50mM HEPES, 250mM NaCl, 1.5mM NaHP04 pH 7.12)
L-Broth (LB)	1% (w/v) Bacto-tryptone, 86mM NaCl, 0.5% yeast extract
LB Agar	1% (w/v) Bacto-tryptone, 86mM NaCl, 0.5% yeast extract; 1.5% (w/v) Agar
Phosphate Buffered Saline (PBS)	170mM NaCl; 3.3mM KCl; 1.8mM Na_2HPO_4; 10.6mM KH_2PO_4
RIPA lysis buffer	0.15M NaCl;1% (v/v) NP-40; 0.5% (v/v) Sodium deoxycholate (DOC); 0.1% (v/v) SDS; 0.05M Tris pH 8.0; 25nM DDT; Protease inhibitors (Complete; Roche); 1mM Vanadate
SDS Running Buffer	0.1% (w/v) SDS; 192mM glycine; 25 mM Tris, pH 8.3
Transfer Buffer	192mM glycine; 25 mM Tris, 20% (v/v) methanol; 0.01% (v/v) SDS
Tris-acetate-EDTA (TAE)	40mM Tris, 0.1% (v/v) glacial acetic acid, 1mM EDTA
Tris-Buffered Saline (TBS)	25mM Tris-HCl, pH 7.4; 137mM NaCl; 5 mM KCl
Tris-Buffered Saline + Tween 20 (TBS-T)	25mM Tris-HCl, pH 7.4; 137mM NaCl; 5 mM KCl; 0.1% (v/v) Tween-20
Tris-EDTA (TE)	10mM Tris-HCl, pH 8.0; 1mM EDTA

Table 2.5: Primary and Secondary antibodies used.

Antibody	**Source**	**Application and working dilution**
Horseradish peroxide (HRP)-conjugated secondary antibody	Cell Signaling	WB; 1:3000
Rabbit anti-Actin	Sigma	WB; 1:5000
Rabbit anti-LC3B	Abcam	WB; 1:1000
Mouse anti-Myc tag (4A6)	Milipore	WB; 1:1000; IF:1:200
Rabbit anti-p42/ERK	Cell Signaling	WB; 1:3000
Mouse anti-p53	BD Pharmingen	WB, 1:5000
Anti-mouse CD4-APC	BioLegend	FC; 1:200
Anti-mouse CD8-APC	BioLegend	FC; 1:200
Anti-mouse CD40-Alexa Fluor®488	BioLegend	FC; 1:200
Anti-mouse CD80-FITC	BioLegend	FC; 1:200
Anti-mouse CD86-FITC	BioLegend	FC; 1:200
Anti-mouse MHC class I-PerCP/Cy5.5	BioLegend	FC; 1:200
Anti-mouse MHC class II-PerCP	BioLegend	FC; 1:500
Anti-mouse CD11c-PE	BioLegend	FC; 1:200
Mouse anti-Cathepsin D	Milipore	IF; 1:200
Mouse anti-GM130	BD Transduction	IF; 1:500
Mouse anti-Rab5	BD Transduction	IF; 1:100
Mouse anti-CD63	BD Transduction	IF; 1:200
Rabbit anti-Calnexin	BD Transduction	IF; 1:200
Rabbit anti-CoxIV	Abcam	IF; 1:201
Mouse anti-Lamp-2	BD Transduction	IF; 1:200
Rabbit-anti TGN 46	Sigma	IF; 1:200
Mouse anti-EEA1	BD Transduction	IF; 1:201
Rabbit anti-GRP78 Bip	Abcam	IF; 1:200
Rabbit anti-PMP70	Abcam	IF; 1:200
Anti-rabbit Tom 20	Santa Cruz	IF; 1:400
Rabbit anti-p53 CM-5	Vector Labs	IHC; 1:250
Alexa Fluor 488® anti-mouse IgG	Molecular Probes	IF; 1:400
Alexa Fluor 488® anti-rabbit IgG	Molecular Probes	IF; 1:400
Alexa Fluor 647® anti-mouse IgG	Molecular Probes	IF; 1:400
Alexa Fluor 647® anti-rabbit IgG	Molecular Probes	IF; 1:400
Rabit anti-P-Histone H3	Upstate	IHC; 1:4000
Rabbit anti-Caspase 3 (Asp-175)	Cell Signaling	IHC; 1:50
Mouse anti-Brdu	BD Biosciences	IHC; 1:200
Rabbit anti-MPO	DAKO	IHC; 1:350
Rat anti-F4/80	Abcam	IHC; 1:150
Rabbit anti-p4EBP-1	Cell Signaling	IHC; 1:500
Rabbit anti-pAkt (Ser473)	Cell Signaling	IHC; 1:25
Rabbit anti-phospho-mTOR	Cell Signaling	IHC; 1:100

(Ser2448)		
Rabbit anti-OLFM4	Abcam	IHC; 1:200
Rabbit Secondary antibody (Vectastain Elite ABC Rabbit kit)	Vector Laboratories	IHC; 1:200
Rabbit secondary antibody solution	DAKO	IHC; Neat

WB=Western Blot; FC=Flow cytometry; IHC = Immunohistochemistry

Table 2.6: List of plasmids or fluorophores used for immunofluorescence studies.

Reagent	**Source**
Adenoviral GFP-LC3	Tumor Cell Death Lab (BICR)
Peroxisome GFP	Molecular Probes
Adenoviral mCherry LC3	Tumor Cell Death Lab (BICR)
Rab7 plasmid	J.Norman (BICR)
DFCP1 plasmid	N. Ktistakis (Babraham)

2.2 Methods

2.2.1 Cell Culture

2.2.1.1 Origin of cell lines

All transformed parental human cell lines and Phoenix-Ampho retroviral packaging cells were generated at the Beatson Institute for Cancer Research by past and current members of the Tumor Cell Death Laboratory. Primary mouse embryonic fibroblasts (MEFs), lymphocytes, and bone marrow progenitors were isolated and cultured as described below.

2.2.1.2 Isolation of MEFs

Pregnant females were culled at day 13.5 to 14.5 *post coitum* by cervical dislocation. The whole carcass was briefly dipped into a solution of distilled water containing virkon tablets to kill any bacteria/fungus present on the animal. The ventral side of animal was sprayed with 70% (v/v) ethanol and laperotomy performed to isolate the uterine horn containing the embryos. Incisions were made at the top of uterus where it joins the oviduct and at the cervix where the oviducts join. The membranes and blood vessels adjoining the oviduct were cut, while taking care not to puncture the oviduct membranes. The oviduct was removed and washed three times in PBS supplemented with gentamycin (33µg/ml). The oviduct membrane was then cut and the embryos dissected away from the placenta and surrounding membranes and placed in PBS/gentamycin. Embryos were decapitated and the internal organs teased out with fine forceps. Following three washes in PBS/gentamycin, embryos were minced as finely as possible and added to 10ml of 0.05% (v/v) trypsin supplemented with 100 µl DNase I and incubated for 45 minutes in a 37^0C water bath with occasional agitation (~ every 10-15 mins). After 30 minutes of incubation, 500ul 2.5% (v/v) trypsin was added and the incubation allowed to proceed for another 15 minutes. DMEM medium (40ml) was then added and the tissue suspension from 4-5 embryos was pooled. The mixture was filtered through a 70µm cell strainer prior to being centrifuged at 200 x *g* for 5 minutes. Cell pellets were re-suspended in 40ml of complete medium and the cells plated out into 15cm dish. The media was changed the next day to

remove dead cells. MEFs were cultured until confluent and then passaged for use in experiments or frozen down and stored in liquid nitrogen.

2.2.1.3 Isolation of T lymphocytes

Mice aged 6 weeks or older were culled using schedule 1(CO_2 asphyxiation).The spleens were removed, meshed with a syringe plunger and flushed through a 40µm cell strainer with cold culture media. The cellular suspension was centrifuged at 200 x *g* for 5 minutes. The supernatant was aspirated and 4ml of red blood cell (RBC) lysis buffer added to the pellet. Following incubation at room temperature for 5-10 minutes, 20ml of cold medium was added and the suspension centrifuged. The cell pellet was re-suspended in RPMI-1640 supplemented with 10% (v/v) heat inactivated FBS, 2mM L-glutamine, 50µM 2-mercaptoethanol, 100µg/ml penicillin, and 100µg/ml streptomycin. The cells were plated at a density of $1x10^6$ into 100mm dishes.

2.2.1.4 Isolation of bone marrow progenitors

Mice aged 6 weeks or older were culled using schedule 1 (CO_2 asphyxiation). The femur and tibia were removed and the ends cut off. Bone marrow progenitor cells were flushed out with cold RPMI-1640 supplemented with 10% (v/v) heat inactivated FBS, 2mM L-glutamine, 100µg/ml penicillin, and 100µg/ml streptomycin using a 25G needle attached to a syringe. The resulting cell suspension was passed through a 70µm cell strainer and either used immediately for analysis (See below) or cultured with different growth factors.

To induce differentiation into dendritic cells, the cell suspension was centrifuged at 200 x *g* for 5 minutes, the medium removed and the cell pellet treated with 4ml of RBC lysis buffer for 5 minutes. Following the addition of 20ml of cold medium was added, cells were pelleted by centrifugation. The cell pellet was re-suspended in complete RPMI-1640 supplemented with 100ng/ml Flt-3L and plated at a density of$1x10^6$ in 100mm dishes. Bone marrow progenitor cells were incubated at 37^oC in a humidified atmosphere containing 5% CO_2 for seven days.

To induce differentiation into macrophages, the bone marrow progenitor cells were cultured in RPMI-1640 supplemented with 10ng/ml M-CSF. Macrophages were plated at $3x10^7$ in 100mm dishes and cultured at 37^oC in a humidified atmosphere

containing 5% CO_2 for a total of 6 days. Macrophage cultures were rinsed and fresh media supplemented with M-CSF was added at day 3-4 in order to remove non-adherent cells. Adherent cells remaining at day 6 exhibited a homogeneous morphology.

2.2.1.5 Maintenance of cell lines

All cells were maintained at 37^{o}C in a humidified atmosphere containing 5% CO_2. Cell culture was performed in either biosafety Class 1 or 2 hoods, under sterile conditions.

With the exception of primary lymphocytes and cells originated from the bone marrow, all other cell lines were cultured in complete Dulbecco's Modified Eagle's medium (DMEM) supplemented with 10% (v/v) fetal calf serum (FCS), 2mM L-glutamine, 100µg/ml penicillin and 100µg/ml streptomycin.

Cell lines were passaged when they reached approximately 80% confluency. Media was removed by aspiration, the monolayer rinsed with PBS, and then 2-4 ml of 0.25% trypsin/TE added. Following incubation at 37°C for 5 minutes, dissociated cells were re-suspended in fresh media and transferred to a clean tissue culture flask at an appropriate ratio.

For long-term storage, cells were trypsinised and pelleted by centrifugation at 200 x *g* for three minutes. They were then re-suspended in 1ml of 10% (v/v) dimethylsulphoxide (DMSO) in FBS, transferred to CryoTube^{TM} vials, insulated by wrapping in cotton wool and slowly frozen at -80°C before storage in liquid nitrogen.

To bring up from storage, cells were thawed quickly at 37^{o}C after removal from liquid nitrogen, mixed with fresh media and centrifuged at 200 x *g* for three minutes. The supernatant was removed completely and the cell pellets re-suspended in fresh culture media and plated out into a small tissue culture flask.

2.2.2 Molecular cloning

2.2.2.1 Restriction digest

Restriction digests were performed using a 5 to 10-fold unit excess of the appropriate enzyme with 2-10µg plasmid DNA for 1 hour at the temperature, as specified by the manufacturer. For sequential digests DNA was purified using Qiagen PCR purification kit following the first restriction digest and then re-suspended in an appropriate reaction buffer for the second restriction digest. Linearized plasmid DNA was treated with 5U Calf Intestine Alkaline Phosphatase to remove 5' phosphate groups, purified using Qiagen PCR purification kit and then re-suspended in an appropriate volume of TE.

2.2.2.2 Ligation

Restriction fragments for ligation were purified by gel electrophoresis followed by excision using a Qiagen Gel Band Purification Kit. Ligations were carried out using Rapid DNA Ligation Kit. An approximate 2-fold molar excess of the insert fragment over the vector fragment was combined in a final volume of 10µl DNA Dilution Buffer. 10µl T4 DNA Ligation buffer was then added along with 5U T4 DNA ligase. This was incubated at room temperature for 16 hours.

2.2.2.3 Transformation of competent cells

Super-competent *E.Coli* DH5α cells were thawed on ice and gently mixed with 10-20ng of plasmid. The cells were incubated on ice for 30 minutes, heat shocked at 42ºC for 30 seconds and then transferred to ice for a further 15 minutes. 250µl of pre-warmed LB broth was added before incubation for 1 hour on an orbital shaker (225-250 rpm). The transformation mix was then plated on LB agar plates containing 50µg/ml ampicillin or kanamycin and the plates were incubated at 37ºC overnight to allow growth and colony formation of the transformed cells.

2.2.2.4 Screening of transformants

Colonies obtained from transformation were grown in overnight cultures of LB with 50µg ampicillin/kanamycin, and plasmid DNA isolated using QIAprep Spin Miniprep Kits. Analytical restriction digests were performed and resolved on

agarose gels to validate the correct orientation of the inserts. Inserts were always sequenced. Sequencing was performed by the Molecular Service unit at the Beatson Institute for Cancer Research.

2.2.2.5 Preparation of plasmid DNA

For large-scale plasmid DNA preparation, a single bacterial colony was picked from a freshly streaked plate and used to inoculate 4 ml LB medium containing 50µg/ml ampicillin or kanamycin. This was incubated at 37ºC with vigorous shaking for about 16 hours to form a mini culture and was subsequently used to inoculate 100 ml LB containing 50µg/ml ampicillin or kanamycin. Following an overnight incubation at 37ºC in an orbital shaker (300 rpm), cells were pelleted by centrifugation at 3000 x *g* for 20 minutes at 4ºC and plasmid DNA isolated using the Qiagen Plasmid Maxi Kit. Briefly, the bacterial pellet was re-suspended in 10 ml of Buffer P1 (50mM Tris pH 8.0, 10mM EDTA, 100µg/ml RNase A) and then gently but thoroughly mixed with 10ml Buffer P2 (200mM NaOH, 1% SDS) to initiate an alkaline lysis reaction. This reaction was allowed to proceed for 5 minutes at room temperature before the addition of 10 ml chilled buffer P3 (3M potassium acetate, pH 5.5) to allow neutralization and the formation of a precipitate of dodecyl sulphate. The SDS-denatured proteins and chromosomal DNA were co-precipitated with the detergent whilst the plasmid DNA remained in solution due to a lack of close protein associations. Precipitation was enhanced by 20 minute incubation on ice and the precipitate was then pelleted by centrifugation at 4000 x *g* for 30 minutes at 4ºC. The supernatant containing plasmid DNA was promptly removed and applied to a QIAGEN-tip 500 pre-equilibrated with 10 ml of Buffer QBT (750mM NaCl, 50mM MOPS pH 7.0, 15% Isopropanol, 0.15% TritonX-100). Gravity flow allowed the supernatant to pass through the anion exchange resin that bound the plasmid DNA. The resin was the washed twice with 30 ml of buffer QC (1M NaCl, 50 mM MOPS pH 7.0, 15% Isopropanol) and the purified plasmid DNA was subsequently eluted with 15 ml Buffer QF (1.25M NaCl, 50mM Tris pH 8.5, 15% isopropanol) and precipitated with 10.5 ml (0.7 volume) of room temperature isopropanol. The eluent was immediately centrifuged at 4000 x *g* centrifugation at 4ºC for 30 minutes. The plasmid DNA pellet was then washed with 70% (v/v) ethanol, dried at room temperature for 5-10 minutes and re-suspended in an appropriate volume of sterile TE buffer.

2.2.2.6 Agarose gel electrophoresis

Agarose was melted by heating in 1xTAE. Prior to solidification, ethidium bromide was added to a final concentration of 0.5µg/ml,. Agarose was allowed to solidify in gel trays. Samples for electrophoresis were diluted with 10x gel loading buffer (30% (v/v) glycerol, bromophenol blue) and loaded onto the gel alongside a suitable DNA ladder. Electrophoresis was carried out at 100V in 1xTAE gel running buffer. DNA was visualised using a UV transilluminator.

2.2.3 Genetic Manipulation

Ectopic over expression of proteins were achieved by calcium phosphate transfection, Xfect transfection, adenovirus infection, retrovirus infection or by inducing stable Saos-2 cell lines which were generated using the Tet-On® Gene Expression Systems with 1µg/ml Doxycycline for protein expression.

Ablation of DRAM-1 isoforms in human cells is achieved by siRNA transfection. DRAM-1$^{fl/fl}$ MEFs were infected with an empty retrovirus (pBabe puro) or retrovirus vector carrying a Cre-recombinase construct.

2.2.3.1 Calcium phosphate transfection

1x10^6 cells were seeded into 10cm dishes one day prior to transfection. 15µg of plasmid DNA in 440 µl distilled water was mixed with 500µl HBS (50mM HEPES, 250mM Nacl, 1.5mM pH 7.12), prior to vigorous mixing with 60 µl 2M $CaCl_2$. Reactants were vortexed and incubated at 37^{o}C for 25 minutes to allow for the formation of DNA-calcium phosphate precipitate, and then added drop-wise to cells. The precipitate was removed after 16 hours by three washes in DMEM before 10%DMEM was added.

2.2.3.2 Xfect transfection (Rab-7 and DFCP-1 constructs)

Saos-2 cells were plated in 35 mm wells 24 hours before transfection at a density of 1.5 x 10^5 cells per well. 5µg of plasmid DNA was added to Xfect reaction buffer to a final volume of 100µl. In another tube 1.5µl Xfect polymer was added to 98.5µl

Xfect. Both tubes were vortexed briefly. The polymer solution was added to the DNA solution and vortexed well at medium speed for 10 sec. Both samples were incubated for 10 min at room temperature to allow nanoparticle complexes to form. The 200µl of nanoparticle complexes were added drop-wise to the cells, and incubated for 4 hours at 37°C. The complexes were removed and replaced with fresh medium. After 48 hours, cells were harvested for immunofluorescence staining.

2.2.3.3 Adenovirus amplification, purification, titration and infection

The recombinant adenoviruses used in this thesis are replication defective human adenovirus serotype 5, and were amplified in HEK-293 cells. 24 hours prior to infection, $4x10^6$ HEK-293 cells were seeded in 10cm dishes. Cells were infected with the appropriate titre of adenovirus. When the cytopathic effect took place, cells were detached, centrifuged at 200 x *g* for five minutes and the pellet re-suspended in DMEM without antibiotics. Adenovirus was recovered by performing four freeze-thaw cycles in dry ice/ethanol and a 37^oC water bath.

Adenovirus was purified using the Adeno-X™ Maxi purification kit according to manufacturer's instruction and a titration performed using the AdEasy™ Viral Titer Kit.

To infect target cells, $1x10^6$ cells were plated in either 100mm dishes or 6 well plates. Adenovirus was added accordingly to cultures and media is replaced after 16 hours.

2.2.3.4 Retrovirus infection

Retroviral infections of mouse embryonic fibroblasts (MEFs) and Saos-2 cells carrying an Eco-receptor were performed using retrovirus produced by Phoenix-Eco retroviral packaging cells. Phoenix-Eco cells were plated at $2x10^6$ cells in a 10 cm dish. The next day cells were transfected with 15µg retroviral vector DNA for 16hours as described in section 2.3.1 Three harvests of retrovirus supernatant were collected in DMEM containing 20% (v/v) FBS at 12 hour intervals.

24 hours prior to infection, MEFs and Saos-2 cells were seeded at 0.8 x10^6 and 1 x10^6 cells per 10cm dish respectively. Retroviral supernatants were passed through a 0.45µm filter to remove any contaminating cells, and then added to the target cells together with polybrene at a final concentration of 5µg/ml. Three rounds of infection were undertaken at 12 hour intervals. Cells were allowed to recover for 24 hours in DMEM supplemented with 10% (v/v) FBS prior to selection with either 2.5µg/ml puromycin, 100µg/ml hygromycin or 10µg/ml blasticidin.

2.2.4 RNA/cDNA techniques

2.2.4.1 RNA preparation

RNA was extracted and purified using the RNeasy® Mini Kit according to manufacturer's instructions. Briefly, media was removed from cells and washed once with PBS. Adherent cells were harvested by scraping in 200µl of RLT buffer per well (6-well plate) or 500µl per 10cm plate and transferred to a sterile eppendorf tub, whereas non-adherent cells were re-suspended in 200µl of RLT buffer after the PBS wash. Both cell and tissue lysates were homogenized by repeated passing through a 20G (0.9 mm) needle attached to a sterile plastic syringe. 1 volume of 70% (v/v) ethanol was added to the homogenized lysate, and mixed well by pipetting. All the contents in the tube were then transferred to the RNeasy spin column placed in a 2 ml collection tube and centrifuged at 8000 x *g* for 15 seconds. After discarding the flow-through, the spin column was sequentially washed with 700µl Buffer RW1 followed by 2 washes of 500µl of RPE, discarding the flow-through each time. The RNeasy spin column was placed in a new 2 ml collection tube and centrifuged at full speed for 1 min to remove residual ethanol. RNA was eluted by adding 30–50µl RNase-free water directly to the spin column membrane, followed by centrifugation for 1 min at 8000 x ginto a new collection tube. The concentration of RNA samples was determined by measuring the absorbance at 260 nm using a Biophotometer plus spectrophotometer (Eppendorf). The ratio of the absorbance readings at 260 nm and 280 nm (A_{260}/A_{280}) gave an indication of the purity of each RNA sample.

2.2.4.2 Reverse transcription (cDNA synthesis)

cDNA was synthesised using the DyNAmo SYBR Green 2-step qRT-PCR kit

according to manufacturer's instructions on a Peltier Thermal Cycler (MJ Research). Briefly, 1-2µg of RNA was mixed with 20µl of 20x RT buffer (containing dNTP mix and 10 mM $MgCl_2$), 2µl of Random Hexamers (300ng/µl) and 4µl M-MuLV RNase H reverse transcriptase to a final volume of 40 µl. Samples were incubated at 25°C for 10 mins to allow primer annealing and extension, then 37°C for 30 mins to allow cDNA synthesis. The reaction was terminated by heating at 85°C for 5 mins and then cooled to 4°C.

2.2.4.3 Quantitative Polymerase Chain Reaction (qPCR)

Quantitative PCRs were carried out using the DyNAmo SYBR Green 2-step qRT-PCR kit (Finzymes) according to manufacturer's instructions in a Peltier Thermal Cycler (MJ research, Helena Bioscience). Briefly, 1µl of cDNA (See Section 2.4.2) was added to 10µl 2x qPCR master mix (contains modified hot start *Tbr* DNA polymerase, SYBR Green I, optimized PCR Buffer, 5mM $MgCl_2$ and dNTP), 7µl H2O and 2µl custom designed primers or validated QuantiTect Primer sets (Qiagen) for the gene of interest. Reactions were pipetted into 96 well optical plate (BioRad) and sealed using optically clear flat cap strips (BioRad). Reactions were carried out in triplicate for each sample. Cycling parameters used were 95°C -15 mins (initial denaturation); [94°C - 10 s (denaturation); 55°C - 30 s (annealing); 72°C - 30 s (extension); plate read (data acquisition)] 40 cycles; 72°C - 10 mins (final extension); melting curve 70-90°C; Read 0.3°C; hold 1 s; 72°C - 10 mins (reannealing); then 15°C hold. Data collection was carried out using a Chromo4 real-time PCR detector (BioRad) and MJ Opticon Monitor software. Gene expression was normalized relative to 18S rRNA levels.

Primers used for qPCR are listed below:

18s Fwd	: 5'-GTAACCCGTTGAACCCCATT-3'
18s Rev	: 5'-CCATCCAATCGGTAGTAGCG-3'
Hs DRAM-1 Fwd	: 5'-GTACAGAAGCAAAATCAAACCTGC -3'
Hs DRAM-1 Rev	: 5'-TCAAATATCACCATTGATTTCTGTGCA -3'
Hs MAP1LC3-B	: Quantitect® Primers (Qiagen; QT01673007)
Mm DRAM-1 Fwd	: 5'-CAGCCTTCATCATCTCCTACG-3'
Mm DRAM-1 Rev	: 5'-ATGCAGAGAAGTTTATCATG-3'
Mm DRAM-2	: Quantitect® Primers (Qiagen; QT00158515)

Mm DRAM-3 /TMEM150b : Quantitect® Primers (Qiagen; QT01163470)
Mm DRAM-4 /TMEM150c : Quantitect® Primers (Qiagen; QT00131901)
Mm DRAM-5 /TMEM150a : Quantitect® Primers (Qiagen; QT00135632)

2.2.4.4 Polymerase Chain Reaction

Amplifications were undertaken using ProofStart™ DNA polymerase (Qiagen) on a PTC-200 PCR machine.Cycling parameters used to amplify human and mouse DRAM-1 splice variants were 95°C 4 min (94°C - 30 s; 52°C - 30 s; 72°C -1 min) for 35 cycles (DRAM-1) or 20 cycles (18S rRNA); 72°C 10 min; hold 4°C. Gene expression was normalized relative to 18S rRNA levels.

Primers were custom designed and synthesized by Dharmacon. A list of primers are listed below:

18S Fwd : 5'-GTAACCCGTTGAACCCCATT-3'
18S Rev : 5'-CCATCCAATCGGTAGTAGCG-3'
Fwd Hs DRAM-1 exon 1 : 5'-ATGCTGTGCTTCCTGAGGGGAATG-3'
Rev Hs DRAM-1 exon 7 : 5'-CACAGAAATCAATGGTGATATTTGA-3'
Fwd Mm DRAM-1 exon 1 : 5'-TTCCTCCTGGTGACTTGGTC-3'
Rev Mm DRAM-1 exon 7 : 5' AGT CGT CAT TGA TTT CTG TGG A -3'

PCR products were resolved on a 3% (w/v) agarose gel and bands visualised using a UV transilluminator as described above.

2.2.5 Protein analysis

2.2.5.1 Protein extraction

Media was removed from cells and washed once with PBS. Adherent cells were harvested by scraping in 200µl of RIPA buffer per well or 500µl per 100 mm plate and transferred to a sterile eppendorf tube, whereas non-adherent cells were re-suspended in 200µl of RIPA buffer after one PBS wash. Insoluble material was pelleted by centrifugation at 14000 x g at 4°C for 15mins and supernatants removed to a clean eppendorf tube. Protein lysates were either processed immediately or stored at -20°C.

2.2.5.2 BCA assay

Bicinchoninic acid (BCA) solution was mixed with $CuSO_4$ solution in a 50:1 ratio. 200µl of this mixture was added to 10µl standards (containing 80, 100, 200, 400, 1000 or 2000µg/ml BSA diluted in distilled water); or 2µl of protein samples diluted in 48µl of distilled water, in a 96 well plate. The samples were incubated at 37^{o}C for 30-60 minutes. Optical density was read at 562nm and the concentration of protein calculated from the BSA standard curve.

2.2.5.3 Separation of proteins by polyacrylamide gel electrophoresis (SDS-PAGE)

Proteins were resolved according to molecular weight by electrophoresis on denaturing polyacrylamide gels in Amersham Biosciences SE400 standard format vertical unit tanks. Samples were mixed with 2x sample buffer, boiled for 10 minutes, briefly centrifuged to collect the sample, and then loaded onto a polyacrylamide gel. Electrophoresis was carried out in 1x SDS Running buffer (See Table 2.4 for composition)at 55V overnight or 200V for three hours until the dye front had reached the bottom of the gel. SDS-PAGE gels consisted of a separating gel overlaid by a stacking gel. Depending on the molecular weight of the protein of interest, the separating gel was between 6% and 15% acrylamide (from 30% stock solution (37.5:1 acrylamide:bis acrylamide) and otherwise constituted 375mM Tris-HCl, pH8.8, 0.1% SDS, polymerised with 0.05% ammonium persulphate, 0.1% TEMED. Stacking gel was 4% acrylamide and otherwise constituted 125mM Tris-HCl, pH 6.8, 0.1% SDS, polymerized with 0.05% ammonium persulphate, 0.1% TEMED.

2.2.5.4 Western Blotting

Proteins resolved by SDS-PAGE were transferred to nitrocellulose membrane in 1x Transfer Buffer (See Table 2.4 for composition) at 0.5A for 4 hours using Hoefer TE 42 Protein Transfer apparatus. Following transfer, the membrane was stained with Ponceau S to check for loading and the fidelity of transfer.

2.2.5.5 Probing

Following transfer, the membrane was blocked in TBS-T containing 5% (w/v) dried skimmed milk for 1 hour at room temperature. Membranes were incubated with primary antibodies (typically a 1:1000 dilution in 5% (w/v) BSA in TBS-T) for 2 hour at room temperature or overnight at 4°C. Excess primary antibody was removed from the membrane by washing 3 times in TBS-T for 10 minutes before incubating for 1 hour at room temperature with the appropriate horseradish peroxidase-conjugated secondary antibody at a dilution of 1:3000. To ensure the removal of excess secondary antibody, the membrane was washed 3 times for 30 minutes in TBS-T. Proteins bound to the membrane were visualized by chemiluminescence using ECL Western Blotting Substrate and autoradiography.

2.2.6 Cell death assays

2.2.6.1 Clonogenic assay

Saos-2 cells were plated on 10cm dishes and transfected the following day with 10µg of either: DRAM-1 SV1, SV4 or SV5, p53 (positive control) or an empty plasmid pcDNA3-Myc/His (Invitrogen) (negative control), as described in section 4.2.1. Two days after transfection, cells were detached and counted. Approximately 0.6 x10^6 cells were cultured in 15cm dishes with 600µg/ml G418 to select for transformed cells. Cells were cultured for two weeks, and fresh medium containing the selection antibiotic replenished every three days. On the day of harvest, the medium was removed, and the cells were washed with PBS prior to staining with 8 ml of Giemsa for 10 minutes at room temperature. Plates were then washed with 10% (v/v) methanol (diluted in distilled water) and left to dry overnight, prior to analysis.

2.2.6.2 Sub-G1 content

After treatment for the indicated times the total populations of cells (both floating and adherent cells) were processed for flow cytometric analysis (FACScan, Becton Dickinson). Adherent cells grown in 6-well plates were harvested by collection of media in 15ml falcon tube. The cells were then washed in 0.5 ml PBS that was also collected into the 15 ml falcon tube and 0.5ml of TE plus 0.25% (v/v)

trypsin was added to remove adherent cells, and subsequently transferred to the falcon tube. The samples were then centrifuged for 5 minutes at 1000 x *g* and the supernatants removed. Cells were re-suspended in 500µl PBS and then 5 ml ice-cold methanol added slowly while vortexing to avoid clumping. Cells were incubated at 4°C for a minimum of 3 hours. Directly before FACS analysis the cells were collected by centrifugation and re-suspended in 400µl PBS, 20µl of 1mg/ml Propidium Iodide (PI) and 0.2µl RNaseA (100 mg/ml) and incubated for 30 minutes at room temperature then sorted for and analysed for DNA content using a FACSCalibur flow cytometer (Becton Dickinson) and CellQuest software. The percentage of cells with sub-G1 DNA content was taken as a measure of the number of apoptotic cells in the total cell population.

2.2.6.3 PI exclusion assay

To assay for apoptosis, floating and adherent cells harvested from 6-well plates were collected as described in 2.6.2 and centrifuged at 200 x *g* after the treatments and times indicated. The pellet was immediately stained with 5µg/ml PI in 200µl of media for 5 minutes, in the dark at room temperature. The cells were then analysed using a FACSCalibur flow cytometer (Becton Dickinson) and CellQuest software. .

2.2.7 Autophagy assays

2.2.7.1 Autophagosome formation (LC3 punctation)

Cells infected with DRAM-1 isoforms or ‘empty virus’ as control, and GFP-LC3 adenovirus (Bampton, Goemans et al. 2005). After 48 hours cells were fixed in 4% (v/v) PFA and imaged on Zeiss Axioplan 2 / ISIS. Cell images were analyzed visually and cells with 8 or more GFP-LC3 puncta were scored as positive for cells with accumulated autophagosomes. At least 200 cells were analyzed for each condition.

2.2.7.2 LC3 immunoblotting

LC3-I to LC3-II conversion was measured by western blotting following infection with either adenoviruses expressing DRAM-1 isoforms or control 'empty' adenovirus that contains no transgene. LC3 levels were analysed as described in section 4.5 and probed with antibodies against LC3B.

2.2.7.3 Long-lived protein degradation

Saos-2 cells and MEFs were plated at a density of 0.2 x 10^6 and 0.1 x 10^6 per 60mm dishes (6-well plate), respectively. The next day, the medium was removed and cells were labeled 5µCi L-[35^S] cysteine/methionine in met/cys free medium (Invitrogen) supplemented with 10% (v/v) FCS, 2mM glutamine, 100µg/ml penicillin and 100µg/ml streptomycin for 8 hours. Cells were then washed 3 times with PBS and incubated overnight in met/cys free medium supplemented with 2mM cold cys/met, 10%FCS, 2mM glutamine, 100µg/ml penicillin and 100µg/ml streptomycin at 37^{o}C. Following the appropriate treatment, 200ul aliquots of media were removed, trichloroacetic acid (TCA) added to give a final concentration of 10% and incubated at 4^{o}C overnight. Meanwhile, the cells were fixed by adding 1ml 10% (v/v) TCA for 15minutes. The cells were then washed with 10% (v/v) TCA and then dissolved with 200µl 0.2M NaOH per well while shaking at 4^{o}C overnight. The next day, the medium was centrifuged at 12000 x *g* for 10 mins. The pellet was discarded and the supernatant added to 3ml scintillation fluid to determine the amount of acid-soluble radioactivity. Similarly, 3ml of scintillation fluid was also added to the cells to determine the amount of acid-precipitable radioactivity. The rate of protein degradation was determined as follows:

$$\% \text{ protein degradation} = \frac{\text{acid-soluble radioactivity in culture medium}}{\text{(acid-soluble + acid-precipitable radioactivities)}}$$

2.2.7.3 RFP-GFP LC3 assays

Tet-On DRAM-1 Saos-2 cells were retro-infected with pBabe puro mRFP-GFP LC3 construct as described in section 2.3.4. The cells were then treated with 1μg/ml Doxycycline to induce expression of full length DRAM-1 protein, and/or infected with adenoviruses expressing DRAM-1 isoforms 4 and 5, or an empty vector. Cells were harvested for immunoflourescence staining as described in section 2.7.5.1.

2.2.7.4 Reactive Oxygen Species (ROS) production assay

Saos-2 cells and MEFs were plated at a density of 0.2 x 10^6 and 0.1 x 10^6 per 60mm dishes (6-well plate), respectively. The next day, cells were treated as indicated. At the end point of the experiment, the medium was removed and the cells were washed 3 times with PBS. Cells were stained with 5μM DCFDA in phenol-red free OPTIMEM supplemented with 10% (v/v) FCS for 20minutes, at 37^{o}C in the dark. Cells were washed 3 times with PBS, detached with trypsin as described in section 2.1.5, and re-suspended in phenol-red free OPTIMEM supplemented with 10% (v/v) FCS. Samples were kept on ice, while being analysed by flow cytometry.

2.2.7.5 Immunofluorescence

Cells seeded on 16mm and 19mm coverslips were washed with PBS, fixed in 4% (v/v) Paraformaldehyde/PBS for 20 minutes and washed 3 times in PBS. Cells were then permeabilised with 0.3% (v/v) Triton-X-100 in PBS for 10 minutes. Following 3 more washes in PBS, non-specific binding sites were blocked with a solution containing 0.3% (w/v) Avid BSA, 10% (v/v) FCS, 5% (w/v) Milk, 0.3% (v/v) Triton-X-100 in PBS for 30 minutes. Primary antibodies diluted in blocking solution (without milk) were applied for 1 hour in 37^{o}C. Coverslips were washed 3 times with 0.1% (v/v) Triton in PBS, stained with the secondary antibody diluted in blocking solution (without milk) for 30 minutes in 37^{o}C. Following 3 washes with PBS, coverslips were incubated with 4% (v/v) paraformaldehyde/PBS at room temperature for 15 minutes, washed with PBS plus a final wash in water, then

mounted in 8µl of Fluorescent Mounting Medium. The antibodies used for immunofluorescence are listed in table 2.7.

Table 2.7: Markers used for validation of DRAM-1 localisation in cellular organelles.

Organelle	**Marker 1**	**Marker 2**
Lysosome	Lamp-2	Cathepsin D
Golgi apparatus	TGN	GM130
Early Endosomes	EEA1	Rab5
Late Endosomes	Rab7	CD63
Autophagosome	mCherry LC3	DFCP1
Endoplasmic reticulum	Bip	Calnexin
Peroxisome	PMP70	Peroxisome GFP
Mitocondria	Tom 20	CoxiV

Cells were imaged on Zeiss Axioplan 2/ISIS for autophagosome formation and Leica Confocal 2 for DRAM-1 isoform co-localisation studies. Images were processed using Leica and Image J software.

2.2.8 T cell activation assay

2.2.8.1 Upregulation of T cell activation signals on APCs upon stimulation

Differentiated bone marrow dendritic cells from section 2.1.4 were plated in 'U bottom' 96 well plates (Nunc) at a density of $1x10^6$ cells/ml and incubated with 1µg/ml LPS for 16 hours. Cells were centrifuged at 200 x *g* and the media removed. Pellets were re-suspended in the appropriate antibodies listed in Table 2.5 in complete RPMI-1640, and incubated for 20 minutes on ice, in the dark. Cells were washed twice by repeated centrifugation at 200 x *g* and re-suspended in 200µl of complete RPMI-1640. Samples were kept on ice and surface marker expression levels were analysed by flow cytometry immediately.

2.2.8.2 Pulsing of APCs with antigen/ antigenic peptide

The antigen presenting cells (APCs) used to stimulate T cells were dendritic cells and macrophages (isolated and cultured as described in section 2.1.4.).Dendritic cells and macrophages were plated in 'U bottom' 96 well plates (Nunc) at a density of $1x10^6$ cells/ml and incubated with 10μM of Nutlin for 16 hours. The cells were centrifuged at 200 x *g*, and the medium removed. The cells were then pulsed with the T cell specific peptide, ovalbumin (OVA) for four hours at 37°C. In addition, dendritic cells were also incubated with MHC class I processed OVA peptides 257-264, or MHC class II processed OVA peptides 323 -329 under identical conditions. At the end-point of the incubation period, the cells were centrifuged and the medium removed as before, prior to the addition of CFSE-labeled CD8+ or CD4+ T cells from transgenic OT-1 or OT-2 mice respectively. These transgenic mice were obtained from Dr. Simon Milling (Institute of Infection, Immunity and Inflammation, University of Glasgow).

2.2.8.3 T cell proliferation assay

T cells were isolated as described in section 2.1.3 and used immediately. To track T cell proliferation, T cells were stained with 50μM CFSE for 5 minutes at 37°C. The cells were washed twice with PBS, and re-suspended at $1x10^6$ cells/ml in complete RPMI-1640. These cells were then mixed with dendritic cells at a ratio of 10:1 (T cells: dendritic cells), or macrophages at a ratio of 2:1 (T cells:macrophages). The T cell/dendritic cell and T cell/macrophage co-culture was incubated at 37°C for three and four days respectively to allow for T cell activation and proliferation. At the end point of the experiment, the medium was removed as before, and the cell pellet stained with anti-CD8 (APC) or anti-CD4 (APC) antibodies diluted in complete RPMI-1640 to identify T cells subsets. Cells were immediately analysed by flow cytometry. T cell activation is associated with proliferation, which was monitored by CFSE intensity.

2.3 Characterisation of *DRAM-1* conditional knockout mice

All Experiments were performed under the UK Home Office guidelines (project license 60/4183 and personal license 12265). All mice were of the mixed background and maintained under non-barrier conditions and given a standard diet (Harlan) and water *ad libitum*. At least 3 mice of each genotype were used for each experimental cohort. The alleles used in this thesis were Cre, *AhCre*, CAGG-Cre ER, *DRAM-1*$^{+}$, *DRAM-1*$^{-}$, *DRAM* ^{fl} and *Mdm2* $^{f/fl}$.

2.3.1 Generation of *DRAM-1* $^{fl/+}$ mice

DRAM-1 $^{fl/+}$ mice (mixed background - 50% 129S6 and 50% C57BL/6J) were generated by Model Animal Research Centre, Nanjing University. Briefly, exon 2 was replaced with the DRAM-1 Flox targeting vector (Fig. 2.1). Upon recombination mediated by *Cre recombinase*, exon 2 of the *DRAM-1* is excised, leading to frame shift in the exons behind exon 2 and subsequently the production of a truncated, non-functional DRAM-1 protein, as illustrated in Fig. 2.2. The DRAM-1 Flox targeting vector was transfected into 129S6/SvEvTac-derived W4 embryonic stem (ES) cells. Clones expressing this targeting vector were microinjected into C57BL/6 pseudo-pregnant females to generate chimeras. The chimeras born were crossed with C57BL/6 mice to obtain heterozygotes.

2.3.2 Generation of DRAM-1$^{-/-}$ null mice

DRAM-1 $^{fl/+}$ *heterozygotes* were back-crossed with each other to obtain *DRAM-1* $^{fl/fl}$ homozygotes. *DRAM-1* $^{fl/fl}$ homozygotes were then bred with a Cre Deleter, which harbours the *Cre*+ allele(s) from a C57BL/6 background (developed by Artemis Pharmaceuticals/Taconic). Offspring which are heterozygous for *DRAM-1*$^{-/+}$ *w*ere back-crossed to each other to obtain *DRAM-1*-null mice, as well as the wild-type and heterozygous littermate controls.

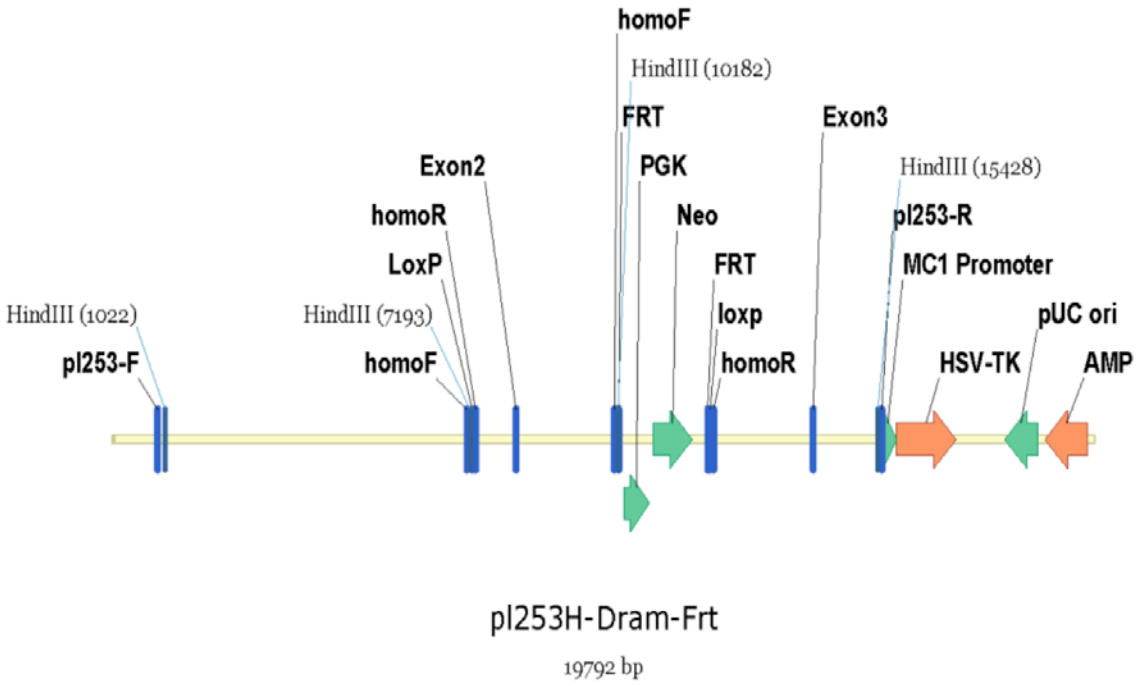

Illustration obtained from Model Animal Research Centre Nanjing University.

Figure 2.1 : DRAM-1 Flox targeting vector
The genomic DNA encoding DRAM-1 gene was digested by HindIII and a 12.3kb fragment encoding exons 2 and 3 of DRAM-1 was cut, purified and ligated with pl253, and subsequently linearized by HindIII for the insertion of a 'LoxP-Neo-LoxP' cassette.

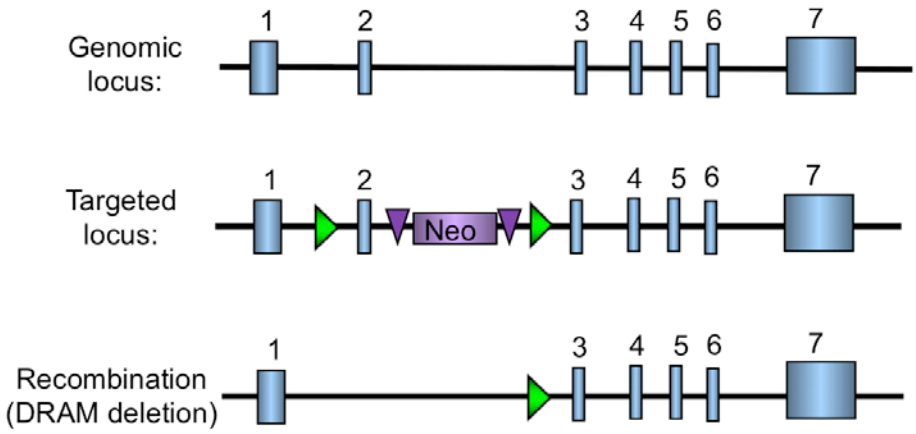

Illustration obtained from Model Animal Research Centre Nanjing University.

Figure 2.2: Illustration of the DRAM-1 'wild-type' , floxed and recombined alleles
Upon recombination, exon 2 is excised, and frame shift occurs behind exon 2, leading to the production of a truncated, non-functional protien.

2.3.3 Genotyping of mice

The initial results to confirm the presence of *DRAM-1*$^{+}$, *DRAM-1*^{fl} and *DRAM-1*$^{-}$ alleles were validated by in-house genomic Polymerase Chain Reaction (PCR) (2.3.6) from DNA extracted from tails (2.3.5). Subsequent genotyping were conducted by Transnetyx, Inc (Cordova, TN).

2.3.4 DNA extraction from tails

DNA was extracted from mice tails using the Puregene DNA Extraction kit. Tails were lysed in eppendorf tubes with 500µl of cell lysis solution (Flowgen) and 10µl of proteinase K (from 20mg/ml stock), and incubated at 37ºC in shaking incubator (70rpm) for 16 hours. Tails were left to cool at room temperature prior to the addition of 200µl of protein precipitation solution (Flowgen) to each tube. Tubes were vortexed and centrifuged at maximum speed for 5 minutes in a microfuge. The supernatant was removed into a clean tube containing 500µl of isopropanol, vortexed and centrifuged at maximum speed for 5 minutes. The supernatant was carefully removed and the DNA pellet was left to dry overnight. DNA was re-suspended in 250µl of nuclease free water.

2.3.5 PCR conditions for *DRAM-1*$^{+}$ *DRAM-1*$^{+}$, *DRAM*^{fl} and *DRAM* $^{-}$ alleles

All PCR reactions were carried out in 50µl volumes with 3.5µl of the genomic DNA preparation using the GoTaq® Flexi DNA Polymerase Kit (Promega). The amount of reagents used per sample is as follows:

Reagent	Volume
Nuclease free water	30.5µl
5x Colourless GoTaq Flexi Buffer	10µl
$MgCl_2$ (25µM)	5µl
dNTP (10mM)	2µl
GoTaq® Flexi DNA Polymerase (5U/µl)	0.5µl
F Primer (5') (100µM)	1µl
R Primer -1 (3') (100µM)	0.5µl
R Primer -2 (3') (100µM)	0.5µl

Add 1µl genomic DNA.

Primers:

F Primer (5') : 5' GTT GAG CCC AGC TAT GAA GG 3'

R Primer -1 (3') : 5' TGCATCCAGTCAACTGCTTC 3'

R Primer -2 (3') : 5' GAA GTG CTT CCT GGA CAA GC 3'

PCR Program:

95°C- 3min (95°C - 30s; 55°C - 30s; 72°C -1min) 36 cycles, then 72°C - 5min, then 4°C - hold.

PCR products were resolved on a 3% agarose gel. The size of the bands corresponding to *DRAM-1*$^{+}$*, DRAM-1*$^{+}$, *DRAM* ^{fl} and *DRAM* $^{-}$ alleles are depicted in Fig. 2.3.

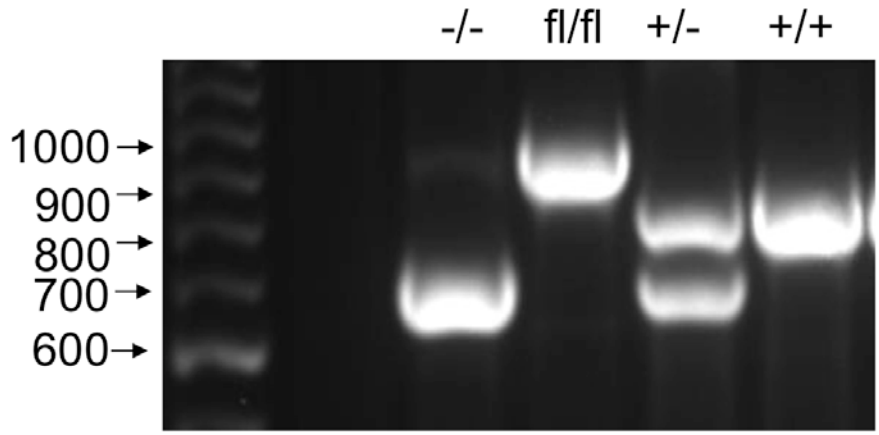

Figure 2.3 : PCR products of *DRAM-1^{fl}*, *DRAM-1^{+}* , and *DRAM-1^{-}* alleles
Genomic DNA were subjected to PCR and products were analysed on a 3% agarose gel. The marker used is a 100bp ladder. *DRAM-1^{fl}*, *DRAM-1^{+}* , and *DRAM-1^{-} runs at* 950, 800 and 700 kb respectively.

2.3.6 Long term aging cohort

To assess the role of DRAM-1 in regulating development and life-span, wild-type, heterozygotes and *DRAM-1*-null mice were aged for up to 650days. Mice were checked routinely to observe for phenotypic differences and disease development. Whole body autopsy was performed on mice that reached the end point of the experiment. The dissection and analysis of the animals in this cohort were performed hand in hand with Dr. Ayala King (Pathologist, The Beatson Institute for Cancer Research).

2.3.7 Blood profiling/ Haematology smear test

Blood profiling was performed by the Veterinary Diagnostic Services, Glasgow University. Mice were culled with rising concentrations of carbon dioxide (CO_2). Peripheral blood was isolated from the vena cavae into plastic whole blood tube spray coated with K_2EDTA. Blood samples incubated on ice were sent immediately to the clinical pathology laboratory for processing. The parameters assessed are summarised in Table 2.8.

Table 2.8: Parameters that were assessed in the haematology smear test of wild type and DRAM-1 null mice at the age of 3 months.

Parameters	**Indication**
Red Blood Cell (RBC)	Number of red blood cells per volume of blood.
Hematocrit (Hct)	Percentage of red blood cells in a given volume of whole blood.
Haemoglobin (Hb)	Amount of oxygen-carrying protein in the blood.
Mean corpuscular volume (MCV)	Average size of RBCs.
Mean corpuscular hemoglobin (MCH)	Average amount of oxygen-carrying hemoglobin inside a red blood cell.
Mean corpuscular hemoglobin concentration (MCHC)	Average concentration of hemoglobin inside a red cell.
Red cell distribution width (RDW)	Calculation of the variation in the size of your RBCs.
White Blood Cell (WBC)	Number of white blood cells per volume of blood.
WBC differential count	Number of different types of white blood cells (Neutrophils lymphocytes, monocytes, eosinophils, basophils) per volume of blood.
Platelet count	Number of platelets in a given volume of blood
Mean platelet volume (MPV)	Average size of circulating platelets (Platelet size corresponds to platelet production in the bone marrow as newly-formed platelets are larger).
Plateletcrit (PCT)	Total circulating platelet mass.
Platelet component composition distribution width (PDW)	Variability in platelet density (The value decreases with platelet activation).

2.3.8 Radiation-induced lymphomagenesis

To investigate whether *DRAM-1* deletion could accelerate the development of radiation-induced tumourigenesis wild-type, heterozygous and *DRAM-1* null mice were treated with 4 Gy and aged for up to 650 days. Mice were checked routinely to observe for phenotypic differences and disease development. Whole body autopsy was performed on mice, which reached the end point of the experiment.

2.3.9 p53-dependent cell death in the small intestine

2.3.9.1 Irradiation

To investigate if *DRAM-1* deletion affects the DNA damage response to ionizing radiation, wild-type and *DRAM-1* knock-out mice were irradiated with 14 Gy irradiation using a Cs^{137} source delivered at a dose rate of 0.423 Gy/min. Mice were harvested at 6, 24, 48 and 72 hour time points following irradiation. At least 5 mice were used for each time point.

2.3.9.2 Inducible activation of p53 in the gastrointestinal tract and liver

For Cre induction, *AhCre*$^{+}$ *DRAM-1*$^{+/+}$ *Mdm2*$^{fl/fl}$ and *AhCre*$^{+}$ *DRAM-1*$^{fl/fl}$ *Mdm2*$^{fl/fl}$ were given 3 intraperitoneal (i.p.) injections of 80mg/kg β-naphthoflavone in a single day, yielding almost 100% constitutive recombination in the crypts of the small intestine, including the stem cells (Muncan et al., 2006b). To induce recombination in the liver, mice were given one i.p. injection of 80mg/kg β-naphthoflavone in one single day and monitored for between two and six days.

2.3.9.3 Tamoxifen preparation for intraperitoneal injection

To facilitate its formulation in sunflower oil, 5mg of 4-hydroxytamoxifen (4-OHT) (>98% active Z-isomer) was first dissolved in 500µL of absolute ethanol. This was then further diluted further with 4500µL of sunflower oil.

2.3.10 Acute colitis and inflammation-driven tumourigenesis

Mice were provided *ad libitum* with 2% (w/v) DSS (MP Biomedicals) for 5 days, after which drinking water was given. The subjects were monitored daily for changes in weight and clinical symptoms of disease were scored as previously described (Bordon, Hansell et al. 2009). The colons of the subjects were harvested at day 2, 5 and 7 post treatment.

To induce colitis-associated cancer, mice were subjected to a single i.p. injection of Azoxymethane (AOM) (12.5mg/kg body weight). Three days later, mice were subjected to three cycles of 2% Dextran Sodium Sulfate (DSS) for 5 days, and normal drinking water for 16 days. Animals were sacrificed at 70 days post AOM treatment and the colon harvested. The schematic diagrams that illustrate the mode of treatment used are shown in Fig. 2.4.

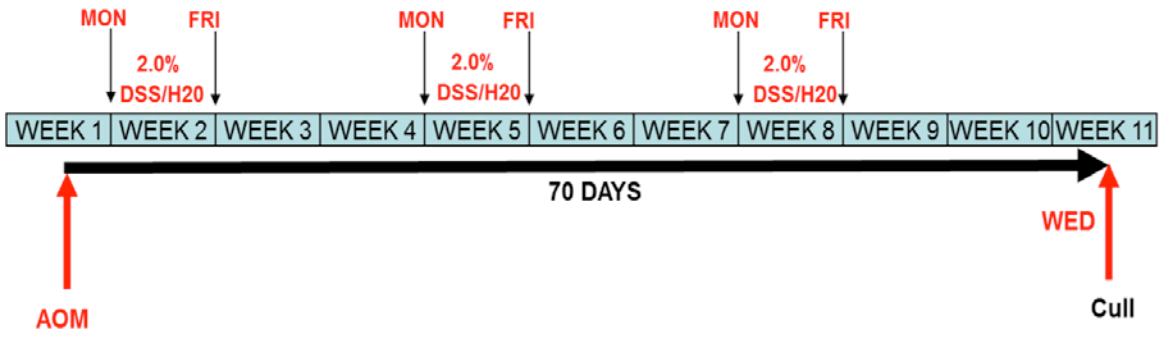

Diagram adapted from Thomas Jamieson (R18, The Beatson Institute for Cancer Research)

Figure 2.4: 2% DSS induced acute colitis
Mice were intraperitoneally injected with AOM and treated 3 cycles of 2% DSS drinking water for five days, followed by normal drinking water, Mice were sacrificed at Day 70 to characterise the onset of inflammation driven dysplasia.

2.3.11 Tissue isolation

All organs and tumours isolated (See sections 2.3.6 and 2.3.8) were fixed in 10% (v/v) formalin for 16 hours. Small intestine and colon were flushed with water and rolled into ‘swiss rolls’ prior to further sectioning and fixation.

For experiment in chapter 2.3.9.1, the proximal length of the small intestine was cut into 10 '1cm' sections, stacked and secured with surgical tape. This 'gut parcel' was then fixed overnight in 10% (v/v) formalin.
For experiments in section 2.3.9.2, the small intestine was were dissected as follows:

- The proximal 5cm was mounted ‘en face’ and fixed overnight in methacarn (methanol, chloroform and acetic acid; 4:2:1).
- The following 3cm was divided into 1cm lengths, bundled using surgical tape and then fixed in 10% (v/v) formalin.
- The next 1cm was stored in RNAlater (Sigma) for subsequent RNA extraction.
- The remaining section was fixed in methacarn overnight.

Additionally, the liver was isolated as follows:

- 3 pieces of 2mm x 2mm and stored in RNA later.
- For SA-β-gal (or senescence associated beta-gal), 1cm x 1cm of the liver was placed onto a cork disk and covered in the embedding medium-OCT before being placed in dry ice.
- The remainder was fixed in 10% (v/v) formalin for 16 hours.

For experiment in section 2.8.10, the colon was flushed with water and fixed in methacarn for 16hours. For acute colitis, the colon was also fixed in 10% formalin for 16 hours. The colon was then wound into ‘swiss rolls’ and transferred to 10% (v/v) formalin and subsequently stored in 70% (v/v) ethanol.

2.3.12 Immunohistochemistry (IHC)

Immunohistochemical stainings of formalin-fixed, paraffin embedded tissue for hematoxylin & eosin (H&E), BrdU, Caspase 3, myeloperoxidase (MPO), p53 and F480 were performed by Colin Nixon of Histology Services (Beatson Institute).

IHC staining for mTOR activity and the stem cell marker OFLM-4 was performed as follows. In brief, formalin-fixed paraffin embedded tissue sections (10µm) on Poly-L-lysine slides were de-waxed in xylene for 20 minutes and then rehydrated through graded ethanol solutions (100% alcohol for 10 minutes, 70 % (v/v) ethanol for 5minutes) and finally into water. Antigen retrieval was performed in 1x Citrate buffer diluted in dH_2O in 95^oC for 30 minutes.
Endogenous peroxidase was blocked using 3% (v/v) H_2O_2 (Sigma) in water for 10 minutes at room temperature. Sections were washed for 5 minutes in TBS-T and blocked for 30 minutes with 5% (v/v) normal goat serum (NGS) in TBS-T for 30 minutes at room temperature (45 minutes for anti-mTOR Ser2448). Sections were incubated with the following primary antibody solutions at 4°C for 16 hours.

- p4E-BP1; 1:500 in 5% (v/v) NGS in TBS-T
- $pAkt^{Ser473}$; 1:25 in 5% (v/v) NGS in TBS-T
- mTOR Ser2448 ; 1:100 in 10% NGS in TBS-T

Following a 10 minute wash in TBS-T, sections were incubated with secondary antibody with biotinylated secondary antibody (Rabbit ABC kit, Vector Laboratories) for 30 mins at room temperature. Sections were then washed for 10 minutes in TBST and incubated with pre-mixed ABC complex (Vectastain Elite ABC Rabbit kit; Vector Laboratories) for 30 mins at room temperature. Staining was visualised by incubation with DAB complex for 5-15 minutes at room temperature. After reaction termination by immersion in distilled water, sections counterstained with hematoxylin. Sections were dehydrated by washing in increasing concentrations of alcohol (70% (v/v) ethanol for 5 minutes, 100% ethanol for 10 minutes), treated with xylene for 15 minutes and then mounted using DPX mounting medium.

IHC staining for the stem cell marker OFLM-4 was performed as in 2.3.12 with the following exceptions. Sections were incubated with the primary antibody to OFLM-4 at 1:200 in 5% (v/v) normal goat serum in PBS for 16 hours at 4°C. Incubation with the secondary rabbit antibody solution (DAKO) was for 1 hour.

2.3.13 Assaying live crypts, apoptosis and regeneration in vivo

Intestinal crypts containing at least 5 consecutive epithelial cells were considered to be live crypts and used as an indicator of crypt survival or regeneration, depending on the experimental time point.

Colonic crypts were identified as straight and narrow crypts that are aligned parallel to the crypt bases. The number of polyps (small benign growths protruding from the colon or rectum) were scored along the whole length of the colon and confirmed by H&E staining.

To quantify for apoptosis, caspase-3 IHC was performed. The number of caspase-3 positive cells in 25 full crypts was noted and compared within each genotype. Additionally, H&E stained sections were analysed under the microscope for cell shrinkage, chromatin condensation, formation of apoptotic bodies, appearance of red 'halo' around the dying cells, and nuclei demonstrating increased 'red' staining (Kerr *et al.,* 1972, Wyllie *et al.,* 1980). Proliferation and mitotic division was determined by performing IHC staining for BrdU (to identify cells in the S-phase of the cell cycle) and phospho-histone H3 respectively. For BrdU assay, mice were injected intraperitoneally with 2.5mg BrdU. For quantification of mitosis in the small intestine, the number of Ki67 or BrdU positive cells in 25 full crypts was noted and compared within each genotype.

2.3.14 SA-β-gal (senescence associated beta-gal) staining

Frozen liver sections (10μm thick) on poly-L-lysine slides were fixed for 15 minutes in a solution of 2% (v/v) paraformaldehyde/ 0.25% (w/v) glutaraldehyde diluted in PBS. Sections were washed 3 times with 1mM $MgCl_2$ diluted in PBS (pH5.5) and then stained with a solution of 1mM $MgCl_2$/PBS (pH5.5) containing 1x potassium cyanide (KC) solution and 20mg/ml X-Gal solution in a wet chamber at 37^{o}C for 16

hours. Following three washes in PBS sections were mounted with DPX mounting medium.

2.3.15 Statistics

Statistical analysis for the qPCR data shown in Fig. 4.4 and Fig. 4.26 was generated using the Relative Expression Software Tool (REST) 2009 (http://www.genequantification.com/). All other statistical analyses were performed using SPSS software. Statistical analyses for results in chapter 3 were undertaken via a univariate general linear model followed by correction using Tukey HSD, except where indicated. Statistical analyses for results in chapter 4 and 5 were undertaken via Mann Whitney U test.

Graphs (with the exception of Fig. 4.4 and Fig. 4.26 which was generated using Prism 5 software) were generated using Microsoft Excel. The error bars were calculated and represented in terms of mean ± SD. The boxplots for Chapter 5 were generated using SPSS.

Chapter 3: Characterisation of DRAM-1 isoforms

3.1 Introduction

The proteome of humans and higher eukaryotes is greatly expanded from the genome by various post -transcriptional and -translational modification events. Of these events, alternative splicing of nascent mRNA, in which exons in a common transcript are ligated in various combinations to generate distinct splice variants, has been regarded as the primary contributor for this diversification of the human genome (Shankarling and Lynch 2010) (Wang, Sandberg et al. 2008). In fact, elegant microarray profiling and EST-cDNA sequence data analysis suggested that almost 70% of human genes are estimated to contain at least one alternatively spliced exon (Johnson, Castle et al. 2003). The protein isoforms that are translated from these splice variants may have similar, different or even antagonizing functions (Hernandez, Moreno et al. 2010) (Boise, Gonzalez-Garcia et al. 1993; Echard, Opdam et al. 2000).

The DRAM-1 protein is encoded by the *DRAM-1* transcript that contains 7 exons. (Crighton, Wilkinson et al. 2006). In this study, eight other splice variants of *DRAM-1* have been identified in human. These transcripts contain exons 1 and 7, but lack different combinations of exons 2-6. Three of these splice variants, nominally termed Splice Variant (SV)1, SV4 and SV5 which code for DRAM-1 isoforms 1, 4 and 5 respectively, were further characterised with respect to their ability to regulate autophagy. In line with this, autophagy was monitored by assessing the changes in two of the well characterised autophagic markers, the conversion of the microtubule-associated protein 1 light chain 1, LC3-I to LC3-II and the degradation of long – lived proteins (Klionsky, Abeliovich et al. 2008).

Mammalian paralogues of Atg8 are categorized into two subgroups based on their amino acid sequence homology - the LC3 subfamily consisting of LC3A, LC3B and LC3C and the GABARAP/GATE 16 subfamily comprising of the GABARAPL1, GATE-16/ GABARAPL2, and GABARAP-L3 (Weidberg, Shvets et al. 2010). LC3B, or more commonly known as LC3, is most commonly used as a marker for autophagy induction, and has been demonstrated to associate with autophagosomes and recruit other autophagic factors such as p62 and NBR1

(Kirkin, Lamark et al. 2009) (Weidberg, Shvets et al. 2010). LC3B exists in three forms, the pre-cursor pro-LC3, LC3-I and the lipidated LC3-II (Klionsky, Abeliovich et al. 2008). Pro-LC3 is processed into the cytosolic LC3-I, which is then cleaved by ATG4 and modified into LC3-II by its conjugation to phosphatidylethanolamine (PE) (Klionsky, Abeliovich et al. 2008). The lipidated LC3-II, which can be visualized as puncta when conjugated to fluorochromes like GFP or mRFP, is present on isolation membranes, autophagosomes and much less on autolysosome, thus making it a reliable marker for autophagy induction (Mizushima and Yoshimori 2007). In light with this, the development of assays to monitor LC3 turn over, such as the tandem mRFP GFP fluorescent-tagged LC3 reporter protein has greatly facilitated the study of autophagic flux. The dynamics of autophagy comprises of the formation of autophagosomes and the subsequent fusion with lysosomes, forming autolysosomes to create an acidic environment for cargo digestion (Klionsky and Emr 2000). Since GFP fluorescence is quenched under acidic conditions whereas mRFP remains stable, the colocalisation of both signals indicates LC3-containing components that are not fused to the lysosomes such as the isolation membrane and immature autophagosomes (Klionsky, Abeliovich et al. 2008). On one hand, when fusion occurs, the GFP signal is quenched, leaving only the mRFP signal – corresponding to amphisomes and autophagosomes (Kimura, Noda et al. 2007). The stepwise visualisation of green and red signals that correspond to autophagosome formation and maturation is illustrated in Fig. 3.1. As such, this assay is able to successfully determine the flux of autophagosomes and autolysosomes.

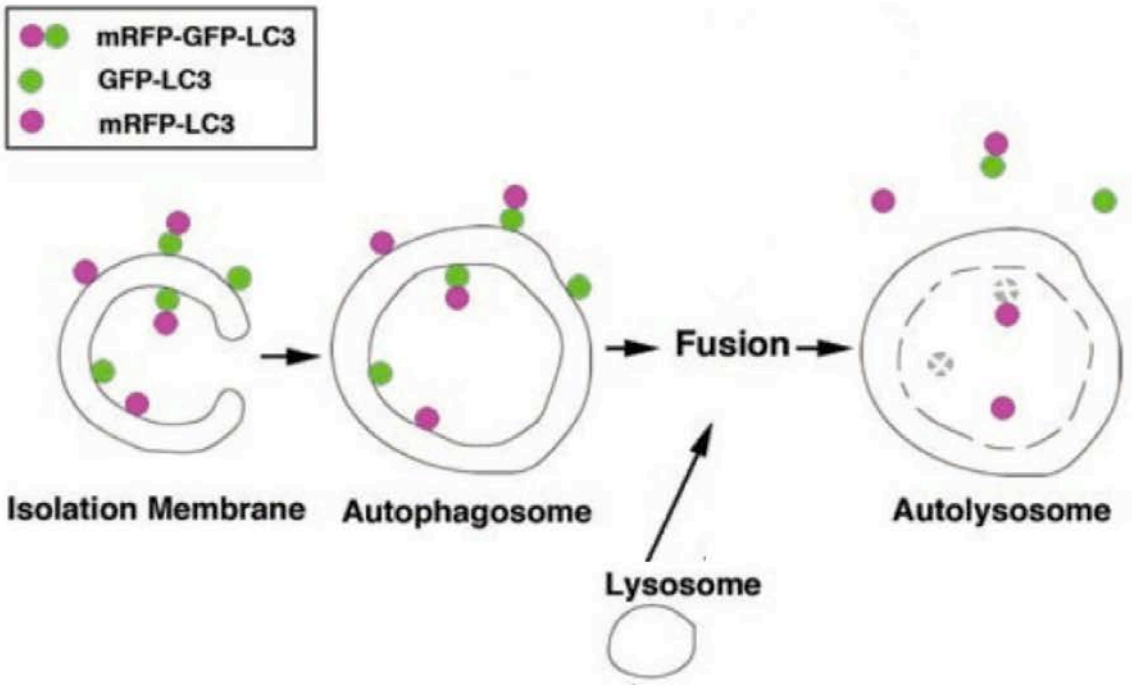

Kimura et. al (2007)

Figure 3.1: Schematic representation of GFP and mRFP fluorescence in the mRFP-GFP-LC3 construct
Colocalisation of GFP and mRFP fluorescence corresponds to isolation membrane and autophagosome that has not fused with a lysosome. mRFP signal without GFP corresponds to autolysosome.

Long-lived protein is also a well-known autophagic substrate and the rate of long-live protein degradation is a well-established method to measure autophagic flux and enables good quantification (Klionsky, Abeliovich et al. 2008). In this context, proteins are usually labelled with a radio-isotope by incorporation of a radioactive amino-acid, followed by a long cold-chase to allow for the degradation of short-lived proteins, and the subsequent release of the acid-soluble radioactivity, which is quantified to reflect autophagic activity (Klionsky, Abeliovich et al. 2008) (Furuta, Hidaka et al. 2004; Mizushima, Yoshimori et al. 2010). Upon autophagy induction, the degradation of long-lived proteins is accelerated, resulting in a mark increase in the release of the radioisotope from intact cells into the medium.

Elevated ROS levels well above the basal level have been demonstrated to induce autophagy (Rouschop, Ramaekers et al. 2009). Furthermore, p53 target genes like TIGAR and PUMA have been demonstrated to modulate ROS levels. In this context, TIGAR supresses ROS formation and the subsequent inhibition of autophagy in a p53-independent manner, with no clear effects on the mTOR pathway when deprived of nutrient or subjected to metabolic stress (Bensaad, Cheung et al. 2009). This discovery adds yet another level of complication to autophagy regulation by p53. Furthermore, the regulation of ROS by TIGAR is also essential to modulate apoptosis (Bensaad, Tsuruta et al. 2006). Enhanced expression of PUMA is also reported to induce ROS formation that contributes to apoptosis in colorectal cancer cells (Liu, Lu et al. 2005). Since DRAM-1 is also a p53 target gene, which is involved in autophagy and apoptosis, we wanted to know if the overexpression and deletion of *DRAM-1* can modulate ROS levels with respect to its ability to induce autophagy and apoptosis.

Following the role of the previously characterised DRAM-1 in facilitating p53-mediated apoptosis (Crighton, Wilkinson et al. 2006), the ability of DRAM-1 isoforms 4 and 5 to induce cell death in a p53-independent and -dependent manner was also assessed. Given that autophagy activation is largely perceived as a cytoprotective mechanism when nutrients are scarce, and that DRAM-1 promotes autophagy, the role of DRAM-1 in modulating cell death in nutrient limiting conditions was also assayed.

3.2 Results

3.2.1 *DRAM-1* encodes multiple splice variants that are induced by p53

The previously characterised p53 tetracycline-inducible (TetOn-p53) Saos-2 osteosarcoma cell line (Ryan, Ernst et al. 2000) were used to determine if *DRAM-1* encodes for other splice variants beyond the one that has been characterised (Crighton, Wilkinson et al. 2006), and if so, whether they are also induced by p53. RNA was isolated from TetOn-p53 cells without or with 24h Doxycycline (Dox) treatment and was subjected to semi-quantitative PCR using primers from exon 1 at the extreme 5' of the *DRAM-1* open reading frame and exon 7 at the extreme 3'. These primers were able to detect eight other mRNA species, nominally named SV 2, 3, 4, 5, 6, 7, 8 and 9 - several of which were upregulated when p53 was activated with Doxycycline (Fig. 3.2). These transcripts were cloned and sequencing confirmed that they harbour different internal deletions of exons 2-6, while retaining exons 1 and 7 (Fig. 3.3) (Analysis by Jim O'Prey, Tumour Cell Death Laboratory). Sequencing also confirmed that only SV4 and SV5 results in mRNA species that continue in-frame to the same stop codon as SV1 at the end of exon 7, and thus it is postulated that they also have mature 3' ends to maintain mRNA stability. These 3 isoforms also retained the highly conserved 'PYISD' motif as described by Crighton et al (2006) (Fig. 3.4). The 'PYISD' domain is required for the efficacy of DRAM-1 to modulate autophagy, as a mutation of the amino acid from Serine (suspected to be the phosphorylation site) to Alanine diminished the formation of GFP-LC3 puncta (Fig. 3.5). Having said that, only DRAM-1 isoform 1 harbours a putative canonical LC3 Interacting Region (LIR) which consists of the WxxL, (Fig. 3.4) that enables the recognition of autophagy receptors by autophagy effectors (Kirkin, Lamark et al. 2009; Rozenknop, Rogov et al. 2011).

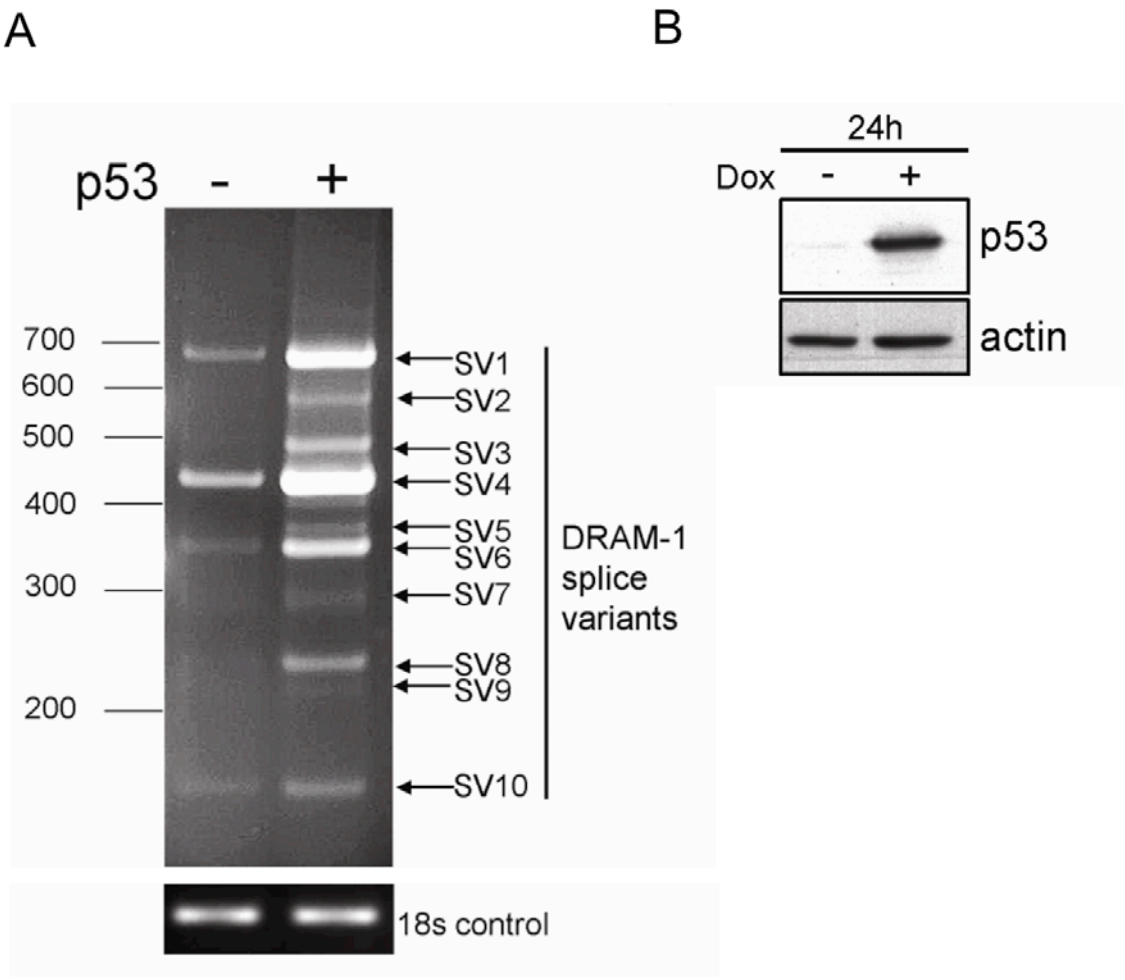

Figure 3.2(A-B): *DRAM-1* splice variants are induced by p53
TetOn-p53 Saos-2 cells were treated with 1µg/ml Doxycycline (Dox) for 24 hours. (A) RNA was harvested and analysed on a 3% agarose gel for DRAM-1 expression.
(B) p53 induction upon Dox treatment was verified by western blotting.

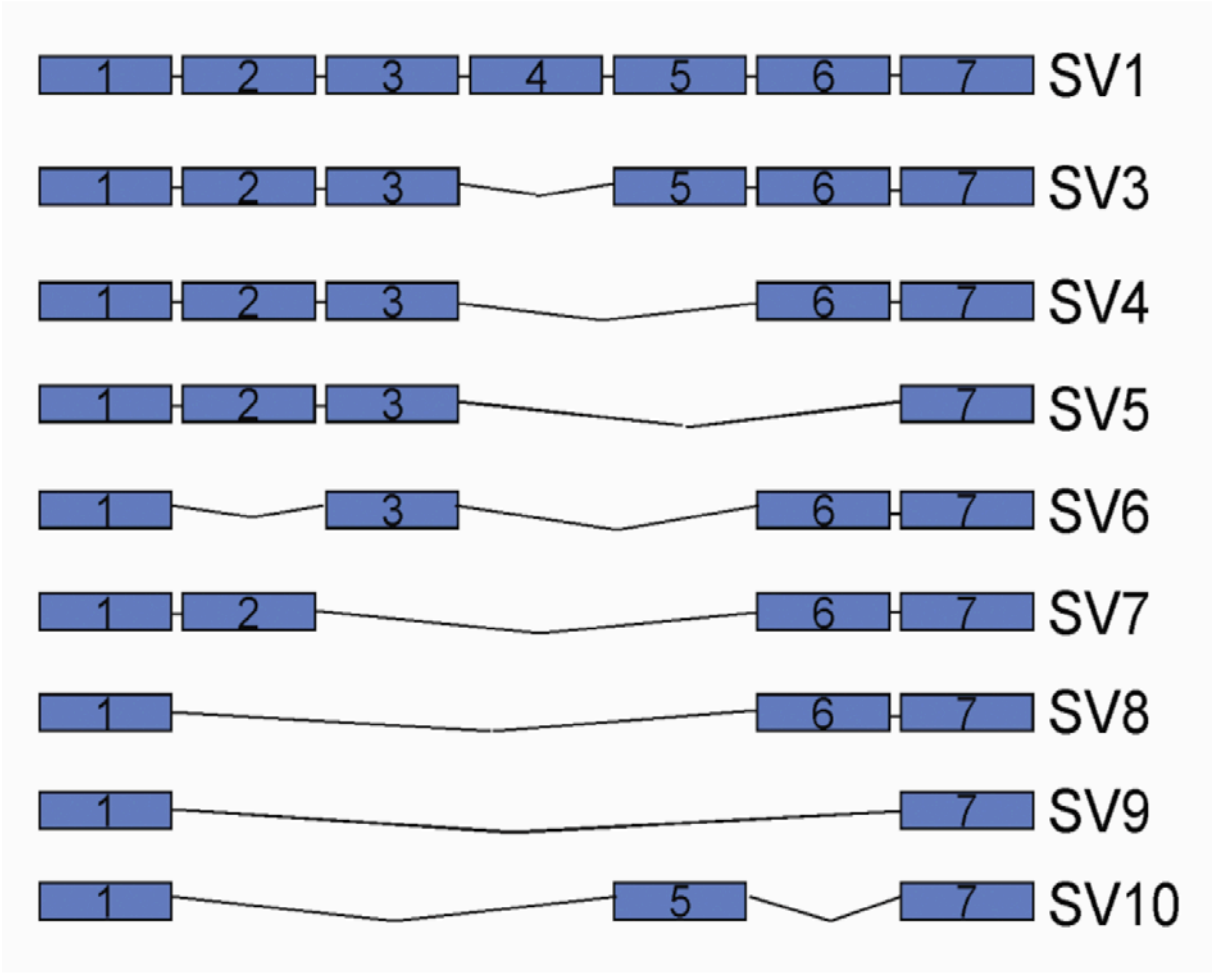

Figure 3.3: Schematic representation of *DRAM-1* splice variants
SV 1-10 is comprised of exons 1 and 7, but harbour different internal exon deletions.

Isoform 1:

MLCFLRGMAFVPFLLVTWSSAAFIISYVVAVLSGHVNPFL**PYISD**T
GTTPPESGIFGFMINFSAFLGAATMYTRYKIVQKQNQTCYFSTPV
FNLVSLVLGLVGCFGMGIVANFQELAVPVVHDGGALLAFVCGVVY
TLLQSIISYKSCPQ**WNSL**STCHIRMVISAVSCAAVIPMIVCASLISIT
KLEWNPREKDYVYHVVSAICEWTVAFGFIFYFLTFIQDFQSVTLRI
STEINGDI

Isoform 4:

MLCFLRGMAFVPFLLVTWSSAAFIISYVVAVLSGHVNPFL**PYISD**T
GTTPPESGIFGFMINFSAFLGAATMYTRYKIVQKQNQTCYFSTPV
FNLVSLVLGLVGCFGMGIVANFQDYVYHVVSAICEWTVAFGFIFYF
LTFIQDFQSVTLRISTEINGDI

Isoform 5:

MLCFLRGMAFVPFLLVTWSSAAFIISYVVAVLSGHVNPFL**PYISD**T
GTTPPESGIFGFMINFSAFLGAATMYTRYKIVQKQNQTCYFSTPV
FNLVSLVLGLVGCFGMGIVANFQSVTLRISTEINGDI

Figure 3.4: Amino acid composition of DRAM-1 isoforms 1, 4, and 5
The conservation of PYISD motifs in all DRAM-1 isoforms is highlighted in red, and the LIR domains (green) is present only in isoform 1.

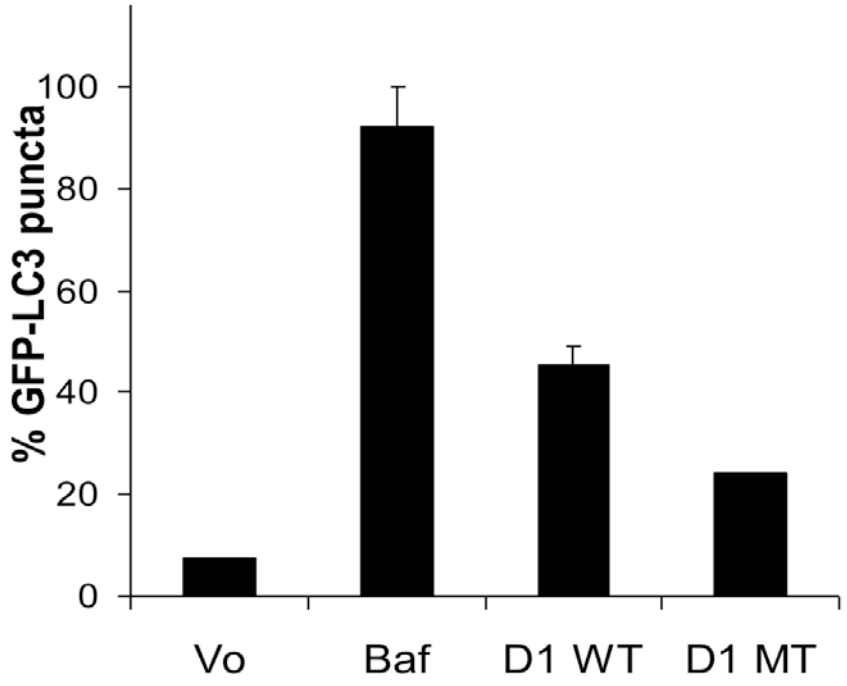

Figure 3.5: Disruption of the PYISD domain diminished DRAM-1 induced GFP-LC3 punctation

Saos-2 cells were co-infected with adenoviruses expressing GFP-LC3 and either DRAM-1 isoform1 (D1 WT), mutant (D1 mt) or empty vector (Vo). Additionally, cells were also treated with 100nM of Bafilomycin-A1 (Baf-A1) as a positive control for autophagosome accumulation. Cells with 8 or more puncta were score as positive for GFP LC3 punctation.

The presence of DRAM-1 isoforms was also confirmed in other cells and tissues by performing PCR amplification using the same primers from various cell lines of different origin. The levels of expression of these splice variants is variable across the different cell lines that were tested (Fig. 3.6). The splicing of *DRAM-1* is not restricted to human, as several *DRAM-1* transcripts were also found to be expressed mouse embryonic fibroblasts (MEFs), and are also upregulated when induced with the p53-inducing agent, Nutlin-3A (Fig. 3.7).

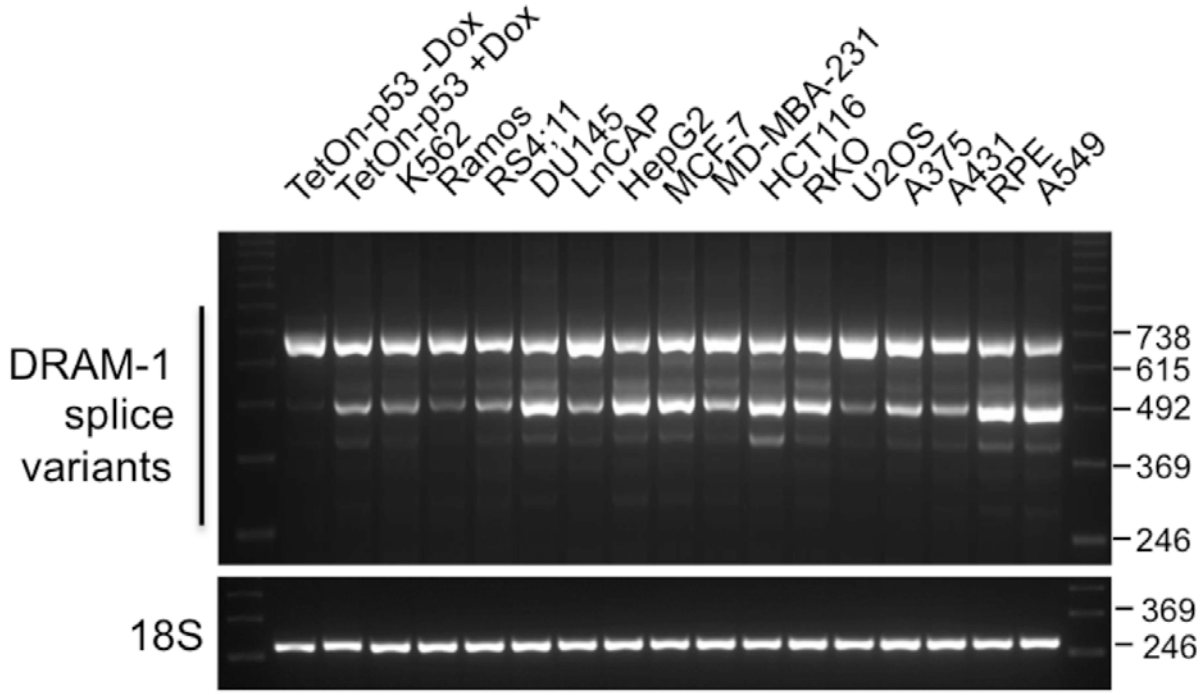

(Figure produced by James O'Prey of the Tumor Cell Death Laboratory)

Figure 3.6: *DRAM-1* splice variants are expressed in multiple human cell lines

RNA from a panel of human cell lines was subjected to semi-quantitative RT-PCR with primers from exon 1 and exon 7 of DRAM-1, and then analysed on a 3% agarose gel.

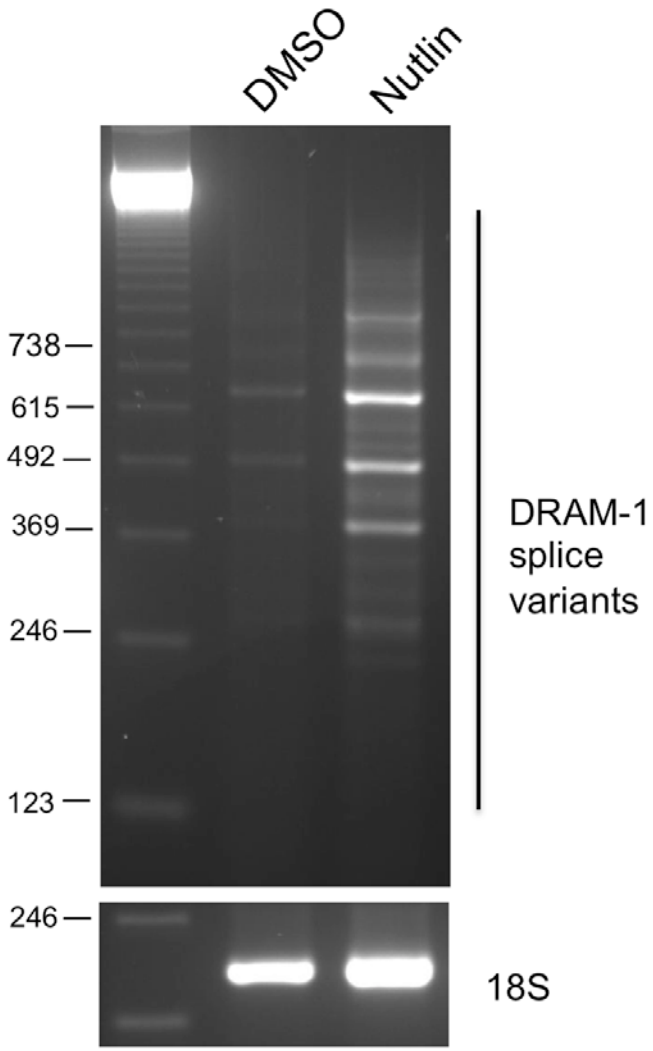

Figure 3.7: *DRAM-1* splice variants are expressed in mouse cells
RNA from MEFs that had been incubated in the absence or presence of the p53 inducing agent, Nutlin-3A (10mM for 48h) were subjected to semi-quantitative RT-PCR with primers from exon 1 and exon 7 of mouse DRAM-1. The PCR products were analysed on a 3% agarose gel.

3.2.2 DRAM-1 isoforms are localised and degraded in distinct cellular compartments

DRAM-1 isoform 1 is localised to lysosomes (Crighton, Wilkinson et al. 2006). To determine the cellular distribution of isoforms 4 and 5, DRAM-1 isoforms were over expressed from adenoviruses in Saos-2 cells and stained with at least two markers for each cellular component that were analysed, as listed in Table 3.1. In addition to the lysosome (Fig. 3.8), DRAM-1 isoform 1 was also found to be present in golgi apparatus, (Fig. 3.9), early and late endosomes (Fig. 3.10 and 3.11), but neither isoforms 4 nor 5 showed convincing colocalisation in these compartments (Fig. 3.8-3.11). Further colocalisation studies were carried out with markers of mitochondria, peroxisomes and the endoplasmic reticulum. DRAM-1 isoform 4 was partially localised to the endoplasmic reticulum and peroxisomes (Fig. 3.12 and 3.13), whereas isoform 5 was partially found in the endoplasmic reticulum (Fig. 3.12). None of the DRAM-1 isoforms were found in the mitochondria (Fig. 3.14). DRAM-1 isoforms were also tested to determine if they colocalise with other autophagy markers, in this case, the previously discussed LC3B and also DFCP1, a novel autophagy regulator which is normally distributed in Golgi and endoplasmic reticulum, but colocalises with LC3B upon autophagy induction (Ridley, Ktistakis et al. 2001). DRAM-1 isoforms 1 and 5 colocalised with the autophagosome marker, LC3, but not isoform 4 (Fig. 3.15). In light of this result, all the DRAM-1 isoforms partially colocalised with DFCP1 (Fig. 3.16).

Table 3.1: Markers used for determination of DRAM-1 localisation in cellular organelles

Organelles	Marker 1		Marker 2	
	Name	**Details**	**Name**	**Details**
Lysosome	Lamp-2	Lysosomal integral membrane protien	Cathepsin D	Lysosomal aspartyl protease
Golgi apparatus	TGN-46	Trans-golgi network protein	GM130	Golgi matrix protein
Early Endosomes	EEA1	A hydrophillic peripheral membrane protein which colocalizes to early endosomes	Rab5	GTP-binding protein that is associated with early endosome and plasma membranes
Late Endosomes	Rab7	GTP-binding protein which is associated with late endosomes.	CD63	A highly glycosylated type-III lysosomal (integral) glycoprotein
Autophagosome	mCherry LC3	Autophagsome marker (refer to section 1.2)	DFCP1	An autophagy regulator normally distributed in Golgi and endoplasmic reticulum, but colocalises with LC3B upon autophagy induction
ER	BiP	GRP78 BiP is localised to the endoplasmic reticulum	Calnexin	An integral membrane protein located primarily in the ER
Peroxisome	PMP70	Peroxisomal Membrane Marker of 70kDa	Peroxisome GFP	A modified baculovirus expressing a fusion construct of a peroxisomal marker and green fluorescent protein
Mitocondria	Tom 20	The mitochondrial preprotein translocases of the outer membrane which is located in the mitochondria	Cox IV	This protein is one of the nuclear-coded polypeptide chains of cytochrome c oxidase, the terminal oxidase in mitochondrial electron transport

Details of all commercial antibodies and reagents were obtained from the data sheet enclosed. Details of Rab 7 and DFCP1 contructs were obtained from Jim Norman (The Beatson Institute for Cancer Research; personal communication) and (Ridley, Ktistakis et al. 2001)

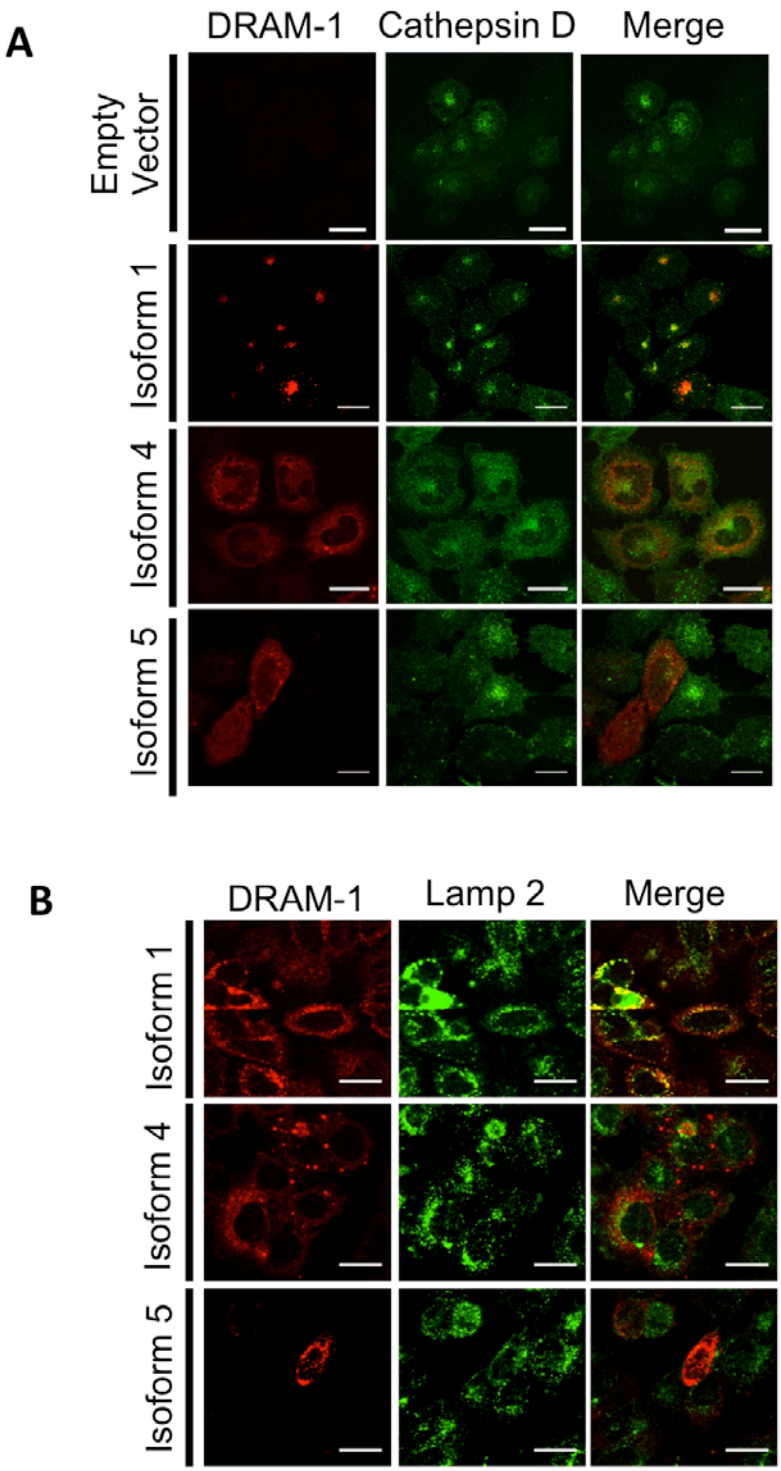

Figure 3.8: DRAM-1 isoform 1, but not isoform 4 and isoform 5, localises to lysosomes

Saos-2 cells were infected with equivalent amounts of DRAM-1 adenoviral lysates for 48 hours. Colocalisation (yellow) of myc-tagged DRAM-1 (red) with cathepsin D (green) (A) and LAMP-2A (green) (B), was assayed by confocal microscopy. The scale bar shown represents 20µm.

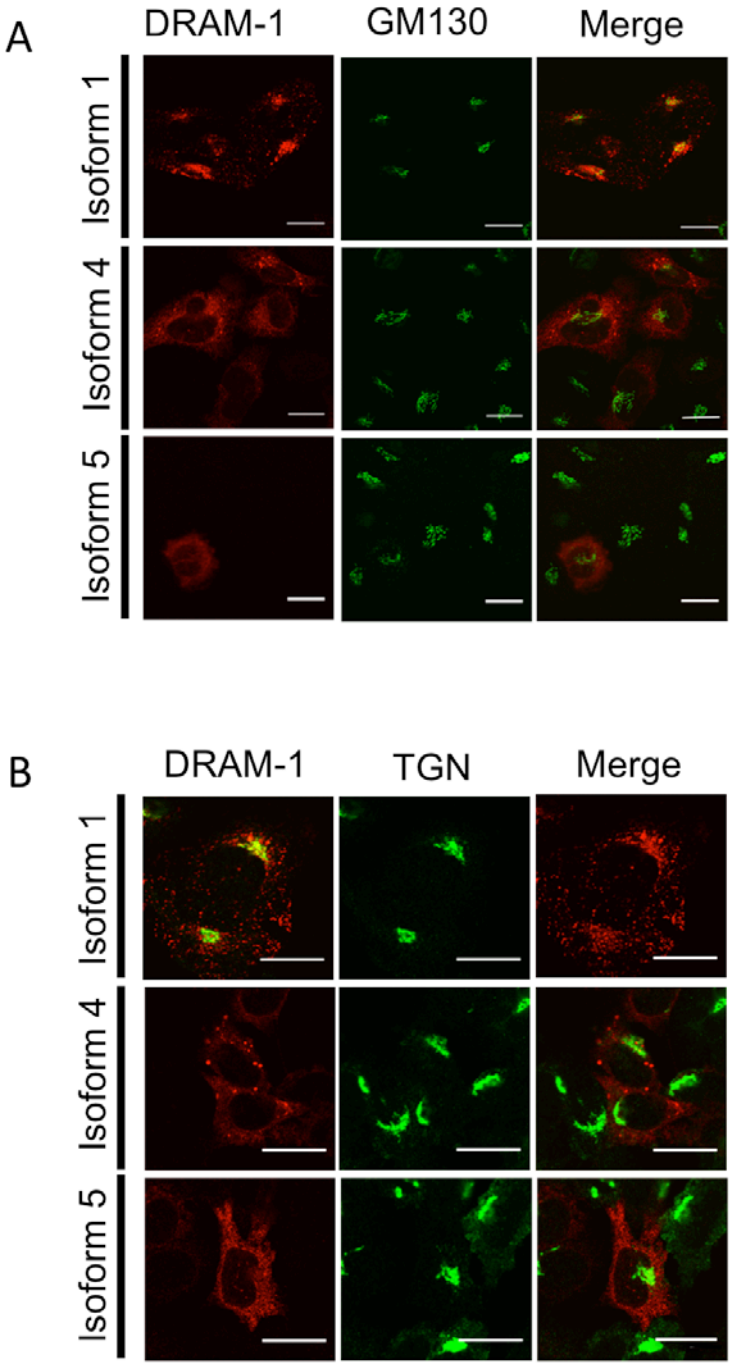

Figure 3.9: DRAM-1 isoform 1, but not isoform 4 and isoform 5, localises to golgi apparatus

Saos-2 cells were infected with equivalent amounts of DRAM-1 adenoviral lysates for 48 hours. Colocalisation (yellow) of myc-tagged DRAM-1 (red) with GM130 (green) (A) and TGN (B) (green), was assayed by confocal microscopy. The scale bar shown represents 20μm.

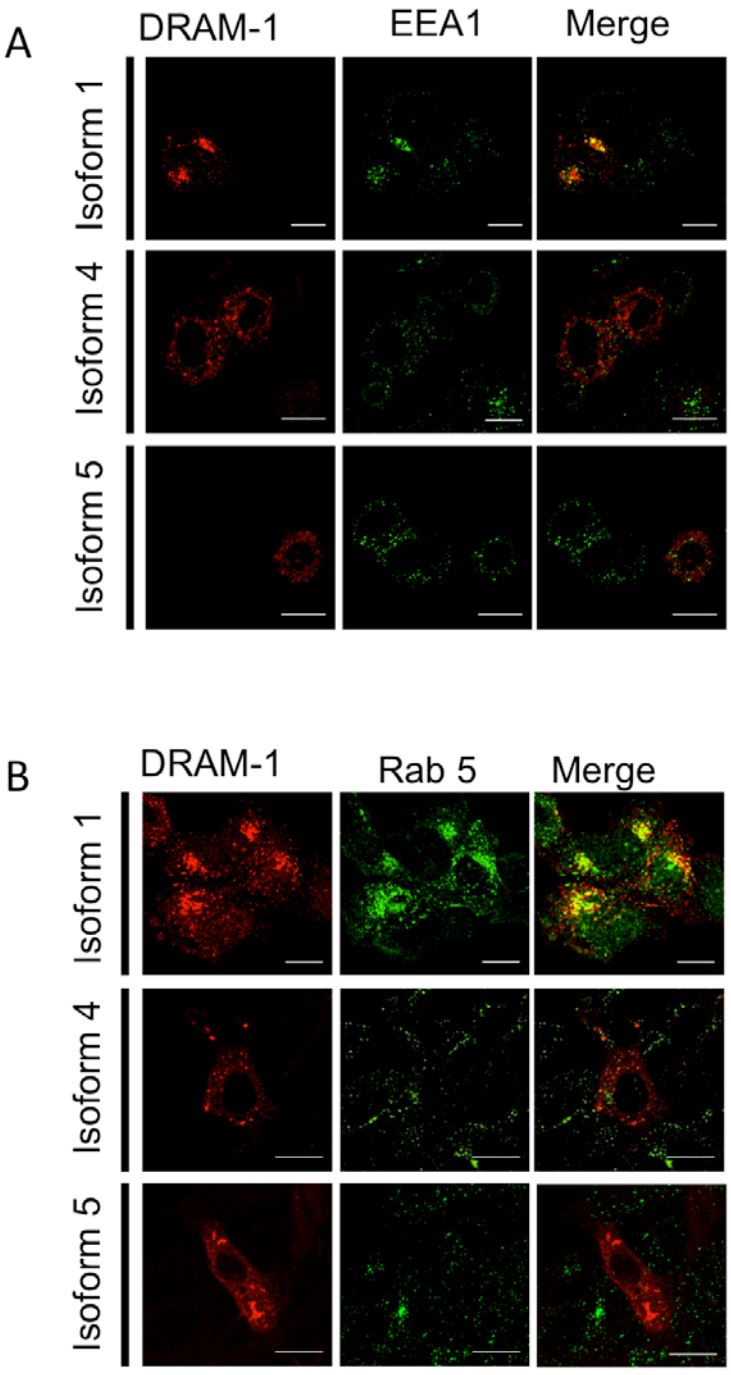

Figure 3.10: DRAM-1 isoform 1, but not isoform 4 and isoform 5, localises to early endosomes

Saos-2 cells were infected with equivalent amounts of DRAM-1 adenoviral lysates for 48 hours. Colocalisation (yellow) of myc-tagged DRAM-1 (red) with EEA1 (green) (A) and Rab5 (green) (B), was assayed by confocal microscopy. The scale bar shown represents 20μm.

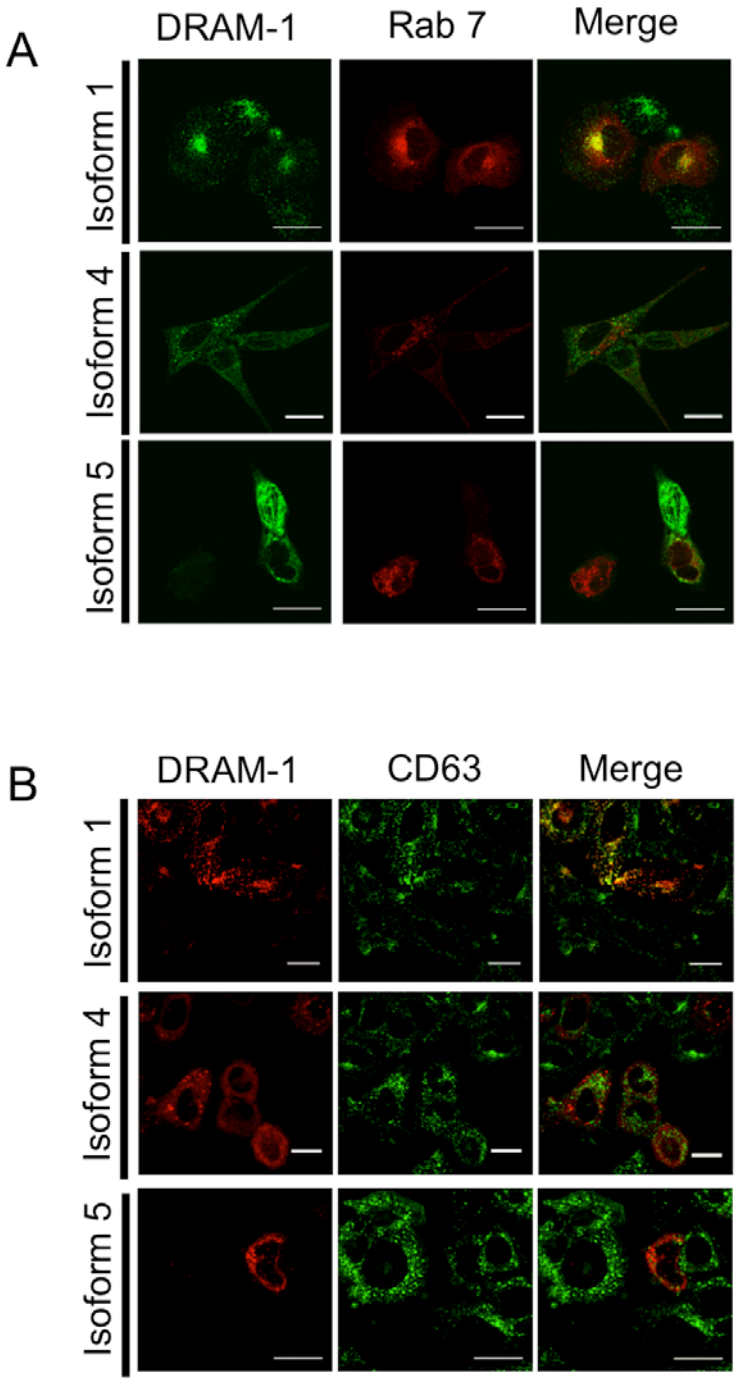

Figure 3.11: DRAM-1 isoform 1, but not isoform 4 and isoform 5, localises to late endosomes

Saos-2 cells were infected with equivalent amounts of DRAM-1 adenoviral lysates for 48 hours. Colocalisation (yellow) of myc-tagged DRAM-1 (red) with Rab7 (green) (A) andCD63 (green) (B), was assayed by confocal microscopy. The scale bar shown represents 20µm.

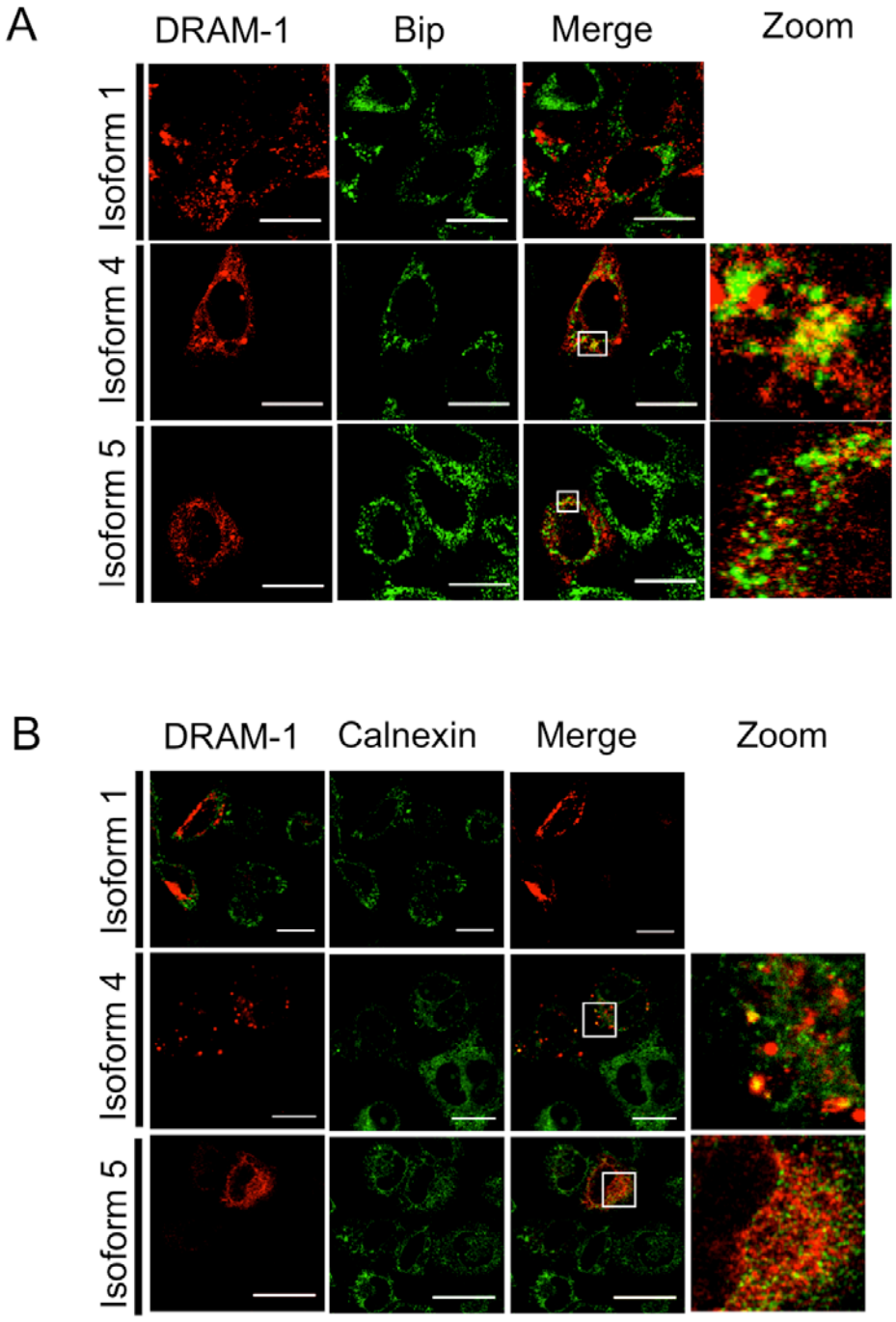

Figure 3.12: Partial colocalisation of DRAM-1 isoforms 4 and 5 to the endoplasmic reticulum

Saos-2 cells were infected with equivalent amounts of DRAM-1 adenoviral lysates for 48 hours. Colocalisation (yellow) of myc-tagged DRAM-1 (red) with Bip (green) (A) and calnexin (green) (B), was assayed by confocal microscopy. The scale bar shown represents 20μm.

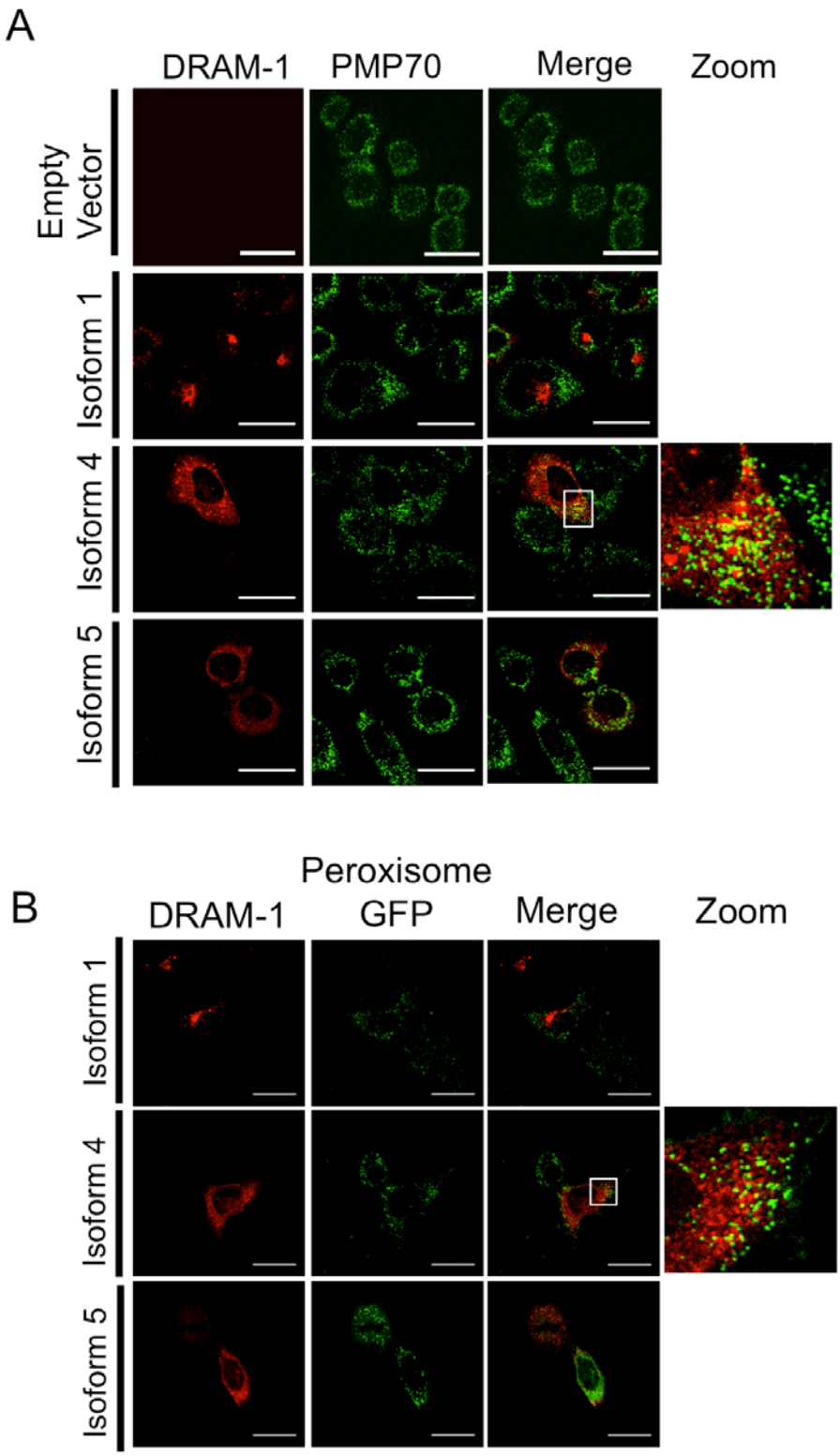

Figure 3.13: Partial colocalisation of DRAM-1 isoform 4 to peroxisomes
Saos-2 cells were infected with equivalent amounts of DRAM-1 adenoviral lysates for 48 hours. Colocalisation (yellow) of myc-tagged DRAM-1 (red) with PMP70 (green) (A) and Peroxisome-GFP Molecular Probes™ (green) (B), was assayed by confocal microscopy. The scale bar shown represents 20μm.

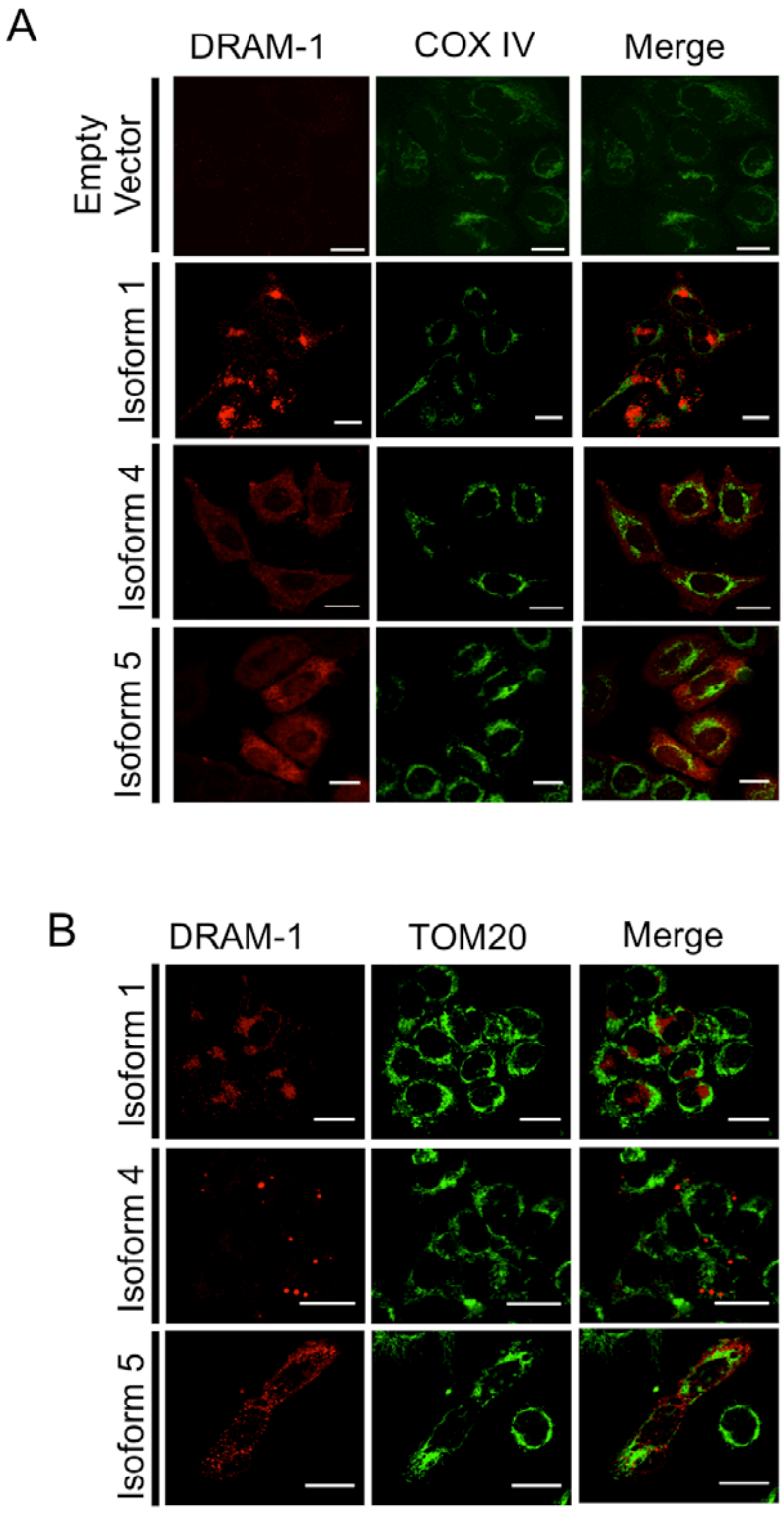

Figure 3.14: DRAM-1 isoforms do not colocalise to the mitochondria

Saos-2 cells were infected with equivalent amounts of DRAM-1 adenoviral lysates for 48 hours. Colocalisation (yellow) of myc-tagged DRAM-1 (red) with COX IV (green) (A) and Tom 20 (green) (B), was assayed by confocal microscopy. The scale bar shown represents 20μm.

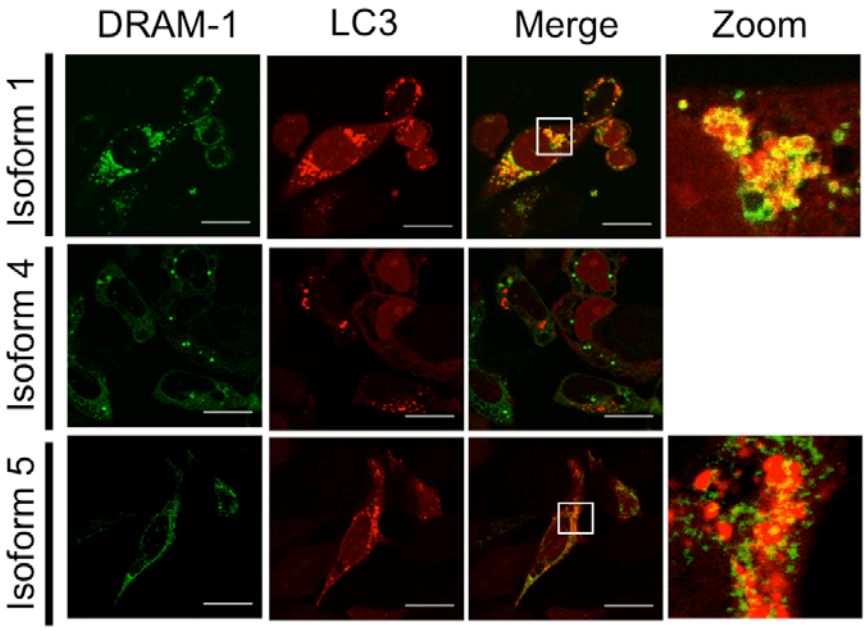

Figure 3.15: Localisation and partial localisation of DRAM-1 isoforms 1 and 5 respectively with the autophagy marker, LC3

Saos-2 cells were infected with equivalent amounts of DRAM-1 adenoviral lysates for 48 hours. Colocalisation (yellow) of myc-tagged DRAM-1 (green) with mCherry-LC3 (red), was assayed by confocal microscopy. The scale bar shown represents 20μm.

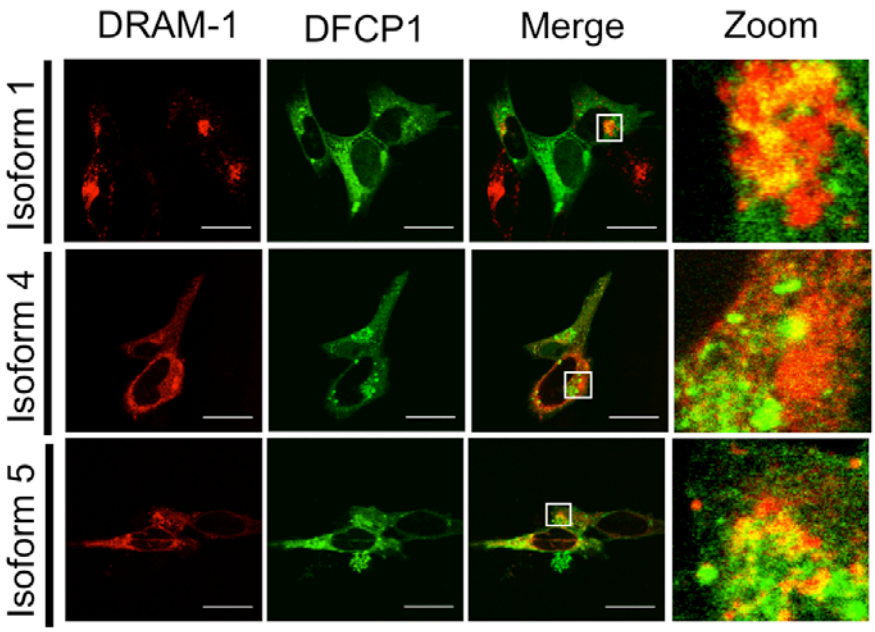

Figure 3.16: Partial colocalisation of DRAM-1 isoforms 1, 4 and to the autophagy marker, DFCP1

Saos-2 cells were infected with equivalent amounts of DRAM-1 adenoviral lysates for 48 hours. Colocalisation (yellow) of myc-tagged DRAM-1 (red) with DCFP1 (green), was assayed by confocal microscopy. The scale bar shown represents 20μm.

It was also found that DRAM-1 isoform 1 turnover occurs at the lysosome, as evident in the increase of the protein level upon lysosomal inhibition with the vacuolar-type H(+)- ATPase inhibitor, Bafilomycin-A1. In the contrary, the protein expression of isoform 4 decreases slightly whereas the protein level of isoform 5 remains the same, upon lysosomal inhibition (Fig. 3.17A). Rather, isoforms 4 and 5 are degraded in the proteasome, as shown by the significant increase in protein levels when the proteasomal function is blocked with the potent and reversible proteasome inhibitor, MG132 whereas isoform 1 protein levels decreases slightly (Fig. 3.17B).

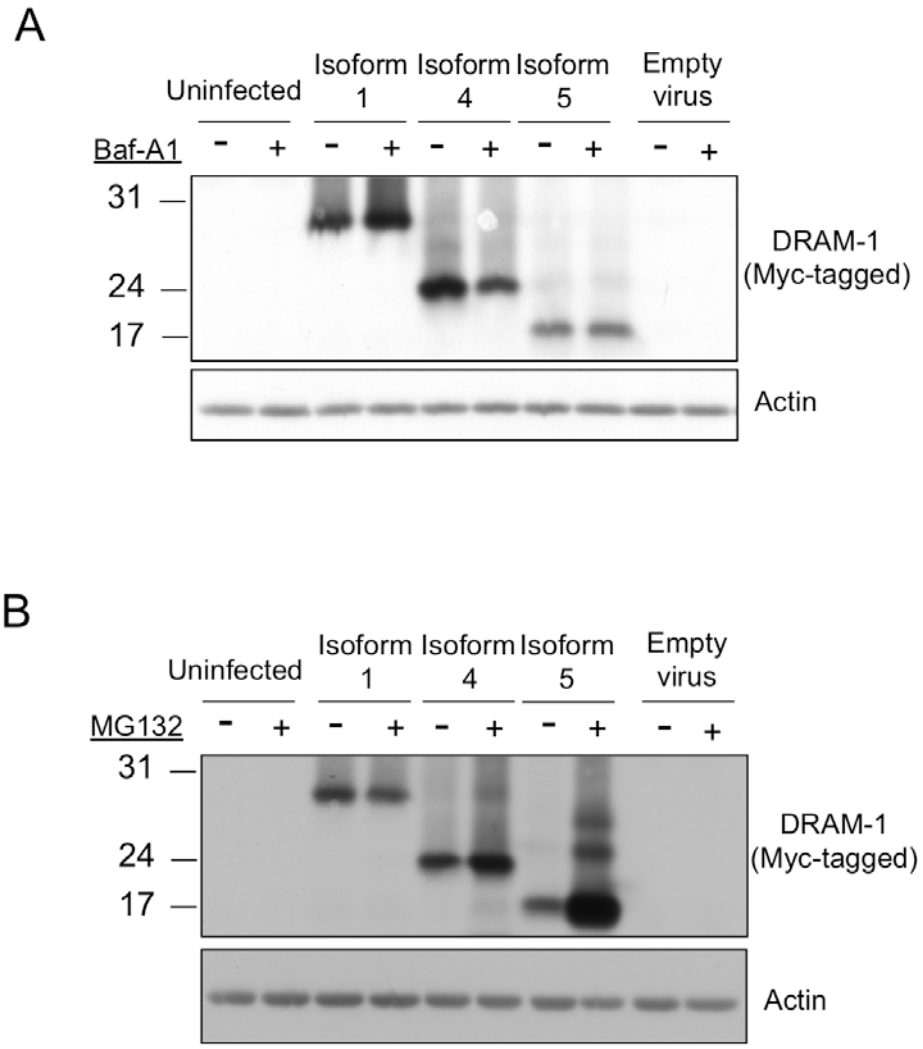

Figure 3.17(A-B): DRAM-1 isoform 1 is degraded in lysosomes, whereas isoform 4 and isoform 5 are degraded in proteasomes

Saos-2 cells were infected with DRAM-1 adenoviral lysates for 48 hours, and treated with either 100nM Bafilomycin-A1 (Baf-A1) (Sigma) (A) or 20μM MG132 (B) for 8h and 4h respectively. Proteins were analysed on a 12% SDS-PAGE gels.

3.2.3 DRAM-1 isoforms and the regulation of autophagy

To test if DRAM-1 isoforms 4 and 5 were also autophagy regulators, Saos-2 cells were simultaneously infected with adenoviruses expressing isoforms 1, 4 and 5, or empty adenoviral vector as control, together with an adenovirus expressing GFP-LC3 (Kabeya, Mizushima et al. 2000; Bampton, Goemans et al. 2005). Consistent with previous findings, cells expressing isoform 1 displayed marked increase in GFP-LC3 punctation, which corresponds to autophagosome formation compared with cells infected with empty viral control ($p = 0.001$) (Fig. 3.18). Significant accumulation of autophagosomes was also observed in cells infected with isoforms 4 and isoform 5 ($p < 0.05$) albeit to a lower extent compared to isoform 1 (Fig. 3.18). This implies that DRAM-1 isoforms 4 and 5 are also autophagy modulators.

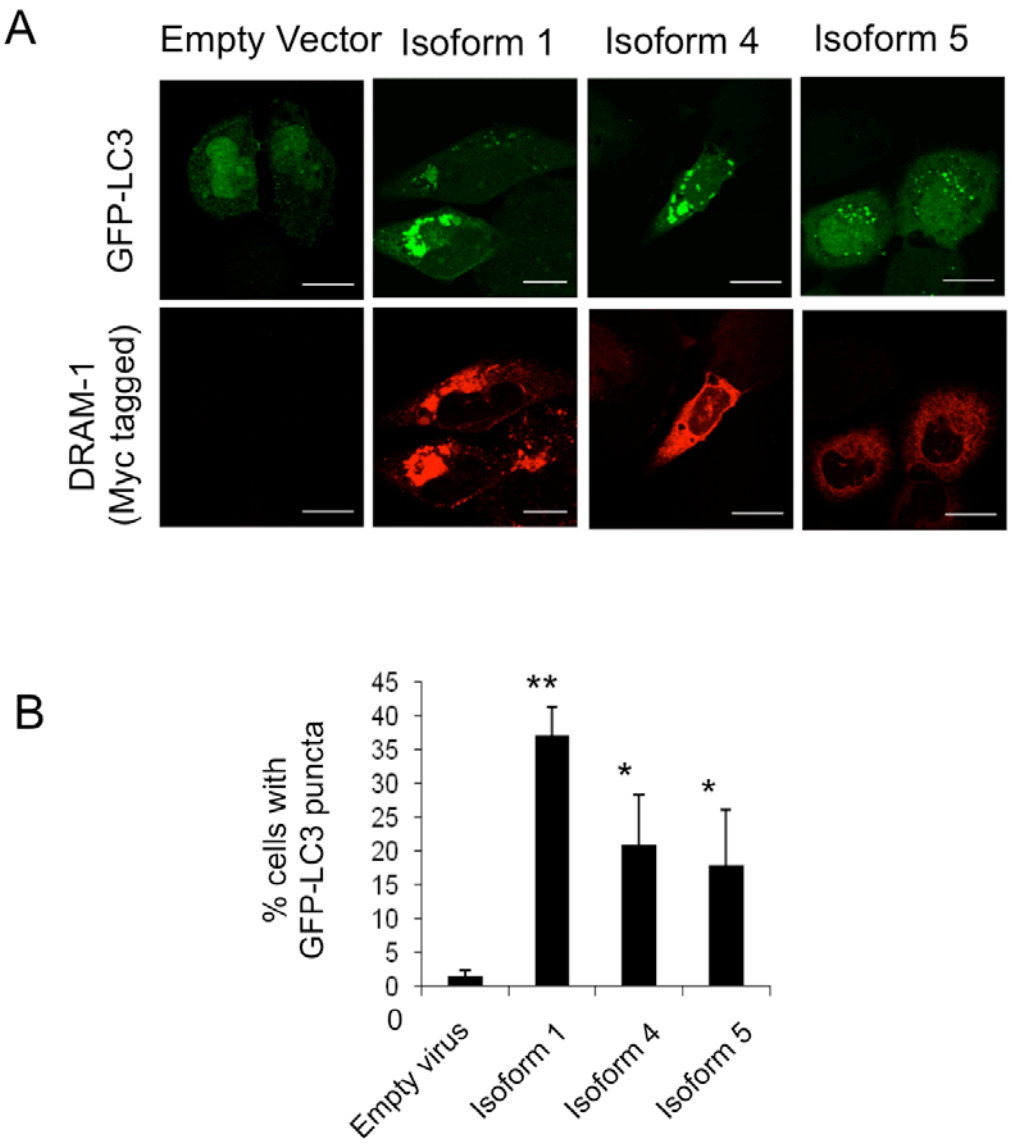

Figure 3.18(A-B): DRAM-1 isoform expression induces autophagosome formation

Saos-2 cells were co-infected with GFP-LC3 and either DRAM-1 isoforms or empty vector for 48 h.

(A) Representative images of cells overexpressing DRAM-1 isoforms displaying autophagosome formation The scale bar shown represents 20μm.

(B) Cells with eight or more GFP-LC3 puncta were scored as positive for cells with accumulated autophagosomes. In each case at least 200 cells were counted and the error bar indicates standard deviation.

To test if DRAM-1 isoforms promote autophagy, autophagic flux was assessed by monitoring the change in ratio of LC3-I to LC3-II by western blot following infection with each of the DRAM-1 isoforms, in the presence or absence of lysosomal degradation. Lysosomal degradation was prevented by treatment with Bafilomycin-A1 – an inhibitor of vacuolar H(+)-ATPase which increases the lysosomal pH to prevent the fusion of autophagosomes and lysosomes (Oda, Nishimura et al. 1991). Autophagy promoters are expected to cause a further increase in LC3-II accumulation upon the inhibition of this final stage of the autophagy machinery (Mizushima and Yoshimori 2007; Klionsky, Abeliovich et al. 2008). Consistent with the previous observation (Fig. 3.18), all the DRAM-1 isoforms increase the ratio of LC3-II to LC3-I, and the change with isoform 1 was greater than that observed with isoform 4 or isoform 5 (Fig. 3.19). Further accumulation in LC3-II levels was observed in all the cells when treated with the lysosome inhibitor, Bafilomycin-A1 compared to conditions when the lysosome function was not perturbed (Fig. 3.19). Additionally, cells that were overexpressing DRAM-1 isoforms 1 and 4 reflected a greater accumulation of LC3-II compared to those infected with the empty vector when the lysosomal function was inhibited, as reflected by the changes in the ratio of LC3-II to the actin control. This implies that both isoforms 1 and 4 promote autophagy. However, there is a slight decrease in the ratio of LC3-II to actin in the cells that were overexpressing the DRAM-1 isoform 5 control compared to those infected with the empty vector upon Bafilomycin-A1 treatment. This suggests that DRAM-1 isoform 5 could possibly repress autophagy.

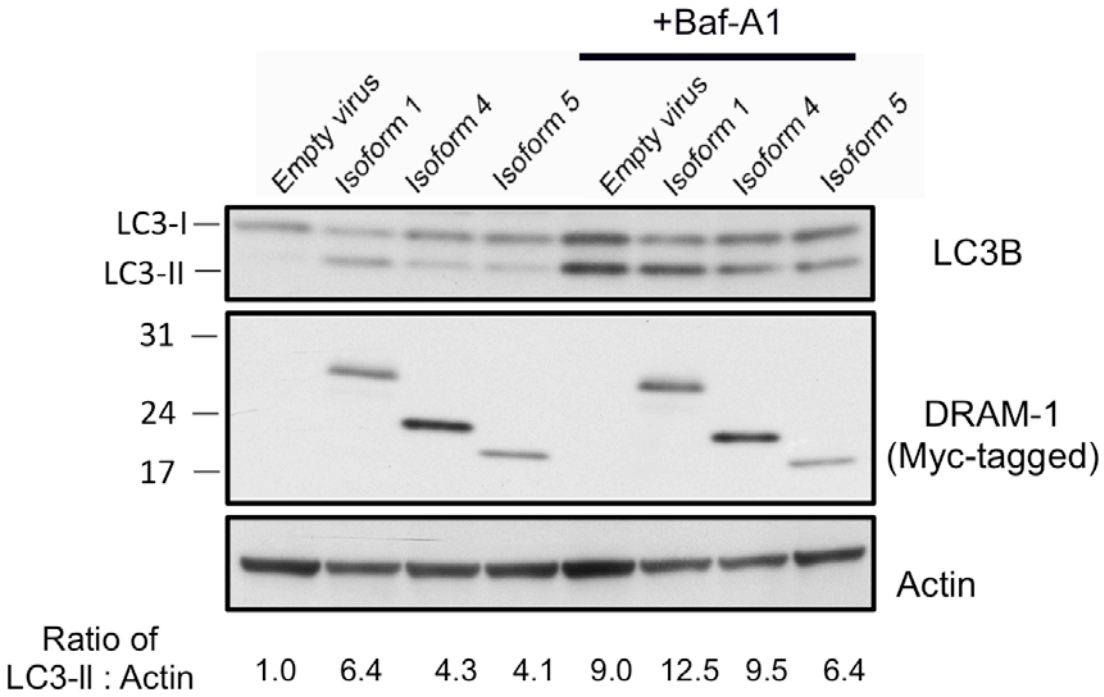

Figure 3.19: DRAM-1 modulates LC3-II to LC3-I
Saos-2 cells were infected with adenoviruses expressing either DRAM-1 isoforms 1, 4, 5 or 'empty' virus as control. Lysosome function was inhibited with 100nM Bafilomycin-A1 for 4h. Cell lysates were analysed on a 15% SDS-PAGE gel and probed for LC3-B, DRAM (myc) and actin. LC3-II levels were normalised against actin as a control. The relative ratio of LC3-II to actin was analysed using Image J.

Thus, it remains plausible that the coexpression of DRAM-1 isoforms 1, 4 and 5 can either cause a synergistic or additive increase in LC3-II levels. To test this, TetOn-DRAM-1 cells (Saos-2 cells which contain a tetracycline inducible DRAM-1 transgene) were infected with adenoviruses expressing either DRAM-1 isoform 4, 5 or an empty vector as control. DRAM-1 expression was achieved by incubating the cells with Doxycycline. It turned out that the total levels of LC3-1 and LC3-II did not increase upon coexpression of either DRAM-1 isoforms 1 and 4 or isoforms 1 and 5, compared to the individual overexpression of DRAM-1 isoform 1 alone (Fig. 3.20). Despite previous speculations that DRAM-1 isoform 5 could potentially repress autophagy, this experiment suggests that the enhanced expression of DRAM-1 Isoforms 1 and Isoforms 4 or 5 does not cause a synergistic and additive increase in LC3 lipidation.

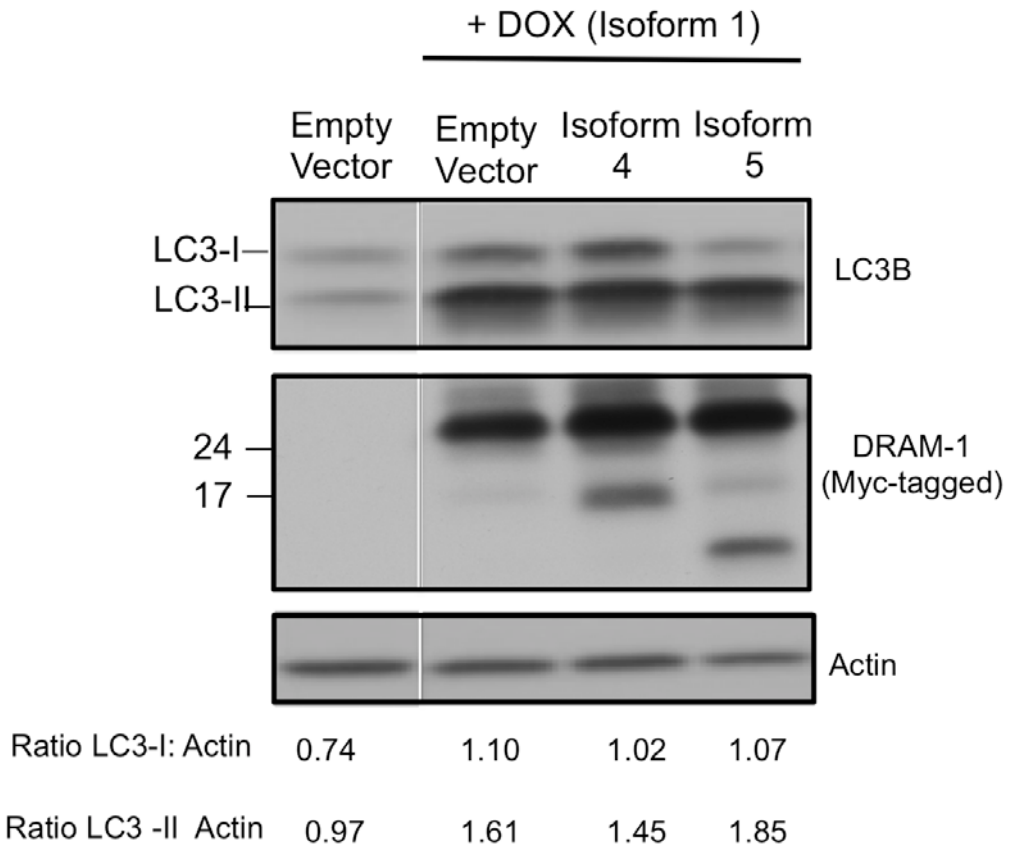

Figure 3.20: Coexpression of DRAM-1 isoforms 1 and 5 decreases LC3-I levels

TetOn-DRAM-1 cells (Saos-2 cells which contain a tetracycline inducible DRAM-1 SV 1 transgene) were either infected with DRAM-1 isoforms 4, 5 or empty vector. 24h later, the cells were treated with 1µg/ml of Doxycycline for 48 hours to induce DRAM-1 isoform 1 expression. Cell lysates were analysed on a 15% SDS-PAGE gel and probed for LC3-B, DRAM (myc) and actin. The relative ratio of LC3-I and LC3-II to actin was analysed using Image J.

Having seen this effect, we sought to determine if the coexpression of DRAM-1 isoforms not only promotes autophagosome biogenesis, but also fusion with lysosomes. To monitor autophagosome turn over, DRAM-1 isoforms were ectopically overexpressed in cells that were stably expressing the tandem monomeric RFP-GFP tagged LC3 to determine the autophagsomes and autolysosomes flux. As discussed in section 3.1, the presence of GFP puncta indicates immature autophagosomes. The presence of mRFP signal (red puncta) indicates mature autophagosomes and amphosomes, and is normally observed when cells are cultured in nutrient-limiting conditions, such as EBSS, which is a potent and well-characterised stimulus for autophagy induction and completion (Fig. 3.21B). At basal levels, both autophagosomes and autolysosomes are present at steady state levels, thus the formation of GFP and RFP puncta is very low (Fig. 3.20A). The colocalisation of both signals (yellow puncta) indicates LC3 II containing autophagosomes that are not fused to the lysosome, and is normally observed when the later stages of autophagy are inhibited with agents that block lysosomal function, such as the vacuolar ATPase inhibitor Bafilomycin-A1 (Fig. 3.21C). Ectopic overexpression of DRAM-1 isoforms 1 (Fig. 3.21D), 4 (Fig. 3.21E) and 5 (Fig. 3.21F) alone increases both mRFP and GFP puncta. Despite the increase in autophagic flux when DRAM-1 isoforms 1 and 5 were coexpressed together, the simultaneous overexpression of neither isoforms 1 and 4 (Fig. 3.20G) nor isoforms 1 and 5 together (Fig. 3.21H) was able to accelerate the fusion of autophagosomes and autolysosomes. Since all DRAM-1 isoforms promote autophagy, as evident with the further increase in LC3 lipidation upon lysosomal inhibition and enhanced autophagic flux, it seems reasonable to imply that DRAM-1 isoforms are potent inducers of autophagosome biogenesis, and that the rate of formation exceeds the rate of fusion with lysosomes.

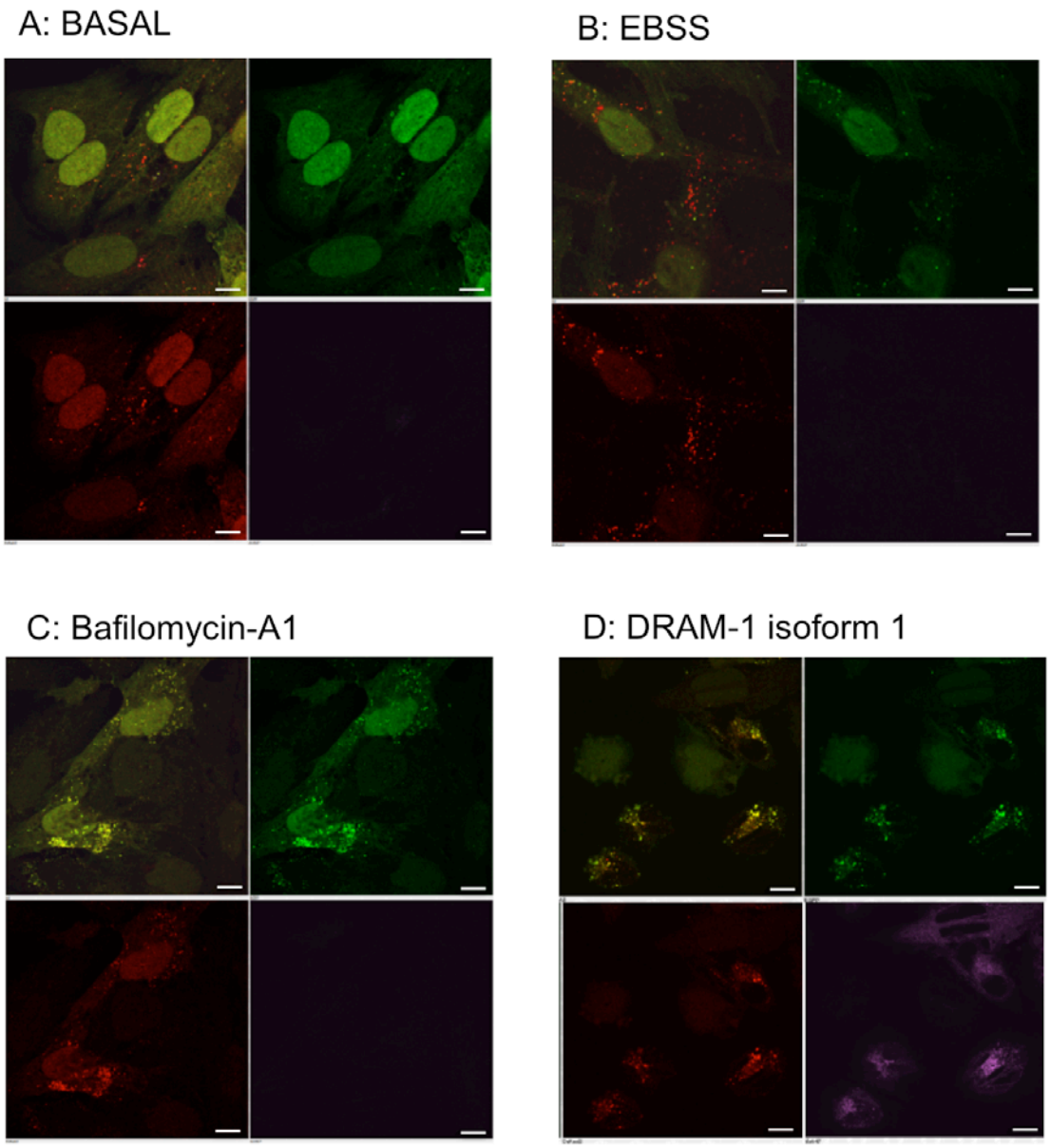

Figure 3.21(A-D): DRAM-1 isoform 1 enhances autophagsome biogenesis, but does not accelerate fusion with lysosomes
TetOn-DRAM-1 cells (Saos-2 cells which contain a tetracycline inducible DRAM-1 SV 1 transgene) were infected with the retrovirus construct carrying the tandem mRFP-GFP-LC3. Cells that constitutively express transgene is selected, and is infected with either empty vector, (A-C). DRAM-1 isoform 1 expression is achieved by treating the cells with 1µg/ml Doxycycline for 48 hours (D). Autophagy at basal level was reflected by (A). Autophagy completion is induced by starving the cells in amino acid-limiting conditions (EBSS) (B). Autophagosome and lysosome fusion is blocked by treating the cells with 100nM Bafilomycin-A1 for 4h (C). Scale bar represents 10µm. Magenta indicates the expression of DRAM-1 isoforms. Red and green indicate LC3 containing compartments. Yellow indicates LC3 II containing autophagosomes that are not fused to the lysosome.

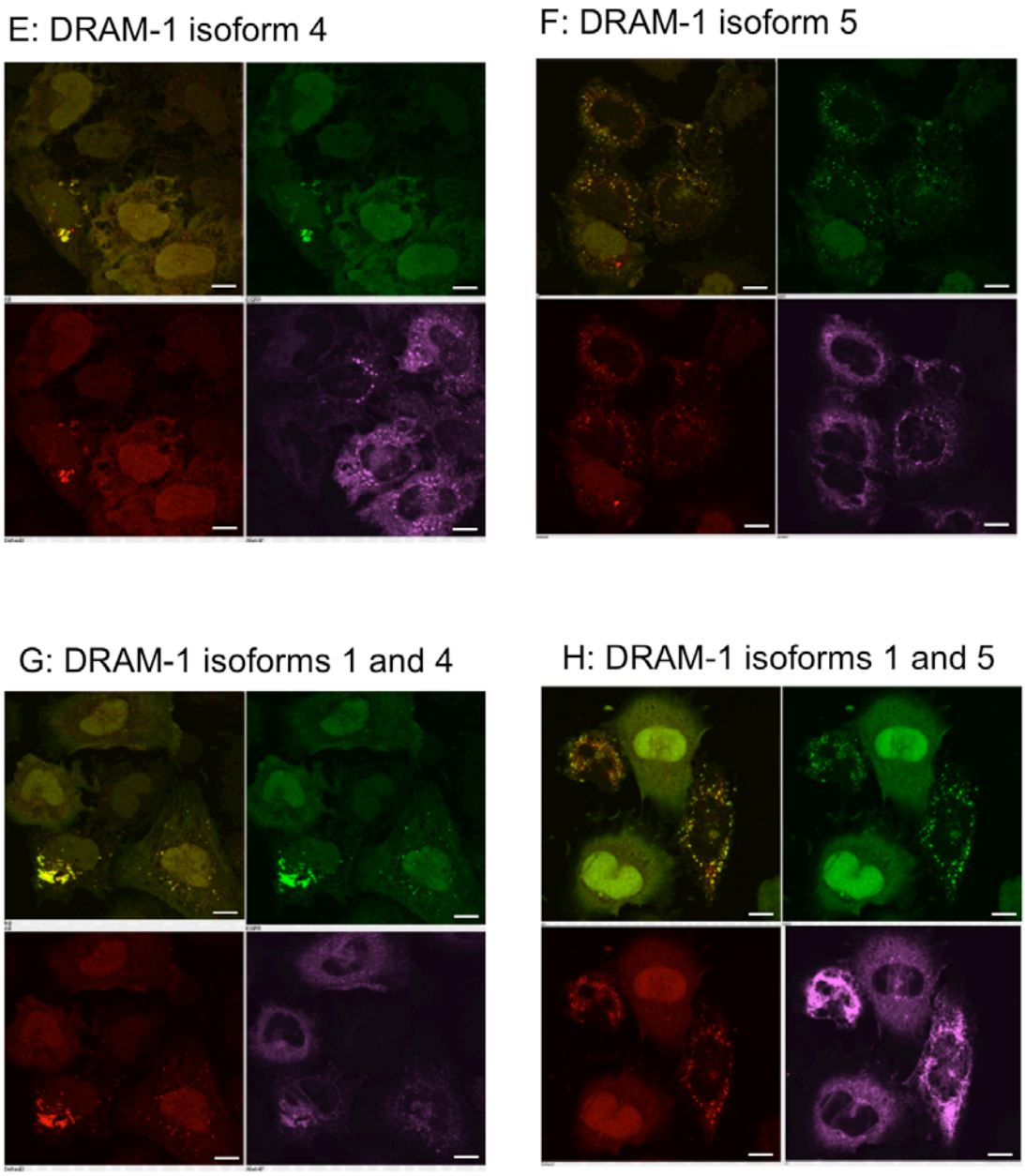

Figure 3.21(E-H): DRAM-1 isoforms 1, 4 and 5 enhance autophagsome biogenesis, but do not accelerate fusion with lysosomes
Tet-on DRAM-1 cells (Saos-2 cells which contain a tetracycline inducible DRAM-1 SV 1 transgene) were infected with the retrovirus construct carrying the tandem mRFP-GFP-LC3. Cells that constitutively express transgene is selected, and is infected with DRAM-1 isoform 4 (E) or DRAM-1 isoform 5 (F). At the same time, DRAM-1 isoform 1 expression is achieved by treating the cells with 1µg/ml of Doxycycline for 48 hours, and were simultaneously infected with either DRAM-1 isoform 4 (G) or DRAM-1 isoform 5 H). Scale bar represents 10µm. Magenta indicates the expression of DRAM-1 isoforms. Red and green indicate LC3 containing compartments. Yellow indicates LC3 II containing autophagosomes that are not fused to the lysosome.

DRAM-1 is required for p53-mediated long-lived protein degradation (Crighton, Wilkinson et al. 2006). In line with this, long-lived protein degradation assay was performed in conditions where DRAM-1 isoforms were ectopically overexpressed. Cellular proteins were labelled with the radioisotope ^{35}S by incorporation of the radioactive amino acids methionine and cysteine for 8 hours. Cells were subjected to an overnight cold chase and the rate of protein degradation was determined as follows:

$$\% \text{ protein degradation} = \frac{\text{Acid-soluble radioactivity in culture medium}}{\text{(Acid-soluble + acid precipitable radioactivity)}}$$

Despite their autophagic roles, long-lived protein turnover was not increased upon the ectopic overexpression of DRAM-1 isoforms (Fig. 3.22). This implies that ectopic overexpression of DRAM-1 isoforms does not modulate long-live protein turn over, in a p53-independent context.

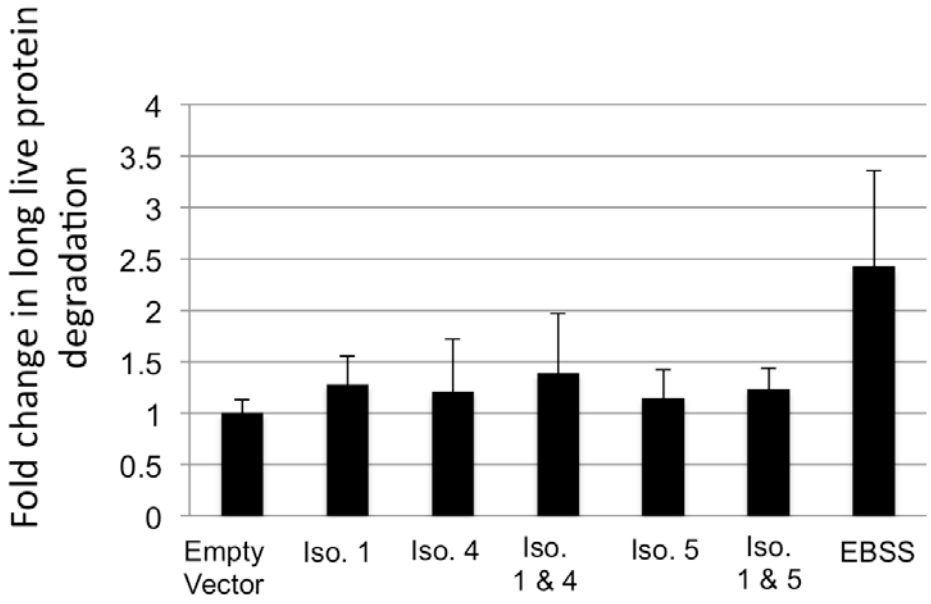

Figure 3.22: Ectopic overexpression of DRAM-1 isoforms do not enhance long-lived protein turn over

TetOn-DRAM-1 cells (Saos-2 cells which contain a tetracycline inducible DRAM-1 SV 1 transgene) were either infected with DRAM-1 isoforms 4, 5 or empty vector as control. At the same time, the cells were treated with 1µg/ml Doxycycline for 48 hours to induce DRAM-1 isoform 1 expression. Cells were labeled with radioactive cysteine and methionine for 8 hours, cold-chased for 16h and long-lived protein turnover was quantified. Cells were subjected to amino acid starvation by culturing them in EBSS for 8 hours as a positive control

Following from the above, the role of DRAM-1 isoforms 1, 4 and 5 in the regulation of reactive oxygen species (ROS) – one of the many signalling molecules involved in the autophagy cascade, was also studied. DRAM-1 inducible Saos-2 cells were treated with the Tetracycline analogue, Doxycycline (1µg/ml) for 48 hours to induce the expression of DRAM-1 isoforms 1, 4 and 5 (Fig. 3.23A). When expression of DRAM-1 isoforms were validated, these cells were incubated with 2',7' - dichloro-dihydrofluorescein diacetate (H_2-DCFDA), which was metabolised by non-specific esterases to the non-fluorescence product, 2',7' dihydrofluorescein (Bensaad, Cheung et al. 2009). 2',7' dihydrofluorescein is then subsequently oxidised to the fluorescent product, DCF, by ROS (Bensaad, Cheung et al. 2009). Ectopic overexpression of neither isoforms 1, 4 or 5 modulates basal and enhanced ROS levels upon treatment with hydrogen peroxide (H_2O_2) (Fig. 3.23B). These results indicate that ectopic expression of DRAM-1 isoforms does not modulate intracellular ROS levels.

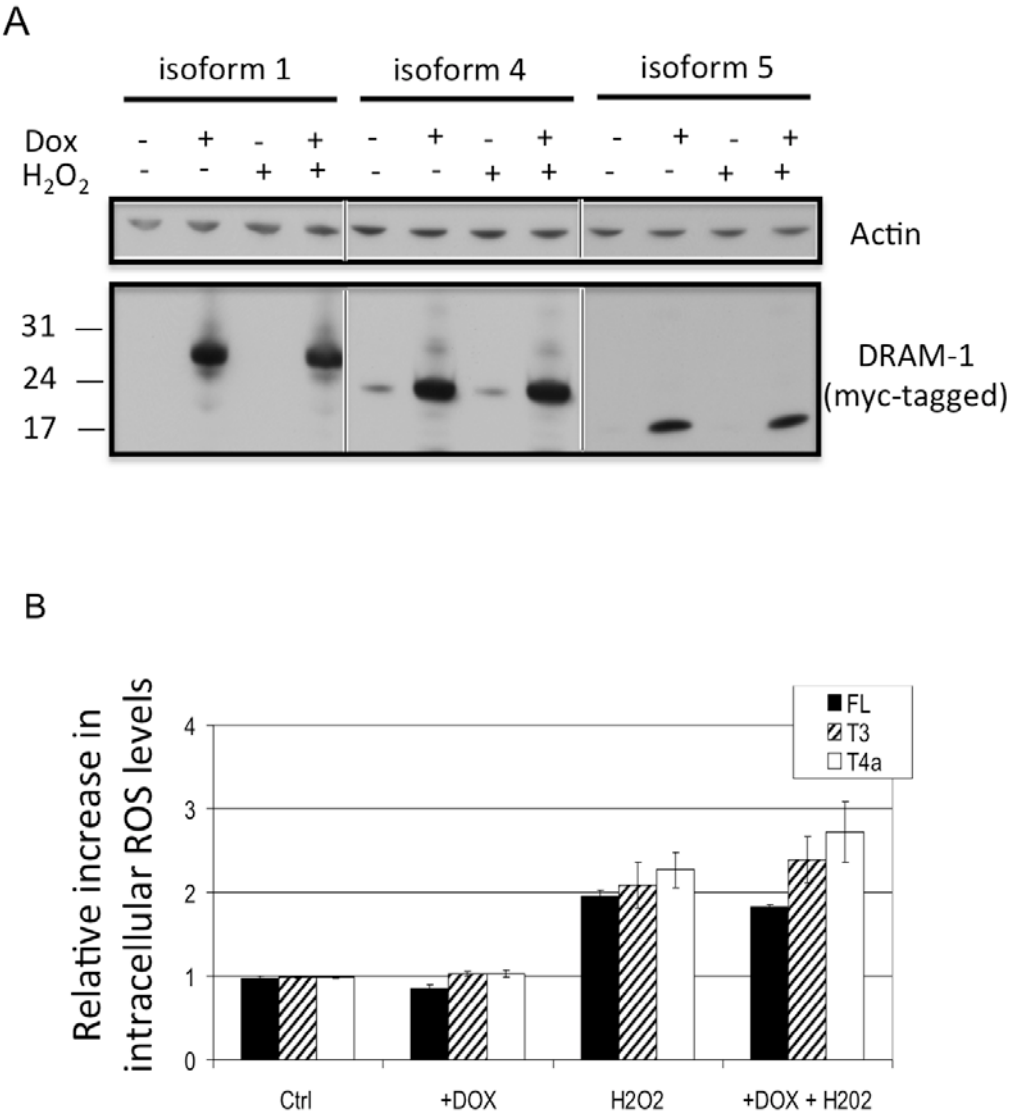

Figure 3.23: DRAM-1 isoforms 1,4 and 5 do not modulate basal and elevated ROS levels

Saos-2 cells harbouring the TetOn inducible myc-tagged DRAM-1 isoforms 1, 4 and 5 were treated with 1µg/ml Doxycycline for 48 hours.

(A) DRAM-1 isoform expression was validated by immunoblotting with myc and actin.

(B) ROS formation was quantified using dichloro-dihydrofluorescein diacetate (H_2-DCFDA), a marker of ROS and was quantified by flow cytometry.

3.2.4 Validation of DRAM-1 effects in mouse cells

We were also interested to know if the genetic ablation of *DRAM-1* affects the above characterised autophagy readouts associated with ectopic overexpression of DRAM-1 isoforms 1, 4 and 5. *DRAM-1* deletion was achieved by infecting *DRAM-1*$^{fl/fl}$ MEFs with a retrovirus expressing Cre recombinase (Fig. 3.24), and the similar autophagy assays were conducted.

Following the convincing LC3-I to –II conversion following forced expression of DRAM-1 isoforms, wild-type (DRAM-1$^{fl/fl}$) and *DRAM-1*-null (*DRAM-1*$^{-/-}$) MEFs were deprived of essential amino acids by culturing them in EBSS for four hours. Surprisingly, *DRAM-1* deletion does not impair the conversion of LC3-I to LC3-II when the cells were cultured in amino acid in limiting conditions (Fig. 3.25). This suggests that DRAM-1 is either functionally redundant, or that the loss of DRAM-1 can be compensated, perhaps by other members of the DRAM-1 family or autophagy regulators.

To validate that DRAM-1 does not play a role in long-live protein turnover, wild-type and *DRAM-1*-null MEFs were incubated with ^{35}S and subjected to a cold chase prior culture in EBSS. Acute *DRAM-1* deletion in *DRAM-1*$^{fl/fl}$ MEFs does not affect the basal levels of long-lived protein turnover, nor does it affect the ability of cells to degrade long-lived proteins upon amino acid starvation (Fig. 3.26), consistent with the above. This confirms that long-lived protein is not a substrate for DRAM-1 mediated autophagy, or that DRAM-1 is not required for long-lived protein degradation under amino acid limiting conditions.

Next in line, we were interested to determine if *DRAM-1* deletion affects basal or modulate elevated ROS levels, a well known signalling molecule for autophagy induction (Section 3.1). Wild–type and *DRAM-1*-null MEFs were incubated with hydrogen peroxide (H_2O_2) and H_2-DCFDA. Basal ROS levels were not affected by DRAM-1 status, and *DRAM-1* deletion does not affect H_2O_2 enhanced intracellular ROS levels (Fig. 3.27).

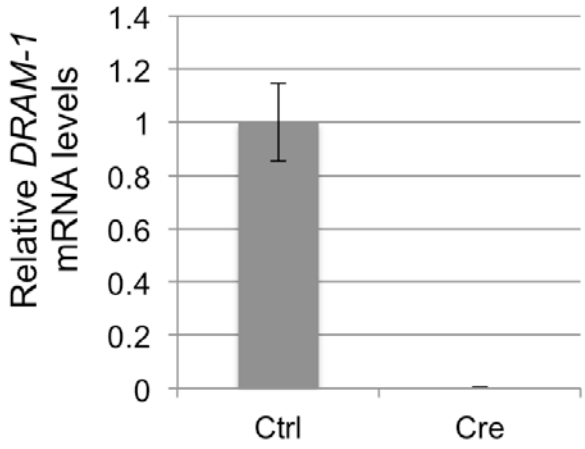

Figure 3.24: Excision of *DRAM-1* in *DRAM-1*$^{fl/fl}$ MEFs
DRAM-1 deletion in *DRAM-1*$^{fl/fl}$ MEFs. *DRAM-1*$^{fl/fl}$ MEFs were infected with retroviruses expressing Cre recombinase or empty vector (Ctr) as control. RNA lysates were harvested, and *DRAM-1* excision was validated by RT-PCR.

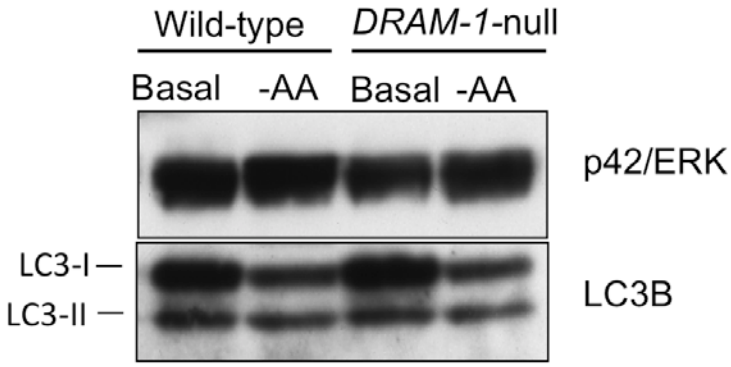

Figure 3.25: *DRAM-1* deletion in MEFs does not affect LC3 lipidation at basal and amino acid-limiting conditions
Wild-type and *DRAM-1*-null MEFs were cultured in complete DMEM (Basal) or in EBSS (-AA) for four hours. Protein lysates were analysed on a 12% SDS-PAGE gel and probed with LC3-B and p42/ERK

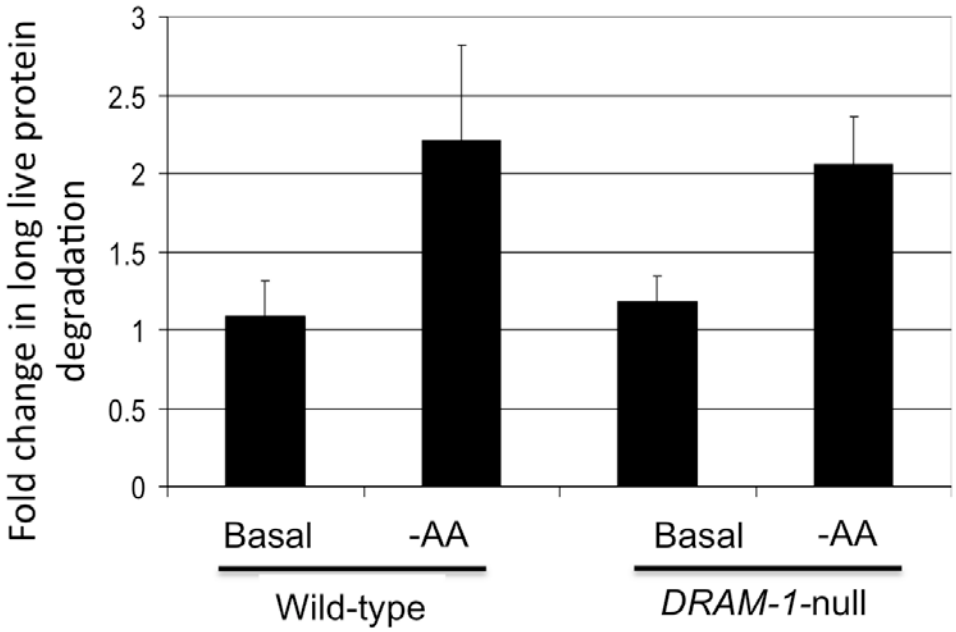

Figure 3.26: *DRAM-1* deletion in MEFs does not impair long-lived protein turnover at basal and amino acid limiting conditions
Wild-type and *DRAM-1*-null MEFs were cultured in complete DMEM (Basal) or in EBSS (-AA) for four hours. Long live protein turnover at basal and amino acid limiting conditions were measured as described.

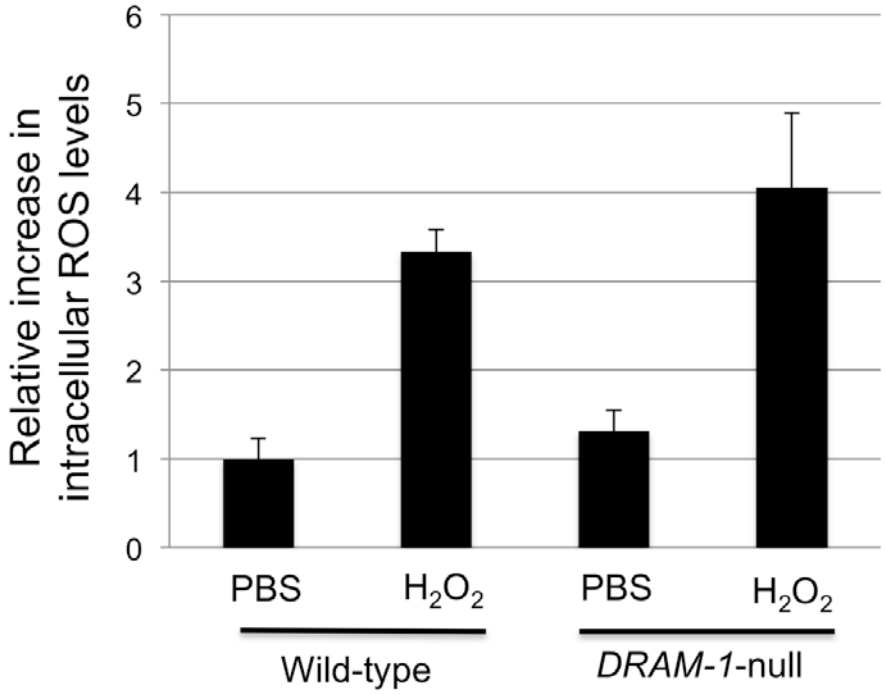

Figure 3.27: *DRAM-1* deletion in MEFs does not affect basal and elevated ROS levels

Wild-type and *DRAM-1*-null MEFs were incubated with H_20_2 or PBS to induce ROS formation, measured using dichloro-dihydrofluorescein diacetate (H_2-DCFDA), a marker for ROS and quantified by flow cytometry.

3.2.5 DRAM-1 isoforms do not induce programmed cell death

The overexpression of DRAM-1 isoform 1 (encoded by SV1) alone does not induce cell death (Crighton, Wilkinson et al. 2006). To investigate if isoforms 4 and 5 (encoded by SV 4 and 5 respectively) are functionally similar, isoforms 1, 4 and 5 were overexpressed alongside p53 at similar levels (Fig. 3.28A) for 48 hours, and assessed for the presence of cells with sub-G1 content – a marker for apoptosis. Although p53 causes significant cell death ($p<0.001$), neither of the DRAM-1 isoforms was able to induce cell death in this short-term assay (Fig. 3.28B). I also investigated if the overexpression of isoforms 1, 4 and 5 affected the long-term viability by monitoring their effects on clonogenic survival. Consistent with the short-term cell death data, neither of the DRAM-1 isoforms affected the clonogenic potential of the cells (Fig. 3.29).

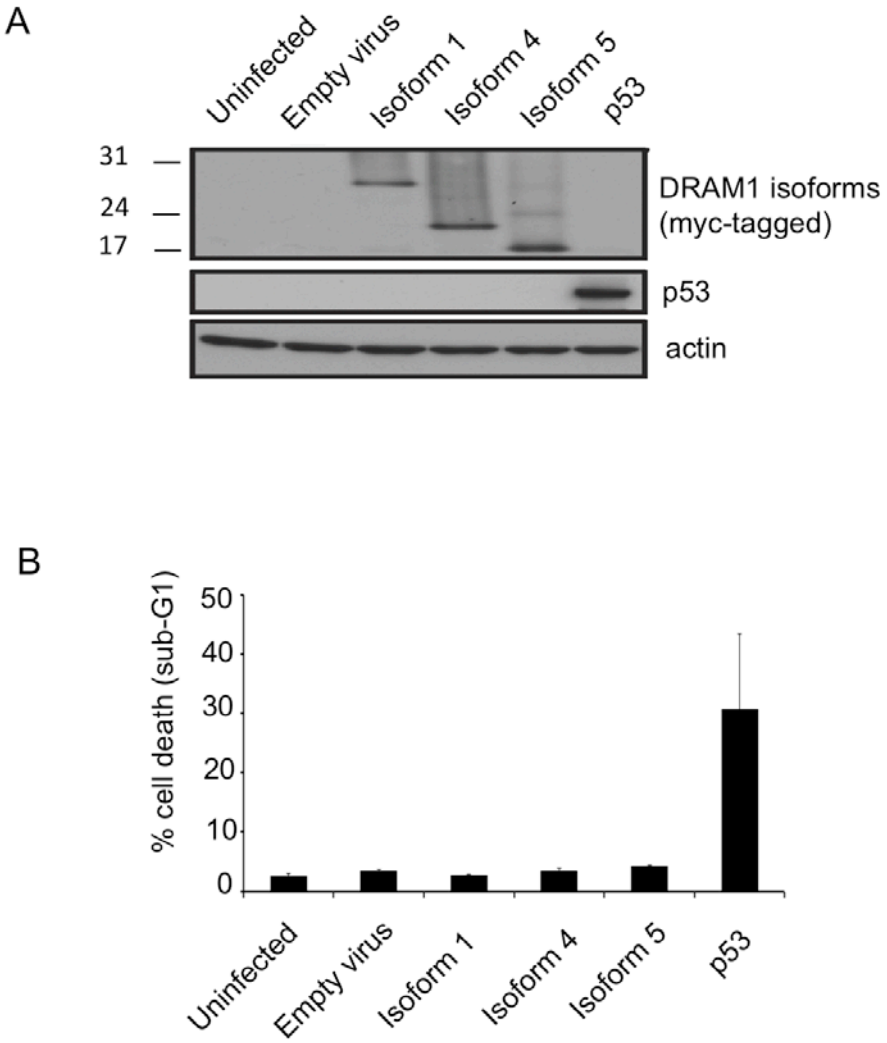

Figure 3.28: DRAM-1 isoforms 1, 4 and 5 do not induce cell death

(A-B) Saos-2 cells were infected with adenoviruses expressing DRAM-1 isoforms 1, 4, or 5, p53 (positive control) or empty vector (negative control).

(A) Protein expression of p53 and DRAM-1 isoforms was validated by western blotting

(B) Adherent and floating cells were harvested and the extent of cell death measured by flow cytometry for the percentage of cells with sub-G1 DNA content. The data represented are from 4 independent experiments and error bars indicate standard deviation (A).

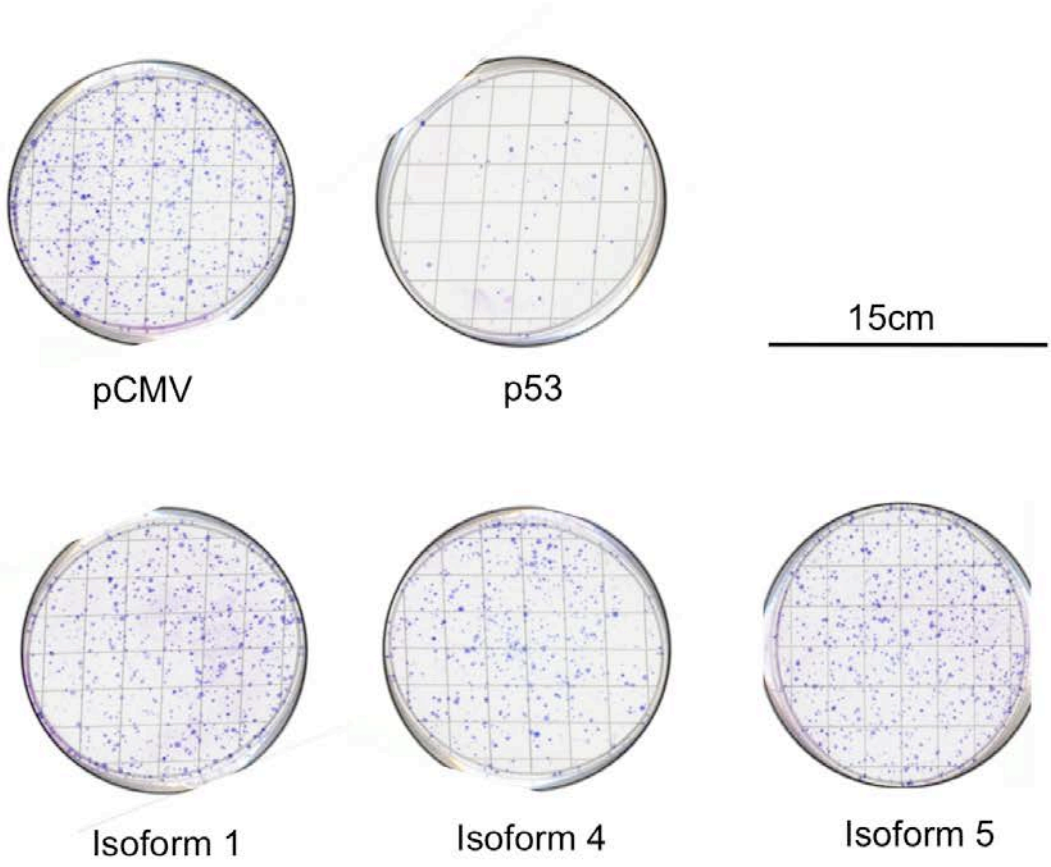

Figure 3.29: DRAM-1 does not affect the clonogenic survival of Saos-2 cells
Saos-2 cells were transfected with 10µg of either: DRAM-1 SV1, SV4 or SV5, p53 (positive control) or an empty plasmid (pCMV; negative control). After 48h, transfected cell populations were re-plated with fresh media containing G418 and assessed for clonogenic survival 2 weeks later.

DRAM-1 isoform 1 expression is required for the enhancement of p53-induced apoptosis, as siRNA ablation of all *DRAM-1* transcripts impeded the extent of cell death (Crighton, Wilkinson et al. 2006). p53 is activated by various forms of genotoxic stress (refer to section 1.7). Thus it is of no surprise that various DNA damaging agents share a common effect in the induction of p53 (Attardi, de Vries et al. 2004). Consistent with this, *DRAM-1* message levels were upregulated in various human cell lines – MDA-MB-231 (breast cancer carcinoma) ($p<0.05$), Saos-2 (*p53*-null osteosarcoma) ($p<0.10$) and U2OS (osteosarcoma) ($p<0.05$) that were treated with etoposide, a Topoisoerase II inhibitor which causes DNA damage and consequently apoptosis (Karpinich, Tafani et al. 2002) (Fig. 3.30).

To identify if any of these three isoforms play an individual role in p53-dependent cell death, *DRAM-1*$^{fl/fl}$ fibroblasts (MEFs) were infected with a retrovirus expressing the E1a oncogene fused to a portion of the estrogen receptor (E1aER). E1aER is bound and inactivated by hsp90 under basal conditions (Helgason, O'Prey et al. 2010). Upon treatment with 4-hydoxytamoxifen, hsp90 binding is abrogated, and E1a is active, sensitising the cells to death induced by the chemotherapeutic drug, doxorubicin (adriamycin) in a p53-dependent manner (Helgason, O'Prey et al. 2010). These E1aER-expressing cells were then sequentially infected with either DRAM-1 isoform 1, 4 and 5, or empty vector as control (Fig. 3.31A) and retrovirus expressing Cre recombinase to ablate all endogenous DRAM-1 expression, or empty retroviral vector as control (Fig. 3.31B). This panel of cells was treated with 4-hydoxytamoxifen and doxorubicin. Activation of E1a sensitised the control cells to doxorubicin and this effect was significantly reduced in cells where endogenous *DRAM-1* expression was loss following recombination when infected with Cre ($p=0.001$) (Fig. 3.31C). Rescue of this effect was not achieved by individual expression of either DRAM-1 isoforms 1, 4 or 5 (Fig. 3.31C), implying that neither of these isoforms, when expressed alone can reconstitute the role of DRAM-1 in p53-mediated programmed cell death.

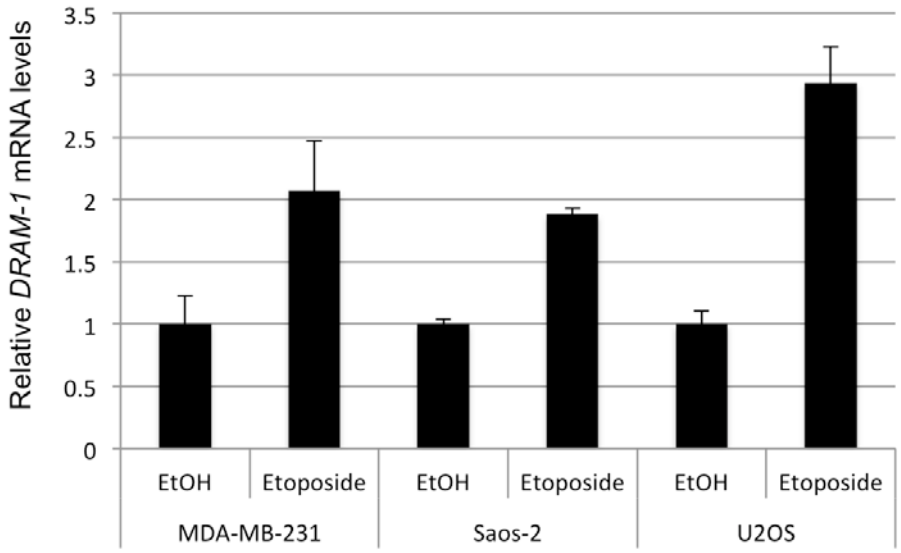

Figure 3.30: *DRAM-1* mRNA levels are upregulated upon exposure to DNA damaging agents

Cells were treated with ethanol (EtOH) as control or etoposide to induce DNA damage. Relative *DRAM-1* mRNA levels were determined by Real-Time PCR.

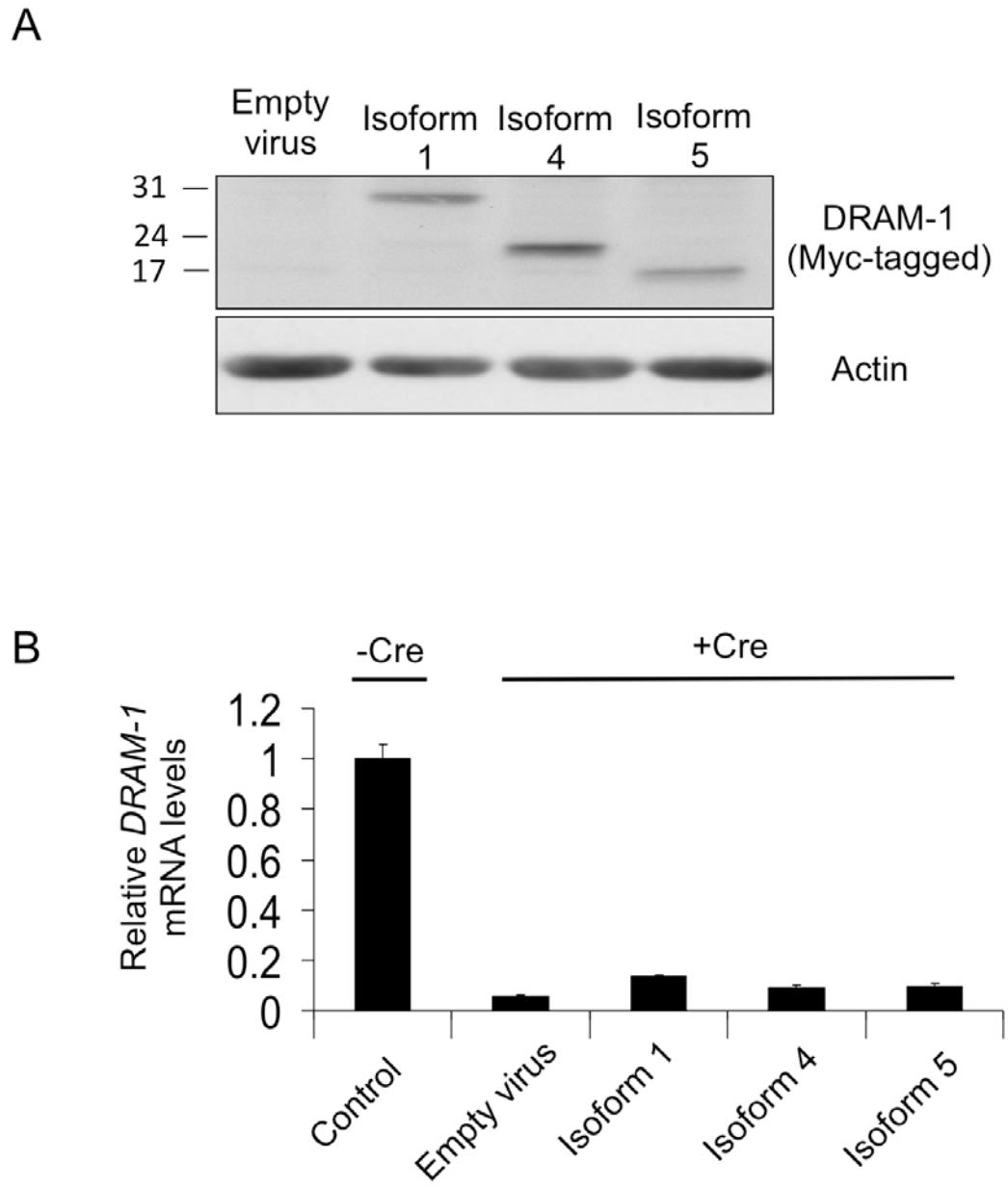

Figure 3.31(A-B): DRAM-1 isoforms 1, 4 or 5 cannot rescue the inhibition of oncogene-induced death caused by total loss of dram-1 expression

(A)DRAM-1$^{fl/fl}$ MEFs expressing the tamoxifen-inducible adenoviral oncoprotein E1A-ER were infected with DRAM-1 isoforms 1,4 and 5 or the empty retrovirus vector. Expression of DRAM-1 SV1, 4 and 5 were validated by western blot.

(B) These panels of cells were then infected with the Cre retrovirus (+Cre) or an empty retrovirus control (-Cre) to induce recombination. *DRAM-1* excision was validated at the message level by RT-PCR.

C

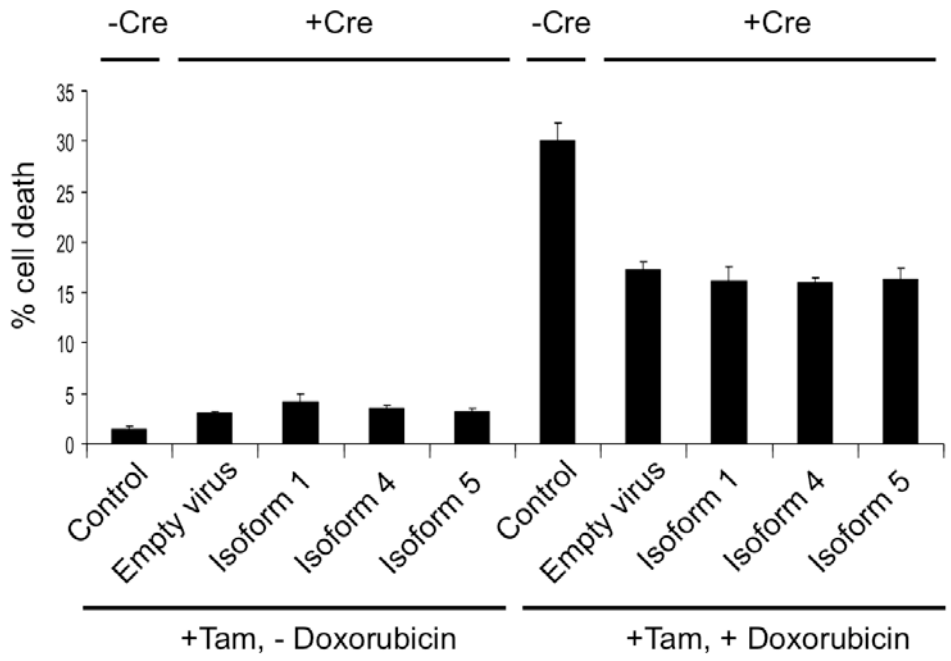

Figure 3.31C: DRAM-1 isoforms 1, 4 or 5 cannot rescue the inhibition of oncogene-induced death caused by total loss of dram-1 expression
MEFs were treated with 500nM of 4-hydroxytamoxifen (TAM) for 8 h to activate E1a in this system. The cells were then treated with 0.2 mg/ml doxorubicin. After 24 h, both adherent and floating cells were harvested and the extent of cell death measured by flow cytometry for the percentage of cells with sub-G1 DNA content.

3.2.6 DRAM-1 is required to sustain survival under nutrient-limiting conditions

Since DRAM-1 isoforms has been demonstrated to positively regulate autophagy, it would be interesting to know if DRAM-1 plays a pro-apoptotic or pro-survival role under nutrient stress. When cells were starved in amino-acid and glucose free medium, human DRAM-1 transcripts were upregulated in a time dependent manner (Mann-Whitney U test; $p<0.05$) (Fig. 3.32).

To elucidate whether DRAM-1 is required for cell death or survival in this context, *DRAM-1*$^{fl/fl}$ fibroblasts (MEFs) were infected with an empty vector, or a retrovirus expressing the Cre recombinase to delete endogenous *DRAM-1*. Wild-type (*DRAM-1*$^{fl/fl}$) and *DRAM-1*$^{-/-}$ MEFs were subjected to amino-acid and glucose starvation for 24h and 48h. Cells were then stained with the vital DNA intercalating dye - propidium iodide, which is taken up by dead cells that have lost their membrane permeability (Galluzzi, Aaronson et al. 2009). Live and dead cells were then quantified by flow cytometry. *DRAM-1*$^{-/-}$ MEFs were highly sensitised to both amino acid and glucose withdrawal (Fig. 3.33), suggesting that DRAM-1 is required for survival under nutrient limiting conditions.

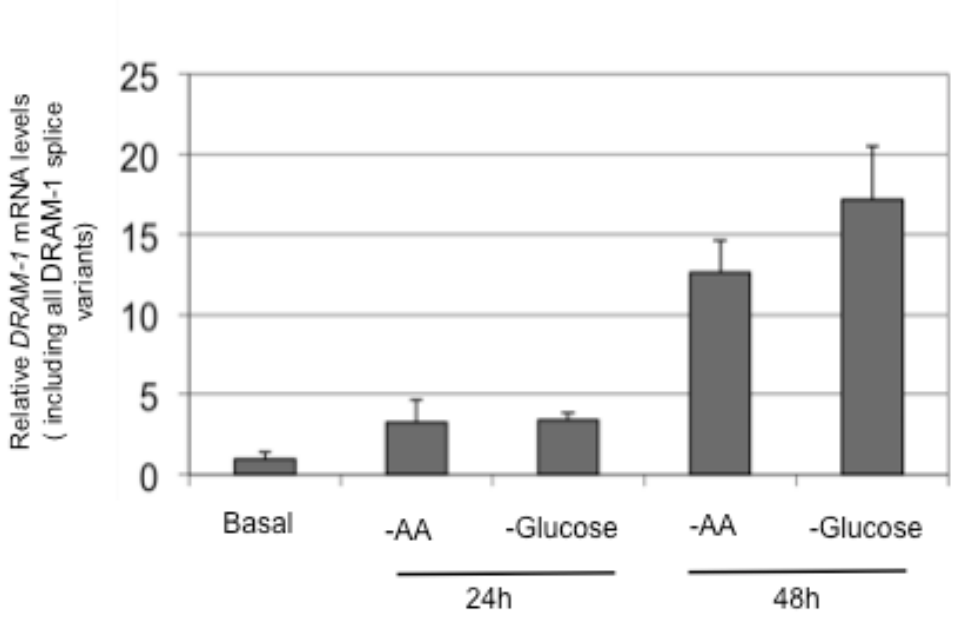

Figure 3.32*: DRAM-1* mRNA levels is upregulated in Saos-2 cells upon nutrient starvation

Saos-2 cells were cultured in complete DMEM (Basal) glucose- and amino-acid-limiting (-AA) conditions for 24 and 48 hours. Cells were harvested and relative expression of DRAM-1 was validated by RT-PCR.

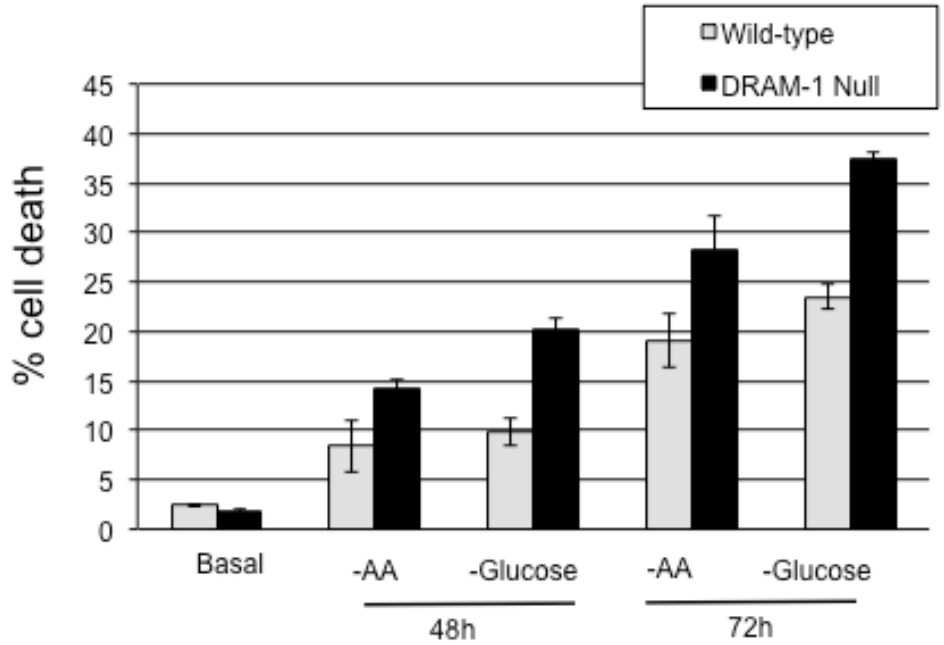

Figure 3.33: DRAM-1 deletion in MEFs sensitises them to cell death upon nutrient starvation

Wild-type and *DRAM-1*-null MEFs were cultured in glucose and amino acid-limiting conditions for 24 and 48 hours. Cells were harvested, and analysed for cell death using PI exclusion assay, as described in the previous section.

3.3 Discussion

DRAM-1 encodes a series of splice variants. In addition to the previously characterised autophagy modulator SV1, (Crighton, Wilkinson et al. 2006) we have identified eight other p53-inducible splice variants, all containing exons 1 and 7 but lacking different combinations of exons 2-6. These mRNA species are expressed at varying levels in multiple human cell lines, suggesting that the expression of DRAM-1 splice variants is widespread and that the relative importance of these isoforms is cell-type dependent. DRAM-1 splice variants are also present in mouse embryonic fibroblasts (MEFs) and are induced by p53, implying that the alternative splicing of *DRAM-1* is also present in higher eukaryotes. Of these 9 mRNA species, we have confirmed that only SV 1, 4 and 5 do not contain a pre-mature stop codon, and thus, were hypothesised to code for a functional protein. DRAM-1 isoforms 1, 4 and 5 contain the PYISD domain, which is critical for the induction of autophagy.

DRAM-1 isoforms were found to localise to different cellular compartments – isoform 1 in the golgi apparatus, endosomes, lysosomes and autophagosomes; isoform 4 partially in the ER and peroxisomes, and isoform 5 partially in the ER and autophagosomes. Both isoforms 4 and 5 are also partially diffused in the cytoplasm. Occasionally, isoform 4 is observed to form puncta in the cells. The conditions that result in the punctate staining pattern remains to be elucidated. Although all DRAM-1 isoforms are predicted to contain a cleavable ER-targeting signal, colocalisation studies revealed that only isoforms 4 and 5 were partially localised in the ER. This implies that only isoforms 4 and 5, but not isoform 1, are retained in the ER upon synthesis. A plausible explanation for this could be that the posttranslational modification of isoform 1 could be different to that of isoforms 4 and 5. As a consequence, the ER-signal peptide might be lost prior to complete protein translation. Further biochemical studies should be conducted to confirm this. Colocalisation studies also revealed that DRAM-1 isoforms 1 and 5, but not isoform 4, might potentially interact with the autophagy marker LC3B. This is consistent with the presence of the canonical WxxL LIR motif on isoform 1. The co-compartmentalisation of isoform 5 and LC3B suggests that Isoform 5 may potentially harbour a non-canonical LIR domain. In the future, the interaction between DRAM-1 isoforms and LC3B should be confirmed by performing

immunoprecipitation assays. Subsequently, the functional significance of this interaction is worth pursuing. The distribution of DRAM-1 isoforms in multiple cellular organelles suggests that autophagy and possibly other cellular effects brought upon by DRAM-1 activation is widespread and occurs in various organelles of the cell. These effects may be mediated by different DRAM-1 isoforms in their respective cellular compartments.

DRAM-1 isoform 1 turnover occurs in lysosomes as evident in the accumulation of protein levels when the lysosomal function is inhibited with Bafilomycin-A1. Bafilomycin-A1 is a vacuolar-H(+)-ATPase inhibitor which increases lysosomal pH and subsequently inactivates the majority of the pH-sensitive lysosomal enzymes, thus leading to a loss of lysosomal activity (Oda, Nishimura et al. 1991). On the other hand, DRAM-1 isoforms 4 and 5 are degraded in the proteasomes, as reflected in the massive accumulation of protein levels when the cells were treated with specific concentrations of cell permeable, reversible proteasomal inhibitor, MG132 (Tsubuki, Saito et al. 1996). Given that lysosomes degrade long-lived protein, whereas proteasomes primarily degrade ubiquitin-tagged short-lived proteins (Qiao and Zhang 2009), (Korolchuk, Mansilla et al. 2009) (Tsuchihara, Fujii et al. 2008), these findings indicate that DRAM-1 isoform 1 is relatively more stable, possibly with a longer half-life compared to isoforms 4 and 5. The proteasomal and lysosomal degradation pathways have been shown to cross-talk to each other to maintain protein homeostasis (Qiao and Zhang 2009). Additionally, pharmacological inhibition of proteasomal activities has been shown to upregulate the levels of lysosomal enzymes that may affect lysosomal transport of selected membrane-bound proteins (Qiao and Zhang 2009) (van Kerkhof, Alves dos Santos et al. 2001). Consistent with the compensatory upregulation of lysosomal activity when the proteasome is inhibited, the turnover of DRAM-1 isoform 1 is slightly enhanced, as evidenced by the subtle decrease in protein levels upon proteasomal inhibition.

Despite lacking the putative WxxL LIR domain (Kirkin, Lamark et al. 2009), DRAM-1 isoforms are functionally similar in terms of autophagy modulation. DRAM-1 isoforms 1, 4 and 5 promote the initial stage of autophagy by inducing autophagosome biogenesis, as reflected by the formation of GFP-LC3 puncta and LC3-I to -II conversion, with isoform 1 evoking a stronger effect compared to isoforms 4 and 5. As such, there could be other non-canonical LIR domains

present on DRAM-1 isoforms 4 and 5, which enables weaker interactions with LC3. This could explain the weaker LC3 lipidation by isoforms 4 and 5. The accumulation of LC3-II may simply imply an enhanced autophagic activity, indicated by an increase in autophagosome formation, or autophagy inhibition when the fusion of autophagosomes to lysosomes is blocked, thus preventing LC3 turnover. Hence, it is crucial to measure autophagic flux by comparing LC3-II levels in the presence and absence of lysosomal protease inhibitors (Mizushima and Yoshimori 2007). As expected of autophagy promoters, LC3-II levels are further enhanced upon lysosomal inhibition in cells overexpressing DRAM-1 isoforms 1, 4 and 5.

The simultaneous overexpression of DRAM-1 isoforms does not promote further accumulation of LC3–II compared to individual overexpression of isoform 1. This suggests that DRAM-1 isoforms 1, 4 and 5 may work independently of one another to promote autophagy.

DRAM-1 isoforms 1, 4 and 5, whether expressed individually or simultaneously, only increase the amount of autophagosomes, but not autolysosomes. This implies that DRAM-1 only modulates the earlier stages of autophagy comprising autophagosome formation, but not fusion with lysosomes. DRAM-1 isoforms are likely potent inducers of autophagosome biogenesis, and the rate of formation is so rapid that it exceeds the fusion with lysosomes.

Despite the fact that DRAM-1 plays an important role in mediating p53-induced autophagy (Crighton, Wilkinson et al. 2006), genetic ablation of *DRAM-1* in MEFs does not affect basal autophagy or starvation-induced autophagy. Wild-type and *DRAM-1*-null MEFs were able to promote LC3-I to LC3-II conversion when cultured under amino-acid limiting conditions (EBSS). This indicates that DRAM-1, like another autophagy modulator, Head Involution Defective (HID) (Juhasz and Sass 2005), and possibly other autophagy regulators that are yet to be identified, can induce but is not required for autophagy activation. This can be attributed to the fact that loss of DRAM-1 can be compensated for by the other DRAM family members, namely DRAM-3, DRAM-4 and DRAM-5 (O'Prey, Skommer et al. 2009).

Having seen the encouraging effects on LC3, the ectopic overexpression of DRAM-1 isoforms does not enhance long-lived protein degradation. Consistent

with this, acute *DRAM-1* deletion in mouse embryonic fibroblast (MEFs) does not affect long-lived protein turnover under basal and nutrient limiting conditions. This suggests that the substrate(s) for DRAM-1-mediated autophagy may differ from those degraded in the canonical starvation-induced autophagy. Alternatively, the cargoes for DRAM-1 might be highly specific, and thus the ectopic overexpression of DRAM-1 may only affect the autophagy adapter protein, LC3. Forced expression of DRAM-1 does not appear to modulate basal or enhanced ROS levels. Likewise, ectopic expression and acute loss of *DRAM-1* in these cells do not affect ROS levels under similar conditions. This implies that the mechanism by which DRAM-1 induces autophagy is ROS-independent. Considering these, it seems that DRAM-1 is a highly specific autophagy modulator, which responds or signals to a narrow range of stimuli and signalling molecules, and affects only a very limited range of substrates, one of them being LC3. Recently, p62 has also been demonstrate to be yet another substrate for DRAM-1 in the execution of autophagy. Galavotti et al. (2012) showed that DRAM-1 is critical for the localisation of p62 to autophagosomes to evoke autophagy. Additionally, the acute silencing of either of these two autophagy modulators in glioblastoma stem cells (GSCs) decreased cellular ATP levels and impaired the invasive and metastatic potentials of these cells (Galavotti, Bartesaghi et al. 2012). Following on from this, it is worthwhile to identify other DRAM-1 interactors, effectors and the autophagic substrates.

DRAM-1 is pro-apoptotic under several conditions. The simultaneous overexpression of DRAM-1 and DRAM-2 induces cell death in a range of human tumour cell lines (Park, Kim et al. 2009). Furthermore, DRAM-1 is required for effective p53-dependent apoptosis by mediating the release of cytochrome *c* from the mitochondria (see section 1.8.1) (Crighton, Wilkinson et al. 2006). We have shown that the role of DRAM-1 in enhancing p53-mediated cell death is conserved, at least, across higher eukaryotes. The acute deletion of *DRAM-1* in mouse embryonic fibroblasts (MEFs) caused a marked reduction in cell death when endogenous p53 levels were upregulated upon treatment with the DNA damaging agent adriamycin (doxorubicin). Doxorubicin is a chemotherapeutic drug that is often used in combination with radiotherapy to treat cancer patients. (Kim and Leeper 1987). However, the ectopic expression of neither DRAM-1 isoforms 1, 4 or 5 alone was able to restore optimum cell death. This suggests that more than one isoform of DRAM-1 is required for effective p53 killing.

Consequently, the mechanism by which DRAM-1 contributes to cytochrome *c* release and cell death downstream of p53 remains to be elucidated. Elegant *in vivo* studies in mice by Mihara et. al (2003) have shown that the translocation of p53 to mitochondria is sufficient to induce apoptosis in the thymus upon exposure to ionising gamma irradiation. They also showed that p53 can directly provoke the permeabilisation of the outer mitochondrial membrane by co-complexing with the anti-apoptotic Bcl-X_L and Bcl-2 proteins to facilitate cytochrome c release (Mihara, Erster et al. 2003). In line with this, it might be interesting to investigate if DRAM-1 mediates the translocation of p53 to the mitochondria to bring about cell death, and the subsequent effects on Bcl-X_L and Bcl-2 proteins. Additionally, the mode of action in which DRAM-1 induces p53-dependent cell death is independent of caspases (Crighton et. al, 2006). Caspase-independent cell death (CICD) may be triggered by several stimuli, such as mitochondrial outer membrane permeabilisation, which results in the release of cytochrome c from the mitochondrial intermembrane space (IMS) (Tait and Green 2008). Besides cytochrome *c*, numerous IMS proteins such as Smac/Diablo, HtrA2/Omi, Endonuclease G (Endo G) and apoptosis-inducing factor (AIF) are also released, and these proteins have also been proposed to actively induce CICD, as reviewed by Tait and Green (2008). Thus, it seems worthwhile to investigate whether DRAM-1 might mediate the release of these factors, in addition to cytochrome *c* in order to characterise the pathways downstream of these factors in evoking p53-dependent apoptosis. Yet another possibility by which DRAM-1 mediates cell death is by inducing autophagy, which may subsequently facilitate p53-dependent apoptosis. Since the simultaneous silencing of *DRAM-1* and *Atg5* does not cause a greater reduction in death than the individual knockdown of *DRAM-1* (Crighton et. al, 2006), it remains possible that DRAM-1 may act upstream of ATG5 to evoke autophagy and subsequently cell death. The interplay of other autophagy regulators that are involved in the autophagic machinery upstream of ATG5 such as Beclin 1 and ATG 101 (see section 1.2) merits further investigation.

DRAM-1 message level was upregulated when cells were subjected to nutrient stress. In this context, *DRAM-1* deletion in MEFs sensitised the cells to death upon amino acid and glucose withdrawal. Given that *DRAM-1-null* MEFs were able to induce LC3 lipidation upon amino-acid starvation (Fig. 3.25 and Fig. 3.26), the requirement for DRAM-1 to promote survival under nutrient-limiting conditions is likely to be independent of autophagy. This implies that there are potentially other

cellular mechanism(s) that are disrupted upon the loss of DRAM-1, which sensitise cells to die under nutrient stress. For instance, serum-starvation has been reported to induce the cleavage of poly (ADP-ribose) polymerase (PARP), the full-length procaspase-3 and procaspase-9, as well as causing decreased expression of endogenous Bid, a BH-3-only proapoptotic protein of the Bcl-2 family (Goyeneche, Harmon et al. 2006). Although the involvement of autophagy in this context is not reported, the role of DRAM-1 in response to nutrient starvation in the regulation of intrinsic, as well as extrinsic apoptosis and other forms of cell death such as necrosis is worth investigating.

In conclusion, results from this section suggest that *DRAM-1* transcripts encode for specific regulators of autophagy, which also participate in p53-mediated cell killing. Given that DRAM-1 SV1, SV4 an SV5 were identified by primers spanning the first and the last exon (exon 7) of the transcript, it remains plausible that there could be other splice variants of *DRAM-1* which do not contain either of the exons 1 and 7, which still might regulate autophagy, cell death or other functions which are yet to be elucidated. Additionally, the cellular effects driven by DRAM-1 expression is hypothesised to require the participation of multiple isoforms of DRAM-1. Since the overexpression of DRAM-1 induces autophagosome formation, it remains highly plausible that DRAM-1 might regulate other autophagy effectors, such as mTOR and the panel of ATG proteins which are involved in the earlier stages of autophagy preceding autophagosome maturation, and is worth investigating.

Chapter 4: Characterisation of conditional DRAM-1 knockout mice

4.1 Introduction

The use of the bacterial- (Cre/*loxP*) and yeast-derived (FLP/*frt*) site-specific DNA recombination systems has facilitated the development of conditional knockout mice models (Vooijs, Jonkers et al. 2001). For instance, the development of the Cre Deleter strain that is driven by the CMV promoter, enables the ubiquitous deletion of a gene flanked by *loxP* sites (Artemis Pharmaceuticals/Taconic).
However, this strategy is not ideal, as the onset of Cre expression may occur at an early developmental period in which the gene is required, thus leading to the accumulation of phenotypic aberrations which may complicate the analysis of later developmental stages, and occasionally may lead to death (Vooijs, Jonkers et al. 2001).

This has prompted the development of spatial and temporal control of Cre-mediated recombination models (Vooijs, Jonkers et al. 2001). For instance, intestinal and liver inducible Cre can be driven using the Cyp1A1 (cytochrome p450 subfamily A1) (Ireland et al., 2004). The Cyp1A1 promoter which is usually transcriptionally inactive, is upregulated upon exposure to lipophilic xenobiotics, such as β- naphthoflavone and binds to the cytoplasmic Aryl Hydrocarbon receptor (hence termed AhCre), allowing it to translocate to the nucleus where it form complexes with other factors to facilitate DNA binding and subsequently transcription (Ireland, Kemp et al. 2004). Alongside this, many mouse models of diseases have been developed to unravel the signalling pathways that are altered in human diseases.

To complement our *in vitro* findings, we have extended our studies of DRAM-1 *in vivo.* In this context, we were interested to determine if the ubiquitous deletion of *DRAM-1* is embryonically lethal, and if DRAM-1 is required for normal organ development. In line with this, *DRAM-1* flox-flox mice were crossed to CMV Cre Deleter to delete DRAM-1 in the whole body. Subsequent to this, we wanted to determine if *DRAM-1*-null mice are predisposed to diseases that arose from autophagy deficiency. Given that DRAM-1 has been shown to enhance p53-

dependent apoptosis *in vitro*, we were also interested to determine if the deletion of *DRAM-1* can modulate p53-dependent and –independent cell death *in vivo*. To address this, wild-type and *DRAM-1*-null mice were exposed to 14 Gy of gamma-irradiation and the small intestines were harvested from these mice after 6h and 24h to assess for apoptosis; and 48h and 72h to assess for regeneration. Additionally, since *DRAM-1* mRNA levels were down regulated in various forms of human cancer (Crighton, Wilkinson et al. 2006), we were also interested to determine if the ubiquitous loss of DRAM-1 predisposes to the development of cancer upon exposure to low dose of gamma-irradiation. Finally, since human *DRAM-1* is upregulated by various cytokines (refer to section 5.2.1), we were interested to determine if the whole-body deletion of *DRAM-1* in mice can modulate the inflammatory response in the colon, as well as inflammation-driven tumourigenesis.

In addition, we wanted to investigate if DRAM-1 is required for p53-mediated senescence in the liver. In this context, MDM2 flox/flox mice harbouring either both copies of the wild type (DRAM-$1^{+/+}$) and DRAM-1 flox/flox alleles were crossed to the AhCre Deleter to drive specific excision of DRAM-1 and MDM2 primarily in the small intestine and liver. The deletion of *MDM2* would result in an increase in p53 levels in the small intestine and the liver, which will enable us to study apoptosis and senescence both in the presence and absence of DRAM-1 (see sections 4.2.2 and 4.2.4 for detailed explanation).

4.1.1 The intestinal crypt as a model to examine apoptosis in vivo

The intestinal tract is composed of three tissue layers – the smooth muscles which enable peristalsis, the stromal muscles and the mucosa layers which comprise of epithelial cells for nutrient absorption (Sancho, Batlle et al. 2004). The epithelium is further characterised by the presence of numerous finger-like protrusions, termed villi, and crypts of Lierberkuhn (Sancho, Batlle et al. 2004). The base of the intestinal crypts constitutes of columnar and antimicrobial peptide and enzyme-secreting paneth cells (Porter, Bevins et al. 2002). Intestinal stem cells, which differentiate into daughter progenitor cells, are found directly above the paneth cells (Hocker and Wiedenmann 1998).

Actively cycling murine intestinal stem cells are identified by leucine-rich repeats containing G-protein coupled receptor 5 (Lgr5), Achaete scute-like 2 (Ascl2) and olfactomedin 4 (Olfm4) expression; whereas slowly cycling stem cells are marked by B cell-specific Moloney murine leukemia virus integration site 1 (Bmi1) and Telomerase Reverse Transcriptase (mTert) (Dehmer, Garrison et al. 2011). Lgr5 was most exclusively expressed in cells intermingled with paneth cells, whereas OLFM4, which display a membranous-staining pattern, is enriched at the bottom of crypts and is expressed to varying degrees above the paneth cell compartment (Munoz, Stange et al. 2012).

These progenitor cells differentiate to form three distinct cell lineages that populate the villus - the enterocytes, which produce hyrdrolases and absorb nutrients; goblet cells which secrete a protective mucous lining, and the enteroendocrine cells which secrete hormones (Hocker and Wiedenmann 1998). It was later revealed that the crypt progenitor cells divide every 12-16 hours to form 200 cells per crypt daily (Sancho, Batlle et al. 2004).

The small intestine is a well characterised model to study DNA damage response *in vivo.* It is highly sensitive to DNA damage-induced apoptosis, and has a high regenerative capacity, which is attributed to the presence of a population of intestinal stem cells (Potten 1998). Upon the deletion of these stem cells, there exists another population of 30-40 clonogenic cells that can repopulate the intestinal crypt in a hierarchical manner, with increasing numbers of new cells being recruited after 1, 8 and 15 Gy of gamma-irradiation (Roberts and Potten 1994). The recruitment and clonogenic repopulation of the crypt is characterised by a marked burst of proliferation within the crypt, thus leading to transient crypt enlargement (Ijiri and Potten 1986). Various cytotoxic agents such as gamma-irradiation (8 Gy and higher) induce apoptosis in the intestinal crypts, with a peak induction at 6-12 hours following DNA damage, and this early wave of apoptosis is mediated by the activation of p53 (Sansom and Clarke 2000) (Potten, Merritt et al. 1994). There is also a second wave of apoptosis at 24 hours following DNA damage (Merritt, Allen et al. 1997). This form of cell death is independent of p53 and is proposed to be attributed to aberrant mitosis post gamma-irradiation (Merritt, Allen et al. 1997).

4.1.2 The colon as a model to examine inflammation *in vivo*

The colon epithelium contains crypts and Lgr5 positive stem cells at the bottom of the crypts, but has a flat surface rather than protruding villi (Sancho, Batlle et al. 2004) (Barker, van Es et al. 2007). The epithelium comprises two main differentiated cell types - the absorptive colonocytes and the goblet cells (Sancho, Batlle et al. 2004)

Animal models of intestinal inflammation have greatly facilitated our understanding of the pathogenesis of Crohn's disease and ulcerative colitis, two of the most common form of inflammatory bowel disease (IBD) in human (Wirtz, Neufert et al. 2007).One of the most established models of inflammation is the dextran sulfate sodium (DSS) colitis model, in which mice are fed with the DSS polymer to stimulate the development of acute colitis characterized by bloody diarrhoea, ulcerations and infiltrations of immune cells (Okayasu, Hatakeyama et al. 1990). DSS is proposed to be toxic to gut epithelial cells of the basal crypts and disrupts the integrity of the mucosal barrier (Wirtz, Neufert et al. 2007). When the integrity of this layer is compromised, pathogens can easily can access into the inflamed niche, resulting in colon inflammation (Wirtz, Neufert et al. 2007). Myeloperoxidase (MPO) is an enzyme that is found in the lysosomes of neutrophil, and is often used as a marker for neutrophil infiltration (Roncucci, Mora et al. 2008). MPO activity has been described to be upregulated in mouse models of colon inflammation (Yamada, Marshall et al. 1992), and is now used as an established marker to monitor intestinal inflammation (Galvez, Garrido et al. 2000).

4.1.3 Mouse models of radiation- and inflammation-induced tumorigenesis

The oncogenic effects of radiation in humans and mice have been extensively studied. The loss of *p53* greatly accelerate the development of lymphoma and other forms of cancer upon exposure to ionising radiation (Kemp, Wheldon et al. 1994). Apoptosis elicited by p53 upon DNA damage mediates the removal of cells that potentially carry mutation(s) to prevent tumourigenesis (Michalak, Jansen et al. 2009). However, regeneration normally follows apoptosis, and the repeated deletion and regeneration of tissues can lead to tumour promotion (Labi, Erlacher et al. 2010). This phenomenon also enhances the propagation of treatment-resistant cancer cells during anti-cancer therapy (Allan and Travis 2005).

Inflammation and tumourigenesis are inherently linked. The infiltration of lymphocytes and the secretion of chemokines have been proposed to be a driving factor for tumour maintenance and progression (Mantovani, Allavena et al. 2008). In line with this, patients with inflammatory bowel disease (IBD) have an increased risk of developing colorectal cancer (Clapper, Cooper et al. 2007). Following from the previous section, DSS in combination with carcinogens such as azoxymethane (AOM) have been demonstrated to enhance tumour incidence, multiplicity and lesion progression in mice, and is a well characterised model for inflammation-driven tumourigenesis (De Robertis, Massi et al. 2011). The major mechanism in the AOM-induced colon carcinogenesis model is the aberrant activation of Wnt signaling which is caused by accumulation of beta-catenin. Apart from *beta-catenin*, *k-ras* is also frequently mutated in this model (Takahashi and Wakabayashi 2004).

4.2 Results

4.2.1 Characterisation of *DRAM-1* knockout mice

Wild-type, heterozygotes and whole body *DRAM-1* knockout mice were generated from a starting cross between DRAM-1 flox/flox (*DRAM-1*$^{fl/fl}$) and Cre Deleter (*Cre*$^{+}$) mice (refer to section 2.3.1). Accordingly, four independent *DRAM-1*$^{+/-}$ intercrosses yielded *DRAM-1*$^{-/-}$ mice in the expected Mendelian ratio [6 *DRAM-1*$^{+/+}$: 14 *DRAM-1*$^{+/-}$: 9 *DRAM-1*$^{-/-}$; Chi-square value = 0.655, p = 0.9] (For calculations, refer to Fig. 4.1). There was also no difference in the number of *DRAM-1*$^{+/+}$, *DRAM-1*$^{+/-}$, *DRAM-1*$^{-/-}$ female and male pups that were born. Thus, *DRAM-1* is deletion is not embryonic lethal, and does not affect neonatal survival. *DRAM-1*-null mice are viable, fertile, and appeared normal, with no obvious phenotypic defects compared to wild-type and heterozygote controls up to 650 day of age (Analysis were verified by Dr. Ayala King, in-house veterinarian, The Beatson Institute for Cancer Research).

DRAM-1 mRNA level has been shown to be downregulated in preleukemic hematopoietic stem cells knocked down for the transcription factor PU.1 (Steidl, Rosenbauer et al. 2006) PU.1 is a transcription factor which is required for myelomonocytic differentiation during normal haematopoiesis (Steidl, Rosenbauer et al. 2006). This suggests that DRAM-1 could be required for haematopoiesis. To investigate this, *DRAM-1*$^{+/+}$ and *DRAM-1*$^{-/-}$ mice at the age of 3 months old were culled, and circulating blood from these mice was harvested and subjected to peripheral blood smear analysis. The number of circulating lymphocytes and platelet per volume of blood is significantly lower in *DRAM-1*-null mice (Fig. 4.2A and 4.2B). However, the number of circulating red blood cells, and the remaining white blood cells - neutrophils, monocytes and eosinophils is indistinguishable between wild-type and *DRAM-1*-null mice (Fig. 4.2C - 4.2F).

A

Formula to calculate Chi-Square (X^2) value

$$\chi^2 = \Sigma \frac{(\text{observed} - \text{expected})^2}{\text{expected}}$$

Probability table

df	Probability (P)									
	0.995	0.99	0.975	0.95	0.9	0.1	0.05	0.025	0.01	0.005
1	---	---	0.001	0.004	0.016	2.706	3.841	5.024	6.635	7.879
2	0.01	0.02	0.051	0.103	0.211	4.605	5.991	7.378	9.21	10.597
3	0.072	0.115	0.216	0.352	0.584	6.251	7.815	9.348	11.345	12.838
4	0.207	0.297	0.484	0.711	1.064	7.779	9.488	11.143	13.277	14.86
5	0.412	0.554	0.831	1.145	1.61	9.236	11.07	12.833	15.086	16.75
6	0.676	0.872	1.237	1.635	2.204	10.645	12.592	14.449	16.812	18.548
7	0.989	1.239	1.69	2.167	2.833	12.017	14.067	16.013	18.475	20.278
8	1.344	1.646	2.18	2.733	3.49	13.362	15.507	17.535	20.09	21.955
9	1.735	2.088	2.7	3.325	4.168	14.684	16.919	19.023	21.666	23.589
10	2.156	2.558	3.247	3.94	4.865	15.987	18.307	20.483	23.209	25.188
	Not Significant					Significant				

df = Degrees of freedom

Adapted from Lobo, 2008

B

	+/+	+/-	-/-
Observed	6.00	14.00	9.00
Expected Ratio	1.00	2.00	1.00
Expected Numbers (E)	7.25	14.50	7.25
O-E	-1.25	-0.50	1.75
$(O-E)^2$	1.56	0.25	3.06
$(O-E)^2/E$	0.22	0.02	0.42

$X^2 = 0.22 + 0.02+0.42 = 0.66$

$X^2 = 0.66 < 0.211$, p=0.9

Figure 4.1: Calculation of Mendelian inheritance ratio from four independent *DRAM-1*$^{+/-}$ intercrosses

(A) The formula for calculating Chi-Square (X^2) value and the establishment of p value from X^2 from the probability table adapted from Lobo (2008).

(B) The calculation X^2 value for actual number of *DRAM-1*$^{+/+}$, *DRAM-1*$^{+/-}$ and *DRAM-1*$^{-/-}$ pups derived from four independent *DRAM-1*$^{+/-}$ intercrosses.

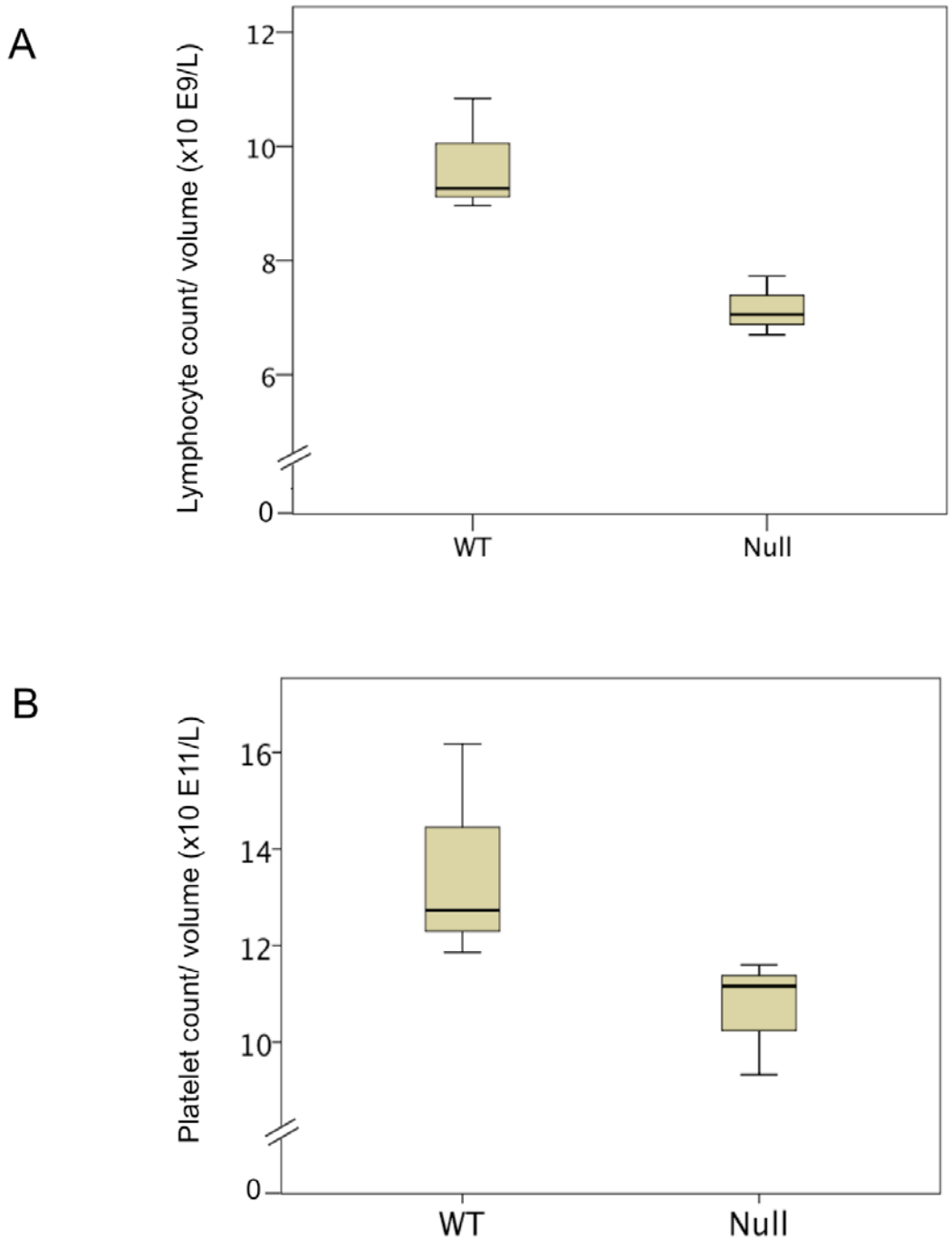

Figure 4.2(A-B): *DRAM-1* deletion decreases circulating lymphocytes and platelets

Peripheral blood from 3 months old wild type and *DRAM-1*-null mice was isolated and subjected to a hematology smear test. N=3.

(A)DRAM-1 deletion significantly reduces lymphocyte count in circulating blood. (Mann-Whitney U test; p=0.05).

(B)DRAM-1 deletion significantly reduces platelet count in circulating blood. (Mann-Whitney U test; p=0.05).

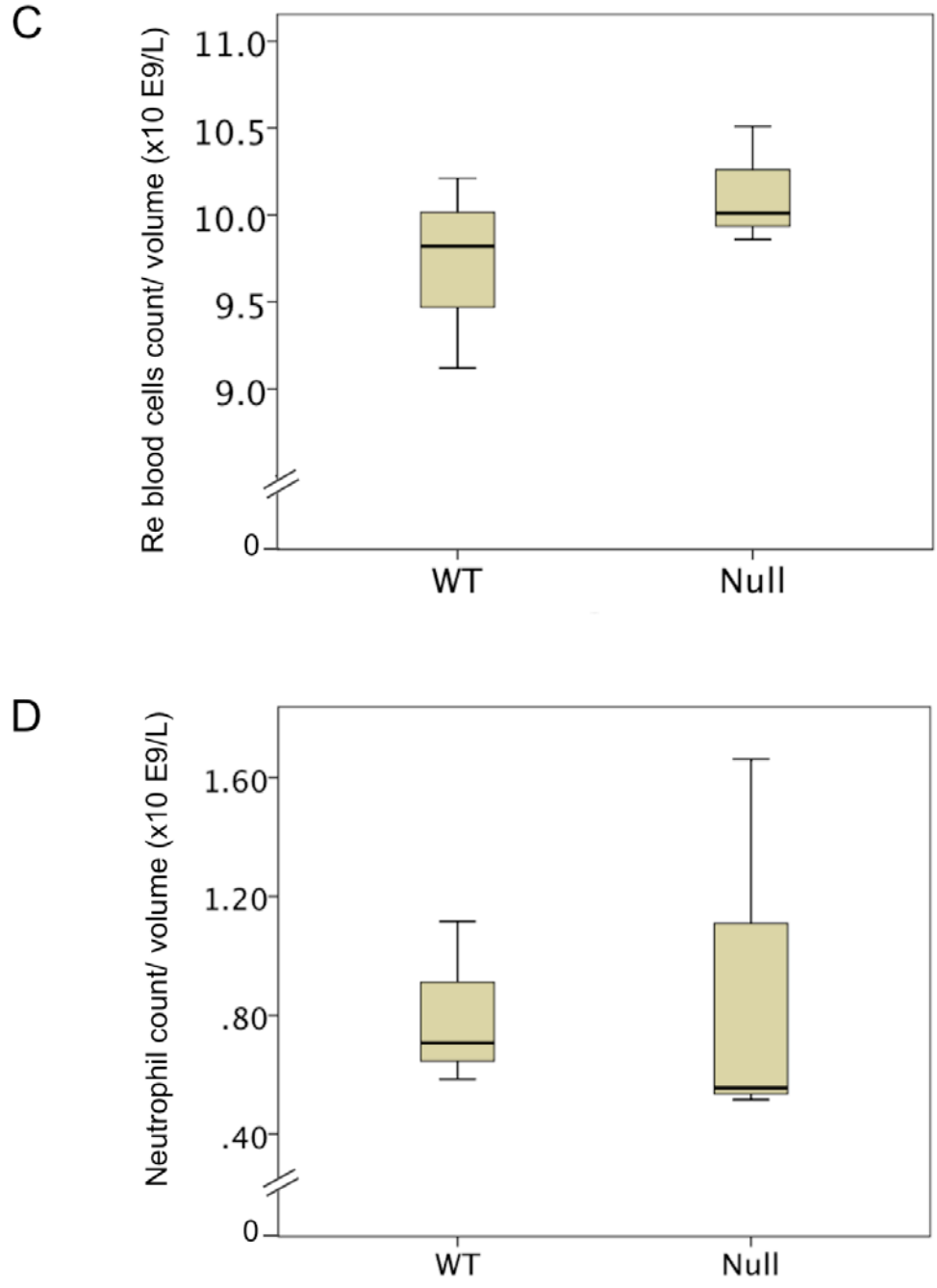

Figure 4.2(C-D): *DRAM-1* deletion does not affect circulating red blood cells and neutrophil

Peripheral blood from 3 months old wild type and *DRAM-1*-null mice was isolated and subjected to a hematology smear test. N=3.

(C) *DRAM-1* deletion does not affect circulating red blood cells. (Mann-Whitney U test; p=0.275).

(D) *DRAM-1* deletion does not affect neutrophil count in circulating blood. (Mann-Whitney U test; p=0.513).

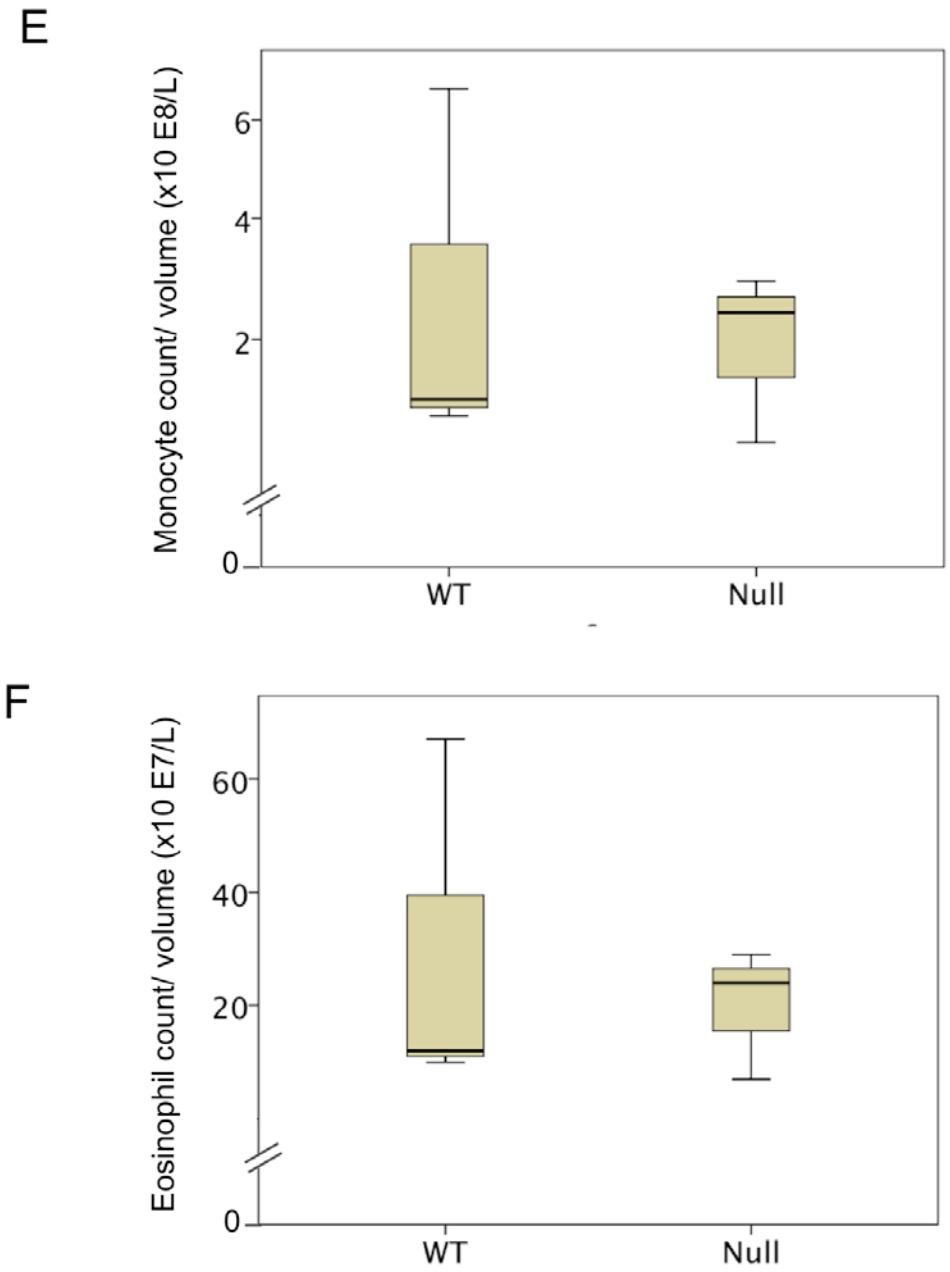

Figure 4.2(E-F): *DRAM-1* deletion does not affect circulating monocyte and eosinophil count

Peripheral blood from 3 months old wild type and *DRAM-1*-null mice was isolated and subjected to a hematology smear test. N=3.

(E) *DRAM-1* deletion does not affect circulating monocyte count. (Mann-Whitney U test; p=0.827).

(F) *DRAM-1* deletion does not affect eosinophil count in circulating blood. (Mann-Whitney U test; p=0.1273).

To determine if *DRAM-1* deletion affects the lifespan or predisposes to spontaneous tumour development, wild-type, heterozygous and *DRAM-1*-null mice were aged under normal conditions and monitored for up to 650 days. Whole body autopsy which was performed at the end point of the experiment, revealed no phenotypic differences between wild-type, heterozygous or *DRAM-1*-null mice (collaboration Dr. Ayala King, in-house veterinarian at the Beatson Institute for Cancer Research). Overall, the loss of *DRAM-1* does not affect the life span of the animals (Fig. 4.3A). Likewise, wild-type and *DRAM-1*-null mice display a similar propensity to develop spontaneous tumourigenesis (Table 4.1 and Fig. 4.3B). However, the % of heterozygous mice which developed spontaneous tumours were higher compared to the wild-type and DRAM-1$^{-/-}$ animals (Table 4.1 and Fig. 4.3B). This could be attributed to the smaller number of animals in this group (N=9) compared to wild-type (N=16) and *DRAM-1*-null mice (N=20).

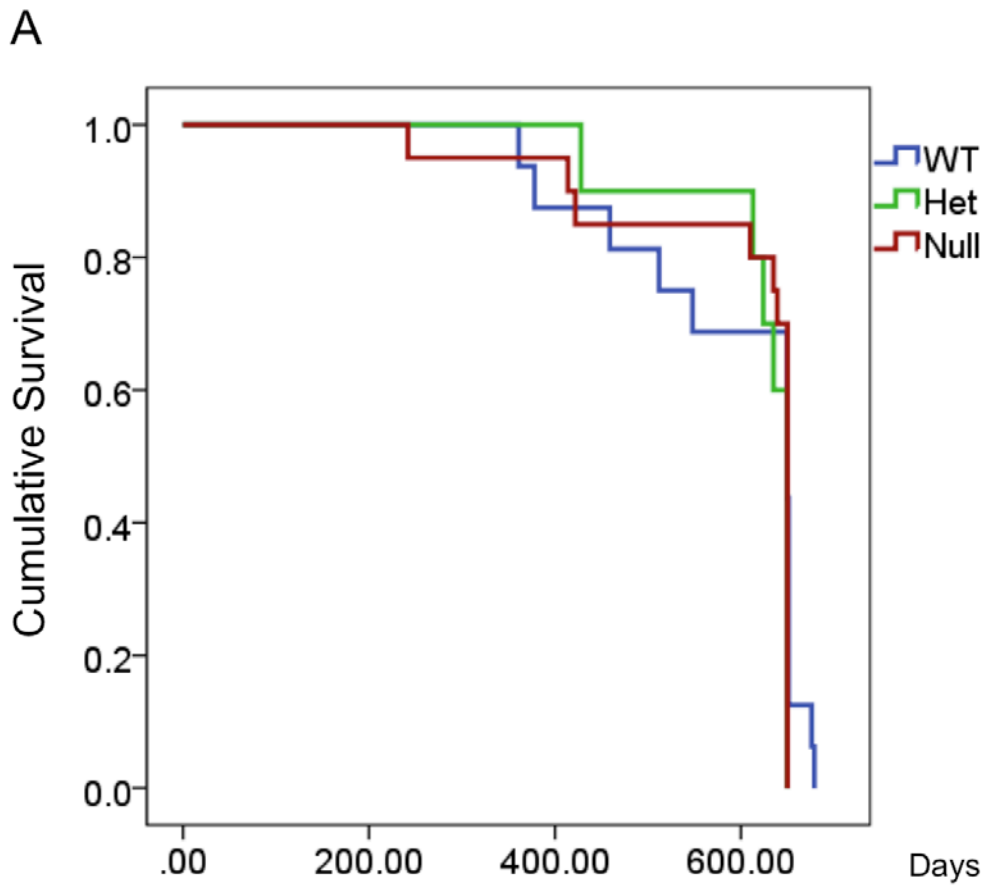

Figure 4.3: Loss of DRAM-1 does not affect life span and spontaneous tumourigenesis

'Wild type', heterozygotes and *DRAM-1*-null mice generated from a starting cross between *Dram-1*$^{fl/fl}$ and Cre Deleter were aged under normal conditions for up to 650 days. Wild-type N=16; Heterozygotes N=9; *DRAM-1*-null N=20.

(A)The lifespan of these mice were monitored and illustrated in a Kaplan-Meier survival curve.

Table 4.1: Cause of death of wild-type, heterozygotes and DRAM-1-null mice aged up to 650 days

Cause of Death	*DRAM-1*$^{+/+}$	*DRAM-1*$^{+/-}$	*DRAM-1*$^{-/-}$
Lymphoma	12.5	30	20
Sarcoma	6.25	10	0
Lung tumour	0	0	5
Liver Tumour	6.25	20	5
Ovary Atrophy	0	0	5
Infection	6.25	0	0
Old Age	12.5	0	35
Healthy	56.25	40	30

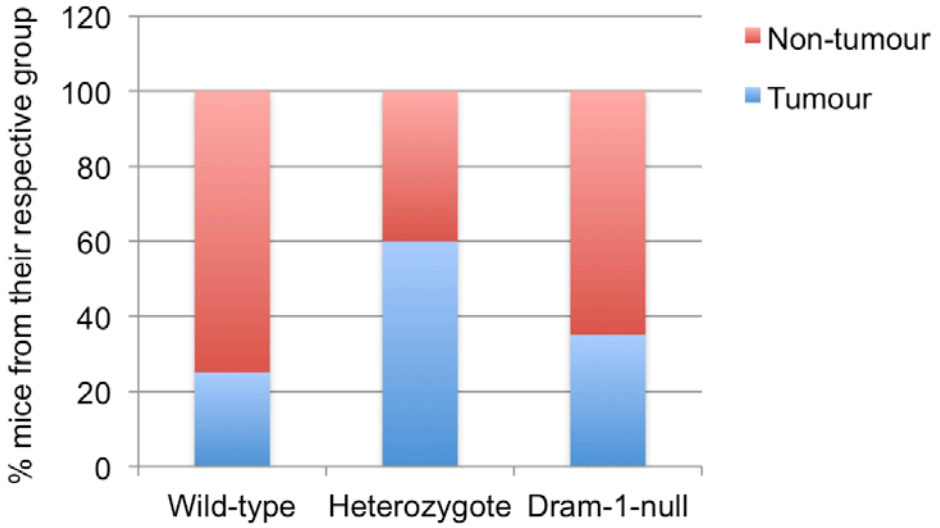

Figure 4.3: Loss of DRAM-1 does not modulate life span and spontaneous tumourigenesis
'Wild type', heterozygotes and *DRAM-1*-null mice generated from a starting cross between *DRAM-1*$^{fl/fl}$ and Cre Deleter were aged under normal conditions for up to 650 days. Wild-type N=16; Heterozygotes N=9; *DRAM-1*-null N=20.
(B) The onset of spontaneous tumorigenesis is summarised in stacked columns.

4.2.2 The role of DRAM-1 in p53-dependent and -independent apoptosis in vivo

Human *DRAM-1* mRNA expression has been shown to be upregulated upon treatment with DNA damaging agents (Fig. 3.24). In line with this, DRAM-1 is also required for effective p53-dependent cell death *in vitro.* We were interested to determine if murine *DRAM-1* mRNA expression is upregulated upon DNA damage and if DRAM-1 is required to mediate both p53-dependent and -independent cell death in the small intestine. Wild-type C57BL/6 mice were subjected to 14 Gy of whole body gamma-irradiation at the age of 6-8 weeks. mRNA from epithelial cells of the small intestine was harvested at 6 hours (early time point) and 48 hours (late time point) post irradiation. At least three mice were used for each condition. DRAM-1 mRNA expression is significantly upregulated 48 hours post irradiation (REST analysis; p = 0.016) (Fig. 4.4).

To determine if *DRAM-1* deletion affects apoptosis *in vivo,* wild-type, and *DRAM-1*$^{-/-}$ knockout mice were subjected to 14 Gy of gamma-irradiation at the age of 6-8 weeks. The small intestines were harvested 6 and 24 hours post irradiation to assess for p53-dependent and –independent apoptosis respectively.

p53 is activated upon DNA damage at 6 hours post irradiation, and the extent of nuclear p53 activation is similar in both wild-type and *DRAM-1*$^{-/-}$ mice (Fig. 4.5). The loss of DRAM-1 is not required for the enhancement of radiation-induced p53-dependent apoptosis, as revealed by caspase 3 scoring of apoptotic cells in the intestinal crypts (Fig. 4.6 A).

Additionally, the loss of *DRAM-1* does not modulate p53-independent apoptosis, as reflected by the indistinguishable number of caspase 3 positive cells per 25 crypts during the later wave of p53-independent apoptosis (Fig. 4.6B).

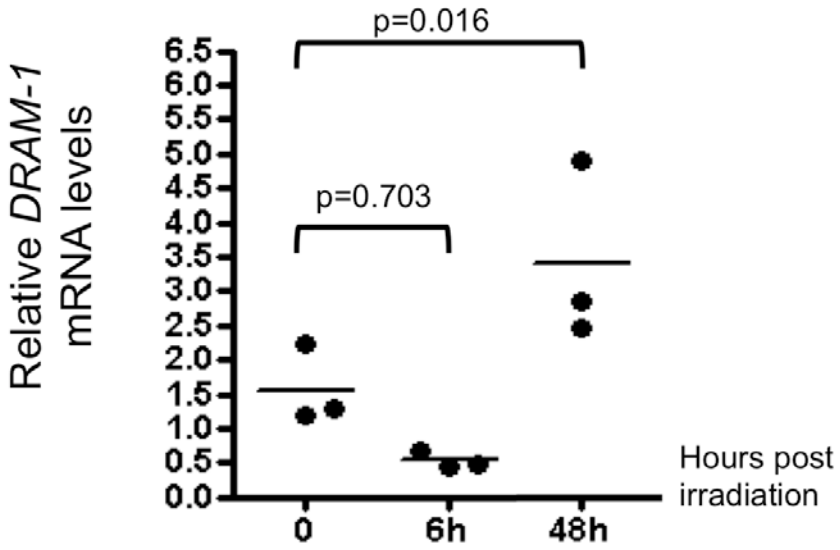

Figure 4.4: *DRAM-1* mRNA expression is upregulated upon DNA damage
Wild type C57BL/6 mice were subjected to 14 Gy of whole body gamma-irradiation. mRNA from the epithelial cells of the small intestine were harvested at 6 hours and 48 hours post irradiation. *DRAM-1* mRNA expression was quantified by real time PCR. (REST analysis; 6h, p = 0.703; 48h, p=0.016)

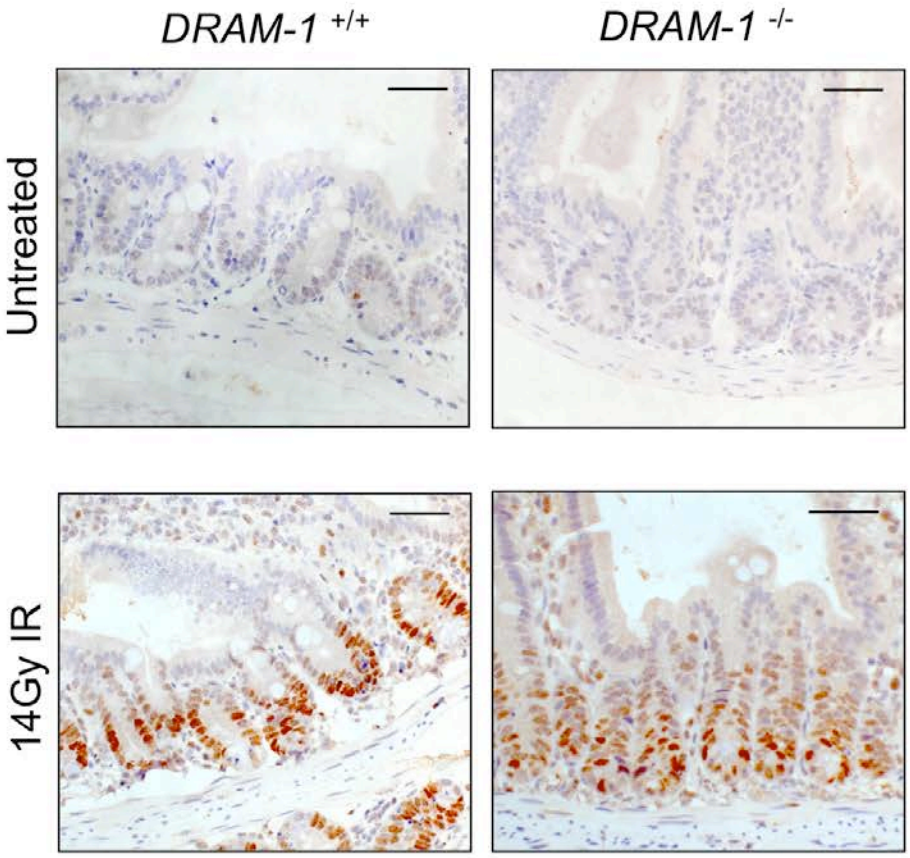

Figure 4.5: p53 is upregulated in wild type and *DRAM-1*-null small intestine
Wild type and *DRAM-1*-null mice were subjected to 14 Gy of whole body gamma-irradiation. Small intestines were harvested at 6 hours post irradiation and stained with p53. The images were taken at original magnification x40, and is a representation of 5 mice from each genotype. Scale bar represents 50μm.

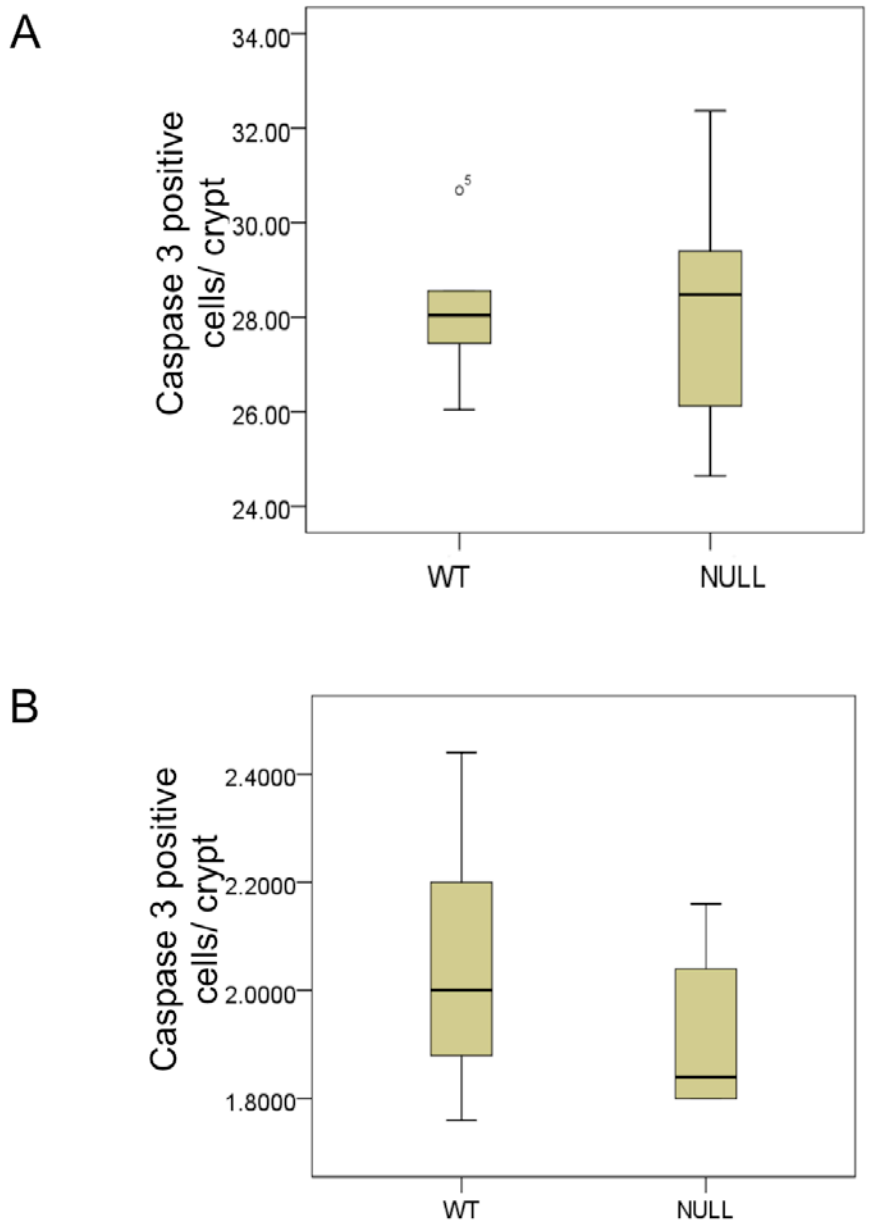

Figure 4.6: *DRAM-1* deletion does not modulate radiation-induced apoptosis

Wild type and *DRAM-1*-null mice were subjected to 14 Gy of whole body gamma-irradiation. The small intestine were harvested at 6 hours and 24 hours post irradiation and stained with caspase 3.

(A) Scoring of Caspase 3 positive cells per crypt at 6 hours (Mann-Whitney U test; p = 0.602).

(B) Scoring of caspase 3 positive cells per crypt at 24 hours (Mann-Whitney U test; p = 0.463)

To rule out the involvement of murine DRAM-1 in p53-dependent cell death in the small intestine, an independent model was used. The *AhCre*$^{+}$ mouse (refer to section 4.1) was crossed with *Mdm2*$^{fl/fl}$ mice (Grier, Yan et al. 2002) and either *DRAM-1*$^{+/+}$ or *DRAM-1*$^{fl/fl}$ mice. Since MDM2 is responsible for directing the proteasomal turnover of p53 (refer to section 1.8), *MDM2* deletion in the small intestine was validated by p53 staining. As demonstrated by others, in the wild-type intestines, high p53 levels were observed in highly proliferative cells of the intervillus pockets and in terminally differentiated cells in the villus region, leading to apoptosis in crypts (Valentin-Vega, Okano et al. 2008) (Fig. 4.7). The intense p53 staining in the nucleus is associated with *DRAM-1* deletion. The nuclear activation of p53 in these areas is independent of DRAM-1 status (Fig. 4.7). Consistent with previous observation, the loss of *DRAM-1* does not modulate p53-dependent apoptosis in the small intestine, as validated by the number of caspase 3 positive cells per crypt (Fig. 4.8).

From these *in vivo* studies, *DRAM-1* deletion does not rescue p53-dependent apoptosis in the small intestine. Additionally, DRAM-1 is also not a regulator of radiation-induced apoptosis in the small intestine.

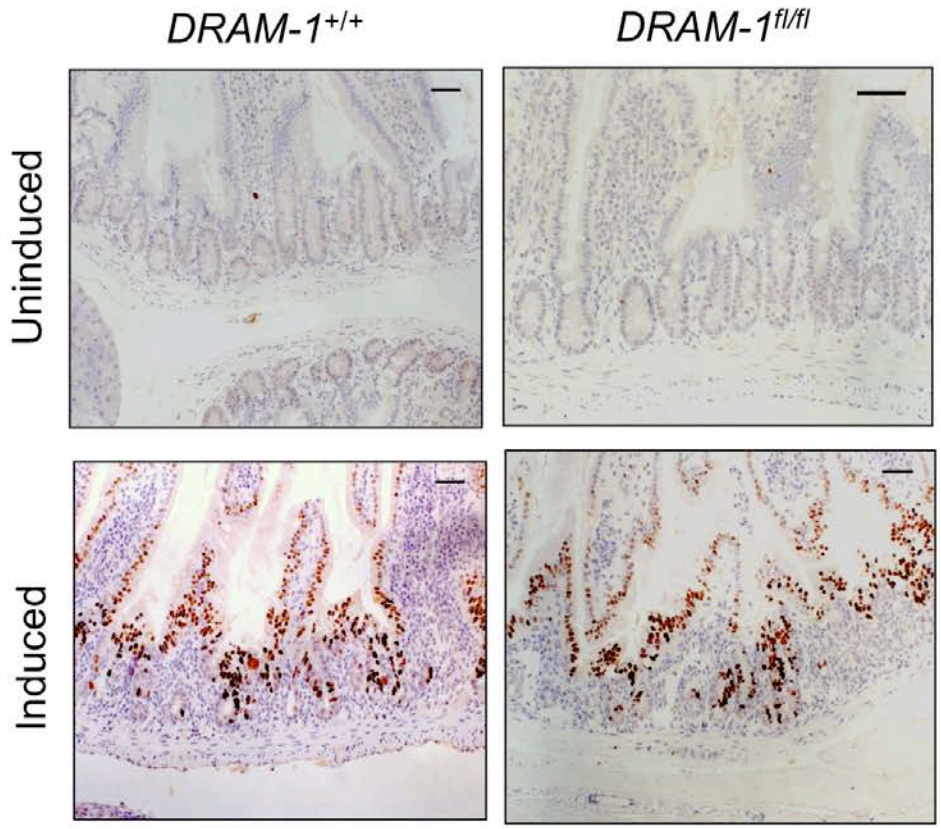

Figure 4.7: p53 is upregulated in wild type and *DRAM-1*-null small intestine upon Mdm2 excision

DRAM-1$^{+/+}$ and *DRAM-1*$^{fl/f}$ mice were subjected to 3x i.p injection of β-naphthoflavone (80mg/kg). The small intestines were harvested at 48 hours later, and stained with p53. The images were taken at original magnification x20, and are a representatives of 3 mice from each genotype. Scale bar represents 50μm.

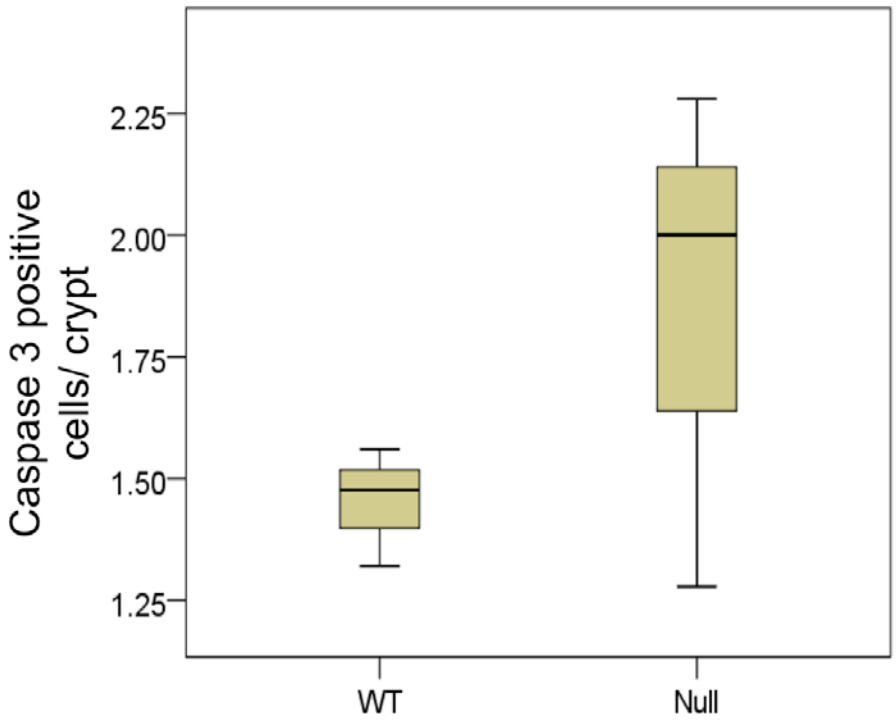

Figure 4.8: *DRAM-1* deletion does not rescue p53-dependent apoptosis
DRAM-1$^{+/+}$ *and DRAM-1*$^{fl/f}$ mice were subjected to 3x i.p injection of β-naphthoflavone (80mg/kg). The small intestine were harvested 48 hours later, and stained with caspase 3. The number of caspase 3 positive cells in 25 live crypts were quantified. Mann Whitney U test; p=0.476. Wild-type N=4; *DRAM-1*$^{fl/f}$ *(DRAM-1*-null) N=3.

4.2.3 DRAM-1 is required for regeneration post radiation-induced injury in the small intestine

Albeit *DRAM-1* deletion does not impair p53-dependent cell death, we were interested to determine if DRAM-1 mediates regeneration. To investigate this, *DRAM-1*$^{+/+}$ and *DRAM-1*$^{-/-}$ mice were subjected to 14 Gy of whole body gamma-irradiation at the age of 6-8 weeks and harvested at 48 and 72 hours later. The first proximal 10cm of the small intestine was harvested and analysed for p53 activation, live crypts, mitosis, proliferation and regeneration.

DRAM-1 deficiency reduced the number of surviving crypts at 48 hours (Mann-Whitney U test; p = 0.021) (Fig. 4.9A) and 72 hours (Mann-Whitney U test; p = 0.018) (Fig. 4.9 B) post irradiation. Consistent with this, the crypt size is significantly reduced in *DRAM-1*$^{-/-}$ animals compared to the wild-type controls at 72 hours (Mann-Whitney U test; p = 0.021) (Fig. 4.9C). The difference in crypt size between wild-type and *DRAM-1*$^{-/-}$ animals is illustrated in Fig. 4.9D.

To confirm the role of DRAM-1 in regulating crypt regeneration, the small intestines harvested at 72 hours post irradiation were stained with the mitotic marker (phospho-Histone H3) and the proliferation marker (BrdU). DRAM-1-deficient intestines show a reduced capacity to undergo mitosis as reflected by a reduction in phospho-Histone H3 positive cells per crypt (Mann-Whitney U test; p = 0.043) (Fig. 4.10A). Likewise, proliferation is also compromised in *DRAM-1*$^{-/-}$ intestines, as reflected by the significant decrease in BrdU positive cells per crypt compared to the wild-type intestines (Mann-Whitney U test; p = 0.009) (Fig. 4.10B).

The defect in crypt regeneration can be attributed to a decrease in the stem cell pool of the small intestine. To determine if *DRAM-1* deletion modulates the stem cell pool, small intestines harvested at 72 hours post radiation was stained with the well established human and murine intestinal stem cell marker, OLFM4. (van der Flier, Haegebarth et al. 2009) (Begus-Nahrmann, Lechel et al. 2009). The population of stem cells remains indistinguishable in wild-type and *DRAM-1*-null intestinal crypts (Fig. 4.11). This suggests that the fast-cycling stem cell pool within regenerating intestinal crypts is not affected upon *DRAM-1* deletion.

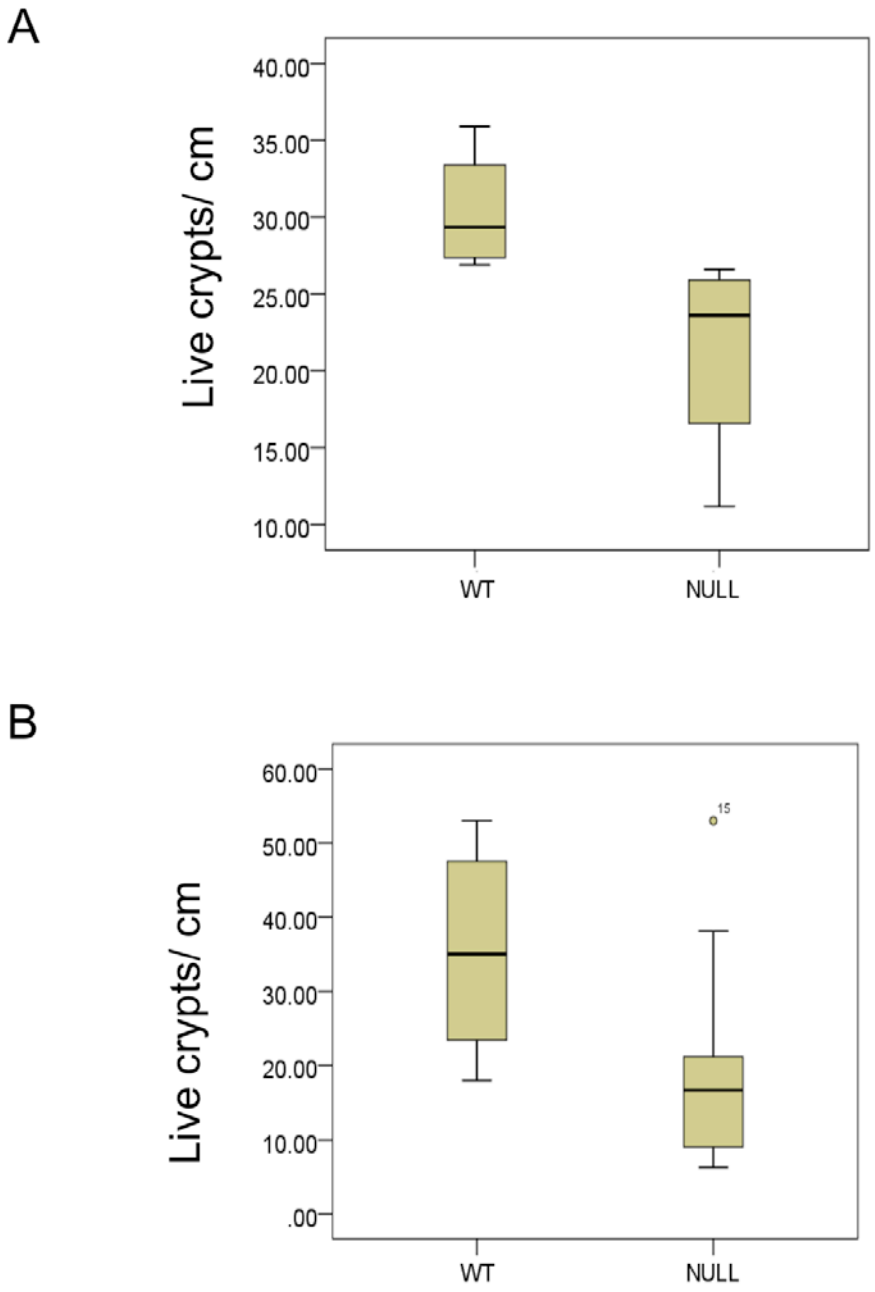

Figure 4.9(A-B) : DRAM-1 is required for regeneration post irradiation
Wild type and *DRAM-1*-null mice were subjected to 14 Gy of whole body gamma-irradiation. Sections of the small intestine were harvested at 48 hours and 72 hours post irradiation and stained with H&E.
(A)The number of live crypts/cm in a total of 10cm length 48 hours post irradiation. (Mann-Whitney U test; p = 0.021).
(B)The number of live crypts/cm in a total of 10cm length 72 hours post irradiation. (Mann-Whitney U test; p = 0.018). N=4.

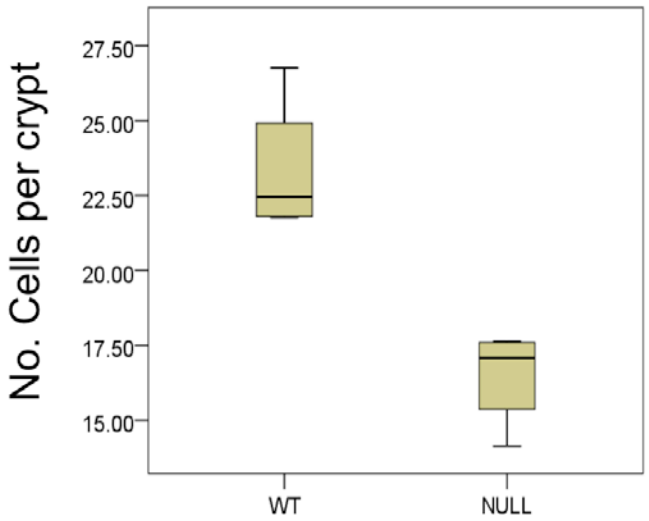

Figure 4.9C: *DRAM-1* deletion reduces crypt size of regenerating crypts
The small intestines of wild type and *DRAM-1*-null mice were harvested 72 hours post irradiation and stained with H&E. The number of live cells per crypt in 25 live crypts were quantified. (Mann-Whitney U test; p = 0.021). N=4.

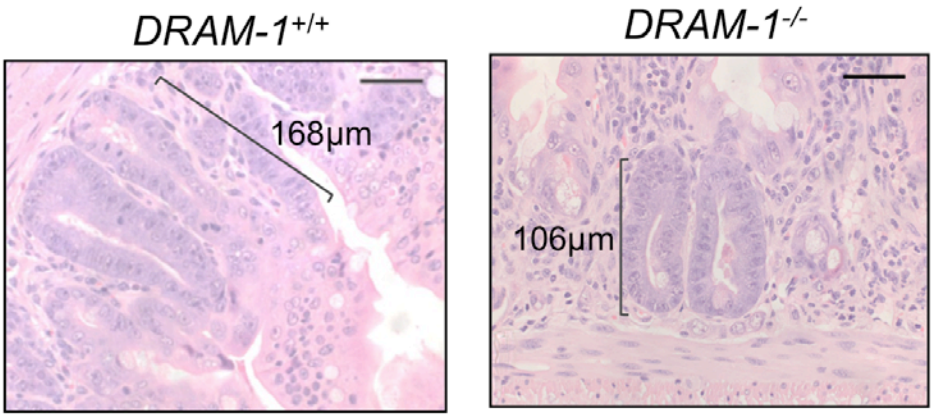

Figure 4.9D: Schematic representation of crypts in wild type and *DRAM-1*-null small intestines 72 hours post irradiation
The small intestines of wild type and *DRAM-1*-null mice were harvested 72 hours post irradiation and stained with H&E. The images were taken at original magnification x40 and are representatives of 5 mice from each genotype. Scale bar represents 50µm.

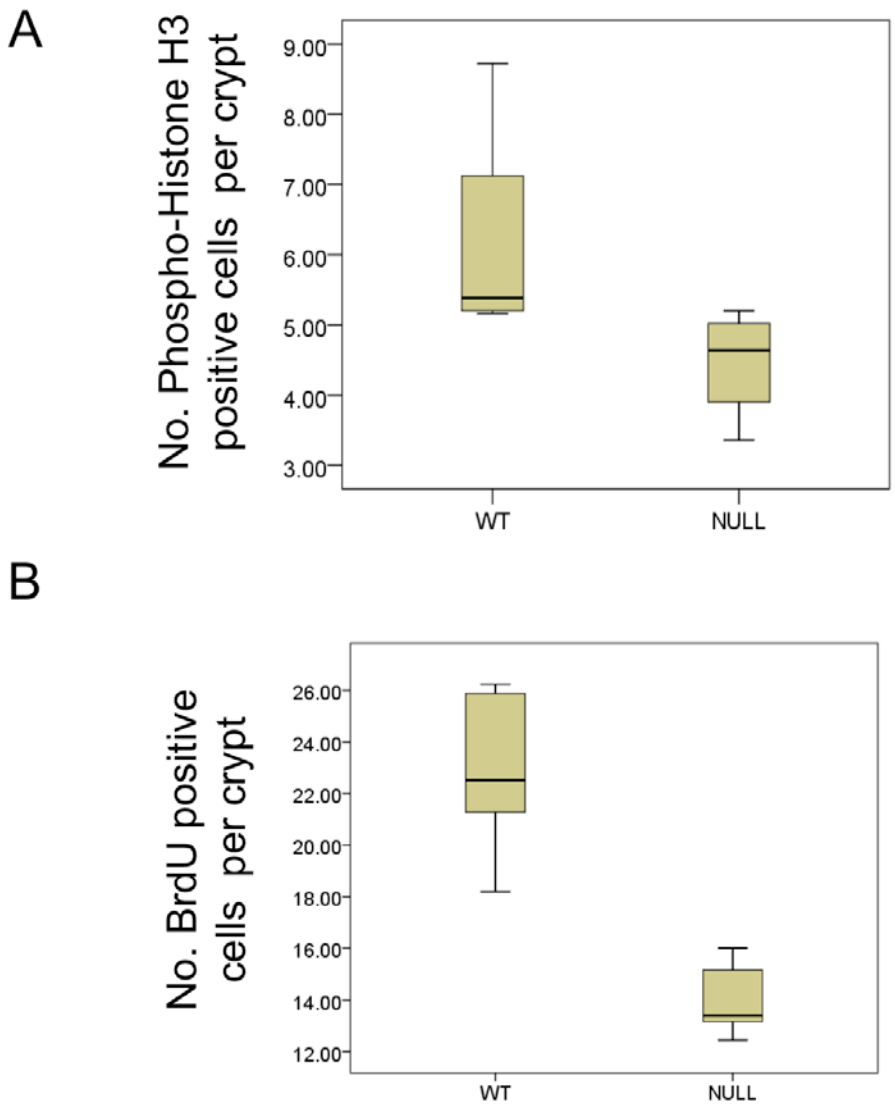

Figure 4.10(A-B): DRAM-1 is required for regeneration post irradiation
The small intestines of wild type and *DRAM-1*-null mice were harvested 72 hours post irradiation and stained with the mitotic marker (Phospho-Histone H3) and the proliferation marker (BrdU).

(A) The number of Phospho-Histone H3 positive cells per crypt in 25 live crypts were quantified. (Mann-Whitney U test; p = 0.043).

(B) The number of BrdU positive cells per crypt in 25 live crypts were quantified. (Mann-Whitney U test; p = 0.009). N=4.

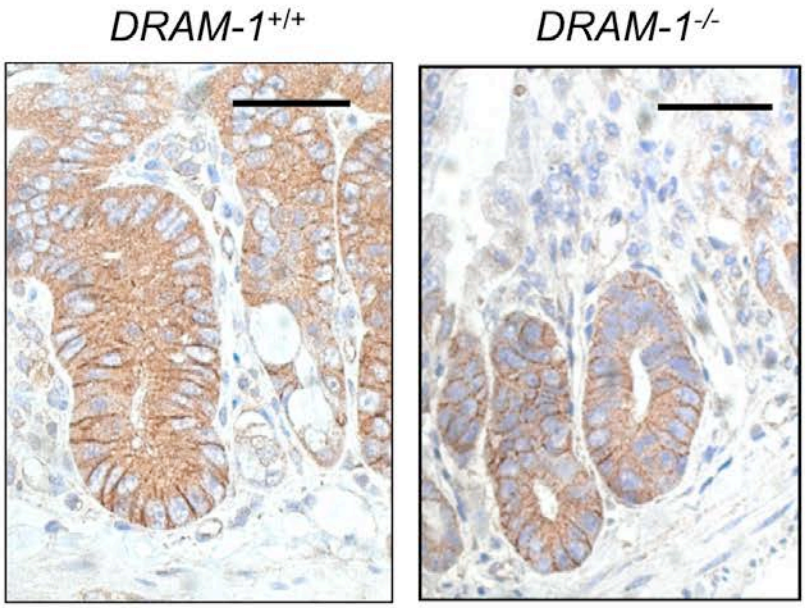

Figure 4.11: OLFM4 positive stem cells are present in regenerating crypts of wild type and *DRAM-1*$^{-/-}$ small intestines

The small intestines of wild type and *DRAM-1*-null mice were harvested 72 hours post irradiation and stained with the stem cell marker, OLFM4. The images were taken at original magnification x40 and are representatives of 5 mice from each genotype. Scale bar represents 50μm.

Yet another regulator of cellular growth and regeneration is the mammalian Target of Rapamycin (mTOR) (Fu, Kim et al. 2009). In line with this, Akt/mTOR signaling has been shown to be required for intestinal regeneration (Ashton, Morton et al. 2010). mTOR activity has been previously demonstrated to be downregulated when the Intestinal cell kinase (ICK), a downstream target of mTOR, is inhibited, leading to a decreased proliferation and differentiation of intestinal epithelial cells (Fu, Kim et al. 2009). Although DRAM-1 has yet to be identified as a downstream target of mTOR, we were interested to determine if the reduced proliferation, mitosis and regeneration in *DRAM-1*$^{-/-}$ small intestine upon injury is attributed to decreased mTOR activity. Wild-type and *DRAM-1*-null small intestine harvested 72 hours post radiation were stained with anti-phospho-AKT, a kinase which phosphorylates and activates mTOR at Ser-2448 (Fu, Kim et al. 2009), and this event is validated by further staining with anti-phospho-mTOR Ser 2448. Additionally, the small intestine was also stained with the downstream target of mTOR, anti-phospho-4EBP1 (Zou, Smith et al. 2009). mTOR activity, as reflected by the levels of phospho-AKT (Fig. 4.12A), phospho-mTOR Ser 2448 (Fig. 4.12B) and phospho-4EBP1 (Fig. 4.12C) is indistinguishable in wild-type and *DRAM-1*-null crypts of the small intestine. This suggests that mTOR activity is not affected in *DRAM-1*$^{-/-}$ cells within regenerating crypts of the small intestine.

To briefly summarise this part, DRAM-1 is required for efficient regeneration of the small intestine post injury by facilitating mitosis and cell proliferation. Additionally, the loss of *DRAM*-1 does not modulate mTOR activity and does not affect the subpopulation of OLFM4 positive fast-cycling stem cells.

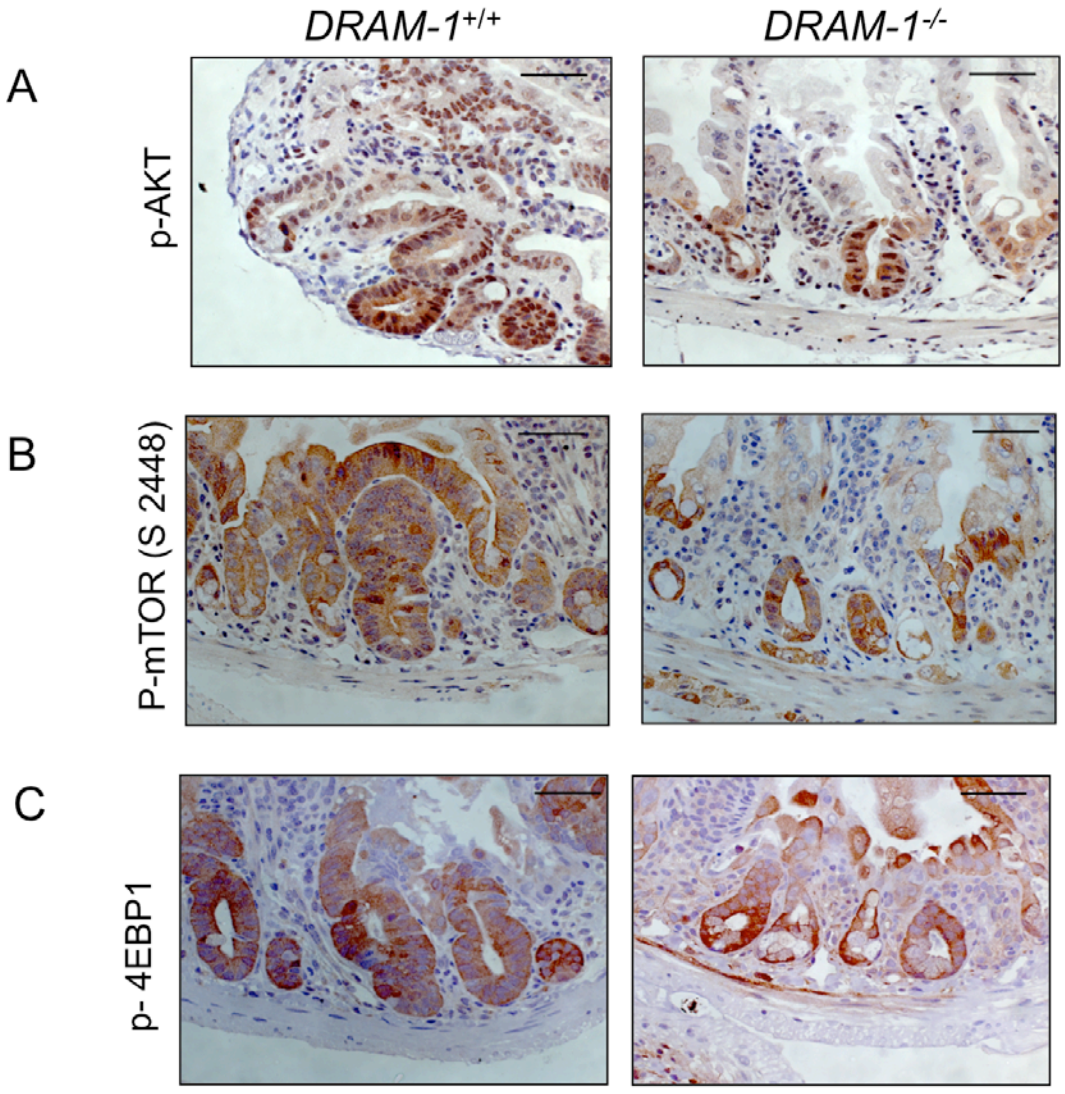

Figure 4.12(A-C) : mTOR activity in regenerating crypts of wild type and *DRAM-1*$^{-/-}$ small intestines

The small intestines of wild type and *DRAM-1*-null mice were harvested 72 hours post irradiation and stained with phospho-AKT (A), mTOR Ser 2448 (B) and phospho-4EBP1 (C). The images were taken at original magnification x40 and are representatives of 4 mice from each genotype. Error bar represents 50μm.

4.2.4 *DRAM-1* deletion does not modulate p53-induced senescence, but increases the frequency of apoptosis and mitosis in the liver

Reactivation of endogenous p53 in *p53*-deficient liver carcinoma cell lines has been shown to promote tumour regression, and the primary response of p53 in this context is to induce cellular senescence instead of apoptosis (Xue, Zender et al. 2007). Along the same lines, autophagy has been documented to mediate the acquisition of the senescence phenotype that was associated with differentiation and the upregulation of inflammatory cytokines (Young, Narita et al. 2009). Given that the interplay of p53, autophagy and senescence is emerging into the limelight, we were interested to determine if DRAM-1 is required for the induction of p53-dependent senescence *in vivo.*

To test this, the livers of *AhCre*$^{+}$ *Mdm2*$^{fl/fl}$ *DRAM-1*$^{+/+}$ ('wild-type') and *AhCre*$^{+}$ *Mdm2*$^{fl/fl}$ *DRAM-1*$^{fl/fl}$ (*DRAM-1*-null after Cre-mediated excision) mice (refer to section 4.2.2) were either fixed in formalin or preserved with OCT 6 days after induction. Similar to section 4.2.2, *Mdm2* and *DRAM-1* recombination events were validated by p53 staining (Fig. 4.13). The frozen liver sections were stained with SA-β-gal (senescence associated beta-gal). From this, the intensity of SA-β-gal staining between 'wild-type' and *DRAM-1*$^{-/-}$ liver is indistinguishable (Fig. 4.14). Since senescent cells do not undergo proliferation, senescence event in livers of 'wild-type' and *DRAM-1*$^{-/-}$mice was quantified by the comparing the number of proliferating hepatocytes. The number of BrdU positive hepatocytes in 'wild-type' and *DRAM-1*$^{-/-}$ liver is indistinguishable (Fig. 4.15). This suggests that *DRAM-1* deletion does not affect cellular senescence upon p53 activation in the liver.

Albeit this, the appearance of a 'condensed chromatin' phenotype in hepatocytes was more frequent in *DRAM-1*$^{-/-}$ liver compared to 'wild-type' upon analysis of H&E stained livers (data not shown). To determine if this morphology is attributed to increased apoptotic or mitotic events, the liver sections were stained with the apoptotic marker- caspase 3 and mitotic marker- phospho-Histone H3. Histone H3 is specifically phosphorylated during mitosis and the phosphorylation event is most pronounced in metaphase (Hans and Dimitrov 2001). In this case, *DRAM-1* deletion increases the rate of apoptosis and mitosis in the liver, as evident by an increase in caspase 3 positive (Mann-Whitney U test; $p = 0.013$) (Fig. 4.16) and

phospho-Histone H3 positive (Mann-Whitney U test; p = 0.05) (Fig. 4.17) hepatocytes respectively. p21 activity remains indistinguishable in wild-type and *DRAM-1*-null livers (Fig. 4.18).

To sum up this part of the experiment, *DRAM-1* deletion in the liver does not enhance p53-mediated cellular senescence. However, DRAM-1 deletion results in an increased rate of apoptosis and mitosis, in conditions when p53 levels are upregulated.

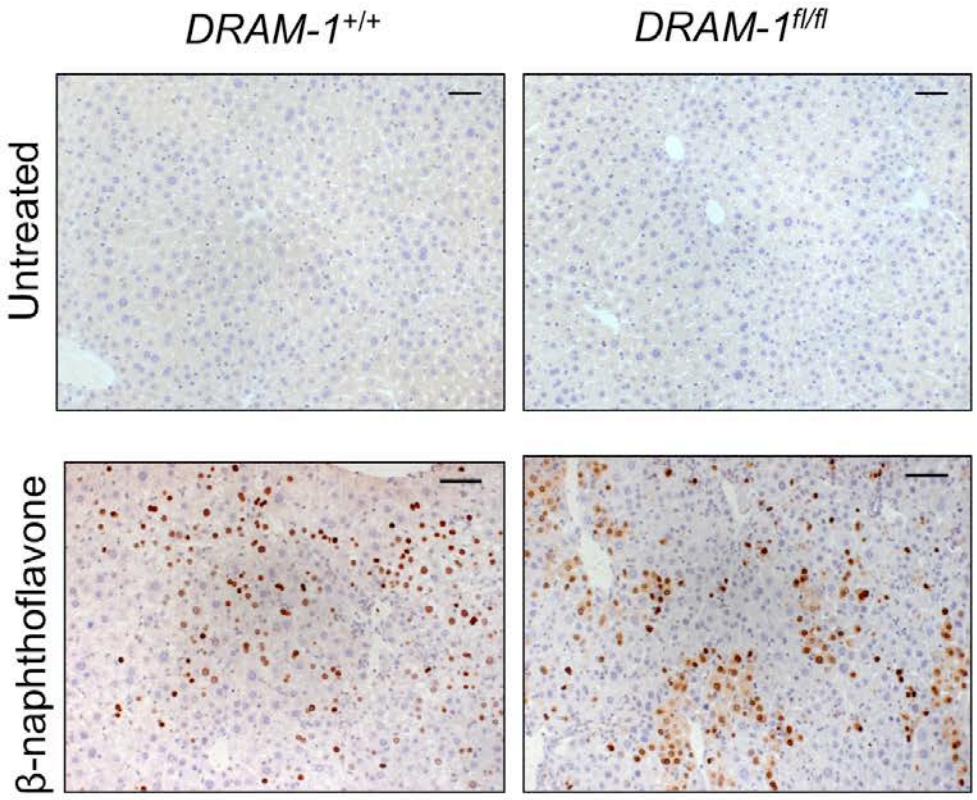

Figure 4.13: p53 is upregulated in wild type and *DRAM-1*-null liver upon *Mdm2* excision

DRAM-1$^{+/+}$ and *DRAM-1*$^{fl/fl}$ mice were subjected to 1x i.p injection of β-naphthoflavone (80mg/kg). The livers were isolated 6 days later, and stained with p53. The images were taken at original magnification x20 and are representatives of five animals from each genotype. Scale bar represents 50μm.

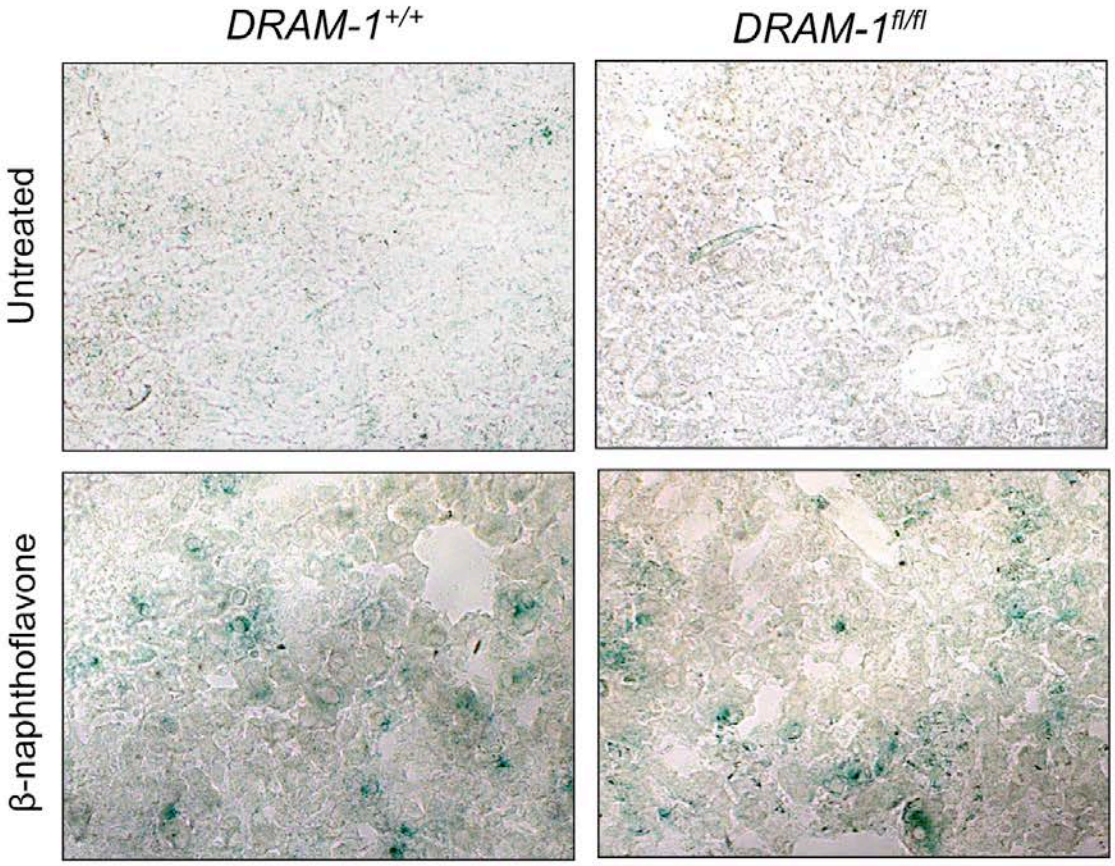

Figure 4.14: p53 activation in wild type and *DRAM-1*-null liver induces senescence

DRAM-1$^{+/+}$ and *DRAM-1*$^{fl/f}$ mice were subjected to 1x i.p injection of β-naphthoflavone (80mg/kg). The livers were isolated 6 days later, and stained for SA-β Gal. The images were taken at original magnification x20 and are representatives of 5 mice from each genotype. Error bar represents 50μm.

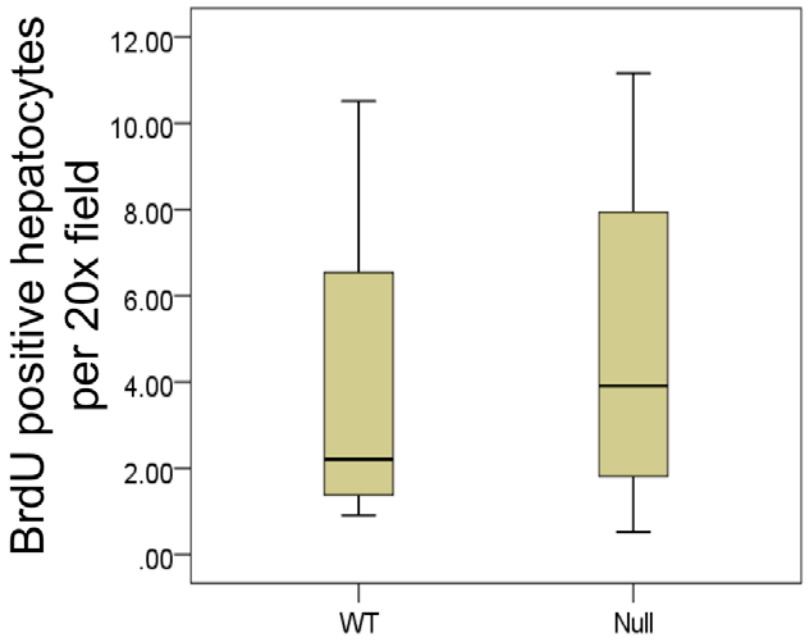

Figure 4.15: *DRAM-1* deletion does not affect proliferation
The livers of wild-type and *DRAM-1*-null mice were harvested 6 days post induction and stained with the proliferation marker (BrdU). The average number of Brdu positive cells in 10 20x fields was quantified. (Mann-Whitney U test; p = 0.564). N=4.

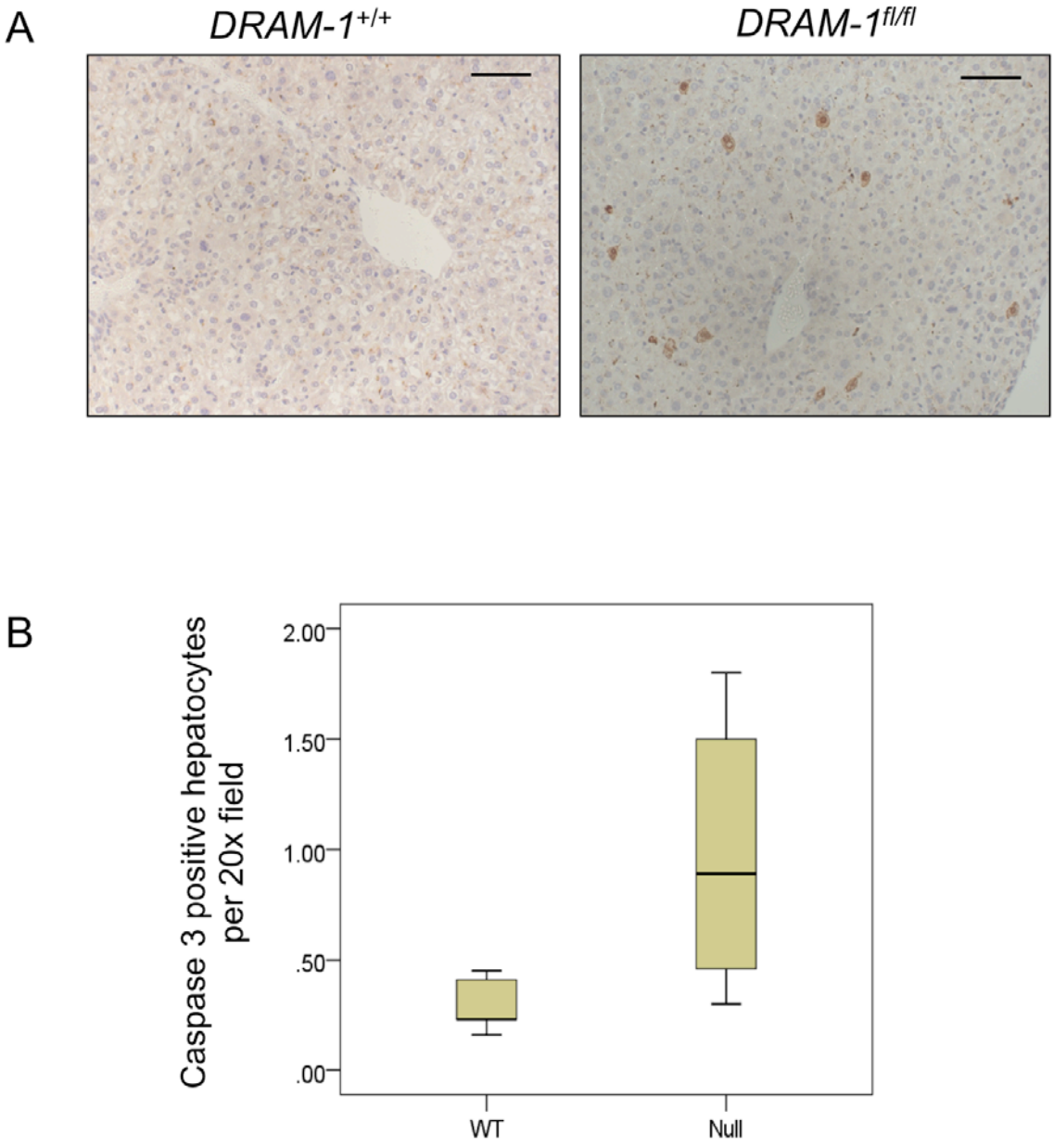

Figure 4.16 : *DRAM-1* deletion increases apoptosis
The livers of wild type and *DRAM-1*-null mice were harvested 6 days post induction and stained with the apoptotic marker (caspase 3). N=4.
(A) Representative images of *DRAM-1*$^{+/+}$ and *DRAM-1*$^{-/-}$ taken at 20x
(B) The average number of caspase 3 positive cells in 10 fields was quantified. (Mann-Whitney U test; p = 0.013).

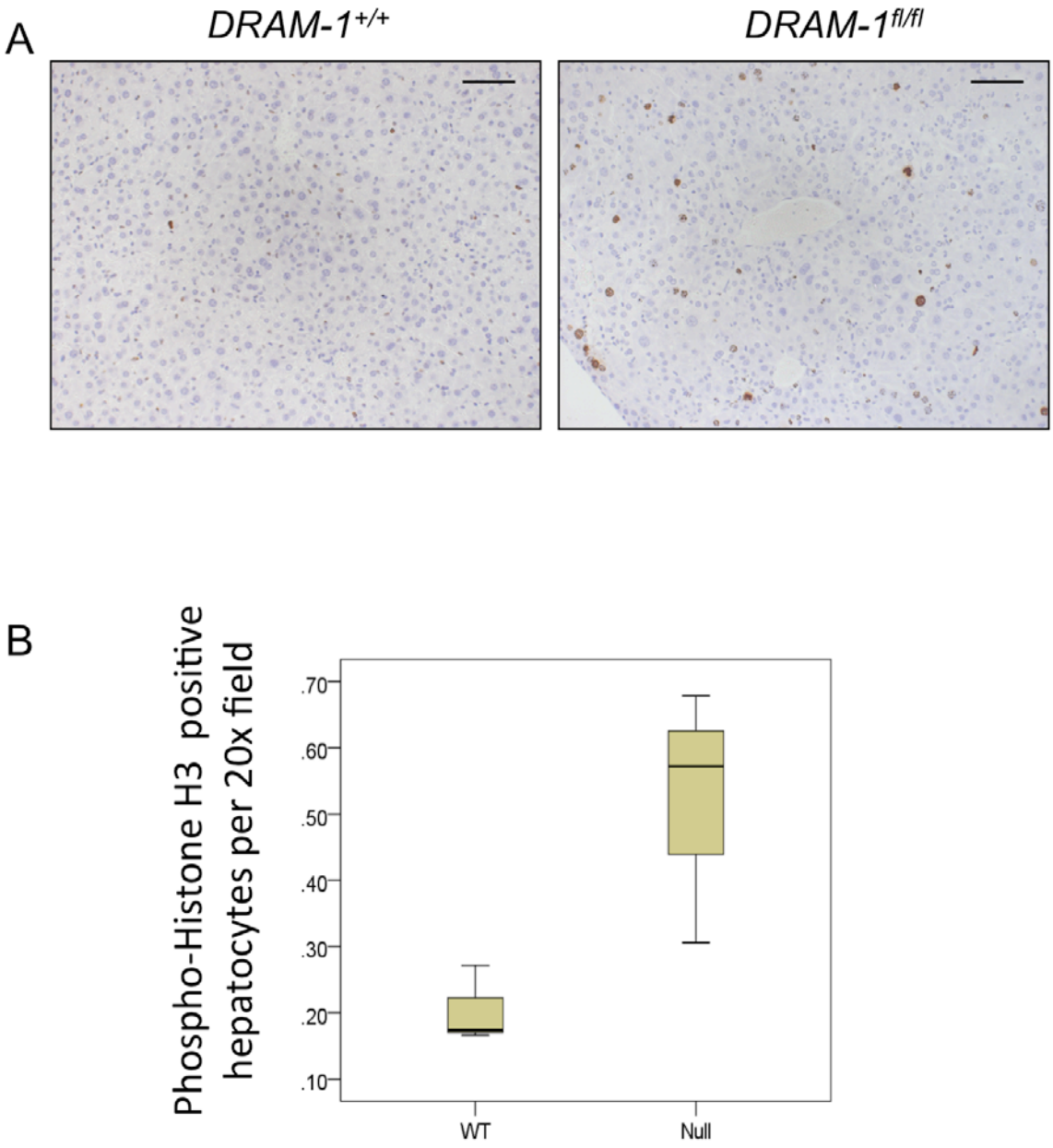

Figure 4.17 : *DRAM-1* deletion increases Histone H3 phosphorylation in the liver upon p53 stabilisation

The livers of wild type and *DRAM-1*-null mice were harvested 6 days post induction and stained with the mitotic marker (phospho-Histone H3). N=4.

(A) Representative images of *DRAM-1*$^{+/+}$ and *DRAM-1*$^{-/-}$ taken at 20x

(B)The average number of phospho-Histone H3 positive cells in 10 fields was quantified. (Mann-Whitney U test; p = 0.013).

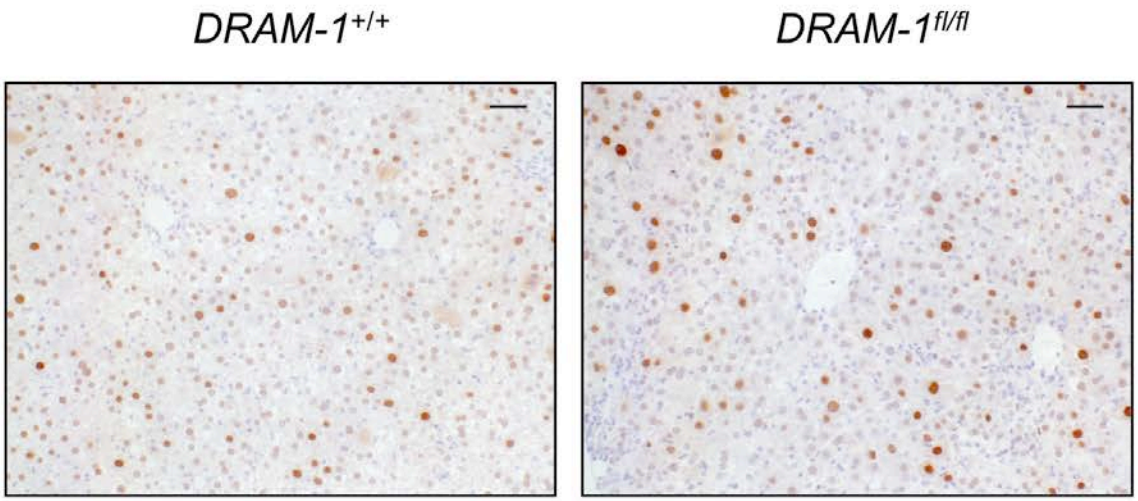

Figure 4.18: p21 is upregulated in wild type and DRAM-1 null liver upon Mdm2 excision

DRAM-1$^{+/+}$ and *DRAM-1*$^{fl/f}$ mice were subjected to 1x i.p injection of β-naphthoflavone (80mg/kg). The livers were isolate 6 days later, and stained with p21. The images were taken at original magnification x20 and are representatives of five animals from each genotype. Scale bar represents 50μm.

4.2.5 *DRAM-1* deletion does not predispose to radiation-induced tumourigenesis

Human *DRAM-1* is downregulated in various forms of cancer (refer to Section 1.7). Furthermore, since the loss of p53 greatly enhances the development of cancer upon exposure to ionizing radiation (Kemp, Wheldon et al. 1994) and that DRAM-1 is a p53 target gene, we sought to investigate if DRAM-1 deletion accelerates tumourigenesis upon exposure to gamma-irradiation.

In this context, wild-type, heterozygous and *DRAM-1*-null mice aged 6-8 weeks were exposed to 4 Gy of gamma irradiation and aged under normal conditions for up to 650 days. The mice were monitored frequently for the development of tumours. From this experiment, the loss of *DRAM-1* does not predispose to radiation-induced tumourigenesis, as indicated by the tumour-free Kaplan Meier survival curves (Fig. 4.19A). The types of tumours, if any, developed by the subjects in this cohort are listed in table 4.2 and the percentage of mice which developed tumours is summarised in Fig. 4.19B.

Table 4.2: Cause of death of wild-type, heterozygotes and *DRAM-1*$^{-/-}$ mice aged up to 650 days post 4 Gy of □amma irradiation

Genotype	***DRAM-1*$^{+/+}$**	***DRAM-1*$^{+/-}$**	***DRAM-1*$^{-/-}$**
Lymphoma	50.0	58.3	31.6
Sarcoma	0.0	0.0	10.5
Lung tumour	0.0	0.0	0.0
Liver Tumour	7.1	8.3	15.8
Unexplained	14.3	0.0	0.0
Infection	7.1	0.0	0.0
Old Age	7.1	16.7	26.3
Healthy	14.3	16.7	15.8

In summary, *DRAM-1* deletion does not accelerate radiation-induced tumourigenesis upon exposure to 4 Gy of □amma irradiation.

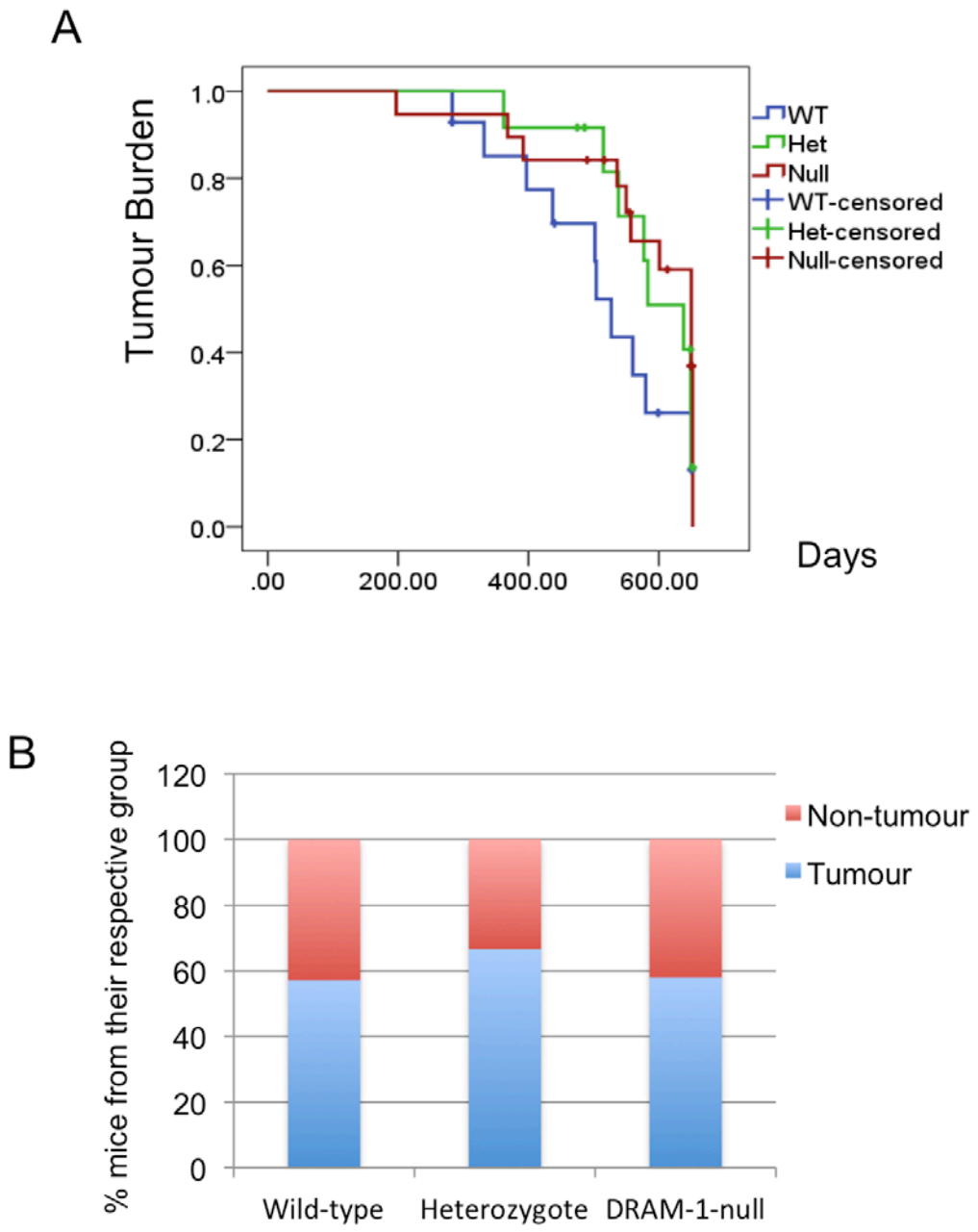

Figure 4.19: Loss of *DRAM-1* does not predispose to radiation-induced tumourigenesis

Wild type, heterozygotes and *DRAM-1*-null mice generated from a starting cross between *DRAM-1*$^{fl/fl}$ and Cre Deleter were subjected to 4Gy of gamma-irradiation and monitored under normal conditions for up to 650 days for:

(A)Kaplan Meier illustrating tumour-free survival

(B)Summary of mice which developed tumours

Wild type = 14, Heterozygotes = 12, *Dram-1*$^{-/-}$ = 19

4.2.6 DRAM-1 is required for colon regeneration post inflammation

We were also interested to determine if *DRAM-1* deletion predisposes to inflammation-driven tumourigenesis. 11 wild-type and 7 *DRAM-1*$^{-/-}$ mice were subjected to intraperitoneal injection of the carcinogen azoxymethane (AOM), and three cycles of 2% DSS. This model reproduces a state of chronic inflammation, which is postulated to be a driving force in tumour progression in colitis associated colorectal carcinoma (De Robertis, Massi et al. 2011).

DRAM-1$^{-/-}$ mice were highly sensitised to the DSS treatment, as 4 out of the 7 mice (57.1%) had lost 20% of their body weight (which is the threshold indicated in our home office personal license) and developed severe clinical symptoms (hunched/moribound), thus leading to a significant decreased lifespan (Fig. 4.20). Healthy wild-type mice were harvested along the same time as the 'sick' *DRAM-1*-null mice as time-point control. Although the length of treatment was too short for polyps formation, the colons of *DRAM-1*$^{-/-}$ mice showed massive epithelial erosion (Fig. 4.21). Upon further analysis, the number of live crypts in the colons of *DRAM-1*$^{-/-}$ mice was significantly lower that the wild-type controls (Mann-Whitney U test; p=0.05) (Fig. 4.22). However, both wild-type and *DRAM-1*$^{-/-}$ mice exhibited a similar degree of neutrophil infiltration, as validated by MPO staining (refer to section 4.1.2) (Fig. 4.23).

The remaining 3 *DRAM-1*$^{-/-}$ mice were able to survive after 3 cycles of DSS treatment, although only one was 'healthy' enough to be kept until the end point of the experiment (70 days). Upon detailed analysis, both wild-type and *DRAM-1*$^{-/-}$ mice developed dysplastic crypts, polyps and lymphocyte infiltration in the colon to a similar extent (Fig. 4.24A and Fig.4.24B). Since the majority of *DRAM-1*$^{-/-}$ mice were unable to complete the course of the treatment, we were unable to determine if the loss of *DRAM-1* predispose to inflammation-driven tumourigenesis.

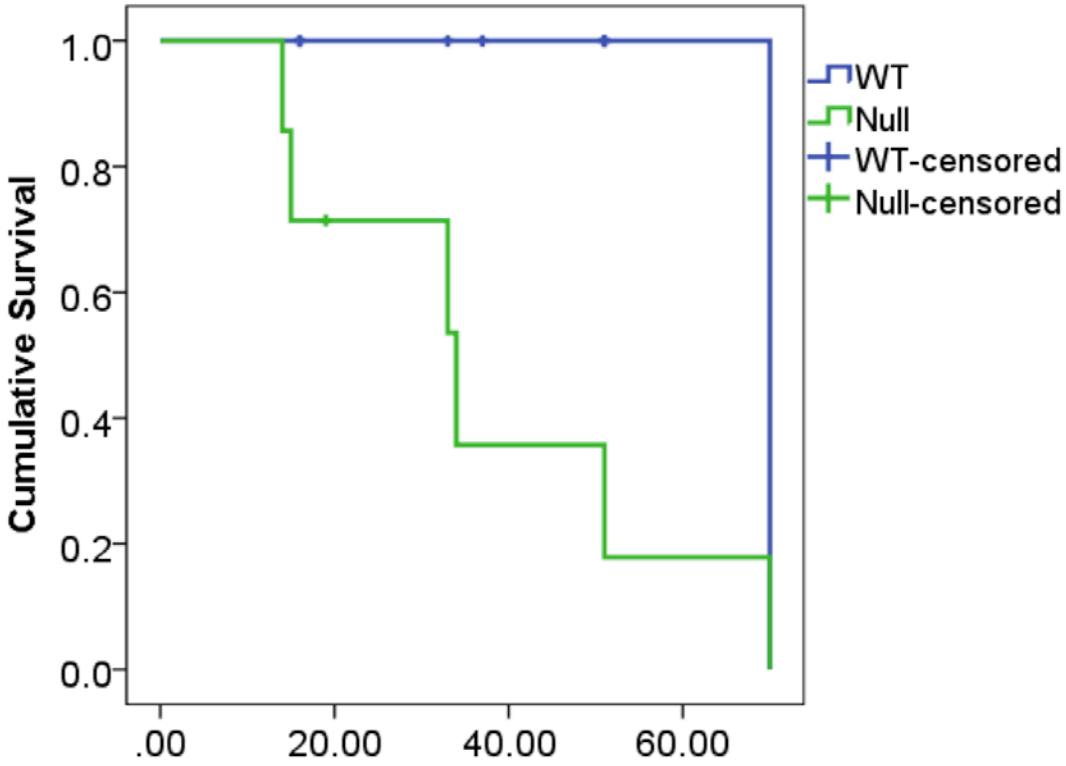

Figure 4.20: DRAM-1 is required for survival upon exposure to 2% DSS
The health status of wild-type and *DRAM-1*-null mice were monitored from the point of AOM injection to the end point of the experiment (70days). Mice which have lost more than 20% of their body weight were culled. For every sick (*DRAM-1*$^{-/-}$) mice which were harvested, a random wild-type animal was sacrificed as a 'time-point' and censored in the Kaplan-Meier curve. (p= Log-rank /Mantel-cox = 0.001).

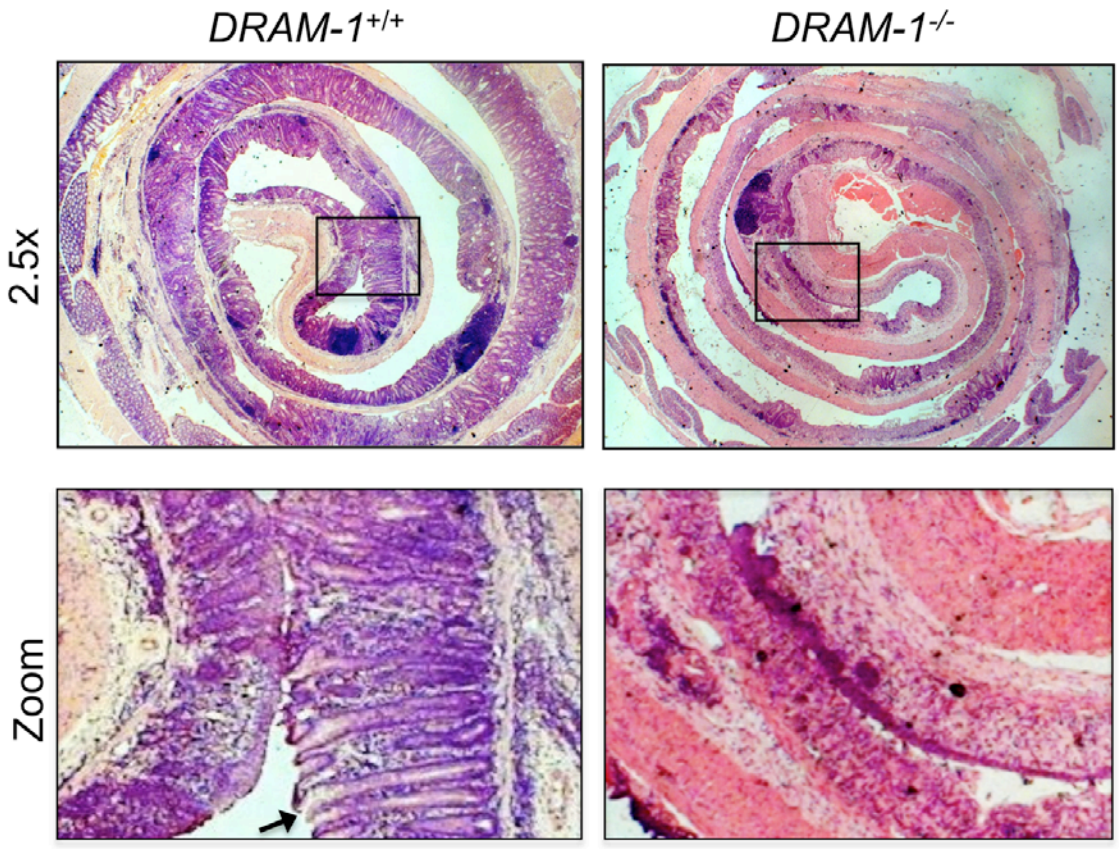

Figure 4.21: DRAM-1 is required for the regeneration of colonic crypts post inflammation-induced injury

The colons of wild-type ('time-point' control) and *DRAM-1*-null mice (poor physiological and clinical symptoms) were harvested and stained with H&E. Representative pictures were taken at 2.5x magnification. Zoomed images of selected areas highlight live crypts in wild-type and the 'denuded' colon in *DRAM-1*-null mice. An example of a live crypt is indicated by the black arrow.

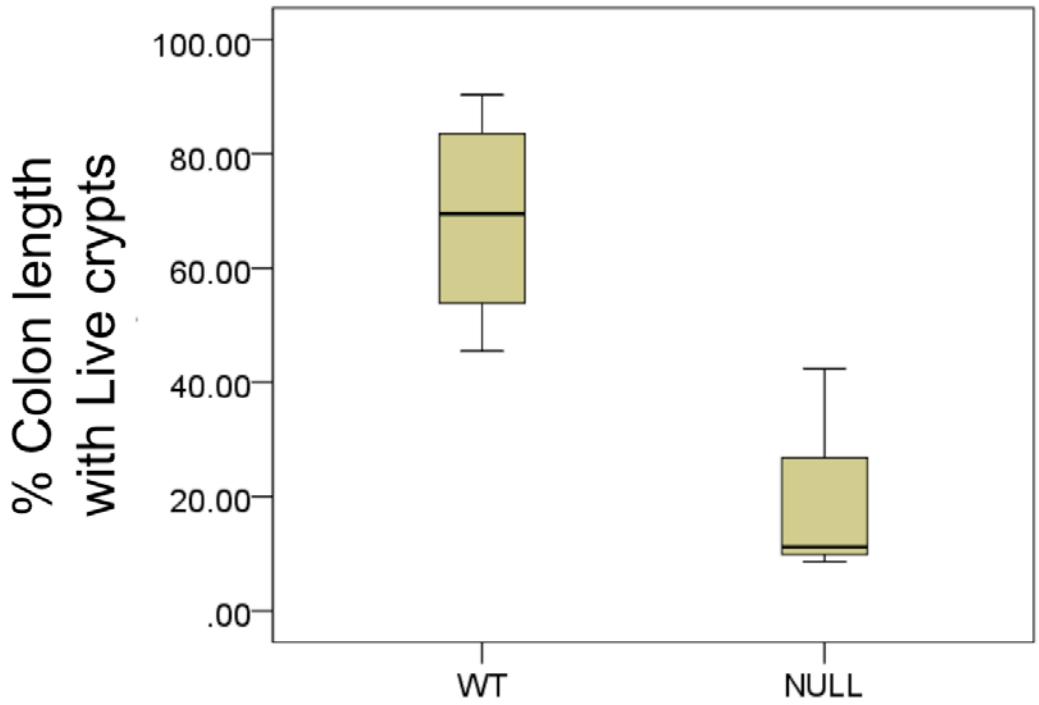

Figure 4.22: *DRAM-1* deletion decreases the number of colonic crypts
Wild type and *DRAM-1*-null mice were subjected to 2% DSS treatment. The colons were harvested and stained with H&E. The number of surviving crypts along the length of the colon is counted and averaged to the total length analysed. (Mann-Whitney U test; p =0.05). N=3

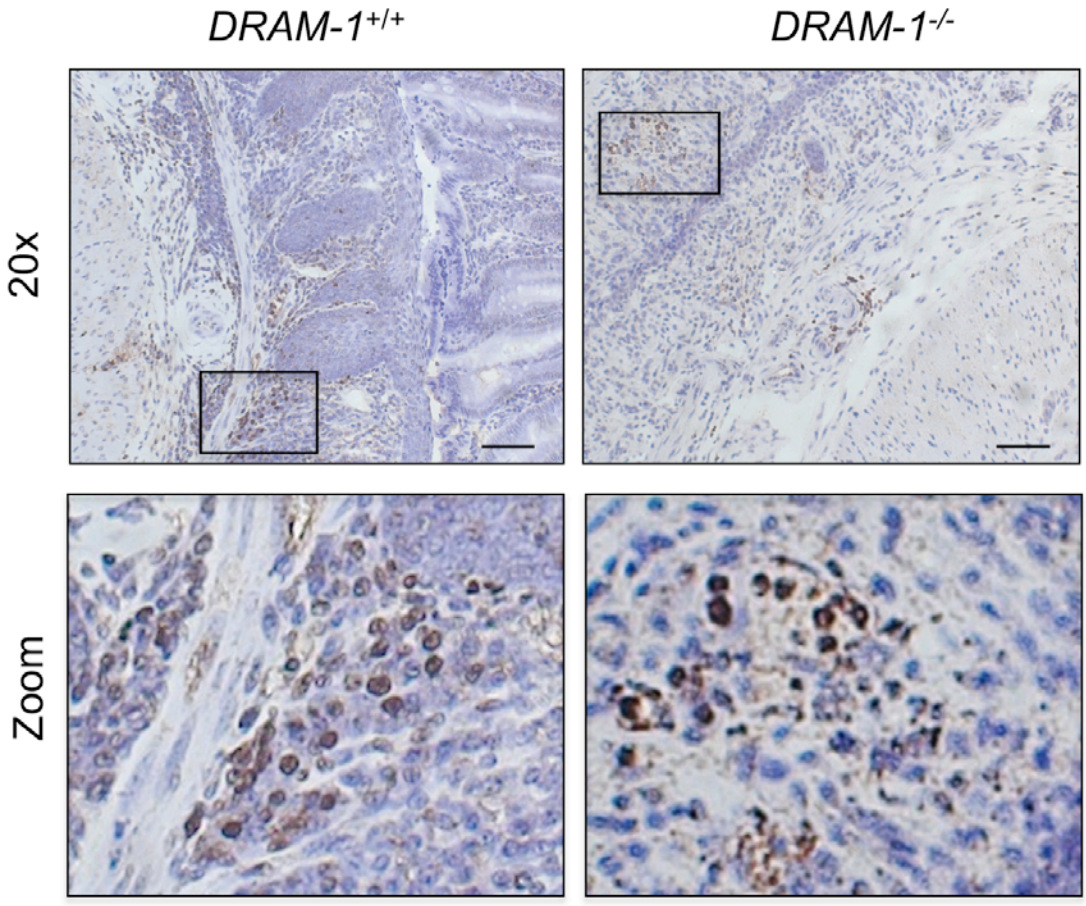

Figure 4.23 : DRAM-1 does not enhance neutrophil inflammation at the later stages of DSS induced inflammation

The colons of wild-type ('time-point' control) and *DRAM-1*-null mice (sick mice) were harvested and stained with MPO. Representative pictures were taken at 20 x magnification. Zoomed images of selected areas highlight the infiltration of neutrophils into the inflamed areas. Scale bar represents 50μm. Wild-type, N=4; *DRAM-1*$^{-/-}$, N=3.

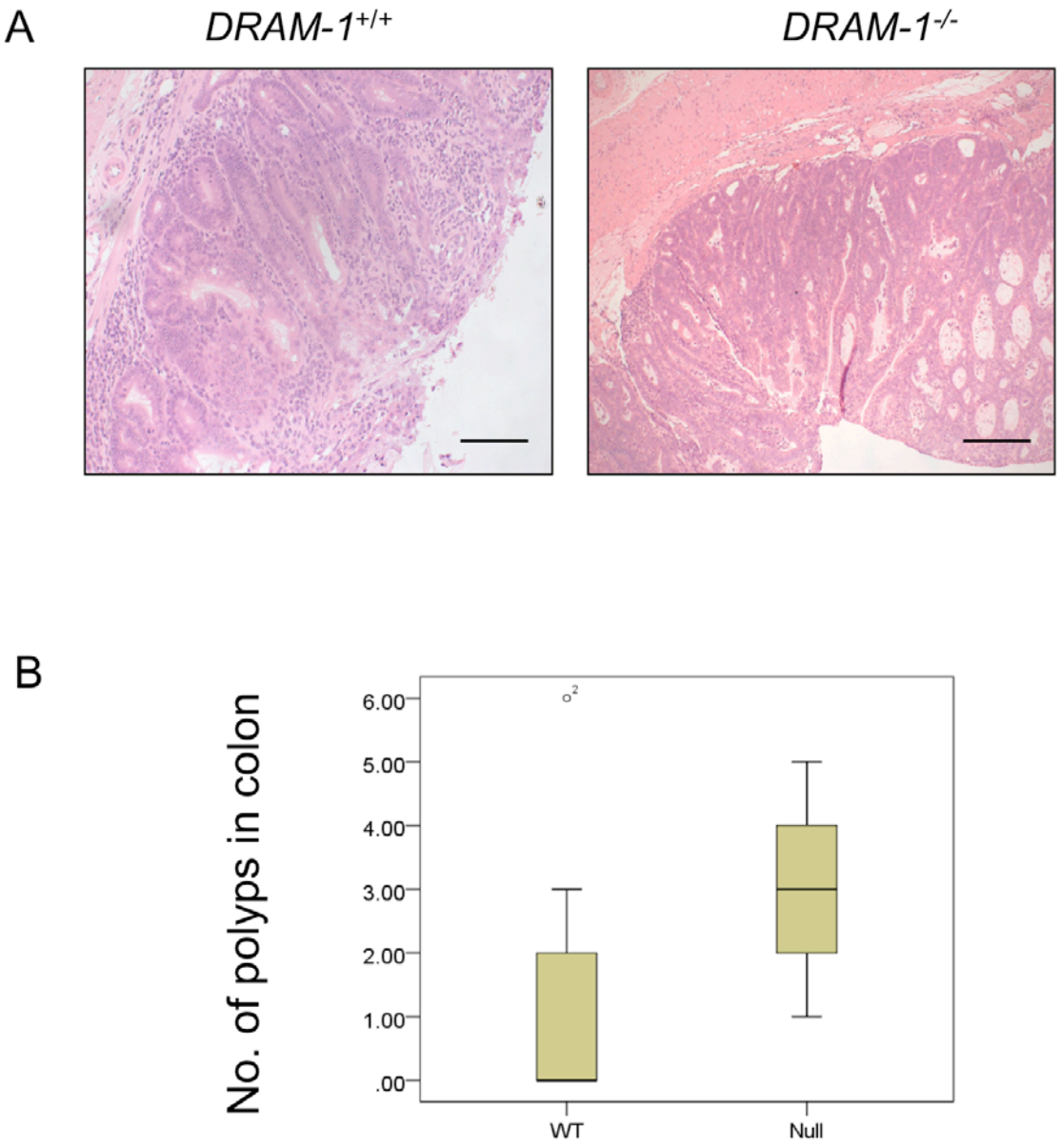

Figure 4.24: AOM/DSS treatment induces morphological changes and polyps formation in wild type and *DRAM-1*-null colon

Wild type and *DRAM-1*-null mice were subjected to 1x intraperitoneal injection of the carcinogen azoxymethane (AOM), and three cycles of 2% DSS. The mice were culled at 70 days post AOM. The colons were harvested and stained with H & E.

(A) The images were taken at original magnification x40. Scale bar represents 50μm.

(B) The number of polyps along wild-type and *DRAM-1*-null colons were quantified (Mann-Whitney U test; p=0.267)

Given that a majority of *DRAM-1*$^{-/-}$ mice suffered severe epithelial erosion and crypt loss upon exposure to 2% DSS, we were interested to investigate if DRAM-1 is involved in the modulation of the mediation of the immune responses, or the regeneration capabilities post inflammation-induced injuries, or both.

Firstly, we were interested to determine if murine *DRAM-1* mRNA expression in the colon is upregulated upon DSS treatment. At least three wild-type C57BL/6 mice were subjected to a 5-day 2% DSS treatment for 2, 5 and 7 days. *DRAM-1* mRNA expression is significantly upregulated 7 days post irradiation (REST analysis; p = 0.016) (Fig. 4.25).

Following from this, *DRAM-1*$^{+/+}$ and *DRAM-1*$^{-/-}$ mice were fed with 2% DSS drinking water for 5 days (refer to section 4.1.2) and monitored for up to seven days. At least three mice each from each genotype were dissected at day 2 to score for early stages of inflammation, day 5 for late stages of inflammation and day 7 for recovery upon inflammation-induced injury.

2 days post treatment, the physiological and clinical symptoms between wild-type and *DRAM-1*$^{-/-}$ mice remain indistinguishable (data not shown). At this point of treatment, the epithelium, crypts (Fig. 4.26) and goblet cells (Fig. 4.27) are still intact. The infiltration of neutrophils and (4.28) and macrophages (4.29) is indistinguishable between wild-type and *DRAM-1*$^{-/-}$ mice.

However, *DRAM-1*$^{-/-}$ mice exhibited a greater degree of weight loss compared to *DRAM-1*$^{+/+}$ animals) (Mann-Whitney U test; p=0.05) 5 days post treatment, although the clinical symptoms between these two groups were not significantly different (Fig. 4.30A & Fig.4.30B). Similar to previous observations, the colons of *DRAM-1*$^{-/-}$ mice showed more severe tissue destruction, and exhibited a significantly lower amount of live crypts (Mann-Whitney U test analysis (p=0.05) (Fig. 4.31). The loss of *DRAM-1*$^{-/-}$ also reduced the number of goblet cells (Fig. 4.32). Both wild-type and *DRAM-1*$^{-/-}$ mice exhibited a similar degree of neutrophil (Fig. 4.33) and macrophage (Fig. 4.34) infiltration.

Despite the preliminary studies in section 4.2.6, whereby the loss of DRAM-1 exacerbates epithelial erosion 2 days after the completion of the 5-day 2% DSS treatment (7 days in total after exposure to DSS), the colons of both *DRAM-1*$^{+/+}$ and *DRAM-1*$^{-/-}$ animals were almost completely 'denuded' at this time point. H&E staining revealed massive epithelial erosion and crypt damage (data not shown). However, the number of goblet cells revealed by Alcian blue staining) (Fig. 4.35) is more abundant in wild type, compared to *DRAM-1*$^{-/-}$ animals. Both wild-type and *DRAM-1*$^{-/-}$ mice exhibited a similar degree of neutrophil (Fig. 4.36) and macrophage (Fig. 4.37) infiltration.

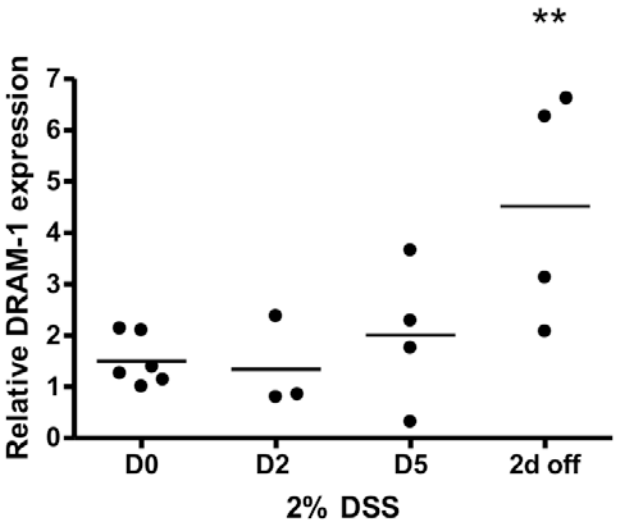

Samples from Tam Jamiesion

Figure 4.25 : *DRAM-1* mRNA level is elevated 7 days after DSS treatment
The colons of wild type mice subjected to 5 days of 3.5% DSS water were harvested 0, 2, 5 and 7 days post 3.5% DSS treatment. (REST analysis; p = 0.016)

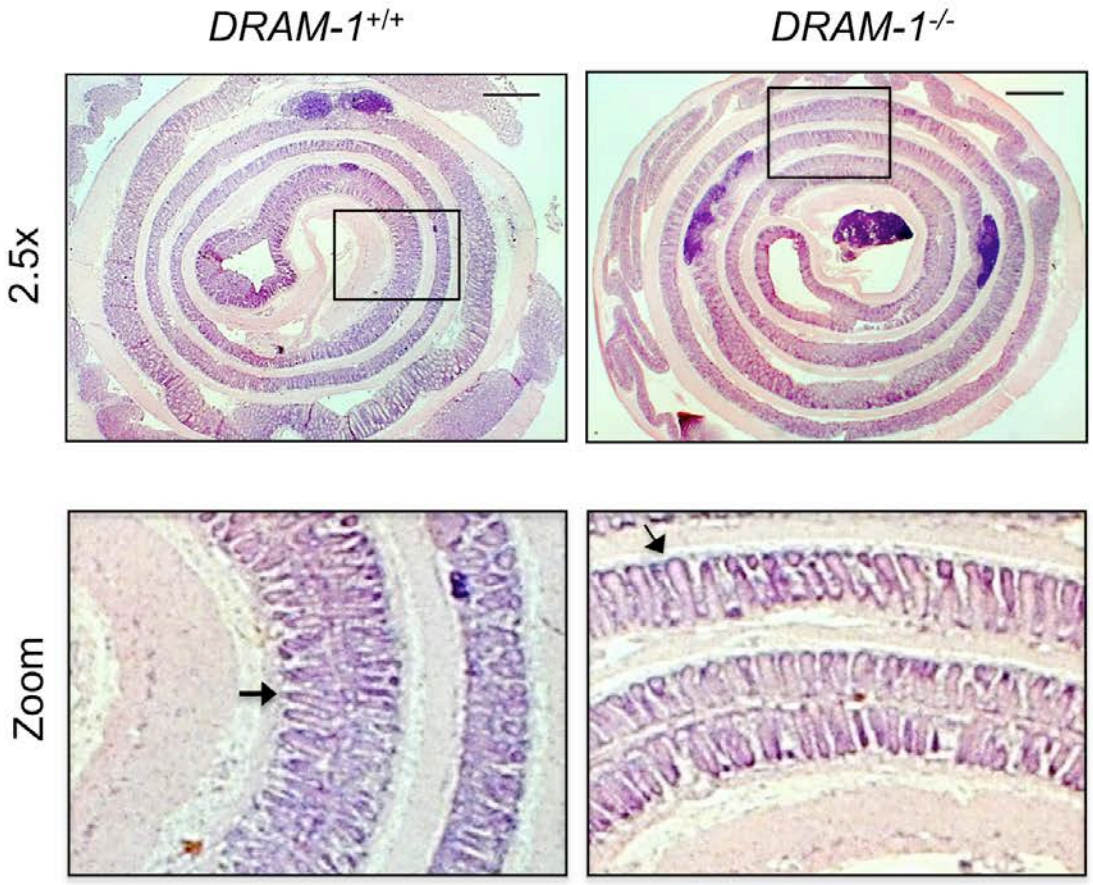

Figure 4.26: *DRAM-1* deletion does not cause epithelium erosion and crypt damage 2 days post 2% DSS treatment

The colons of wild-type and *DRAM-1*-null mice were harvested and stained with H&E. Representative pictures were taken at 2.5x magnification. Zoomed images of selected area highlights live crypts. Scale bar represents 500μm. N=3. An example of a live crypt is indicated by the black arrow.

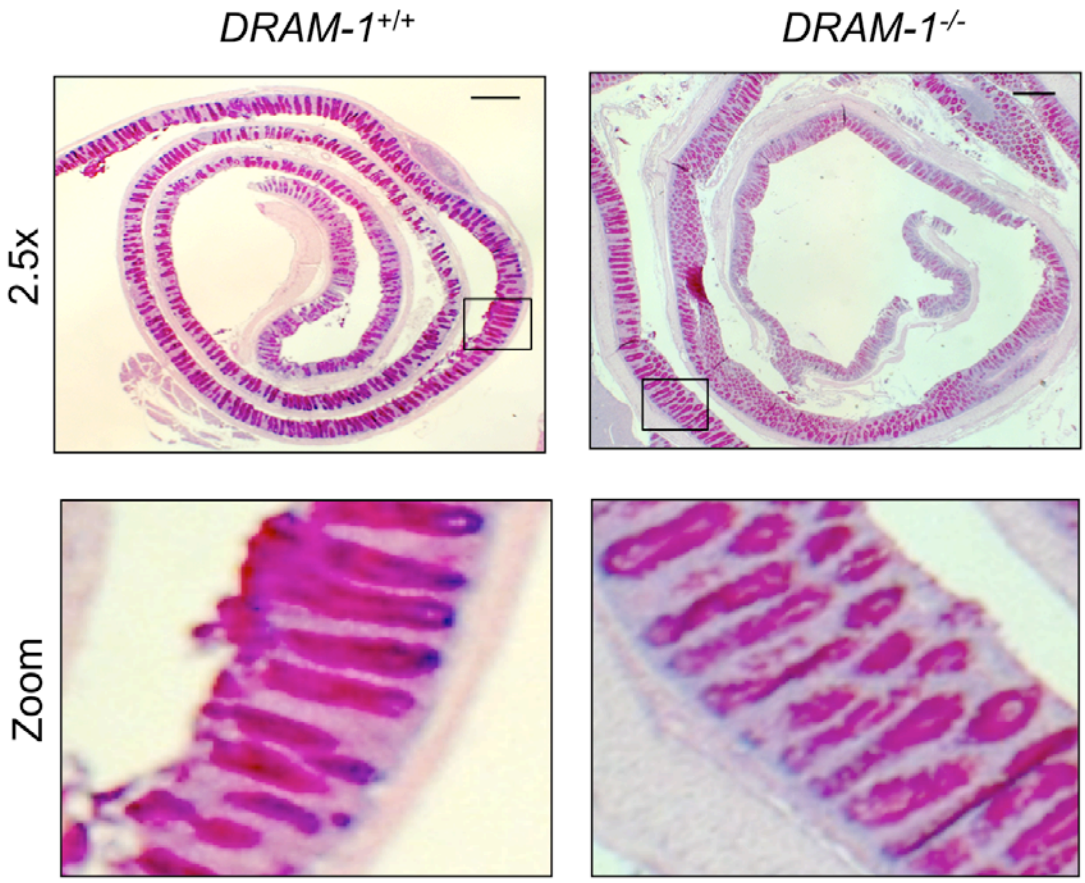

Figure 4.27 :*DRAM-1* deletion does not cause epithelium erosion or the loss of goblet cells 2 days post 2% DSS treatment

The colons of wild-type and *DRAM-1*-null mice were harvested and stained with Alcian Blue for goblet cells (stained pink). Representative pictures were taken at 2.5x magnification. Zoomed images of selected area highlights goblet cells. Scale bar represents 500μm. N=3.

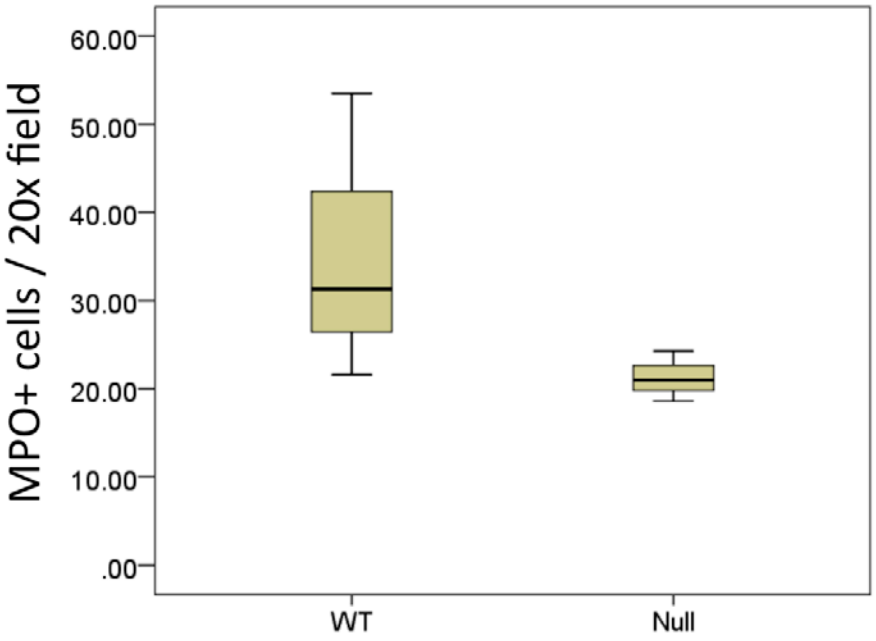

Figure 4.28: *DRAM-1* deletion does not modulate neutrophil infiltration 2 days post 2% DSS treatment

Wild type and *DRAM-1*-null mice were subjected to 2% DSS treatment. The colons were harvested 2 days post treatment hours and stained with MPO. MPO positive cells were scored at 10 successive fields from the anus under 20x magnification. Quantification of neutrophil infiltration is represented in the box plot (Mann-Whitney U test; p = 0.127). N=3.

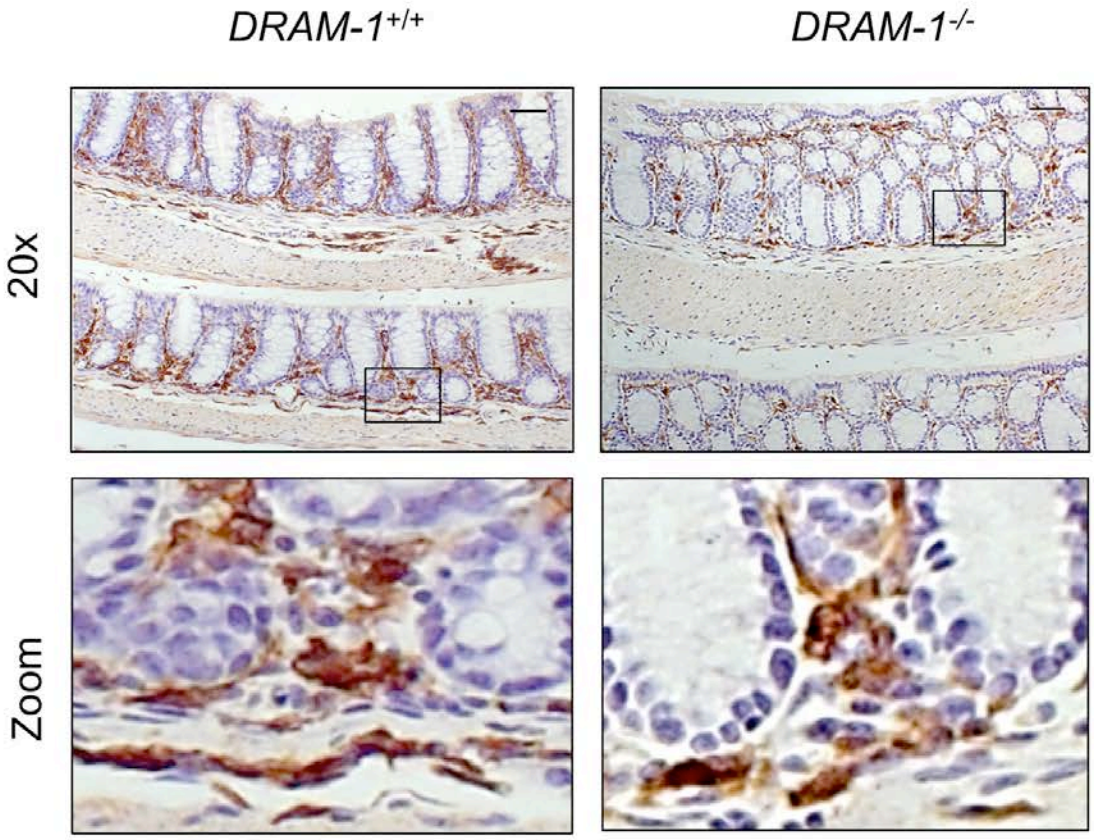

Figure 4.29: *DRAM-1* deletion does not modulate macrophage infiltration 2 days post 2% DSS treatment

Wild type and *DRAM-1*-null mice were subjected to 2% DSS treatment. The colons were harvested 2 days post treatment hours and stained with F480, a marker for macrophage. Representative images were taken at 20x. Zoomed images highlight macrophage infiltration in wild-type and *DRAM-1*$^{-/-}$ mice. Scale bar represents 50μm. N=3.

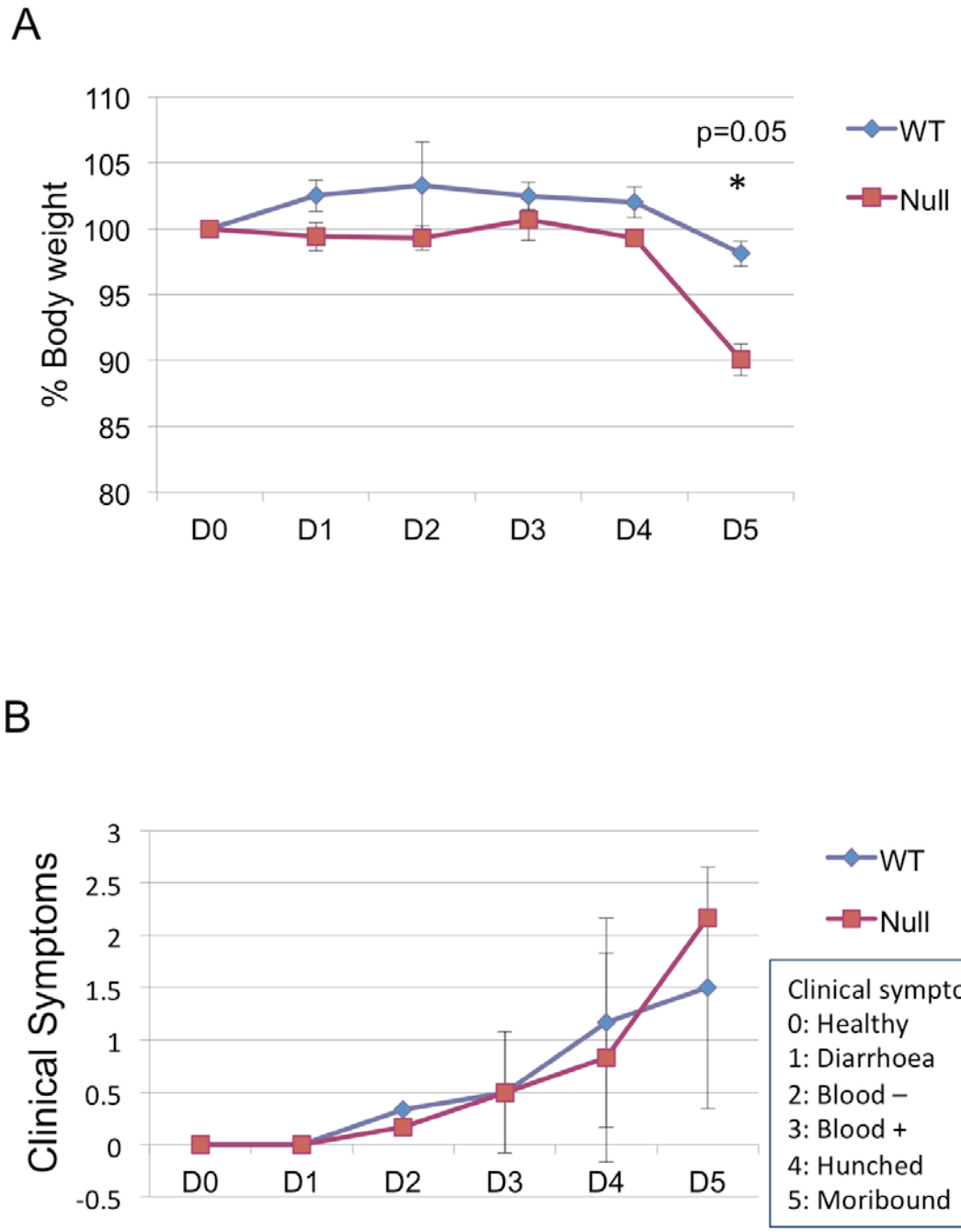

Figure 4.30(A-B): Physiological and clinical symptoms (5 days post 2% DSS treatment)

Wild type and *DRAM-1*-null mice were subjected to 2% DSS treatment.

(B)The mice were monitored daily for changes in body weight (Mann-Whitney U test; p =0.05).

(C)The mice were monitored daily for clinical symptoms and a score (0-5) is assigned each day

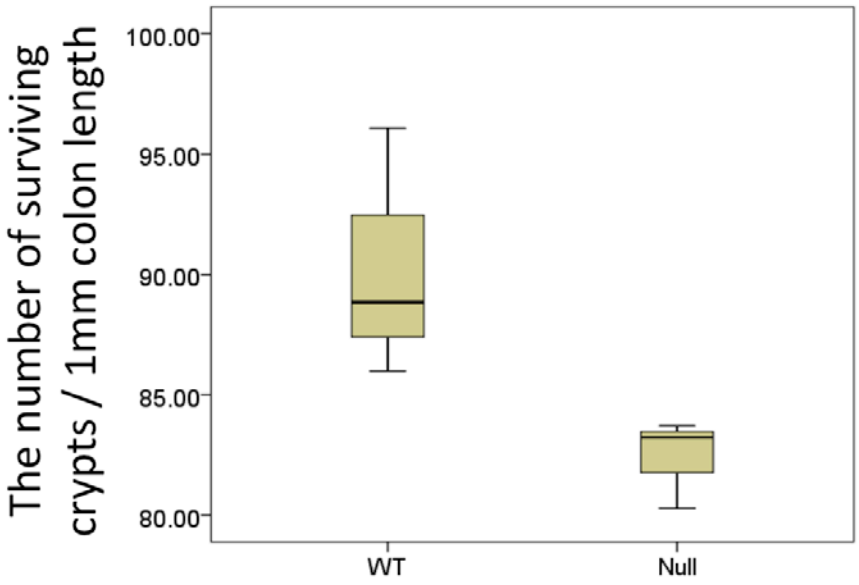

Figure 4.31: *DRAM-1* deletion decreases the number of colonic crypts 5 days post 2% DSS treatment

Wild type and *DRAM-1*-null mice were subjected to 2% DSS treatment. The colons were harvested 5 days post treatment and stained with H & E. The number of surviving crypts along the length of the colon is counted and averaged to the total length counted. (Mann-Whitney U test; p =0.05). N=3

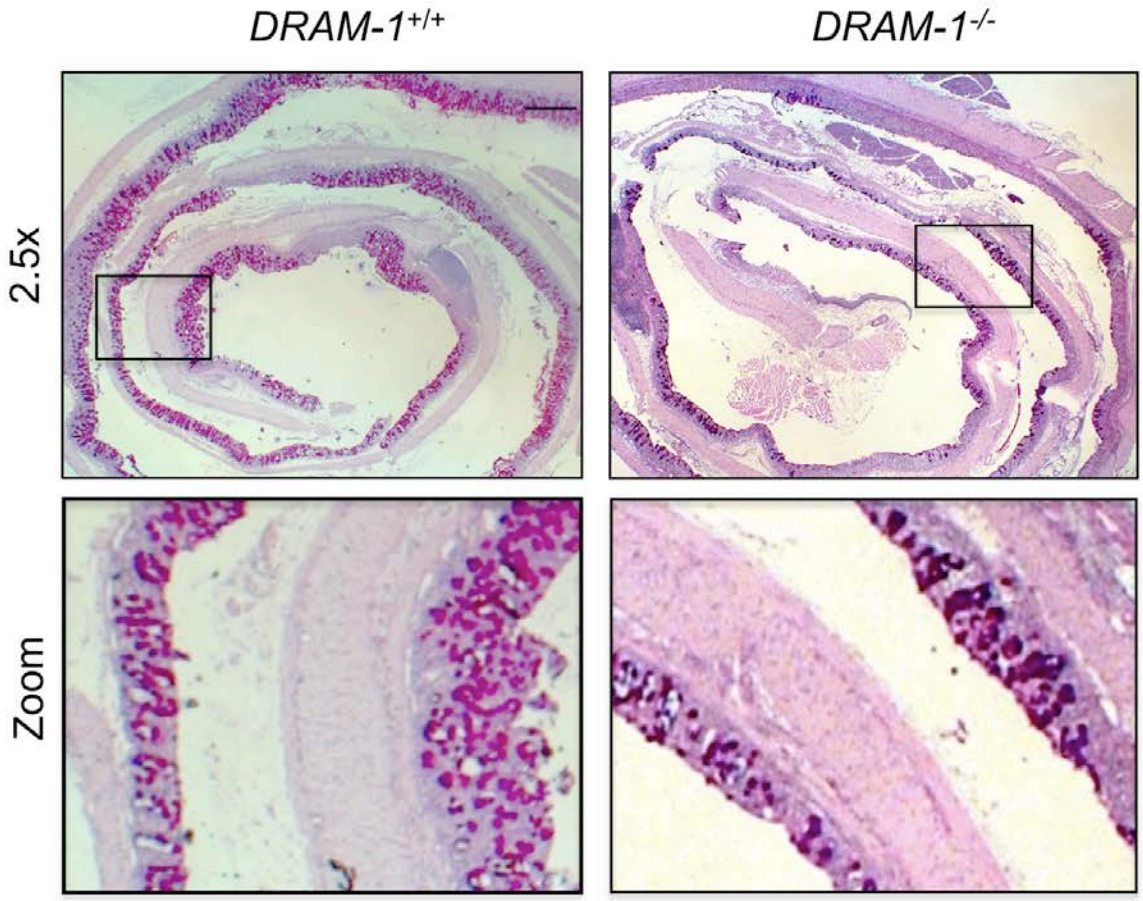

Figure 4.32 :*DRAM-1* deletion decreases the number of goblet cells 5 days post 2% DSS treatment

The colons of wild-type and *DRAM-1*-null mice were harvested and stained with Alcian Blue for goblet cells (stained pink). Representative pictures were taken at 2.5x magnification. Zoomed images of selected area highlights the distribution of goblet cells in the colon.

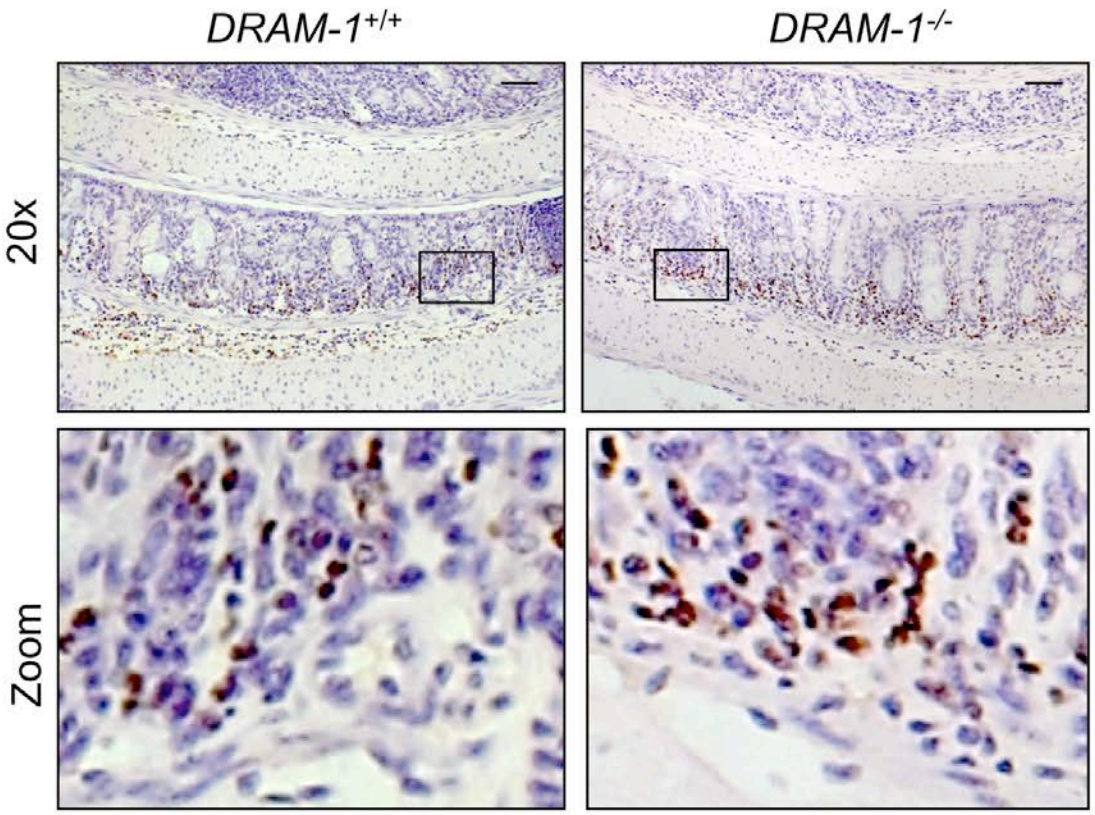

Figure 4.33: *DRAM-1* deletion does not modulate neutrophil infiltration 5 days post 2% DSS treatment

Wild type and *DRAM-1*-null mice were subjected to 2% DSS treatment. The colons were harvested 5 days post treatment hours and stained with MPO, a marker for neutrophils. Representative images were taken at 20x. Zoomed images highlight neutrophil infiltration in wild-type and *DRAM-1*$^{-/-}$ mice. Scale bar represents 50μm. N=3.

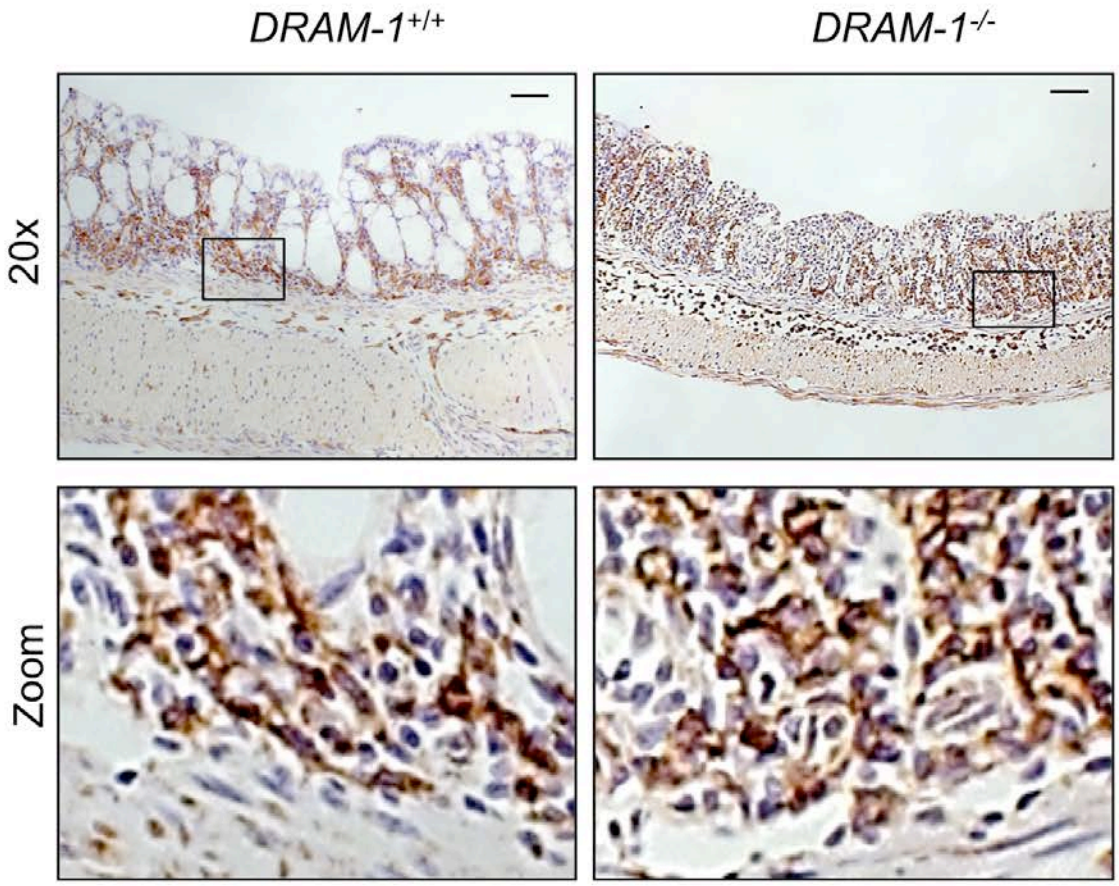

Figure 4.34: *DRAM-1* deletion does not modulate macrophage infiltration 5 days post 2% DSS treatment

Wild type and *DRAM-1*-null mice were subjected to 2% DSS treatment. The colons were harvested 5 days post treatment hours and stained with F480, a marker for macrophage. Representative images were taken at 20x. Zoomed images highlight macrophage infiltration in wild-type and *DRAM-1*$^{-/-}$ mice. Scale bar represents 50μm. N=3.

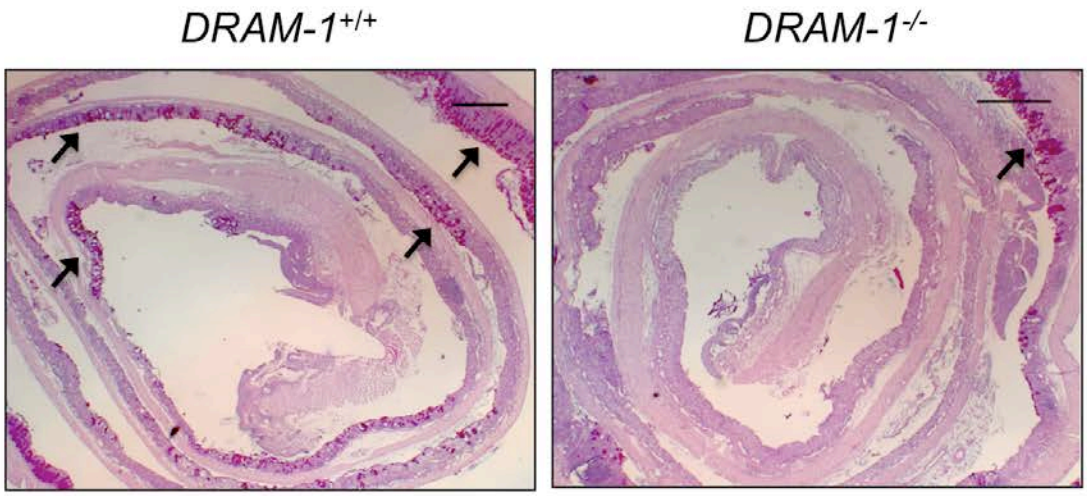

Figure 4.35: *DRAM-1* deletion decreases the number of goblet cells 7 days post 2% DSS treatment

Wild type and *DRAM-1*-null mice were subjected to 2% DSS treatment for 5 days and subjected to normal drinking water for 2 days. The colons were harvested and stained with Alcian Blue for goblet cells (stained pink). Representative pictures were taken at 2.5x magnification. Arrows indicate areas with live goblet cells.

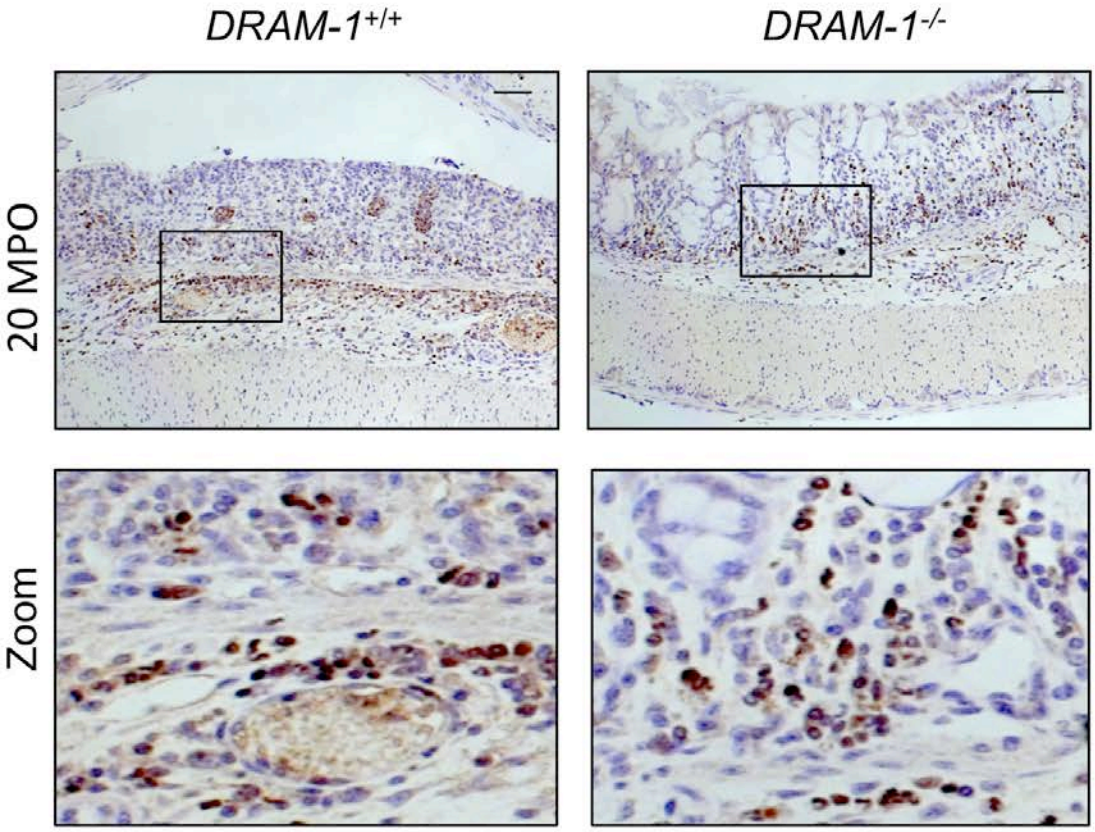

Figure 4.36: *DRAM-1* deletion does not modulate neutrophil infiltration 7 days post 2% DSS treatment

Wild type and *DRAM-1*-null mice were subjected to 2% DSS treatment for 5 days and subjected to normal drinking water for 2 days. The colons were harvested and stained with MPO, a marker for neutrophil. Representative images were taken at 20x. Zoomed images highlight neutrophil infiltration in wild-type and *DRAM-1*$^{-/-}$ mice. Scale bar represents 50μm. N=3.

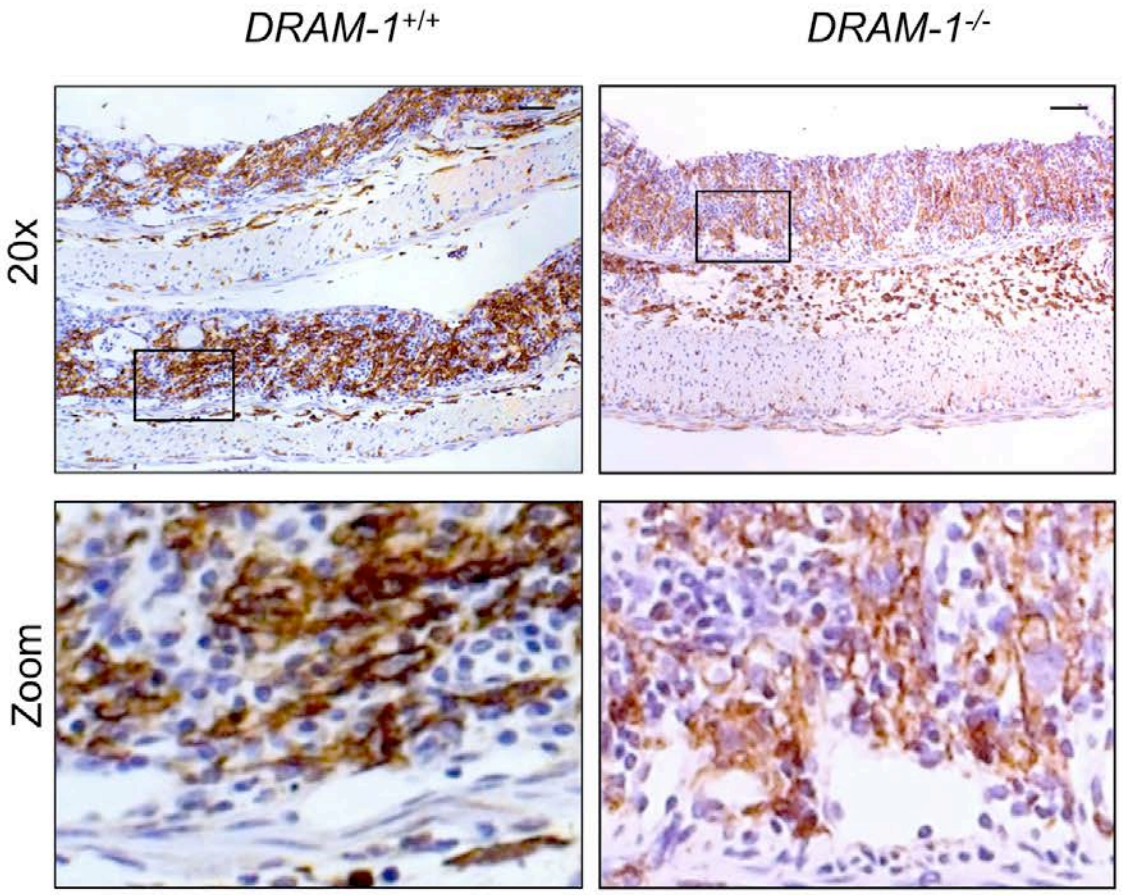

Figure 4.37: *DRAM-1* deletion does not modulate macrophage infiltration 7 days post 2% DSS treatment

Wild type and *DRAM-1*-null mice were subjected to 2% DSS treatment. The colons were harvested 7 days post treatment hours and stained with F480, a marker for macrophage. Representative images were taken at 20x. Zoomed images highlight macrophage infiltration in wild-type and *DRAM-1*$^{-/-}$ mice. Scale bar represents 50μm. N=3.

From this study, the loss of *DRAM-1* does not cause epithelial erosion or aggravate neutrophil and macrophage infiltration in the early stages of inflammation (2 days post treatment). However, the deletion of *DRAM-1* exacerbates the loss of epithelium integrity, as revealed by a reduced number of live goblet cells and crypts in the later stages of inflammation (5 days post treatment), with no difference between neutrophil and macrophage infiltration. The exacerbated colon damage observed in *DRAM-1*$^{-/-}$ mice could be attributed to an intensified immune response mediated by other immune cells such as plasma cells, B cells, T cells and monocytes. Alternatively, this can also be caused by a reduced regeneration capacity post inflammation-induced injury. Albeit preliminary results shown earlier in this section imply that the loss of *DRAM-1* exacerbates inflammation, the colons of both *DRAM-1*$^{+/+}$ and *DRAM-1*$^{-/-}$ animals were almost completely 'denuded' at day 7. As before, neutrophil and macrophage infiltration remained indistinguishable between wild-type and *DRAM-1*$^{-/-}$ mice. However, wild-type colons appear to retain more live goblet cells compared to DRAM-1 deficient mice.

4.3 Discussion

DRAM-1$^{+/-}$ intercrosses yielded *DRAM-1*$^{-/-}$ mice in the expected Mendelian ratio. There was also no difference in the number of *DRAM-1*$^{+/+}$, *DRAM-1*$^{+/-}$, *DRAM-1*$^{-/-}$ female and male pups that were born. DRAM-1 deletion is not embryonic lethal as *DRAM-1*$^{-/-}$ mice are viable, fertile, and appeared normal, with no obvious phenotypic defects compared to wild-type and heterozygote controls. Furthermore, *DRAM-1*$^{-/-}$ mice do not show an increased propensity to the spontaneous development of cancer or autophagy disorders. Given that there are other DRAM family members identified (O'Prey, Skommer et al. 2009), it remains plausible that the loss of DRAM-1 can be compensated by these proteins, implying the need to generate multiple DRAMs conditional knockout mouse models. In relation to this, DRAM-1 is highly conserved in a number of species including mouse, zebrafish, Drosophila, and *C. elegans*, as demonstrated by sequence alignment studies performed by Crighton et. al (2006). This suggests that DRAM-1 must have a very important function since the protein sequence does evolve drastically from lower organisms to higher eukaryotes. Alternatively, DRAM-1 could form part of a huge regulatory complex in which the subunits comprising the complex have structural roles. The evolution of one subunit would also require the co-evolution of other subunits. The conservation of DRAM-1 may also allow for a flexibility to be involved in the regulation of a variety of cellular pathways, which could explain the diverse roles of DRAM-1 in the regulation of autophagy and cell death (discussed in chapter 3); mitosis, proliferation, regeneration and inflammation/innate immunity (discussed in chapter 4) and potentially adaptive immunity (discussed in chapter 5).

Due to the high degree of similarity the involvement of other DRAM family members can also be confirmed by deleting DRAM in simpler metazoans like *C.elegans* and zebrafish, or organisms which only encode one copy of DRAM, such as Drosophila (O'Prey, Skommer et al. 2009). If the deletion of DRAM is lethal, this would suggest that the DRAM family members in higher eukaryotes may have evolved to share functional similarities with DRAM-1.

DRAM-1$^{-/-}$ mice have a reduced number of circulating lymphocytes and platelets. Since DRAM-1 is modulates autophagsome formation, it would be plausible to

investigate if *DRAM-1*-null lymphocytes are still capable of undergoing autophagy, using methods described by Phadwal et. al (2012). Additionally, given that autophagy has been implicated in the clearance of mitonchondria (Pua, Guo et al. 2009), the regulation of endoplasmic reticulum homeostasis and calcium mobilization in T lymphocytes (Jia, Pua et al. 2011), it seem plausible to investigate if these processes can still take place normally in *DRAM-1*-null T lymphocytes.

Furthermore, *DRAM-1* mRNA expression is downregulated in PU.1 knockdown cells (Steidl, Rosenbauer et al. 2006). Thus, it remains plausible that DRAM-1 is involved in haematopoiesis, and that this defect does not progress due to the compensatory effects by other members of the DRAM family. Following from this, it would be interesting to determine which population of circulating lymphocytes (i.e. T cells, B cells, and/or natural killer (NK) cells that are affected upon *DRAM-1* deletion. Additionally, It is also crucial to investigate if *DRAM-1* deletion affects the population of myeloid and lymphoid bone marrow progenitors, as well the activity of haematopoietic stem/progenitor cell (HSPC) by performing colony-forming cell assay (CFC) and *in vivo* repopulation assays (Mortensen, Soilleux et al. 2011) using bone marrow cells isolated from wild type and *DRAM-1*$^{-/-}$ mice.

Although DRAM-1 is required to enhance p53-dependent apoptosis *in vitro* (Crighton, Wilkinson et al. 2006), DRAM-1 does not modulate p53-dependent apoptosis and radiation-induced apoptosis *in vivo.* Given that the previous *in vitro* assays were conducted in Saos-2 osteosarcoma cells and MEFs, this suggests that the involvement of DRAM-1 in p53-dependent apoptosis is maybe specific to certain cell(s) or tissue(s).

However, DRAM-1 is required for the intestinal crypt regeneration upon radiation-induced injury by modulating cellular proliferation and mitosis. Consistent with this, crypt size is significantly reduced in *DRAM-1*$^{-/-}$ mice compared to the wild-type control. Given this, *DRAM-1* deletion does not affect the population of OLFM4 positive fast cycling intestinal stem cells in regenerating crypts. Nonetheless, the stem cell pool in regenerating crypts of wild-type and *DRAM-1*$^{-/-}$ mice should be confirmed with other stem cell markers, such as Lgr5, Bmi1 and Musashi (Barker,

van Es et al. 2007). This can be ascertain by further IHC validation or by crossing *DRAM-1*$^{-/-}$ and *Lgr5-GFP*$^{+}$ mice (Barker, van Es et al. 2007).

While Akt/mTOR signaling is required for intestinal regeneration (Ashton, Morton et al. 2010), Akt and mTOR activity is not affected upon *DRAM-1* deletion in regenerating crypts. Thus, the defect in crypt regeneration is most likely not attributed to a block in the Akt/mTOR signaling pathway.

Autophagy activity has been shown to be upregulated in the small intestine paneth cells upon exposure to ionising radiation and this process is partly mediated by the iNOS signalling mechanism (Gorbunov and Kiang 2009). Similarly, high autophagy activity is also associated with the intestinal proliferative and undifferentiated progenitor cell populations (Groulx, Khalfaoui et al. 2012). Thus, it might be worth while to investigate if autophagic activity in the paneth cells, stem cells or other cells that reside in the small intestine is disrupted upon the loss of DRAM-1 when exposed to gamma irradiation. This can be confirmed by monitoring LC3-II puncta by immunohistochemistry, as described by Rosenfeldt et. al (2012).

Following from the above, the link between paneth cells and the maintenance of intestinal stem cells is well established both *in vitro* and *in vivo*. Genetic removal of paneth cells *in vivo* by mutating *Gfi1*, transgenic expression of diphtheria toxin A under the paneth-cell-specific cryptdin 2 promoter (*CR2-tox176*), and conditional deletion of *Sox9*, results in the concomitant loss of Lgr5 stem cells (Sato, van Es et al. 2011). In addition, Paneth cells have been reported to express EGF, TGF-α, Wnt3 and the Notch ligand Dll4, all essential signals for stem-cell maintenance in culture (Sato, van Es et al. 2011). It is thus concluded that paneth cells provide a niche for intestinal stem cells, which drives clonogenic repopulation of the intestinal crypt (see section 4.1). Given that the loss of *DRAM-1* is proposed to decrease the clonogenic repopulation of intestinal crypts upon irradiation, it would be interesting to establish if this is a DRAM-1 is required for paneth cell function, and subsequently stem cell maintenance. This can be tested by conditionally deleting *DRAM-1* in the paneth cells using the cryptdin 2 promoter (*CR2-tox176*) (Garabedian, Roberts et al. 1997) , followed by assessing paneth cell function and number by staining for markers of the paneth cells - lysozyme 1 and 2 and

defensins (Wang, Peregrina et al. 2011). Lysozymes and defensins are anti-microbial that are produced by the paneth cells (Sato, van Es et al. 2011).

DRAM-1 mRNA expression level is downregulated in oncogene-induced senescent cells. However, *DRAM-1* deletion does not modulate p53-induced senescence in the liver, quantified by the indistinguishable proliferative events in *DRAM-1*$^{+/+}$ and *DRAM1*$^{-/-}$. However, the role of DRAM-1 in oncogene-induced senescence *in vitro* and *in vivo* has yet to be elucidated and is certainly worth pursuing.

Although the *in vivo* model of moderate p53 activation in the liver does not induce apoptosis, a significant population of *DRAM-1*$^{-/-}$ hepatocytes exhibited an elevated level of histone H3 phosphorylation. The increase in mitosis does not contribute to increased proliferation (indistinguishable BrdU incorporation), but rather, *DRAM-1*-null hepatocytes display a greater propensity to cell death, as revealed by caspase 3 staining. Given that the phosphorylation of histone H3 is initiated in late G2/interphase and dephosphorylated takes place upon anaphase, (Hendzel, Wei et al. 1997), it is very likely that the DRAM-1$^{-/-}$ hepatocytes are arrested in the metaphase stage, at spindle assembly checkpoint (SAC) (refer to section 1.8.2). This could be attributed to a defect in the formation of the mitotic spindle, which disables the attachment of the chromosomes to the mitotic spindle, or the alignment at equatorial plane (Zhou, Yao et al. 2002). In this case, *DRAM-1*$^{-/-}$ hepatocytes may eventually exit mitosis without proper sister chromatid segregation and cell division, and then undergo apoptosis by p53-dependent tetraploidy checkpoint activation (Huang, Chang et al. 2009). To ascertain this, it would be useful to determine if the loss of *DRAM-1* affects centrosomes and spindle formation, as well as the attachment of sister chromatids on the spindles and the alignment of the metaphase plate. Additionally, it would be interesting to determine if the loss of DRAM-1 modulates the expression of BubR1, a key component of the mitotic spindle checkpoint machinery, which is also regulated by p53 (refer to section 1.8.2). In any case, it may also be interesting to establish the role of DRAM-1 in in vivo models of liver cancer, ranging from carcinogen- and virus-induced to genetically engineered mouse model for HCC (Leenders, Nijkamp et al. 2008). This would determine if the plausible defects in mitosis and increased apoptosis upon *DRAM-1* deletion can result in tumourigenesis.

DRAM-1 deletion does not predispose to radiation-induced tumourigenesis, as the onset of tumourigenesis is indistinguishable between *DRAM-1*$^{+/+}$, *DRAM-1*$^{+/-}$ *and DRAM-1*$^{-/-}$ mice. It remains plausible that the tumour suppressive roles of DRAM-1 can be compensated by other members of the DRAM family, which explains why the loss of *DRAM-1* does not predispose to radiation-driven tumourigenesis. Thus, it would be of great interest to determine if the tumours arising from *DRAM-1*$^{-/-}$ mice displayed an increased expression of *DRAM-2, DRAM-3, DRAM-4* or *DRAM-5*, or if the simultaneous deletion of *DRAM-1* and other DRAM family members increases the risk of tumour development. Yet another explanation is that the tumour suppressive (or promoting) effects of DRAM-1 are highly specific to the carcinogenic stimuli or tissue type.

In our efforts to investigate if the loss of DRAM-1 predisposes to inflammation-driven colorectal carcinogenesis using the AOM/DSS model, we found that *DRAM-1*$^{-/-}$ mice are susceptible to 2% DSS. This indicates that the loss of *DRAM-1* predisposes to inflammation, at least in the colon. To investigate this further, *DRAM-1*$^{+/+}$ and *DRAM-1*$^{-/-}$ mice were subjected to the acute colitis model (2% DSS) and monitored for changes in physiological and clinical symptoms for 7 days as before, without the AOM injection.

DRAM-1 deletion does not affect epithelium integrity, as well as the infiltration of neutrophils and macrophages in the early stage of inflammation.

However, *DRAM-1* deficiency exacerbates the loss of epithelium integrity, crypt damage and the loss of goblet cells in the later stages of inflammation (5 days post treatment). As before, the infiltration of neutrophils and macrophages at this stage remained indistinguishable between *DRAM-1*$^{+/+}$ and *DRAM-1*$^{-/-}$ colons.

Recapitulating the preliminary results in the beginning of section 4.2.6, the colons of *DRAM-1*$^{-/-}$ animals assessed at day 7 (after the 5 days 2% DSS treatment and 2 days recovery period on normal drinking water) exhibited complete epithelial destruction. However, the colons of both *DRAM-1*$^{+/+}$ and *DRAM-1*$^{-/-}$ animals were almost completely ‘denuded’ at the endpoint of the acute colitis experiment, although there were more live goblet cells in the wild-type compared to *DRAM-1*$^{-/-}$ colons. An explanation for the variation is possibly due to the different animal

density in the animal facility between the period of preliminary studies and the 'controlled' DSS experiment. Furthermore, the strain of mice used in this experiment normally survive past 7 days of this regimen (Clapper, Cooper et al. 2007). Again, this implies that the exacerbated inflammation and irreparable tissue damage in wild-type may be attributed to varying hygiene conditions between different animal facilities in different institutions. Thus, it would be critical to optimise and tailor the dosage of DSS treatment to the hygiene condition in order to reach a comparable end-point between the wild-type experimental controls and the published wild-type cohorts.

The loss of the autophagy regulator, ATG16L1 has been shown to drastically disrupt the function of paneth cells of the small intestine, thus leading to an increase in the expression of a subset of inflammatory cytokines (Cadwell, Liu et al. 2008). In line with this, it seems plausible to investigate if the expression of the genes (by qPCR) encoding these subset of cytokines is different in the wild-type and *DRAM-1*-null small intestine when exposed to DSS. Additionally, the production of inflammatory cytokine may be exacerbated upon the loss of DRAM-1 during inflammation, which could explain the sensitisation of *DRAM-1*-null mice to DSS. This could be determined by performing a cytokine array on blood samples, which would indicate the level of systemic cytokine production (personal communication, Dr. Simon Milling). In addition, regulators of the unfolded protein response (UPR) such as XBP1 and ORMDL3 have been shown to genetically associated with Crohn's disease and ulcerative colitis (Fritz, Niederreiter et al. 2011). Since the loss of DRAM-1 predisposes to DSS-induced colitis, it would be interesting to investigate if the functions of these regulators might be disrupted upon the loss of *DRAM-1.* Additionally, it might be interesting to investigate if other inflammatory markers, such as granulocyte marker proteins (GMP) are expressed differently in *DRAM-1*$^{+/+}$ and *DRAM-1*$^{-/-}$ mice (Nysoeter, Erichsen et al. 2007).
The normal colon has been reported to contain a diverse population of immune cells ranging from T cells, plasma cells, macrophages and class II antigen-expressing cells (Banner, Savas et al. 1993). Although we have demonstrated that the loss of *DRAM-1* does not modulate neutrophil and macrophage infiltration, it would be interesting to investigate if other immune cells such as the ones mentioned above, are involved in modulating the immune responses in the inflamed colon (Banner, Savas et al. 1993).

Perhaps the most interesting facet associated with this study is to determine whether the intensified damage in the colon upon *DRAM-1* deletion is attributed to an exacerbated inflammation (which could lead to excessive tissue damage beyond repair), loss of epithelial integrity, a defect in the regenerative capacity of the colonic crypts post injury, or a combination of all the above. To investigate this, it *DRAM-1* can be conditionally deleted in the colon under the control of the Vil-Cre promoter, which deletes specifically in the gut epithelium (el Marjou, Janssen et al. 2004). If the loss of *DRAM-1* in the gut causes colon destruction, this may imply that DRAM-1 is required to maintain the integrity of epithelial cells. Additionally, the regeneration capacity could also be affected, and this can be determined by assessing proliferative and mitotic indices, as well as stem cell activity, similar to methods as described in section 4.2.3.

Likewise, to investigate if DRAM-1 is required to control the extent of the immune response upon pathogen attack, *DRAM-1* deletion in the immune cells can be driven by the Vav-Cre promoted which deletes *DRAM-1* in the hematopoietic cells thus giving rise to *DRAM-1*$^{-/-}$ immune cells (de Boer, Williams et al. 2003). If *DRAM-1* deletion in this context causes colon destruction, this may imply that DRAM-1 is required to regulate the magnitude of immune response. As mentioned above, DRAM-1 may also regulate all these processes, and thus is an exciting area worth pursuing.

Lastly, to determine if DRAM-1 is required to prevent the onset of colitis-associated colorectal cancer, it would seem plausible to reduce the dosage of DSS in order to limit the extent of inflammation so that *DRAM-1*-null mice can recover and stay alive until a point where they are able to develop polyps for accurate comparison with wild-type mice. Additionally, it would be interesting to establish if the infiltration of immunes cells, such as neutrophils, mast cells, natural killer (NK) cells, dendritic cells (DC), and tumor-associated macrophages is modulated in *DRAM-1-null* tumours, as suggested by Terzic and colleagues (2010) (Terzic, Grivennikov et al. 2010).

In conclusion, the loss of *DRAM-1* maybe compensated by other DRAM family members, thus explaining the lack of diseased phenotypes upon *DRAM-1*

deletion. However, the role of DRAM-1 in the cell cycle, particularly in the maintenance of the spindle assembly checkpoint and the progression from metaphase and anaphase is worth investigating. Furthermore, DRAM-1 is also very likely to be involved in tissue regeneration, at lease in the gastrointestinal tract upon radiation-induced injuries. The loss of *DRAM-1* does not predispose to radiation-induced tumourigenesis, but its role in modulating cancer development driven by inflammation remains unknown and is worth pursuing. DRAM-1 is also required to limit the extent of damage in the colon upon pathogen attack. The direct function of DRAM-1 in the colon, whether to control the magnitude of the immune response, maintain epithelium integrity or mediate crypt regeneration upon damage is yet to be elucidated and merits further investigations.

Chapter 5: The role of p53 and DRAM-1 in the regulation of antigen processing via the MHC pathway

5.1 Introduction

Dendritic cells (DCs) are potent antigen presenting cells (APCs) that capture antigens in peripheral tissues and migrate to lymphoid organs where the processed antigenic fragments are presented to T cells (Pierre, Turley et al. 1997; Vidalain, Azocar et al. 2000). Immature DCs express low levels of MHC class I, MHC class II molecules, and T cell costimulatory molecules, and they are specialised to endocytose antigen (Banchereau and Steinman 1998). Mature DCs, which have acquired antigens, have increased expression of MHC molecules and T cell costimulatory molecules (Banchereau and Steinman 1998). Effective T cell activation by antigen presenting cells requires the interaction of the MHC molecules and T cell costimulatory molecules on APCs with the receptors on T cells (Fig. 5.1) (Rovere, Vallinoto et al. 1998) (Pierre, Turley et al. 1997) (Tripathi, Bruch et al. 2008). In addition to DCs, macrophages have also been shown to process and present peptides on MHC molecules for the activation of T cells (Unanue 1984) (Ceddia and Woods 1999). MHC class II molecules and T cell costimulatory molecules have also shown to be upregulated on macrophages upon exposure to antigens (Damoiseaux, Yagita et al. 1998) (O'Keefe, Nguyen et al. 2002).

Apart from antigens, the presence of a high number of apoptotic cells can also induce DC maturation and the presentation of intracellular antigen from these dying cells (Rovere, Vallinoto et al. 1998). However, the acquisition of apoptotic and necrotic neutrophils causes an increase in CD83 and MHC class II but a decrease in the classical T cell costimulatory molecules, CD40, CD80 and CD86, hence a decrease in the ability to stimulate T cells (Clayton, Prue et al. 2003).

The development of T cell receptor (TCR) transgenic mice has greatly facilitated the study of T cell response to a variety of different antigens (Barnden, Allison et al. 1998). For instance, the MHC class I and II restricted TCR transgenic lines - OT1 and OT2 respectively, have been modified to respond to the highly manipulable antigen ovalbumin (OVA) (Ehst, Ingulli et al. 2003) (Hogquist, Jameson et al. 1994) (Barnden, Allison et al. 1998). Ovalbumin (OVA), the protein

of hen's egg white, is universally used as the main allergen to induce asthma, food and dermal allergy in animal models (Sun, Elsayed et al. 2010). The allergenic epitopes of OVA are mainly determined by the primary structure and are dependent on a certain peptide chain length (Sun, Elsayed et al. 2010). OVA 323-339 has been demonstrated to include the CD4+ T cell epitope and is widely used to study the nature of class II MHC-peptide binding and CD4+ T cell activation (Sun, Elsayed et al. 2010). Similarly, OVA 257-264 is mainly used to study class I MHC-peptide binding and the concomitant activation of CD8+ T cells (Svensson and Wick 1999). T cell activation and proliferation can be monitored by utilizing the well-established carboxyfluorescein diacetate succinimidyl ester (CFSE) tracking method (Quah, Warren et al. 2007). CFSE is a non-fluorescent dye that readily crosses intact cell membranes and is subsequently converted into the fluorescent carboxyfluorescein molecule by intracellular esterases (Last'ovicka, Budinsky et al. 2009). The succinimidyl ester group reacts with amino groups and results in stable long-term intracellular retention (Last'ovicka, Budinsky et al. 2009). CFSE is inherited equally by daughter cells after division, thus cell division can be measured as successive halving of the fluorescent intensity of CFSE, which can be visualized as distinct peaks and can be used to track division when analysed by flow cytometry (Last'ovicka, Budinsky et al. 2009).

p53 has been shown to participate in the regulation of adaptive immunity (refer to section 1.6). Given that *DRAM-1* is a p53 target gene, and is primarily localised to the lysosomes, which are critical intermediate compartments involved in the regulation of immune responses (refer to section 1.6), we were interested to explore the potential of p53 and DRAM-1 as regulators of the MHC processing pathway in the professional antigen presenting cells DCs and macrophages.

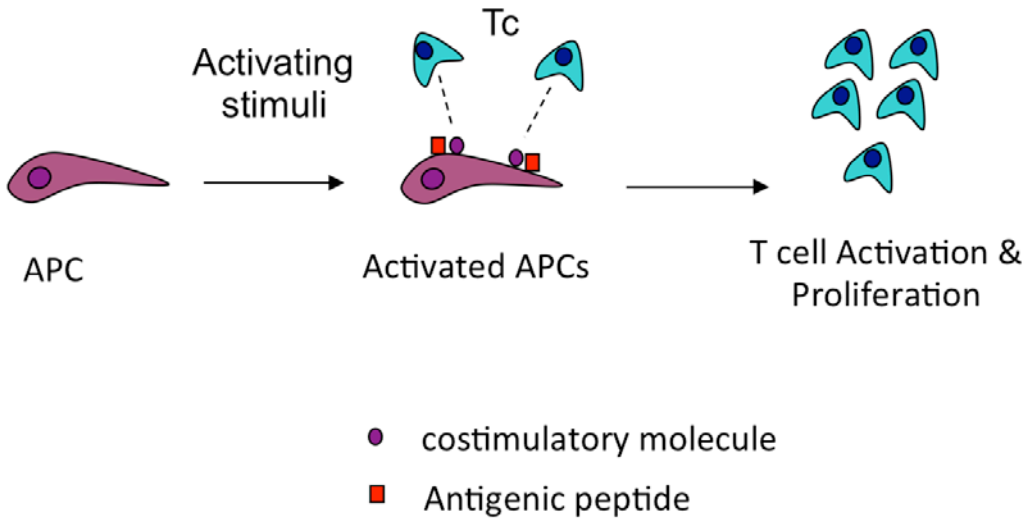

Figure 5.1: Regulation of MHC molecules and T cell costimulatory molecules in DCs
Immature DCs expresses low levels on MHC molecule and T cell costimulatory molecules on the sell surface. Mature DCs, which have acquired antigens have an increased expression of MHC molecules and T cell costimulatory molecules. These two signals are required for activating T cells.

5.2 Results

5.2.1 DRAM-1 expression is coregulated with regulators of the antigen presenting pathway

Network analysis is an approach that identifies a cluster of genes from the genetic architecture that are functionally related (Quigley, To et al. 2011) (Quigley, To et al. 2009). The identification of these sets of genes can be subsequently exploited to map the whole pathways that are involved in the progression of various processes and diseases, such as inflammation and cancer (Quigley, To et al. 2011) (Quigley, To et al. 2009). A preliminary network analysis of normal skin reveals that *DRAM-1* is closely coregulated with *Lymphocyte cytoplasmic protein-1 (LCP-1)*. LCP-1 is an actin remodeling protein that facilitates antigen presentation and T cell activation (Wabnitz, Kocher et al. 2007). Further analysis was conducted in a panel of 25 epithelial cell lines to build an expression network, and we found that *DRAM-1* is highly coregulated with *CD80*. CD80, also known as the B7 protein, is required for T cell activation and costimulation (Bhatia, Sun et al. 2010). These results suggest that DRAM-1 may be involved in antigen presentation and T cell activation.

Consistent with this, *DRAM-1* mRNA levels were upregulated upon challenge with bacterial lipopolysacharride (LPS) in mouse splenocytes, bone marrow-derived dendritic cells and macrophages (Fig. 5.2A-C). *DRAM-1* mRNA levels are also upregulated in human breast cancer cells (MDA-MB-231) and osteosarcoma cells (Saos-2) upon stimulation with the bacterial lipopolysacharride (LPS) and the inflammatory cytokines interferon-gamma (IFN-γ) and tumour-necrosis factor alpha (TNF-α) (Fig. 5.3). Since Saos-2 cells do not express p53, the upregulation of *DRAM-1* is independent of p53.

Given that DRAM-1 expression is upregulated in response to elevated levels of inflammatory cytokines or upon exposure to pathogens, it seems plausible that DRAM-1 may be involved in the regulation of immune response.

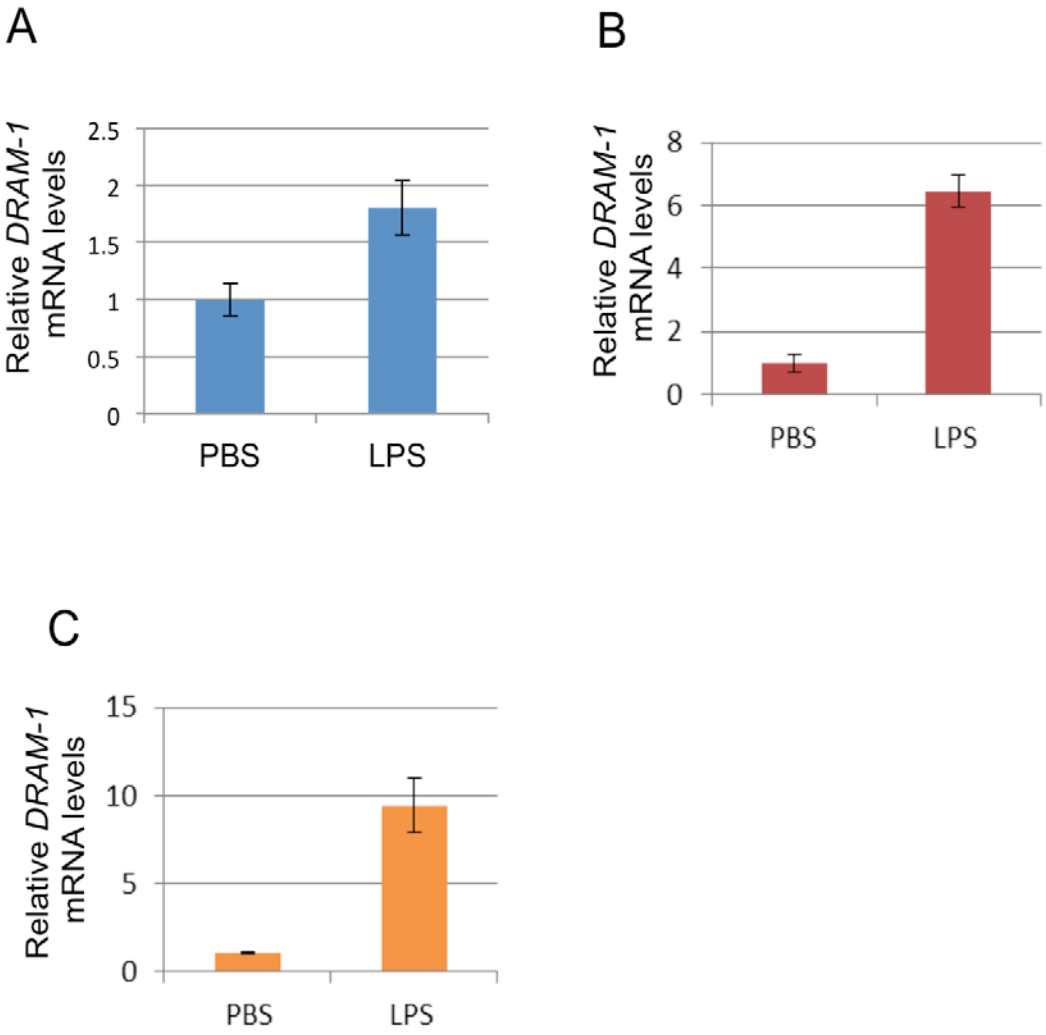

Figure 5.2 (A-C): *DRAM-1* mRNA levels are upregulated upon LPS treatment
Mouse splenocytes (A), bone marrow-derived macrophages (B) and bone marrow-derived dendritic cells (C) were incubated with 1µg/ml LPS for 16 hours. RNA was harvested and DRAM-1 levels quantified by RT-PCR. Results shown are representative of what was observed in at least three separate experiments.

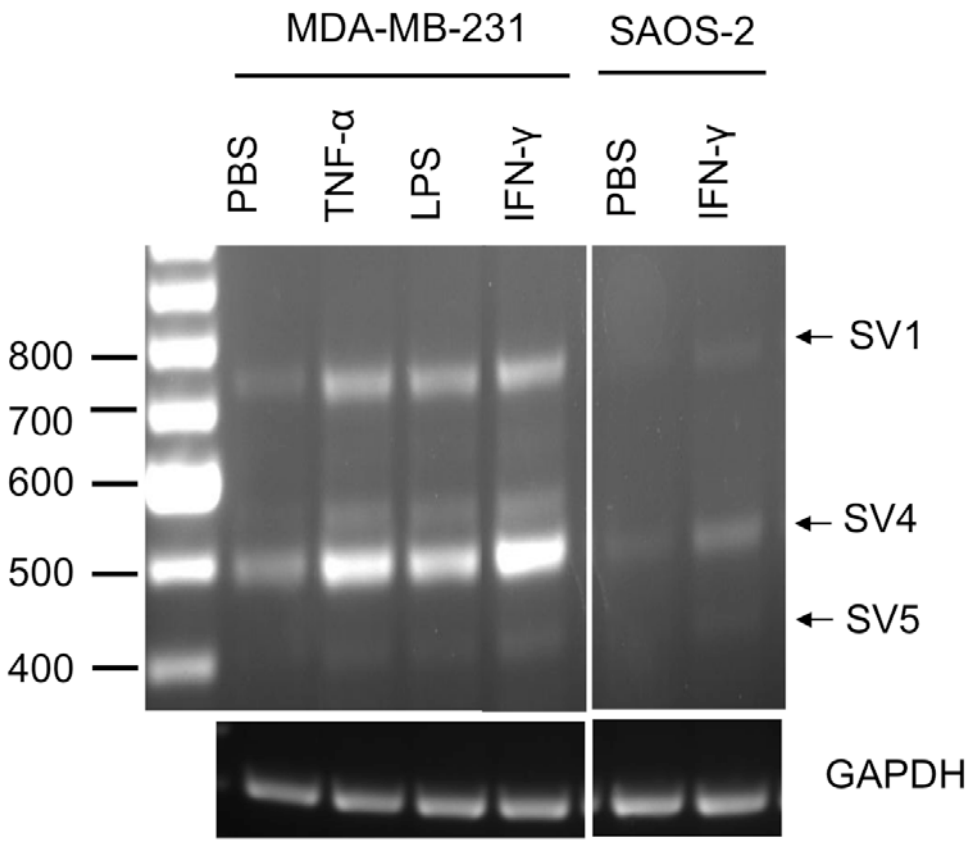

Figure 5.3: *DRAM-1* mRNA levels are upregulated upon treatment with inflammatory cytokines in human cells
MDA-MB-231 breast cancer cell line were incubated with 100ng/ml IFN-γ and 5μg/ml TNF-α and LPS for 16 hours. Saos-2 cells were treated with 100ng/ml IFN-γ. RNA was harvested and relative *DRAM-1* mRNA levels were compared via PCR and resolved on 3% agarose gel.

5.2.2 DRAM-1 regulates MHC class I and CD40 expression in DCs

To determine if *DRAM-1* deletion modulates antigen processing and presentation in dendritic cells, bone marrow progenitors were isolated from 'wild-type' and *DRAM-1*-null (DRAM-$1^{-/-}$) mice. These cells were cultured in 100ng/ml Flt-3L for 7 days to induce differentiation into dendritic cells. The cells were subjected to incubation with LPS for 16 hours, and stained for CD11c, CD19 and CD3e. The population of cells expressing CD11C+, cD19- and CD3e- were categorized as DCs (Fig. 5 .4). *DRAM-1* deletion does not affect the ex-vivo differentiation of bone marrow progenitors into dendritic cells, both at untreated and LPS-stimulated conditions (Fig. 5.5).

The surface expression of MHC molecules, as well as the panel of T cell costimulatory molecules – CD40, CD80 and CD86 was analysed by flow cytometry. *DRAM-1* deletion does not affect the ability of differentiated bone marrow-derived dendritic cells (BMDCs) to upregulate the surface expression MHC class II (Fig. 5.6 B), CD80 and CD86 (Fig. 5.7 A-B) upon treatment with LPS. However, *DRAM-*$1^{-/-}$ DCs have a reduced capacity to upregulate MHC class I (Mann-Whitney U test; $p = 0.05$) (Fig. 5.6A) and CD40 (Mann-Whitney U test; $p = 0.05$) (Fig. 5.7 C) upon exposure to LPS, compared to the wild-type control.

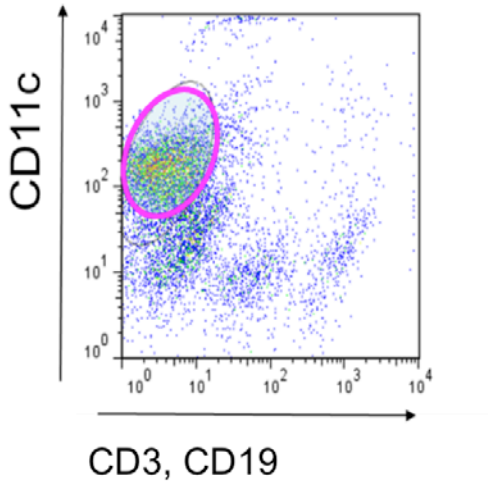

Figure 5.4: Gating of DCs from bone-marrow culture
Bone marrow progenitors cultured in 100ng/ml Flt-3L .for 7 days were stained with CD11c conjugated to PE, CD19 conjugated to APC and CD3e conjugated to APC. CD19 and CD3e are markers used to exclude B and T cells.

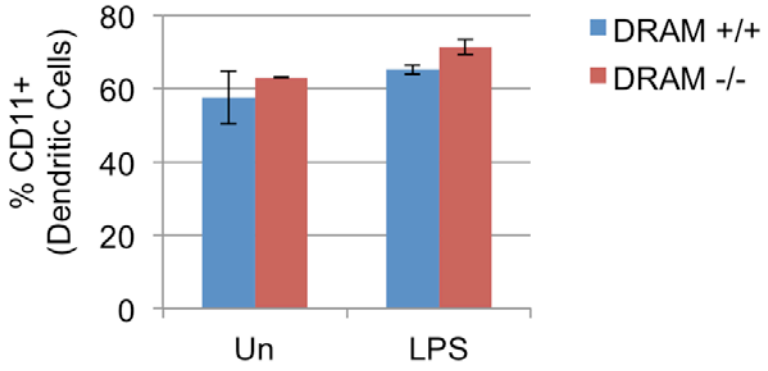

Figure 5.5: DRAM-1 deletion does not affect the ability of bone marrow progenitors to differentiate into dendritic cells *ex-vivo*
Bone marrow progenitors were isolated and cultured in 100ng/ml Flt-3L for 7 days. The cells were incubated with PBS or 1µg/ml LPS for 16 hours. The cells were stained with CD11c –conjugated to the PE fluorochorme (a marker to identify dendritic cells) and subjected to flow cytometry analysis.

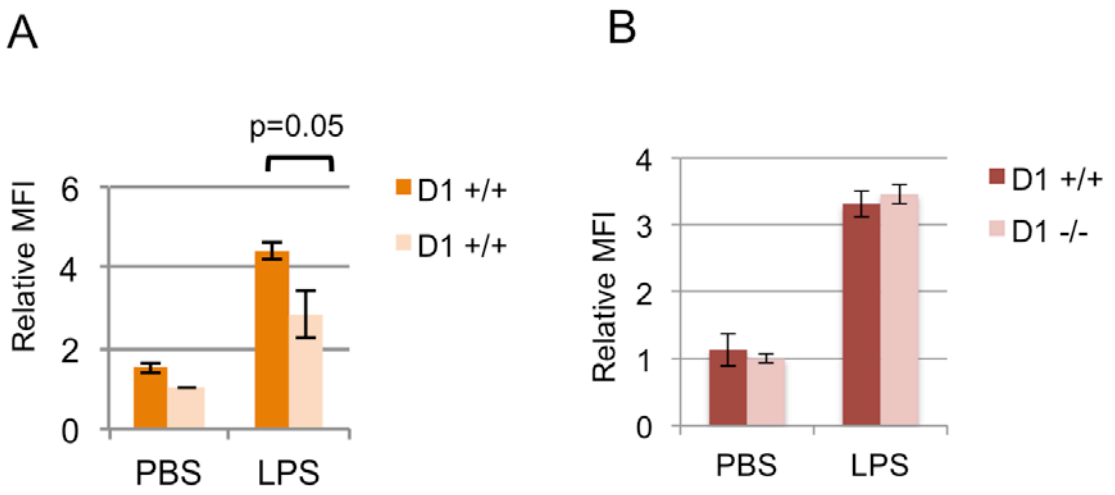

Figure 5.6 (A-B): *DRAM-1* deletion and the modulation of MHC molecules on DCs

Bone marrow-derived dendritic cells were treated with 1µg/ml LPS for 16 hours. The cells were stained with anti-CD11c+ and anti-MHC class I conjugated to PerCP/Cy5.5 (A) or anti-MHC class II conjugated to PerCP-eFlour®710 (B), and subjected to flow cytometry analysis. The surface expression of MHC molecules on CD11c+ DCs is quantified using the mean fluorescent intensity (MFI). Mann-Whitney U test for (A); p = 0.05 . Results shown are representative of what was observed in at least three separate experiments

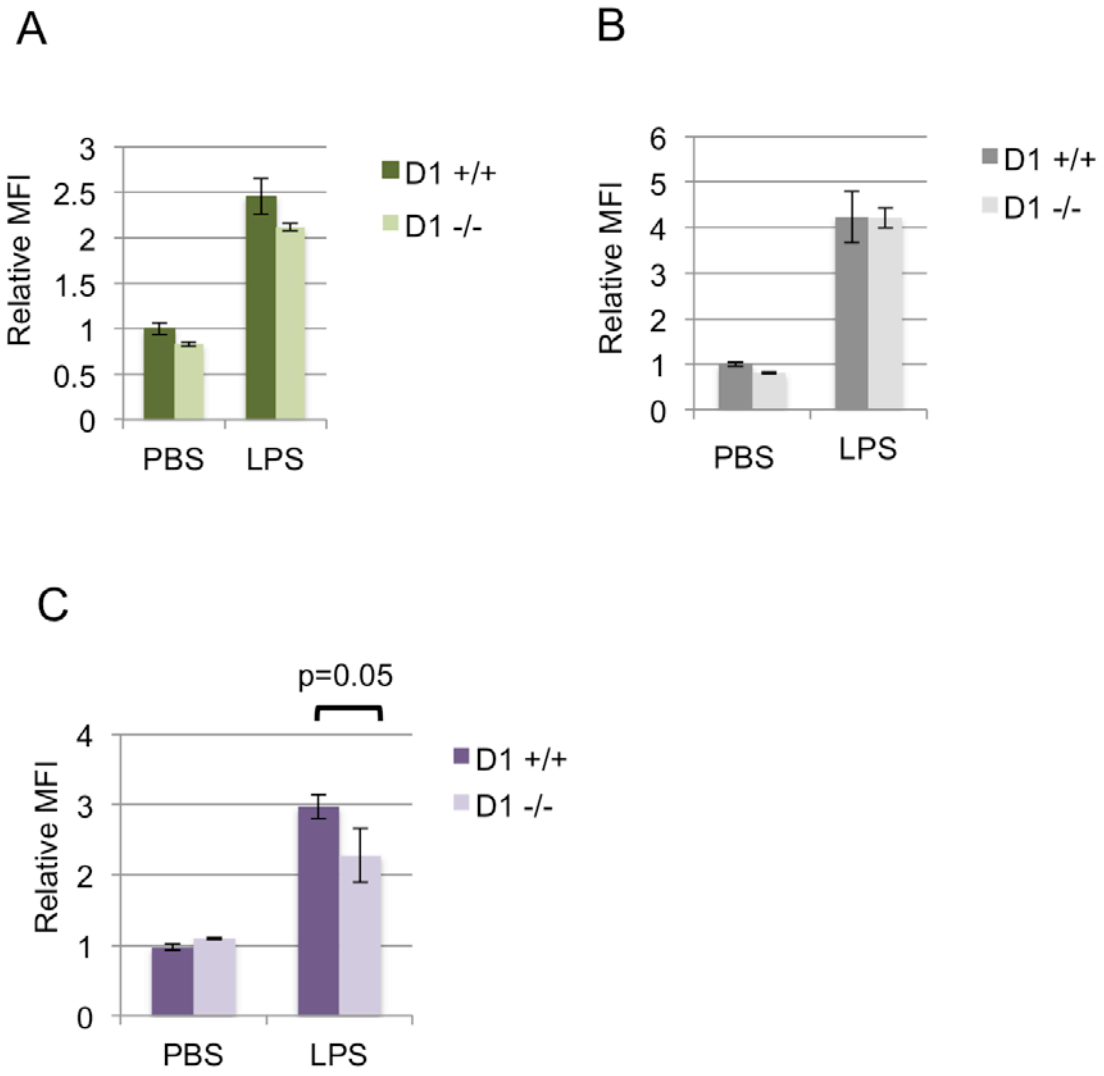

Figure 5.7 (A-C): *DRAM-1* deletion and the modulation of T cell costimulatory molecules on DCs

Bone marrow-derived dendritic cells were treated with 1µg/ml LPS for 16 hours. The cells were stained with anti-CD11c and anti-CD80 conjugated to FITC (A), anti-CD86 conjugated to FITC (B), or anti-CD40 conjugated to Alexa Fluor®488 (C). The cells were subjected to flow cytometry analysis. The surface expression of these molecules on CD11c+ DCs is quantified using the mean fluorescent intensity (MFI). Mann-Whitney U test for (C); $p = 0.05$. Results shown are representative of what was observed in at least three separate experiments

5.2.3 The role of p53 and DRAM-1 in the regulation of T cell activation

Since *DRAM-1* deletion interferes with the optimal expression of MHC class I and CD40, we were interested to determine if *DRAM-1*-null DCs have a reduced capacity to activate CD4+ and CD8+ T cells upon exposure to pathogens. Since DRAM-1 is induced by p53, it could be plausible that the effect of DRAM-1 in antigen presentation is emphasized in conditions where p53 levels are present above basal levels. To address this, p53 level was stabilised in 'wild-type' and *DRAM-1*$^{-/-}$ DCs by incubating the cells with the Mdm2 antagonist, Nutlin-3A (refer to section 1.7.1). DCs were subsequently pulsed with Ovalbumin (OVA) for three hours and co-cultured with the CFSE labeled transgenic CD4+ and CD8+ T cells isolated from OT-2 and OT-1 mice respectively. The activation and proliferation of T cells is indicated by a dilution of the CFSE dye (Fig 5.8).

CD4+ and CD8 T+ cell activation was not affected when *DRAM-1* is deleted in bone marrow-derived DCs, irrespective of p53 status (Fig. 5.9 A-B). Rather, the stabilisation of p53 protein levels impedes the ability of DCs to activate CD4+ (Fig. 4.9A) and CD8+ (Fig. 5.9B) T cells. p53 stabilisation by Nutlin-3A was validated by an increase in the mRNA expression of the p53 target gene, p21 (Fig. 5.9C).

The decreased activation of T cells could be attributed to the pathways downstream of p53 such as apoptosis. To rule out this possibility, and also to confirm that T cell activation is not a result of off-target effects caused by Nutlin-3A, bone marrow derived DCs isolated from 'wild-type' and *p53*-null mice were incubated with Nutlin-3A as before, and harvested for sub-G1 analysis. Nutlin-3A induces a low amount of apoptosis in both *p53*$^{+/+}$ and *p53*$^{-/-}$ DCs to a similar extent, which can be rescued by the pan-caspase inhibitor, zVAD-fmk (Fig. 5.10). zVAD-fmk has been demonstrated to be able to diminish apoptosis in array of cell lines (Kim, Mohan et al. 2000) (Ilangovan, Marshall et al. 2003), including dendritic cells (You, Chang et al. 2008).This suggests that Nutlin-3A treatment could result in p53-independent apoptosis, and that the decreased ability to activate T cells is not a direct result of cell death.

Alongside this, *p53*$^{+/+}$ and *p53*$^{-/-}$ DCs were incubated with Nutlin-3A and pulsed with OVA, as before. Consistent with the previous finding, Nutlin-3A treated *p53*$^{+/+}$ DCs were unable to stimulate both CD4+ and CD8+ proliferation (Figure 5.11A & Figure 5.11B). However, Nutlin-3A treated *p53*$^{-/-}$ DCs were able to induce both

CD4+ and CD8+ T cell proliferation (Figure 5.11 A & B) to similar levels as the DMSO treated *p53*$^{-/-}$ DCs. This suggests that the defect in T cell stimulation is not attributed to the off-target effects of Nutlin-3A, but is solely caused by the increased expression of p53. This is well reflected in the observation that DMSO and Nutlin-3A treated *p53*$^{-/-}$ DCs were able to induce a bigger magnitude of CD4+ and CD8+ T cell proliferation compared to the *p53*$^{+/+}$ DCs (Figure 5.11 A & B).

Given that macrophages are also professional antigen presenting cells, we were interested to investigate if p53 and DRAM-1 modulation in these cells would affect their ability to induce T cell activation upon exposure to antigen. Similarly, bone marrow progenitors were isolated from *DRAM*$^{+/+}$ and *DRAM*$^{-/-}$ mice and cultured in 10ng/ml M-CSF for 6 days to induce differentiation into macrophages. These bone marrow-derived macrophages were pulsed with OVA, and co-cultured with T cells from OT-2 and OT-1 mice as before. Consistent with the previous findings in dendritic cells, DRAM-1 deletion in macrophages does not affect their ability to stimulate T cell proliferation upon incubation with OVA (Fig. 5.12 A & B). However, macrophages that were pre-treated with Nutlin-3A prior to incubation with OVA have a decreased ability to activate both CD4+ (Fig. 5.13 A) and CD8 + T cells (Fig. 5.13 B).

To summarise this part, DRAM-1 deletion does not impair the ability of DCs and macrophages to activate CD4+ and CD8+ T cells upon incubation with OVA. On the other hand, p53 stabilisation in DCs and macrophages inhibits the activation of T cells upon exposure to OVA, implying that p53-mediated inhibition of T cell stimulation is probably applicable to other antigen presenting cells upon pathogen attack.

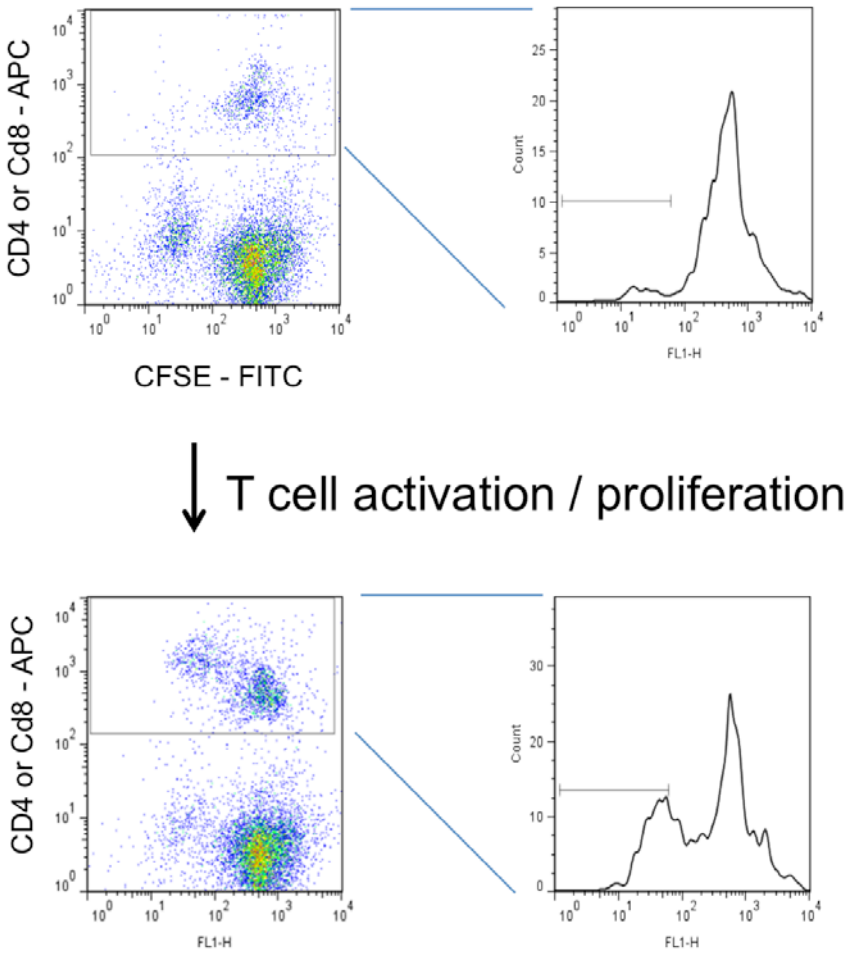

Figure 5.8: Tracking CFSE-labeled T cell activation and proliferation
CD4+ or CD8+ T cells isolated from OT-2 and OT-1 mice were incubated with 5μM CFSE and co-cultured with PBS or OVA pulsed DCs for 3 days to allow for T cell activation. These heterogenous population of cells were stained with anti-CD4 conjugated to APC (A) or anti-CD8 conjugated to APC. The cells were subjected to flow cytometry analysis. T cell proliferation is monitored by the successive dilution of the CFSE dye. The percentage of proliferating T cells was quantified using Cell Quest software . The schematic diagram is generated using FlowJo.

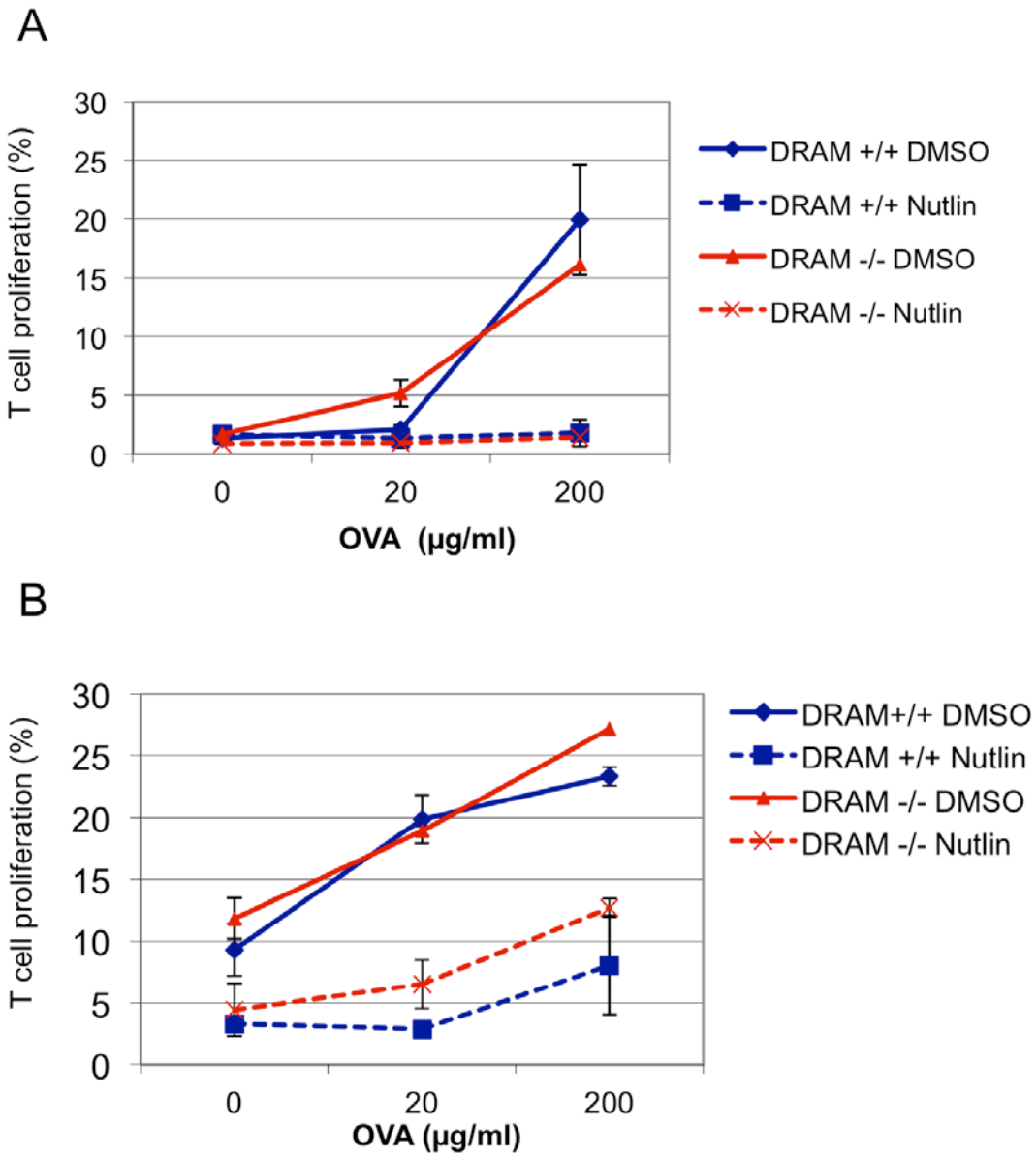

Figure 5.9 (A-B): Effect of p53 stabilisation and *DRAM-1* deletion in DCs with respect to the ability of DCs to activate T cells

Bone marrow-derived dendritic cells were incubated with 8µM Nutlin-3A for 16 hours and pulsed with OVA for 3 hours. Both the Nutlin-3A and OVA compounds were washed off. DCs were then co-cultured with CFSE labeled CD4+ (A) or CD8+ (B) T cells for three days and subjected to flow cytometry analysis. Results shown are representative of what was observed in at least three separate experiments

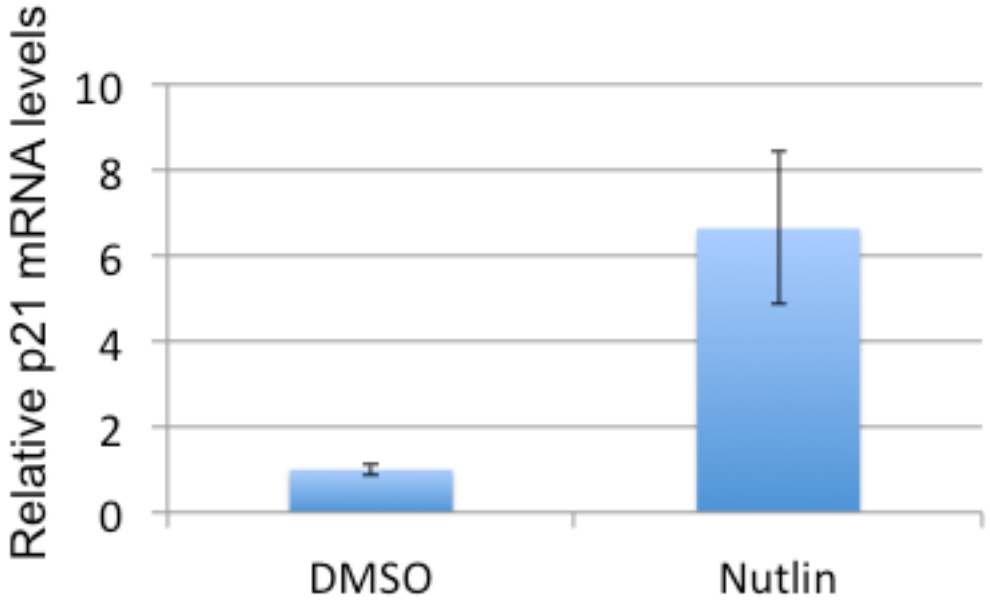

Figure 5.9C: Nutlin-3A treatment induces p21 mRNA levels
Bone marrow-derived dendritic cells were incubated with 8µM Nutlin-3A for 16 hours. p53 stabilisation was validated by quantifying p21 mRNA expression using RT-PCR. Results shown are representative of what was observed in at least three separate experiments

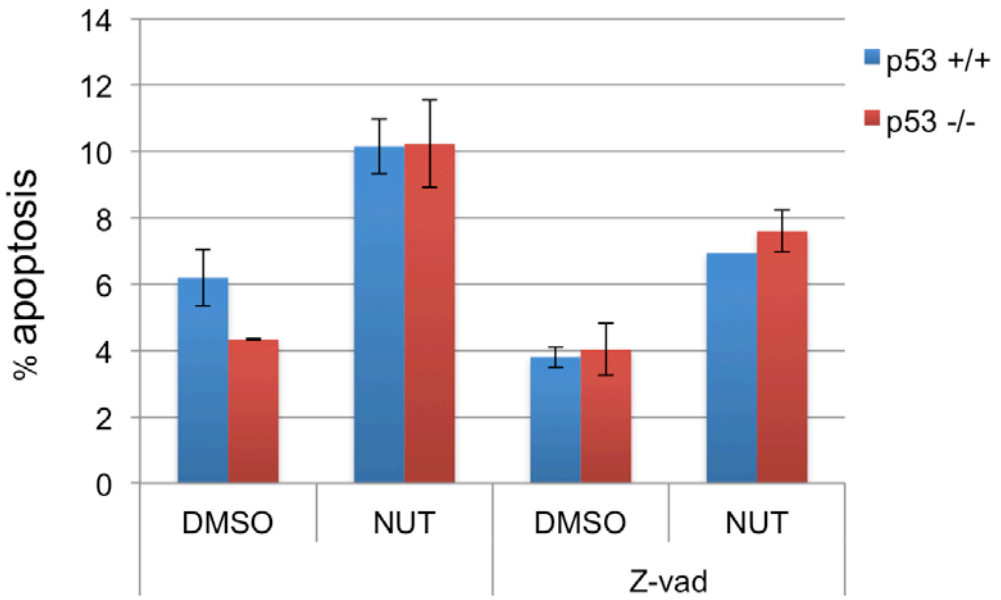

Figure 5.10: Nutlin-3A induces p53-independent apoptosis in wild-type and *p53*-null DCs

Bone marrow-derived dendritic cells were incubated with 8μM Nutlin for 16 hours. DCs were harvested, fixed in methanol, stained with propidium iodide and subjected to flow cytometry analysis to determine Sub-G1 content. Results shown are representative of what was observed in at least three separate experiments

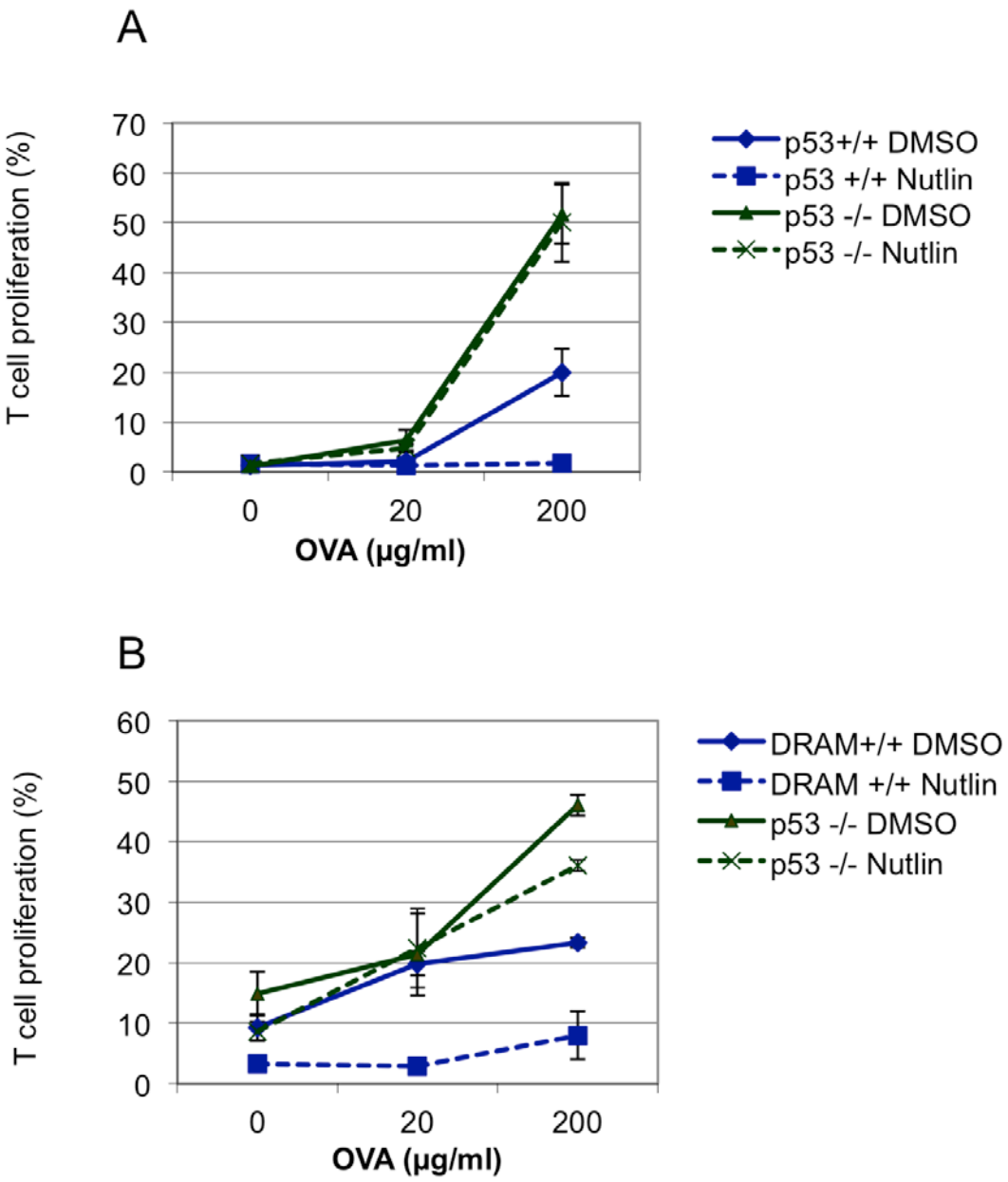

Figure 5.11 (A-B): Effect of p53 stabilisation and *DRAM-1* deletion in DCs with respect to the ability of DCs to activate T cell

Bone marrow-derived dendritic cells were incubated with 8µM Nutlin for 16 hours and pulsed with OVA for 3 hours. Both the Nutlin and OVA compounds were washed off. DCs were then co-cultured with CFSE labeled CD4+ (A) or CD8+ (B) T cells for three days and subjected to flow cytometry analysis.

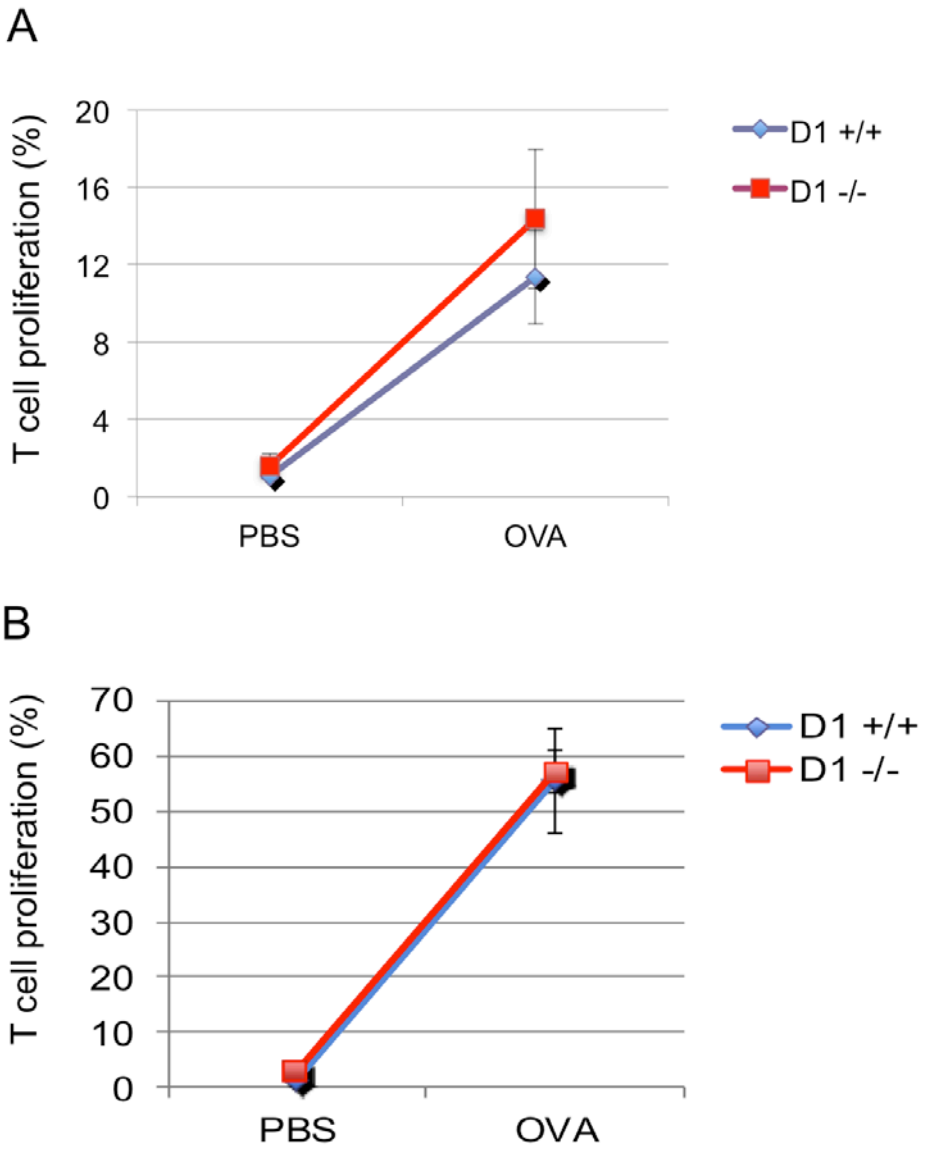

Figure 5.12 (A-B): *DRAM-1* deletion in macrophages does not impede T cell activation

Bone marrow-derived macrophages were incubated with 8μM Nutlin for 16 hours and pulsed with OVA for 3 hours. They are then co-cultured with CFSE labeled CD4+ (A) or CD8+ (B) T cells for three days and subjected to flow cytometry analysis. Results shown are representative of what was observed in at least three separate experiments

A

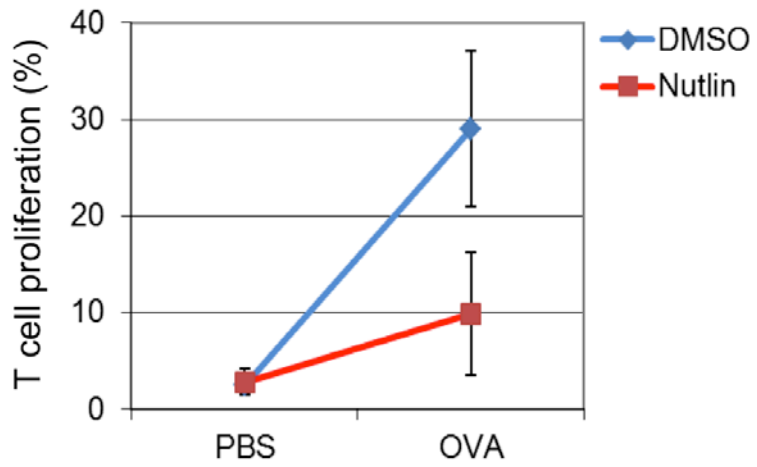

B

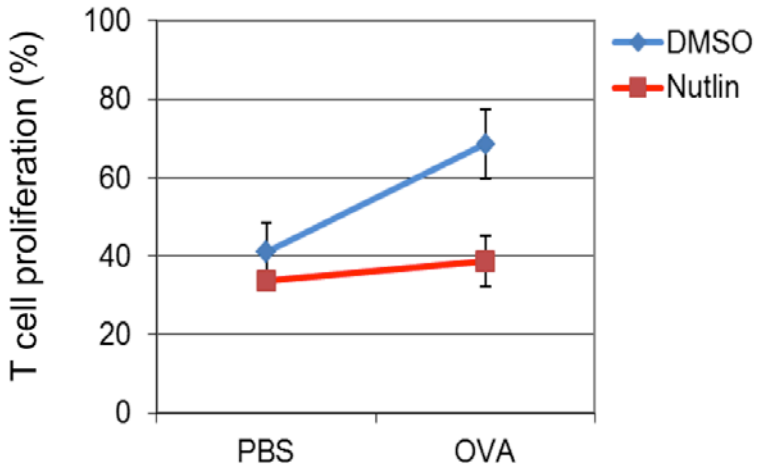

Figure 5.13 (A-B): p53 stabilisation in macrophages impedes T cell activation

Bone marrow-derived macrophages were incubated with 8μM Nutlin for 16 hours and pulsed with OVA for 3 hours. They are then co-cultured with CFSE labeled CD4+ (A) or CD8+ (B) T cells for three days and subjected to flow cytometry analysis. Results shown are representative of what was observed in at least three separate experiments

5.2.4 p53 modulates MHC peptide processing and presentation

Having established that p53 inhibits the ability of DCs to activate T cells, we were interested to determine if this inhibition occurs because p53 inhibits the engulfment and processing of the antigen, or the presentation of the processed antigenic peptide/MHC complex on the cell surface. To address the second question, Nutlin-3A treated DCs were pulsed with the processed OVA peptides - OVA 323-339 which contains the epitope for CD4+ T cell, and OVA 257-264 which harbours the epitope for CD8+ T cell. DCs will engage these antigen fragments on the MHC molecules, thus bypassing the endocytosis and cytoplasmic processing of the antigen (S. Milling, personal communication, The University of Glasgow).

If DCs that are peptide-pulsed and pre-treated with either PBS or Nutlin-3A can stimulate T cell proliferation equally, this would imply that p53 does not affect the presentation of the processed antigenic peptide. Otherwise, if Nutlin-3A treated DCs were unable to induce T cell proliferation to the same extent as the mock control (PBS), this would imply that p53 inhibits the presentation of the processed peptide.

Upon incubation with OVA 257-264, both PBS and Nutlin-3A treated DCs were able to stimulate CD8+ T cell proliferation to a similar extent (Fig. 5.14). This suggests that p53 inhibits the presentation of the MHC class I peptide complex, without affecting antigen engulfment and processing.

Likewise, Nutlin-3A treated DCs also induced T cell proliferation, albeit to a lower extent compared to PBS treated DCs upon incubation with OVA 323-339 (Fig. 5.15). This implies that p53 partially affects the presentation of processed MHC class II antigenic peptides.

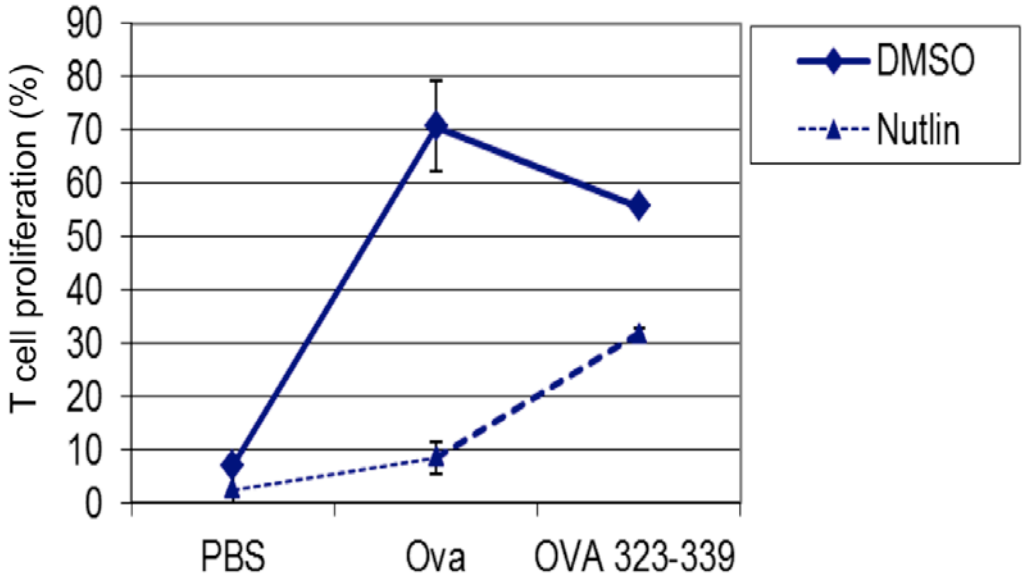

Figure 5.14: p53 partially impairs the presentation of MHC class II peptide
Bone marrow-derived dendritic cells were incubated with 8μM Nutlin for 16 hours and pulsed with OVA or OVA 323-339 for 3 hours. They are then co-cultured with CFSE labeled CD4+ T cells for three days to allow for T-ccellactivation and proliferation. The cells were stained for anti-CD4 conjugated to APC. The cells were subjected to flow cytometry analysis. The proliferation of T cells were measured by the extent of CFSE dilution. Results shown are representative of what was observed in at least three separate experiments

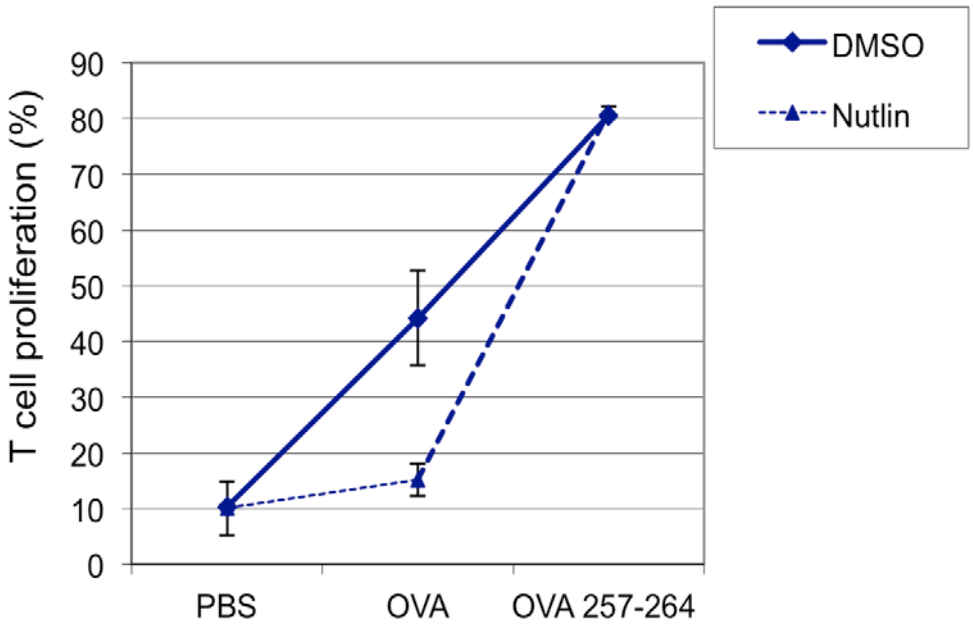

Figure 5.15: p53 does not impair the presentation of MHC class I peptide
Bone marrow-derived dendritic cells were incubated with 8μM Nutlin for 16 hours and pulsed with OVA or OVA 257-264 for 3 hours. They are then co-cultured with CFSE labeled CD8+ T cells for three days to allow for Tc activation and proliferation. The cells were stained for anti-CD8 conjugated to APC. The cells were subjected to flow cytometry analysis. The proliferation of T cells were measured by the extent of CFSE dilution. Results shown are representative of what was observed in at least three separate experiments

In line with this, the role of p53 in the modulation of MHC class II molecules and the T cell costimulatory molecule, in this case, CD40 was also investigated. In this context, *p53*$^{+/+}$ and *p53*$^{-/-}$ bone marrow-derived DCs were incubated with the pan-caspase inhibitor, zVAD to prevent apoptosis (Fig. 4.16). Upon exposure to LPS, the surface expression of MHC class II and CD40 is upregulated in both *p53*$^{+/+}$ and *p53*$^{-/-}$ DCs (Fig. 4.16). Albeit the mean fluorescent intensity (MFI) for both MHC class II and CD40 is slightly higher in *p53*$^{-/-}$ DCs, this difference is not statistically significant, implying that both of these T cell activation signals are not affected by p53. However, Nutlin-3A treatment impairs the ability of *p53*$^{+/+}$ and *p53*$^{-/-}$ DCs to upregulate MHC class II and CD40 upon exposure to LPS. This suggests that Nutlin-3A causes a downregulation of T cell activation signals, independent of p53 status. Alternatively, the downregulation of MHC class II and CD40 could be a direct result of Nutlin-3A induced p53-independent apoptosis, as discussed in section 4.1.2 (Fig. 5.10). On a different note, the upregulation of MHC class II and CD40 upon stimulation with LPS was also abrogated when DCs were treated with the pan-caspase inhibitor, Z-VAD, irrespective of p53 status (Fig. 5.16). This was consistent with the study by Santambrogio et al. (2005) which demonstrates that caspase 3 is required for the localisation of the MHC class II invariant chain in activated (mature) DCs (Santambrogio, Potolicchio et al. 2005). Having said that, the mechanism that governs p53-mediated downregulation of CD40 has yet to be elucidated.

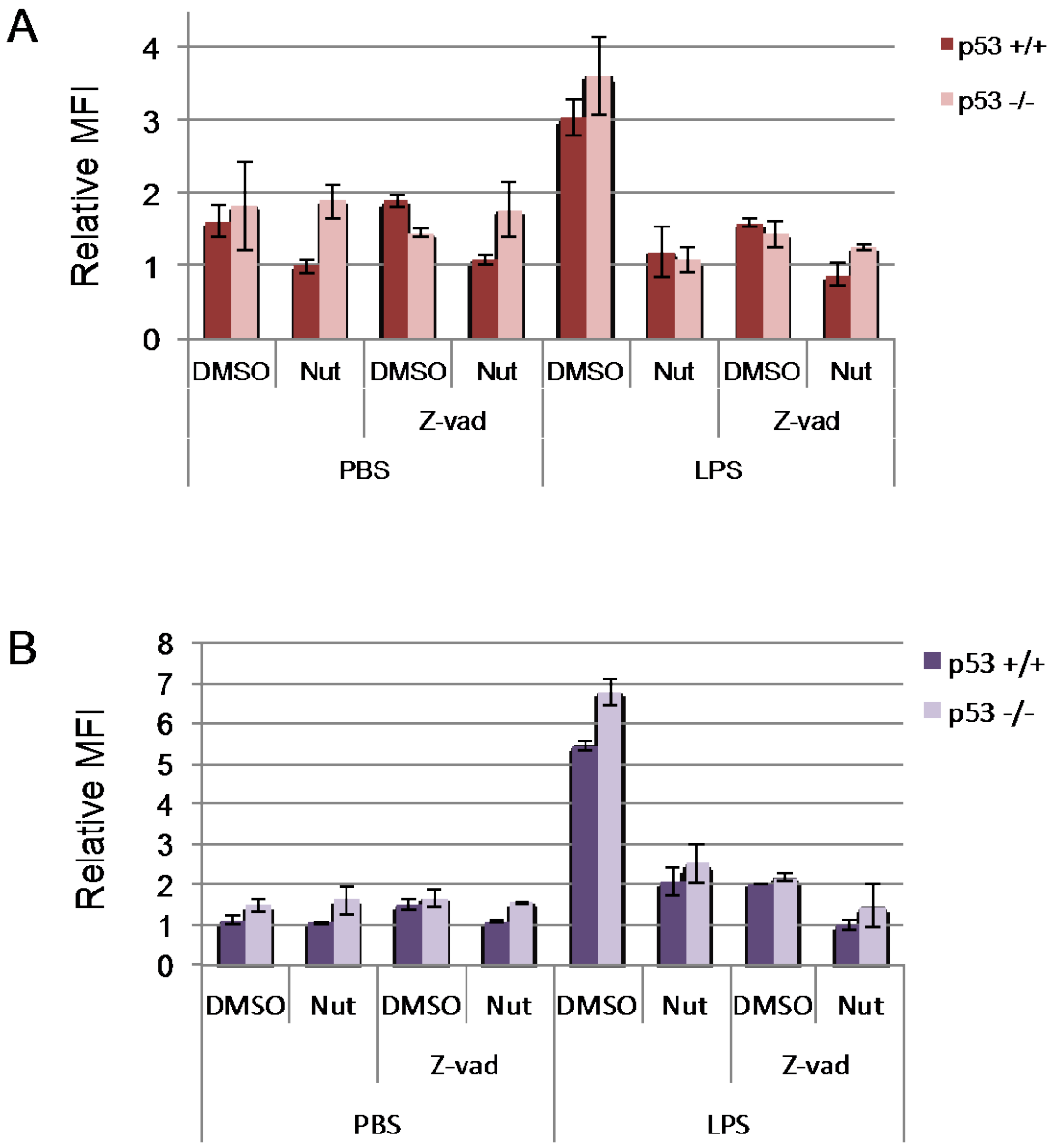

Figure 5.16 (A-B): Nutlin-3A and zVAD-fmk impairs the surface expression of MHC class II independent of p53 status

Bone marrow-derived dendritic cells were treated with 8µM Nutlin-3A, 500µM zVAD-fmk, and or 1µg/ml LPS for 16 hours.

The cells were stained with anti-CD11c+ and anti-MHC class I conjugated to PerCP/Cy5.5 or anti-MHC class II conjugated to PerCP-eFlour®710, and subjected to flow cytometry analysis. The surface expression of MHC class II (A) and CD40 (B) on CD11c+ DCs is quantified using the mean fluorescent intensity (MFI). Results shown are representative of what was observed in two separate experiments

5.3 Discussion

DRAM-1 mRNA expression is upregulated in human cells and mouse professional antigen presenting cells – dendritic cells and macrophages upon exposure to bacterial lipopolysacharride (LPS) and other inflammatory cytokines such as interferon gamma (IFN-γ) and tumour-necrosis factor alpha (TNF-α). Additionally, *DRAM-1* is closely coregulated with regulators of antigen presentation such as the *Lymphocyte cytoplasmic protein-1 (LCP-1)* and *CD80* in an array of human epithelial cell lines. These observations suggest that DRAM-1 is a potential regulator of the immune response, particularly in mediating antigen presentation. However, loss of DRAM-1 in dendritic cells does not affect the upregulation of the T cell activating signals like MHC class II, as well as the T cell costimulatory molecules CD80 and CD86 upon exposure to LPS. On the other hand, the surface expression of MHC class I (see section 1.5.2) and CD40 is downregulated in *DRAM-1*-null DCs compared to their wild-type counterparts.

CD40, is another T cell co-stimulatory molecule which is facilitates the maturation of dendritic cells (DCs), and the subsequent ability of these cells to activate T cells (Gerlach, Steimle et al. 2012). The ligation of CD40 on DCs by CD40L leads to an upregulation in the expression of CD80 and CD86 molecules on DCs (Cella, Scheidegger et al. 1996). Like CD80 and CD86, the ligation of CD40 to its ligand also increases the capacity of DC to trigger proliferative responses, in addition to IFN-gamma production by T cells (Cella, Scheidegger et al. 1996).

Despite being a strong trigger for CD80 and CD86, the downregulation of CD40 in *DRAM-1*-null DCs does not seem to affect the regulation of CD80 and CD86. Furthermore, the deletion of *DRAM-1* in DCs and macrophage does not impair the ability of these professional antigen presenting cells (APCs) to stimulate T cell proliferation upon exposure to the model antigen Ovalbumin (OVA). This suggests that *DRAM-1*-null APCs can still trigger T cell proliferative responses despite expressing lower levels of MHC class I and CD40 levels. Albeit this, the production of IFN-gamma by T cells upon CD40-CD40L ligation in the absence of DRAM-1 may be affected, and remains to be elucidated. We have also shown that the loss of DRAM-1 (and the subsequent downregulation of CD40) does not affect the differentiation of bone marrow progenitors into DCs upon treatment with Flt-3L *in*

vitro. However, the maturation of DCs *in vivo* upon the loss of DRAM-1 remains to be unknown and is worth pursuing.

This suggests a redundancy in DRAM-1 mediated expression of MHC class I and CD40. Alternatively, the loss of *DRAM-1* can be compensated by other family members of the DRAM family. This notion is supported by the cluster analysis of *DRAM-1*, which revealed that *DRAM-1* and *DRAM-2* are strongly associated with regulators of the immune system in papillomas (A. Balmain, personal communication). Despite this, the deletion of DRAM-1 in B cells and T cells, or facultative APCs like skeletal muscles (as discussed in section 5.1) has yet to be investigated and is certainly worth pursuing.

On the other hand, p53 is found to negatively regulate T cell activation. Stabilisation of p53 levels in dendritic cells and macrophages with the specific Mdm2 antagonist Nutlin-3A impairs the ability of these cells to stimulate CD4+ and CD8+ T cell proliferation. In line with this, *p53*-null DCs are able to stimulate a greater magnitude of T cell activation compared to the wild-type counterpart when pulsed with OVA. The defect in CD8+ T cell activation upon p53 stabilisation is not attributed to a disruption in the presentation of the processed antigenic peptide, as DCs incubated with the 'processed class I MHC peptide' (OVA 257-264) can induce a similar magnitude of T cell proliferation, irrespective of p53 status. The impairment in CD4+ T cell activation is partially attributed to the presentation of the processed antigenic peptide, as the inhibitory effect of T cell proliferation upon p53 stabilisation can be partially rescued when DCs were pulsed with the processed class II MHC peptide (OVA 323-339).

Further mechanistic studies to elucidate if p53 affects antigen engulfment and processing are worth pursuing. For instance, we have yet to establish if the loss of p53 affects the expression, or the trafficking of MHC class I and MHC class II molecules, as well as T cell molecules to the cell surface. Albeit this, p53 has been shown the positively regulate the transporter associated with antigen processing (TAP) 1 and the subsequent transport of MHC class I peptides on a panel of non-professional antigen presenting cells to facilitate antigen presentation (Zhu, Wang et al. 1999). This seem to contradict with our findings in which p53 activation in dendritic cells is proposed to inhibit the ability of these cells to activate T cell

proliferation/ activation. However, this discrepancy could be attributed to the different cell types and the nature of the antigen that are used in the experiments. Thus, it would seem plausible to investigate if the loss of p53 in professional antigen presenting cells (such as dendritic cells and macrophages) would modulate TAP1 activity, or the expression and the trafficking of MHC class I and the panels of T cell costimulatory molecules.

The decrease in the ability of DCs to present processed peptide on MHC class ll, but not MHC class l upon p53 activation indicates that the surface expression of MHC class ll may be downregulated by p53. This reiterates the importance of studying the effects of p53 on the expression and the trafficking of MHC class II molecules on antigen presenting cells.

Our system to study antigen processing by MHC class l in DC is limited by the way the antigen is introduced (See Section 1.5.2). In this context, Ovalbumin is introduced as an extracellular antigen, which is cross-presented on MHC class l. Thus, we have yet to establish an accurate model to measure the effects of p53 and DRAM-1 on intracellular / endogenous antigen processing. One category of intracellular antigen that is conventionally recognised by class I originates from viruses. To recapitulate viral infection, it would be interesting to introduce ovalbumin by infecting DCs with lentiviral vectors expressing cytoplasmic (OVAcyt) (Rowe, Lopes et al. 2006). This model is proposed to be a much more accurate method to stimulate viral infection, and MHC class l responses to intracellular / endogenous antigens, since ovalbumin is now synthesised within the cells.

The role of p53 in regulating antigen presentation and the efficacy of APCs to evoke T cell function has been studied extensively. Human dendritic cells that were pulsed with the wild-type p53 protein could induce the specific antitumor effect against p53-overexpressing tumors (Tokunaga, Murakami et al. 2005) (Nikitina, Clark et al. 2001). The contradictory results between these studies and our findings could be attributed to the different nature of stimuli used to pulse DCs. The activation of T cells in response to p53 activation is demonstrated upon exposure to tumour antigens. On the other hand, the inhibition of T cell activation, which is demonstrated in this thesis occurs when DCs were pulsed with ovalbumin

and ovalbumin-derived peptides, which are components of allergens and thus is classified as extracellular antigens (refer to section 5.1). Furthermore, many tumour antigens are intracellular molecules (Noguchi, Kato et al. 2012), while ovalbumin is added as an extracellular antigen in our studies. Thus, it remains plausible that p53 activation could turn down allergen or extracellular mediated T cell activation to promote tumour antigen pulsed-DCs and the subsequent T cell activation for enhanced tumour immunity, as illustrated in Fig. 5.17.

In any case, if the inhibition of the adaptive immune responses via APCs by p53 is thorough and effective, it should be accompanied by inhibition of antibody production by B cells. This can be done by irradiating wild-type and *p53*-null mice to activate p53 (in the wild-type), followed by inoculation with OVA and recombinant IL-1 (as adjuvant) via intraperitoneal injection. Two weeks later, mice will be irradiated and inoculated with OVA for a second time. Mice will subsequently be exsanguinated and the presence of OVA-specific antibodies will be detected by end-point ELISA, as illustrated in Fig. 5.18. If the ability of p53 to block antigen processing and presentation in DCs, macrophages (and B cells) is robust enough to block activation of humoral immunity this should easily be detected in this assay. These aspects would bring us closer to unraveling the role of p53 in the mediation of adaptive immune response, and ultimately tumor immunity.

The roles of p53 in mediating the immune response - inflammation and autoimmunity, have long been established (see section 1.7.2). Our result indicates that the stabilisation of p53 in professional antigen presenting cells represses T cell activity, resulting in a weaken immune response when challenge with pathogen.

Testing this hypothesis in vivo might be limited by the fact that mice are generally resistant to infections with human-specific pathogens like HIV, *Plasmodium falciparum*, and *Shigella flexneri*, especially if the pathogen is administered through the natural route of infection (Coers, Starnbach et al. 2009). This limitation has led to the development of humanised mouse models of human infectious diseases. These mice, which are transplanted with human cells or tissues, have

been utilised widely to study the response of the human immune system in response to viral infection (Legrand, Ploss et al. 2009). For instance, NOD/SCID mice that were transplanted with human hematopoietic fetal liver CD34+ cells and previously implanted with human fetal thymic and liver tissues were able to mount specific adaptive and innate immune responses to Epstein-Barr virus (EBV) and the superantigen toxic shock syndrome toxin 1 (TSST-1) (Melkus, Estes et al. 2006). Taking this a step further, it would be interesting to modulate p53 and DRAM-1 levels in the cells of the immune system prior to exposure to viruses, and monitor the magnitude of immune responses.

Despite harnessing anti-tumorigenic potentials, as discussed in this section, our results suggest that the stabilsation of p53 downregulates the ability of professional antigen presenting cells to stimulate T cell activation upon exposure to the extracellular antigen ovalbumin. This finding is important physiologically as it may imply that tumour therapy targeted at restoring or stabilising wild-type p53 levels might sensitise the patients to diseases caused by extracellular pathogen attack, and should be approached with caution.

In addition, we also found that Nutlin-3A induces apoptosis in $p53^{+/+}$ and $p53^{-/-}$ DCs, independent of p53. Of p53 status Additionally, $p53^{+/+}$ and $p53^{-/-}$ DCs that were pre-treated with Nutlin-3A were unable to upregulate the T cell activation signals, MHC class II and CD40 upon exposure to LPS. The upregulation of MHC class I, CD80 and CD86 is yet to be determined. To rule out that this downregulation of T cell activation signals is caused by apoptosis, DCs were treated with the pan-caspase inibitor, zVAD-fmk, to prevent apoptosis. Given that caspase 3 is required for the expression of MHC class II molecules on mature DCs (Santambrogio, Potolicchio et al. 2005), the inhibition of caspase(s) also results in the downregulation of CD40 in these cells upon exposure to LPS. This observation implies that beyond the regulation of cell death, caspases may also play a critical role in the regulation of DC maturation, antigen presentiation or T cell activation, at least by controlling the expression of MHC class II and CD40 on DCs.

These findings suggest that the administration of Nutlin-3A, and perhaps other compounds that modulate p53 and caspase levels can interfere with adaptive immunity. Thus these potential therapeutic agents should be used with caution.

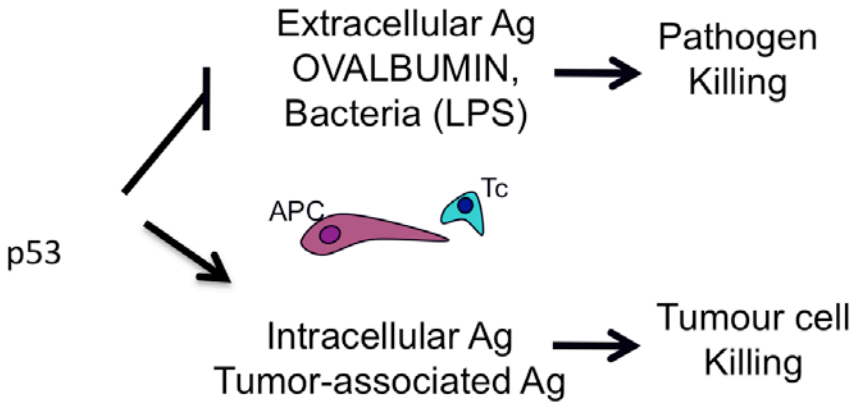

Figure 5.17: Working hypothesis of p53 and tumour immunity
p53 activation could repress extracellular-mediated T cell activation to allocate for the increase in the propensity of intracellular tumour-derived antigen to promote tumour immunity.

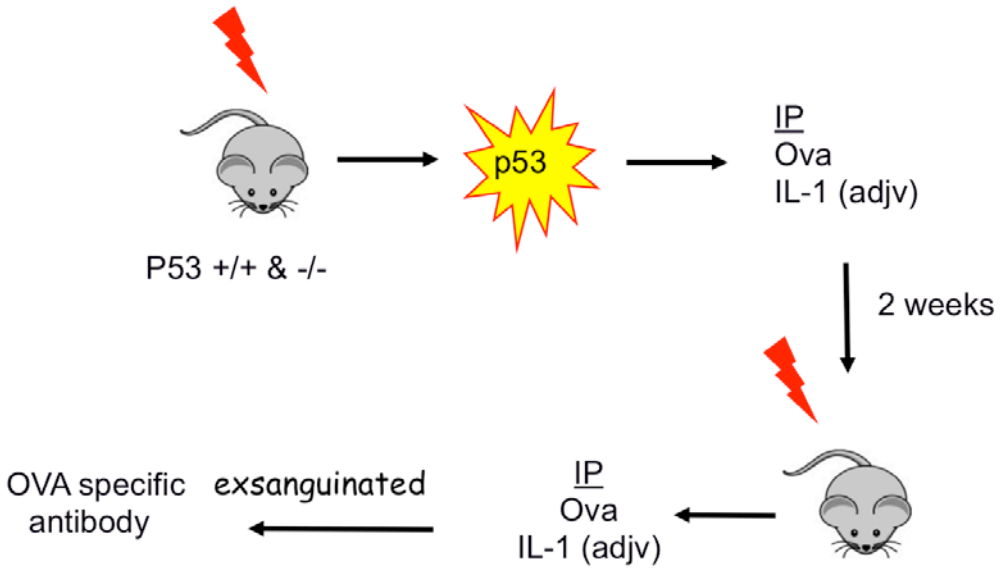

Figure 5.18: Future plan to study the effects of p53 in adaptive immunity
Wild-type and *p53*-null mice would be irradiated to activate p53 (in the wild-type), followed by inoculation with OVA and recombinant IL-1 (as adjuvant) via intraperitoneal injection. Two weeks later, mice will be irradiated and inoculated with OVA for a second time. Mice will subsequently be exsanguinated and the differences in the abundance of OVA-specific antibodies will be detected by end-point ELISA.

Chapter 6: Conclusions

This section summarises the main conclusions of this thesis.

DRAM-1, a p53 target gene, encodes for a series of splice variants both in human and mouse. This implies that the splicing of *DRAM-1* may be widespread and evolutionarily conserved across species, at least in higher eukaryotes.

In the first part of this thesis (Chapter 3), three of the the *DRAM-1* splice variants, namely SV 1, SV 4 and SV 5, all which contains the first and the last exons but lack different combinations of internal exons, have been characterised. These transcripts give rise to different fully functional proteins, all which possessed the conserved 'PYISD' domain, which is critical for DRAM-1-mediated autophagosome formation. DRAM-1 isoforms localise to different cellular compartments spanning the secretory pathway - ER, golgi apparatus, endosomes, and lysosomes, in addition to autophagosomes and peroxisomes. These isoforms are believed to modulate autophagy in parallel, and occasionally coordinatedly in different regions of the cell. Isoform 1 is degraded in lysosomes, whereas isoforms 4 and 5 are degraded in the proteasome.

DRAM-1 isoforms 1, 4 and 5 cause autophagosome accumulation, with isoform 1 evoking a stronger effect of GFP-LC3 punctation and LC3 lipidation compared to isoforms 4 and 5. The simultaneous overexpression of DRAM-1 isoforms does not result in a synergistic accumulation of autophagosomes or an enhanced fusion of autophagosomes to lysosomes.

Interestingly, deletion of *DRAM-1* does not impair LC3 lipidation upon starvation. It is very likely that autophagy mediated by DRAM-1 can be substituted by the other DRAM family members, namely DRAM-2, DRAM-3, DRAM-4 or DRAM-5, all which show significant homology to DRAM-1 (O'Prey, Skommer et al. 2009). This is supported by the observation that *DRAM-2, DRAM-3, DRAM-4* and *DRAM-5* mRNA expression is upregulated in different cell types upon *DRAM-1* deletion, as illustrated in Fig. 6.1.

The autophagic substrates for DRAM-1 appear rather specific. Forced expression

of DRAM-1 induces LC3 accumulation, but ectopic overexpression or genetic ablation of DRAM-1 isoforms does not enhance long-lived protein degradation and ROS, a susbtrate of autophagy which is generated as a byproduct of variuos cellular processes (refer to section 1.3.2).

Consistent with previously published results, DRAM-1 is required for p53-dependent apoptosis (Crighton, Wilkinson et al. 2006). In line with this, the role of DRAM-1 in enhancing p53-dependent cell death also occurs in mouse embryonic fibroblasts, as discussed previously in this thesis. Although the individual overexpression of DRAM-1 isoforms does not modulate cell death, they (or at least one - DRAM-1 isoform 1) are required to sustain cellular viability under amino-acid and glucose-limiting conditions.

In the second part of this thesis (Chapter 4), the investigation of DRAM-1 has been extended to *in vivo* studies. *Dram-1*$^{-/-}$ mice were born at the expected Mendelian frequency and are viable, fertile, and appeared normal, with no obvious phenotypic defects compared to wild-type and heterozygote controls. Although human DRAM-1 has convincingly shown to be a strong promoter of autophagy, loss of *DRAM-1* neither affects the lifespan nor predisposes to autophagy-related diseases in either heterozygotes or *DRAM-1*-null mice aged up to 650 days old.

Albeit DRAM-1 is required for effective p53-mediated cell death in human osteosarcoma cells (Crighton, Wilkinson et al. 2006) and MEFs, loss of DRAM-1 does not modulate apoptosis in the small intestine upon exposure to gamma irradiation *in vivo*, regardless of p53 status. This suggests that involvement of DRAM-1 in p53-dependent apoptosis is highly specific to the type of cell or tissue.

DRAM-1 is required for optimal regeneration in the small intestine, at least in the crypts upon radiation-induced injury by promoting cellular proliferation and mitosis. In this case, mTOR activity and the population of OLFM4 positive fast-cycling stem cells are not affected by loss of DRAM-1, assessed at 72 hours post irradiation.

The reactivation of p53 in the liver has been demonstrated to induce senescence and promote tumour regression (Xue, Zender et al. 2007). Albeit *DRAM-1* is a p53

target gene, the genetic ablation of *DRAM-1* is not required for p53-induced senescence in the liver. However, human *DRAM-1* mRNA expression is downregulated during oncogene-induced senescence (Fig.6.2A and Fig. 6.2B). Thus, it would be interesting to investigate if DRAM-1 modulates the onset of oncogene-induced senescence *in vitro* and *in vivo.*

Using the same model, the simultaneous loss of DRAM-1 and p53 activation in the liver is very likely to cause mitotic arrest in the metaphase stage, thus leading to an increase in apoptosis. This may suggest that DRAM-1 is required to regulate the formation of the mitotic spindle and the attachment of sister chromatids to the spindle. This also highlights the role of DRAM-1 as a tumour suppressor in the liver to maintain the fidelity of mitosis. Thus, it might be worthwhile to confirm the role of DRAM-1 as a tumour suppressor using *in vivo* models of liver cancer.

DRAM-1 knockout mice were not predisposed to spontaneous or radiation-induced tumorigenesis. In line with the previous scenario, loss of *DRAM-1* could be compensated by other DRAM family members. Given this, the deletion of *DRAM-1* in conjunction with other DRAM family members and its impact on the lifespan, susceptibility to autophagy-associated diseases and tumourigenesis is of great interest. We also showed that the loss of *DRAM-1* does not predispose to inflammation-driven colorectal cancer. However, the number of *DRAM-1*$^{-/-}$ subjects in this cohort is relatively small (N=3) because *DRAM-1*$^{-/-}$ mice are susceptible to DSS treatment. To consolidate this observation, this experiment ought to be repeated with a lower dosage of DSS to a reasonable threshold in order to increase the number of *DRAM-1*$^{-/-}$ survivors, at least until a time point where they are able to develop colonic polyps for accurate analysis.

In the last section of chapter 4, we found that the loss of *DRAM-1* exacerbates epithelium erosion, as characterised by the loss of live crypts and goblet cells. However, *DRAM-1*$^{-/-}$ do not exhibit an increase in neutrophil and macrophage infiltration to the colon during the early and late stages of inflammation. In future, it would be of great interest to determine if DRAM-1 is required for regulating inflammation establishing an increase in inflammatory markers, such as cytokine secretion and by monitoring the infiltration of other immune cells such as monocytes, T and B cells (refer to section 4.3). It may be possible that DRAM-1

does not regulate the inflammatory responses, but is required for optimal regeneration of colonic crypts after injury. This is yet another facet that is worth pursuing.

In the third part of this thesis (Chapter 5), it was found that human DRAM-1 is coregulated with regulators of the antigen presentation pathway, and as such might be involved in regulating cellular immune responses. In line with this, *DRAM-1* mRNA expression is upregulated upon exposure to the pathogens, bacterial LPS and inflammatory cytokines. Although loss of *DRAM-1* in dendritic cells affects the upregulation of MHC class I and CD40, other T cell activating signals – MHC class II, CD80 and CD86 remains unperturbed upon exposure to LPS. However, loss of *DRAM-1* in professional antigen presenting cells – dendritic cells and macrophages do not affect their ability to stimulate T cell activation. Given this, studying the loss of *DRAM-1* in B cells (another professional APC) and facultative APCs like skeletal muscle cells is worth pursuing.

Instead, stabilisation of p53 in APCs inhibits antigen processing and impairs CD4+ and CD8+ T cell stimulation. Given that p53 has been shown to increase TAP1 expression and the subsequent trafficking of of MHC class I peptides in non-professional antigen presenting cells (Zhu, Wang et al. 1999), the inhibitory or promoting role of CD8+ T cell activation by p53 is possibly cell-type specific. In line with this, the thorough effect of p53 on the adaptive immunity and its significance in tumour immunity is of great interest.

In efforts to delineate the role of p53 in modulating antigen presentation in dendritic cells (DCs), it was found that the p53 modulator, Nutlin-3A, which is a potential chemotherapeutic drug in the pre-clinical developmental phase, can result in p53-independent apoptosis. Consistent with previous findings in which caspase 3 is required for the expression of MHC class II molecules on mature DCs (Santambrogio, Potolicchio et al. 2005), the pan-caspase inhibitor zVAD-fmk, represses the upregulation of a panel of classical T cell co-stimulatory molecules on antigen presenting cells upon exposure to stress signals.

Clearly, efforts to elucidate the role of DRAM-1 in autophagy, apoptosis, regeneration, senescence and immunity is complicated due to the fact that the

loss of DRAM-1 can likely be compensated by other DRAM family members. Thus, studies to identify the role of DRAM-1 should be conducted alongside the studies to characterise other DRAM family members.

Additionally, the role of p53 in the modulation of adaptive and tumour immunity is worth pursuing in efforts to aid the development of cancer therapeutics.

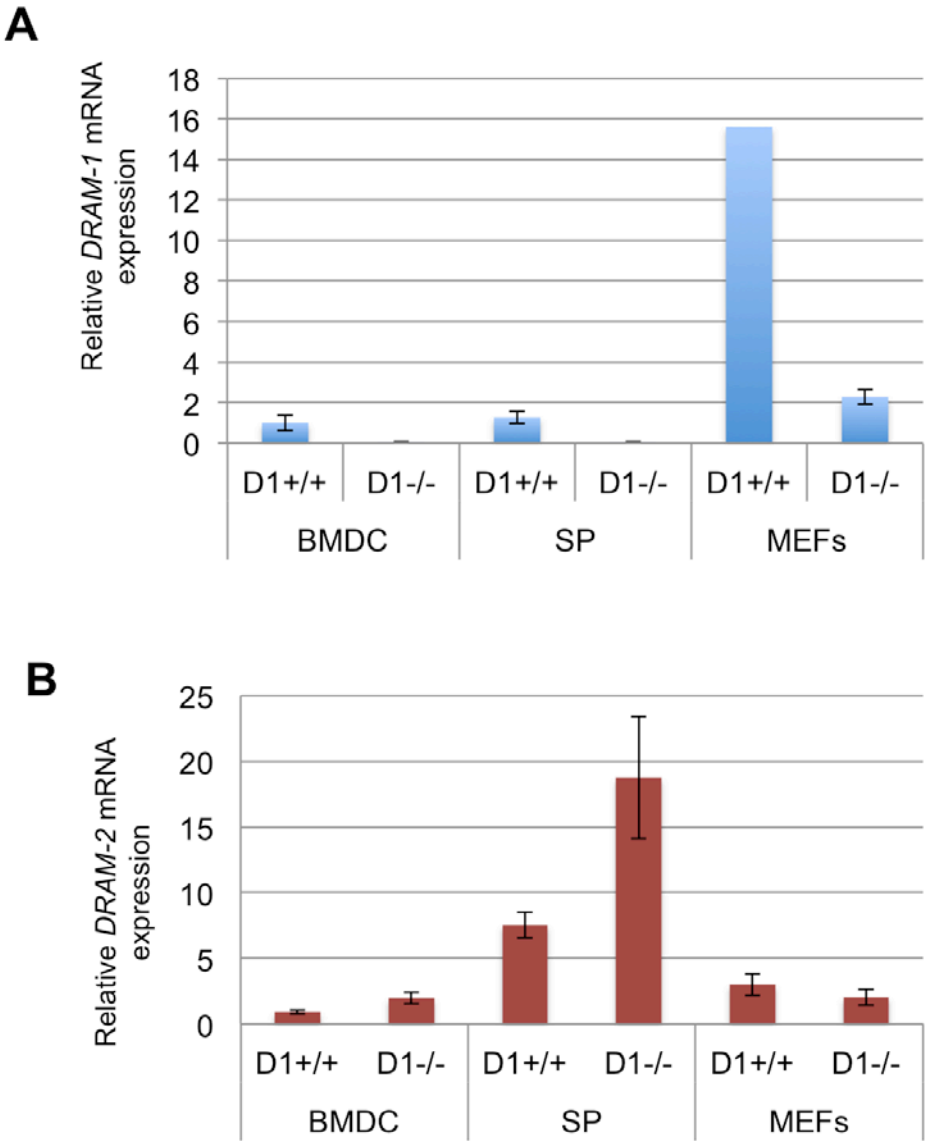

Figure 6.1 (A-B): *DRAM*s mRNA expression in wilde type and *DRAM-1*-null bone-marrow-derived dendritic cells (BMDC) , splenocytes (SP) and MEFS.
(A)*DRAM-1* deletion was validated using RT-PCR.
(B)DRAM-2 mRNA expression was quantified using RT-PCR (B).

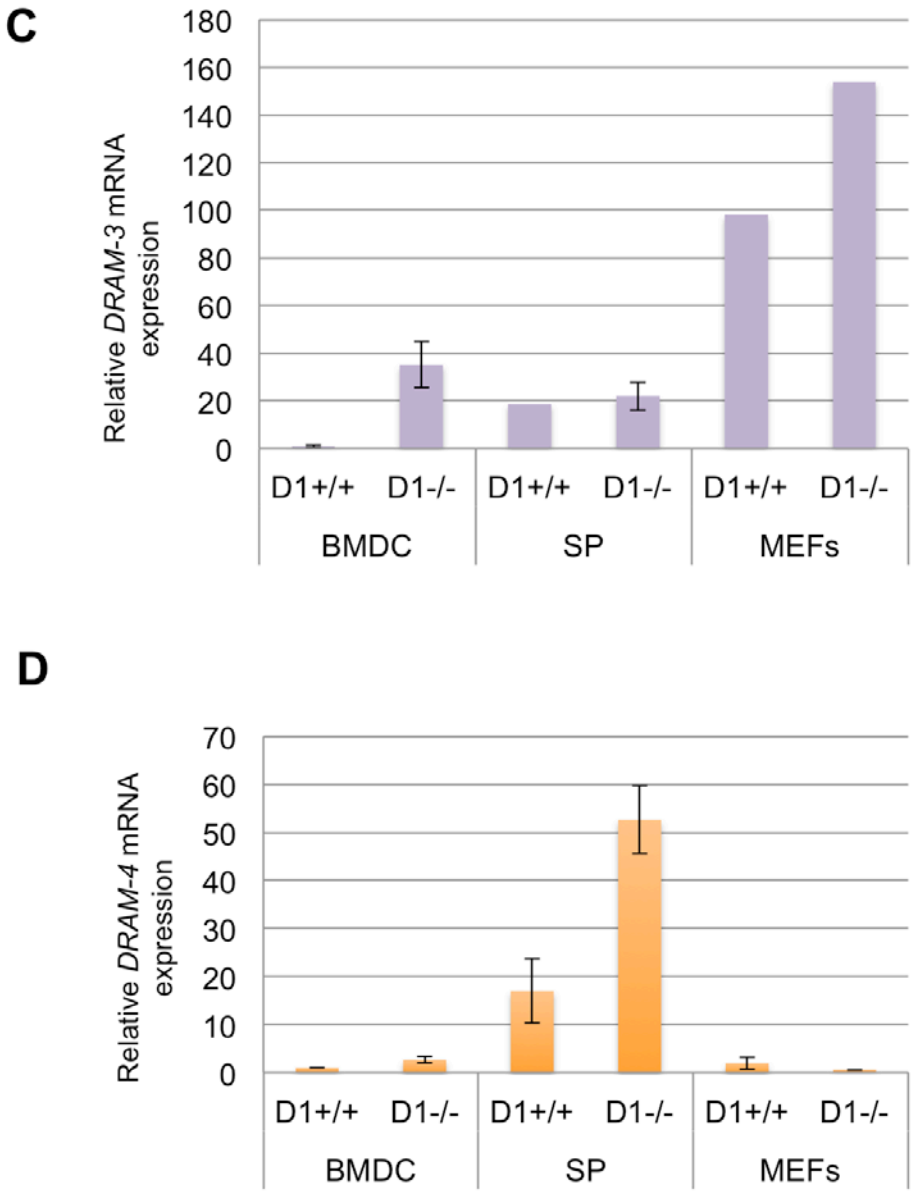

Figure 6.1 (C-D): *DRAM*s mRNA expression in wilde type and DRAM-1 null bone-marrow-derived DCs (BMDC) , splenocytes (SP) and MEFS. *DRAM-3* (C) and *DRAM-4* (D) mRNA expression was quantified using RT-PCR.

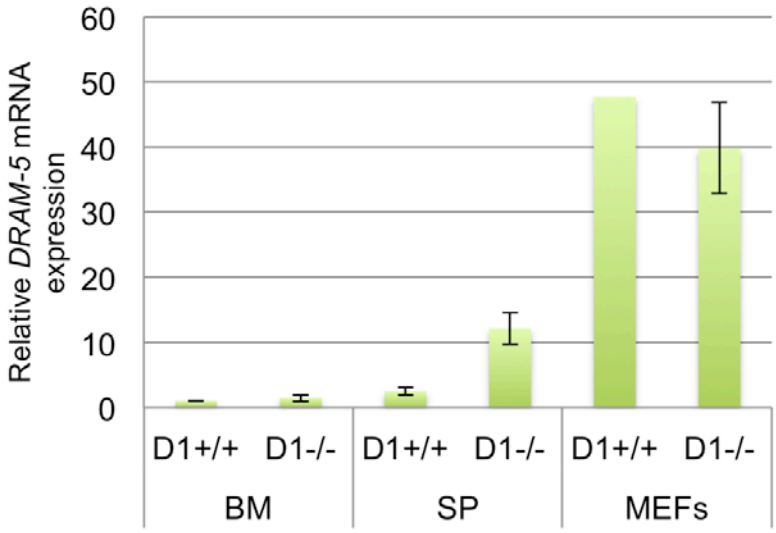

Figure 6.1 (E): DRAMs mRNA expression in wilde type and DRAM-1 null bone-marrow-derived DCs (BMDC) , splenocytes (SP) and MEFS. *DRAM-5* mRNA expression was quantified using RT-PCR.

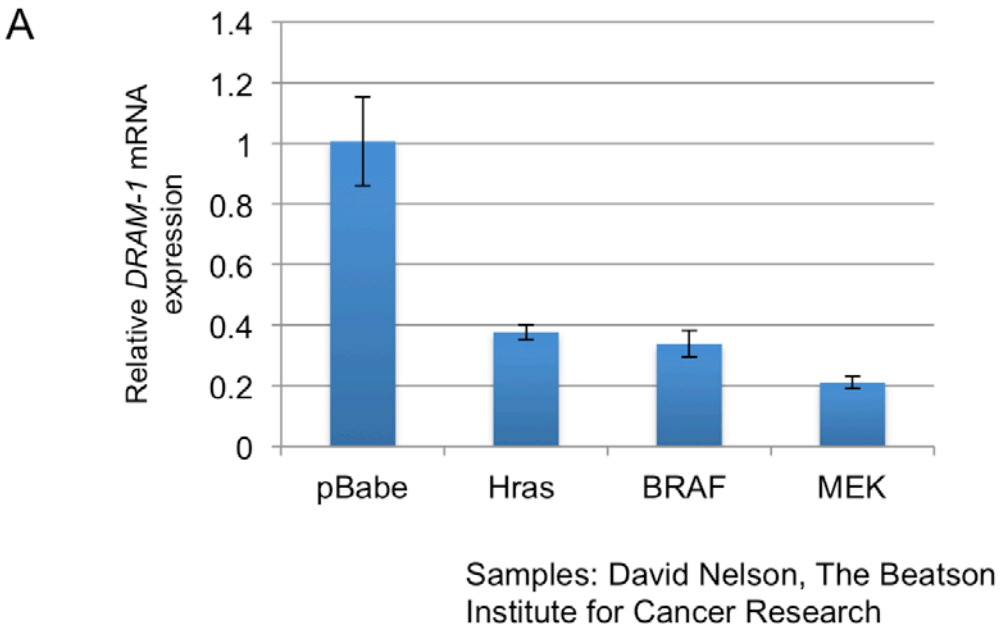

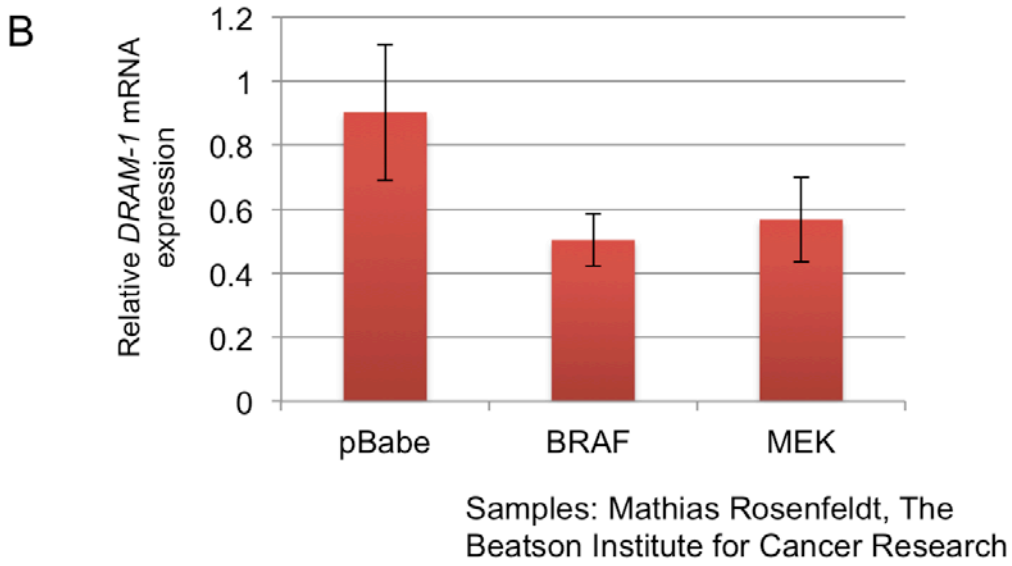

Figure 6.2(A-B): *DRAM-1* mRNA expression is downregulated during oncogene-induced senescence

RNA lysates from IMR-90 (A) or hTERT-immortalised Tig3ET (B) human fibroblasts which were infected with an empty retroviral vector, or retroviruses expressing the oncogenes HrasG12V, BRAFV600E, and MEKQ56P were analysed for DRAM-1 expression by Real Time PCR.

Bibliography

Agarwal, M. L., A. Agarwal, et al. (1995). "p53 controls both the G2/M and the G1 cell cycle checkpoints and mediates reversible growth arrest in human fibroblasts." Proc Natl Acad Sci U S A **92**(18): 8493-8497.

Al-Gubory, K. H., P. A. Fowler, et al. (2010). "The roles of cellular reactive oxygen species, oxidative stress and antioxidants in pregnancy outcomes." Int J Biochem Cell Biol **42**(10): 1634-1650.

Allan, J. M. and L. B. Travis (2005). "Mechanisms of therapy-related carcinogenesis." Nat Rev Cancer **5**(12): 943-955.

Amigorena, S. and A. Savina (2010). "Intracellular mechanisms of antigen cross presentation in dendritic cells." Curr Opin Immunol **22**(1): 109-117.

Ashton, G. H., J. P. Morton, et al. (2010). "Focal adhesion kinase is required for intestinal regeneration and tumorigenesis downstream of Wnt/c-Myc signaling." Dev Cell **19**(2): 259-269.

Attardi, L. D., A. de Vries, et al. (2004). "Activation of the p53-dependent G1 checkpoint response in mouse embryo fibroblasts depends on the specific DNA damage inducer." Oncogene **23**(4): 973-980.

Axe, E. L., S. A. Walker, et al. (2008). "Autophagosome formation from membrane compartments enriched in phosphatidylinositol 3-phosphate and dynamically connected to the endoplasmic reticulum." J Cell Biol **182**(4): 685-701.

Bampton, E. T., C. G. Goemans, et al. (2005). "The dynamics of autophagy visualized in live cells: from autophagosome formation to fusion with endo/lysosomes." Autophagy **1**(1): 23-36.

Banchereau, J. and R. M. Steinman (1998). "Dendritic cells and the control of immunity." Nature **392**(6673): 245-252.

Banner, B. F., L. Savas, et al. (1993). "Characterization of the inflammatory cell populations in normal colon and colonic carcinomas." Virchows Arch B Cell Pathol Incl Mol Pathol **64**(4): 213-220.

Barker, N., J. H. van Es, et al. (2007). "Identification of stem cells in small intestine and colon by marker gene Lgr5." Nature **449**(7165): 1003-1007.

Barnden, M. J., J. Allison, et al. (1998). "Defective TCR expression in transgenic mice constructed using cDNA-based alpha- and beta-chain genes under the control of heterologous regulatory elements." Immunol Cell Biol **76**(1): 34-40.

Begus-Nahrmann, Y., A. Lechel, et al. (2009). "p53 deletion impairs clearance of chromosomal-instable stem cells in aging telomere-dysfunctional mice." Nat Genet **41**(10): 1138-1143.

Bensaad, K., E. C. Cheung, et al. (2009). "Modulation of intracellular ROS levels by TIGAR controls autophagy." EMBO J **28**(19): 3015-3026.

Bensaad, K., A. Tsuruta, et al. (2006). "TIGAR, a p53-inducible regulator of glycolysis and apoptosis." Cell **126**(1): 107-120.

Bernales, S., S. Schuck, et al. (2007). "ER-phagy: selective autophagy of the endoplasmic reticulum." Autophagy **3**(3): 285-287.

Berry, D. L. and E. H. Baehrecke (2007). "Growth arrest and autophagy are required for salivary gland cell degradation in Drosophila." Cell **131**(6): 1137-1148.

Bhatia, S., K. Sun, et al. (2010). "Dynamic equilibrium of B7-1 dimers and monomers differentially affects immunological synapse formation and T cell activation in response to TCR/CD28 stimulation." J Immunol **184**(4): 1821-1828.

Blanchet, F. P., A. Moris, et al. (2010). "Human immunodeficiency virus-1 inhibition of immunoamphisomes in dendritic cells impairs early innate and adaptive immune responses." Immunity **32**(5): 654-669.

Boise, L. H., M. Gonzalez-Garcia, et al. (1993). "bcl-x, a bcl-2-related gene that functions as a dominant regulator of apoptotic cell death." Cell **74**(4): 597-608.

Bond, J., M. Haughton, et al. (1996). "Evidence that transcriptional activation by p53 plays a direct role in the induction of cellular senescence." Oncogene **13**(10): 2097-2104.

Bond, J. A., F. S. Wyllie, et al. (1994). "Escape from senescence in human diploid fibroblasts induced directly by mutant p53." Oncogene **9**(7): 1885-1889.

Bordon, Y., C. A. Hansell, et al. (2009). "The atypical chemokine receptor D6 contributes to the development of experimental colitis." J Immunol **182**(8): 5032-5040.

Cadwell, K., J. Y. Liu, et al. (2008). "A key role for autophagy and the autophagy gene Atg16l1 in mouse and human intestinal Paneth cells." Nature **456**(7219): 259-263.

Cann, G. M., C. Guignabert, et al. (2008). "Developmental expression of LC3alpha and beta: absence of fibronectin or autophagy phenotype in LC3beta knockout mice." Dev Dyn **237**(1): 187-195.

Castedo, M., J. L. Perfettini, et al. (2004). "Cell death by mitotic catastrophe: a molecular definition." Oncogene **23**(16): 2825-2837.

Ceddia, M. A. and J. A. Woods (1999). "Exercise suppresses macrophage antigen presentation." J Appl Physiol **87**(6): 2253-2258.

Cella, M., D. Scheidegger, et al. (1996). "Ligation of CD40 on dendritic cells triggers production of high levels of interleukin-12 and enhances T cell stimulatory capacity: T-T help via APC activation." J Exp Med **184**(2): 747-752.

Chang, Y. T., H. C. Tseng, et al. (2011). "Relative down-regulation of apoptosis and autophagy genes in colorectal cancer." Eur J Clin Invest **41**(1): 84-92.

Chen, Y. and D. J. Klionsky (2011). "The regulation of autophagy - unanswered questions." J Cell Sci **124**(Pt 2): 161-170.

Chene, P. (2003). "Inhibiting the p53-MDM2 interaction: an important target for cancer therapy." Nat Rev Cancer **3**(2): 102-109.

Cho, D. H., Y. K. Jo, et al. (2009). "Caspase-mediated cleavage of ATG6/Beclin-1 links apoptosis to autophagy in HeLa cells." Cancer Lett **274**(1): 95-100.

Ciechanover, A. (2005). "Proteolysis: from the lysosome to ubiquitin and the proteasome." Nat Rev Mol Cell Biol **6**(1): 79-87.

Clapper, M. L., H. S. Cooper, et al. (2007). "Dextran sulfate sodium-induced colitis-associated neoplasia: a promising model for the development of chemopreventive interventions." Acta Pharmacol Sin **28**(9): 1450-1459.

Clayton, A. R., R. L. Prue, et al. (2003). "Dendritic cell uptake of human apoptotic and necrotic neutrophils inhibits CD40, CD80, and CD86 expression and reduces allogeneic T cell responses: relevance to systemic vasculitis." Arthritis Rheum **48**(8): 2362-2374.

Codogno, P. and A. J. Meijer (2005). "Autophagy and signaling: their role in cell survival and cell death." Cell Death Differ **12 Suppl 2**: 1509-1518.

Coers, J., M. N. Starnbach, et al. (2009). "Modeling infectious disease in mice: co-adaptation and the role of host-specific IFNgamma responses." PLoS Pathog **5**(5): e1000333.

Colosetti, P., A. Puissant, et al. (2009). "Autophagy is an important event for megakaryocytic differentiation of the chronic myelogenous leukemia K562 cell line." Autophagy **5**(8): 1092-1098.

Cooney, R., J. Baker, et al. (2010). "NOD2 stimulation induces autophagy in dendritic cells influencing bacterial handling and antigen presentation." Nat Med **16**(1): 90-97.

Crighton, D., J. O'Prey, et al. (2007). "p73 regulates DRAM-independent autophagy that does not contribute to programmed cell death." Cell Death Differ **14**(6): 1071-1079.

Crighton, D., S. Wilkinson, et al. (2006). "DRAM, a p53-induced modulator of autophagy, is critical for apoptosis." Cell **126**(1): 121-134.

Cuervo, A. M. (2004). "Autophagy: in sickness and in health." Trends Cell Biol **14**(2): 70-77.

Damoiseaux, J. G., H. Yagita, et al. (1998). "Costimulatory molecules CD80 and CD86 in the rat; tissue distribution and expression by antigen-presenting cells." J Leukoc Biol **64**(6): 803-809.

de Boer, J., A. Williams, et al. (2003). "Transgenic mice with hematopoietic and lymphoid specific expression of Cre." Eur J Immunol **33**(2): 314-325.

De Botton, S., S. Sabri, et al. (2002). "Platelet formation is the consequence of caspase activation within megakaryocytes." Blood **100**(4): 1310-1317.

De Duve, C., B. C. Pressman, et al. (1955). "Tissue fractionation studies. 6. Intracellular distribution patterns of enzymes in rat-liver tissue." Biochem J **60**(4): 604-617.

De Robertis, M., E. Massi, et al. (2011). "The AOM/DSS murine model for the study of colon carcinogenesis: From pathways to diagnosis and therapy studies." J Carcinog **10**: 9.

Degterev, A., M. Boyce, et al. (2003). "A decade of caspases." Oncogene **22**(53): 8543-8567.

Dehay, C. and H. Kennedy (2007). "Cell-cycle control and cortical development." Nat Rev Neurosci **8**(6): 438-450.

Dehmer, J. J., A. P. Garrison, et al. (2011). "Expansion of intestinal epithelial stem cells during murine development." PLoS One **6**(11): e27070.

Delgado, M. A., R. A. Elmaoued, et al. (2008). "Toll-like receptors control autophagy." EMBO J **27**(7): 1110-1121.

Demarchi, F., C. Bertoli, et al. (2006). "Calpain is required for macroautophagy in mammalian cells." J Cell Biol **175**(4): 595-605.

Deng, C., P. Zhang, et al. (1995). "Mice lacking p21CIP1/WAF1 undergo normal development, but are defective in G1 checkpoint control." Cell **82**(4): 675-684.

Deng, L., J. Feng, et al. (2010). "The novel estrogen-induced gene EIG121 regulates autophagy and promotes cell survival under stress." Cell Death Dis **1**: e32.

Deretic, V. (2005). "Autophagy in innate and adaptive immunity." Trends Immunol **26**(10): 523-528.

Donehower, L. A. and G. Lozano (2009). "20 years studying p53 functions in genetically engineered mice." Nat Rev Cancer **9**(11): 831-841.

Dorfel, D., S. Appel, et al. (2005). "Processing and presentation of HLA class I and II epitopes by dendritic cells after transfection with in vitro-transcribed MUC1 RNA." Blood **105**(8): 3199-3205.

Dunkelberger, J. R. and W. C. Song (2010). "Complement and its role in innate and adaptive immune responses." Cell Res **20**(1): 34-50.

Echard, A., F. J. Opdam, et al. (2000). "Alternative splicing of the human Rab6A gene generates two close but functionally different isoforms." Mol Biol Cell **11**(11): 3819-3833.

Ehst, B. D., E. Ingulli, et al. (2003). "Development of a novel transgenic mouse for the study of interactions between CD4 and CD8 T cells during graft rejection." Am J Transplant **3**(11): 1355-1362.

el Marjou, F., K. P. Janssen, et al. (2004). "Tissue-specific and inducible Cre-mediated recombination in the gut epithelium." Genesis **39**(3): 186-193.

Elgendy, M., C. Sheridan, et al. (2011). "Oncogenic Ras-induced expression of Noxa and Beclin-1 promotes autophagic cell death and limits clonogenic survival." Mol Cell **42**(1): 23-35.

Eskelinen, E. L. and P. Saftig (2009). "Autophagy: A lysosomal degradation pathway with a central role in health and disease." Biochim Biophys Acta **1793**(4): 664-673.

Fader, C. M. and M. I. Colombo (2009). "Autophagy and multivesicular bodies: two closely related partners." Cell Death Differ **16**(1): 70-78.

Feng, Z., H. Zhang, et al. (2005). "The coordinate regulation of the p53 and mTOR pathways in cells." Proc Natl Acad Sci U S A **102**(23): 8204-8209.

Fimia, G. M., A. Stoykova, et al. (2007). "Ambra1 regulates autophagy and development of the nervous system." Nature **447**(7148): 1121-1125.

Fritz, T., L. Niederreiter, et al. (2011). "Crohn's disease: NOD2, autophagy and ER stress converge." Gut **60**(11): 1580-1588.

Fu, Z., J. Kim, et al. (2009). "Intestinal cell kinase, a MAP kinase-related kinase, regulates proliferation and G1 cell cycle progression of intestinal epithelial cells." Am J Physiol Gastrointest Liver Physiol **297**(4): G632-640.

Furuta, S., E. Hidaka, et al. (2004). "Ras is involved in the negative control of autophagy through the class I PI3-kinase." Oncogene **23**(22): 3898-3904.

Galavotti, S., S. Bartesaghi, et al. (2012). "The autophagy-associated factors DRAM1 and p62 regulate cell migration and invasion in glioblastoma stem cells." Oncogene.

Galluzzi, L., S. A. Aaronson, et al. (2009). "Guidelines for the use and interpretation of assays for monitoring cell death in higher eukaryotes." Cell Death Differ **16**(8): 1093-1107.

Galvez, J., M. Garrido, et al. (2000). "Intestinal anti-inflammatory activity of UR-12746, a novel 5-ASA conjugate, on acute and chronic experimental colitis in the rat." Br J Pharmacol **130**(8): 1949-1959.

Garabedian, E. M., L. J. Roberts, et al. (1997). "Examining the role of Paneth cells in the small intestine by lineage ablation in transgenic mice." J Biol Chem **272**(38): 23729-23740.

Gerlach, A. M., A. Steimle, et al. (2012). "Role of CD40 ligation in dendritic cell semimaturation." BMC Immunol **13**(1): 22.

Ghavami, S., M. M. Mutawe, et al. (2011). "Mevalonate cascade regulation of airway mesenchymal cell autophagy and apoptosis: a dual role for p53." PLoS One **6**(1): e16523.

Glas, R., M. Bogyo, et al. (1998). "A proteolytic system that compensates for loss of proteasome function." Nature **392**(6676): 618-622.

Gonzalez-Estevez, C., D. A. Felix, et al. (2007). "Gtdap-1 promotes autophagy and is required for planarian remodeling during regeneration and starvation." Proc Natl Acad Sci U S A **104**(33): 13373-13378.

Gorbunov, N. V. and J. G. Kiang (2009). "Up-regulation of autophagy in small intestine Paneth cells in response to total-body gamma-irradiation." J Pathol **219**(2): 242-252.

Gozuacik, D. and A. Kimchi (2004). "Autophagy as a cell death and tumor suppressor mechanism." Oncogene **23**(16): 2891-2906.

Grier, J. D., W. Yan, et al. (2002). "Conditional allele of mdm2 which encodes a p53 inhibitor." Genesis **32**(2): 145-147.

Griffiths, G. S., M. Grundl, et al. (2011). "Bit-1 mediates integrin-dependent cell survival through activation of the NFkappaB pathway." J Biol Chem **286**(16): 14713-14723.

Groulx, J. F., T. Khalfaoui, et al. (2012). "Autophagy is active in normal colon mucosa." Autophagy **8**(6): 893-902.

Hailey, D. W., A. S. Rambold, et al. (2010). "Mitochondria supply membranes for autophagosome biogenesis during starvation." Cell **141**(4): 656-667.

Han, Y. K., Y. G. Kim, et al. (2010). "Hyperosmotic stress induces autophagy and apoptosis in recombinant Chinese hamster ovary cell culture." Biotechnol Bioeng **105**(6): 1187-1192.

Hans, F. and S. Dimitrov (2001). "Histone H3 phosphorylation and cell division." Oncogene **20**(24): 3021-3027.

Harris, C. C. (2006). "Protein-protein interactions for cancer therapy." Proc Natl Acad Sci U S A **103**(6): 1659-1660.

He, C., M. Baba, et al. (2008). "Self-interaction is critical for Atg9 transport and function at the phagophore assembly site during autophagy." Mol Biol Cell **19**(12): 5506-5516.

Helgason, G. V., J. O'Prey, et al. (2010). "Oncogene-induced sensitization to chemotherapy-induced death requires induction as well as deregulation of E2F1." Cancer Res **70**(10): 4074-4080.

Hendzel, M. J., Y. Wei, et al. (1997). "Mitosis-specific phosphorylation of histone H3 initiates primarily within pericentromeric heterochromatin during G2 and spreads in an ordered fashion coincident with mitotic chromosome condensation." Chromosoma **106**(6): 348-360.

Herberts, C. A., M. S. Kwa, et al. (2011). "Risk factors in the development of stem cell therapy." J Transl Med **9**: 29.

Hermeking, H., C. Lengauer, et al. (1997). "14-3-3 sigma is a p53-regulated inhibitor of G2/M progression." Mol Cell **1**(1): 3-11.

Hernandez, I., J. L. Moreno, et al. (2010). "Novel alternatively spliced ADAM8 isoforms contribute to the aggressive bone metastatic phenotype of lung cancer." Oncogene **29**(26): 3758-3769.

Hocker, M. and B. Wiedenmann (1998). "Molecular mechanisms of enteroendocrine differentiation." Ann N Y Acad Sci **859**: 160-174.

Hogquist, K. A., S. C. Jameson, et al. (1994). "T cell receptor antagonist peptides induce positive selection." Cell **76**(1): 17-27.

Hosokawa, N., T. Hara, et al. (2009). "Nutrient-dependent mTORC1 association with the ULK1-Atg13-FIP200 complex required for autophagy." Mol Biol Cell **20**(7): 1981-1991.

Huang, Y. F., M. D. Chang, et al. (2009). "TTK/hMps1 mediates the p53-dependent postmitotic checkpoint by phosphorylating p53 at Thr18." Mol Cell Biol **29**(11): 2935-2944.

Ijiri, K. and C. S. Potten (1986). "Radiation-hypersensitive cells in small intestinal crypts; their relationships to clonogenic cells." Br J Cancer Suppl **7**: 20-22.

Ilangovan, R., W. L. Marshall, et al. (2003). "Inhibition of apoptosis by Z-VAD-fmk in SMN-depleted S2 cells." J Biol Chem **278**(33): 30993-30999.

Ireland, H., R. Kemp, et al. (2004). "Inducible Cre-mediated control of gene expression in the murine gastrointestinal tract: effect of loss of beta-catenin." Gastroenterology **126**(5): 1236-1246.

Itakura, E., C. Kishi, et al. (2008). "Beclin 1 forms two distinct phosphatidylinositol 3-kinase complexes with mammalian Atg14 and UVRAG." Mol Biol Cell **19**(12): 5360-5372.

Itakura, E. and N. Mizushima (2010). "Characterization of autophagosome formation site by a hierarchical analysis of mammalian Atg proteins." Autophagy **6**(6): 764-776.

Jia, K., C. Thomas, et al. (2009). "Autophagy genes protect against Salmonella typhimurium infection and mediate insulin signaling-regulated pathogen resistance." Proc Natl Acad Sci U S A **106**(34): 14564-14569.

Jia, W., H. H. Pua, et al. (2011). "Autophagy regulates endoplasmic reticulum homeostasis and calcium mobilization in T lymphocytes." J Immunol **186**(3): 1564-1574.

Jin, S. (2006). "Autophagy, mitochondrial quality control, and oncogenesis." Autophagy **2**(2): 80-84.

Johnson, J. M., J. Castle, et al. (2003). "Genome-wide survey of human alternative pre-mRNA splicing with exon junction microarrays." Science **302**(5653): 2141-2144.

Jones, S. N., A. E. Roe, et al. (1995). "Rescue of embryonic lethality in Mdm2-deficient mice by absence of p53." Nature **378**(6553): 206-208.

Jounai, N., F. Takeshita, et al. (2007). "The Atg5 Atg12 conjugate associates with innate antiviral immune responses." Proc Natl Acad Sci U S A **104**(35): 14050-14055.

Juhasz, G. and M. Sass (2005). "Hid can induce, but is not required for autophagy in polyploid larval Drosophila tissues." Eur J Cell Biol **84**(4): 491-502.

Kabeya, Y., N. Mizushima, et al. (2000). "LC3, a mammalian homologue of yeast Apg8p, is localized in autophagosome membranes after processing." EMBO J **19**(21): 5720-5728.

Kang, C., Y. J. You, et al. (2007). "Dual roles of autophagy in the survival of Caenorhabditis elegans during starvation." Genes Dev **21**(17): 2161-2171.

Kang, M. R., M. S. Kim, et al. (2009). "Frameshift mutations of autophagy-related genes ATG2B, ATG5, ATG9B and ATG12 in gastric and colorectal cancers with microsatellite instability." J Pathol **217**(5): 702-706.

Kang, R., D. Tang, et al. (2010). "The receptor for advanced glycation end products (RAGE) sustains autophagy and limits apoptosis, promoting pancreatic tumor cell survival." Cell Death Differ **17**(4): 666-676.

Kanzawa, T., I. M. Germano, et al. (2004). "Role of autophagy in temozolomide-induced cytotoxicity for malignant glioma cells." Cell Death Differ **11**(4): 448-457.

Karantza-Wadsworth, V., S. Patel, et al. (2007). "Autophagy mitigates metabolic stress and genome damage in mammary tumorigenesis." Genes Dev **21**(13): 1621-1635.

Karpinich, N. O., M. Tafani, et al. (2002). "The course of etoposide-induced apoptosis from damage to DNA and p53 activation to mitochondrial release of cytochrome c." J Biol Chem **277**(19): 16547-16552.

Kemp, C. J., T. Wheldon, et al. (1994). "p53-deficient mice are extremely susceptible to radiation-induced tumorigenesis." Nat Genet **8**(1): 66-69.

Kerr, J. F., A. H. Wyllie, et al. (1972). "Apoptosis: a basic biological phenomenon with wide-ranging implications in tissue kinetics." Br J Cancer **26**(4): 239-257.

Kim, J. H. and R. D. Leeper (1987). "Treatment of locally advanced thyroid carcinoma with combination doxorubicin and radiation therapy." Cancer **60**(10): 2372-2375.

Kim, W. J., R. R. Mohan, et al. (2000). "Caspase inhibitor z-VAD-FMK inhibits keratocyte apoptosis, but promotes keratocyte necrosis, after corneal epithelial scrape." Exp Eye Res **71**(3): 225-232.

Kimura, S., T. Noda, et al. (2007). "Dissection of the autophagosome maturation process by a novel reporter protein, tandem fluorescent-tagged LC3." Autophagy **3**(5): 452-460.

King, J. S., D. M. Veltman, et al. (2011). "The induction of autophagy by mechanical stress." Autophagy **7**(12): 1490-1499.

Kirkin, V., T. Lamark, et al. (2009). "A role for NBR1 in autophagosomal degradation of ubiquitinated substrates." Mol Cell **33**(4): 505-516.

Klionsky, D. J. (2007). "Autophagy: from phenomenology to molecular understanding in less than a decade." Nat Rev Mol Cell Biol **8**(11): 931-937.

Klionsky, D. J., H. Abeliovich, et al. (2008). "Guidelines for the use and interpretation of assays for monitoring autophagy in higher eukaryotes." Autophagy **4**(2): 151-175.

Klionsky, D. J. and S. D. Emr (2000). "Autophagy as a regulated pathway of cellular degradation." Science **290**(5497): 1717-1721.

Komatsu, M., S. Waguri, et al. (2005). "Impairment of starvation-induced and constitutive autophagy in Atg7-deficient mice." J Cell Biol **169**(3): 425-434.

Kondo, Y., T. Kanzawa, et al. (2005). "The role of autophagy in cancer development and response to therapy." Nat Rev Cancer **5**(9): 726-734.

Koneri, K., T. Goi, et al. (2007). "Beclin 1 gene inhibits tumor growth in colon cancer cell lines." Anticancer Res **27**(3B): 1453-1457.

Korolchuk, V. I., A. Mansilla, et al. (2009). "Autophagy inhibition compromises degradation of ubiquitin-proteasome pathway substrates." Mol Cell **33**(4): 517-527.

Kraft, C., A. Deplazes, et al. (2008). "Mature ribosomes are selectively degraded upon starvation by an autophagy pathway requiring the Ubp3p/Bre5p ubiquitin protease." Nat Cell Biol **10**(5): 602-610.

Kroemer, G., G. Marino, et al. (2010). "Autophagy and the integrated stress response." Mol Cell **40**(2): 280-293.

Kubbutat, M. H. and K. H. Vousden (1998). "Keeping an old friend under control: regulation of p53 stability." Mol Med Today **4**(6): 250-256.

Kulju, K. S. and J. M. Lehman (1995). "Increased p53 protein associated with aging in human diploid fibroblasts." Exp Cell Res **217**(2): 336-345.

Kuma, A., M. Hatano, et al. (2004). "The role of autophagy during the early neonatal starvation period." Nature **432**(7020): 1032-1036.

Labi, V., M. Erlacher, et al. (2010). "Apoptosis of leukocytes triggered by acute DNA damage promotes lymphoma formation." Genes Dev **24**(15): 1602-1607.

Lambert, L. A., N. Qiao, et al. (2008). "Autophagy: a novel mechanism of synergistic cytotoxicity between doxorubicin and roscovitine in a sarcoma model." Cancer Res **68**(19): 7966-7974.

Lapenna, S. and A. Giordano (2009). "Cell cycle kinases as therapeutic targets for cancer." Nat Rev Drug Discov **8**(7): 547-566.

Last'ovicka, J., V. Budinsky, et al. (2009). "Assessment of lymphocyte proliferation: CFSE kills dividing cells and modulates expression of activation markers." Cell Immunol **256**(1-2): 79-85.

Lee, C. Y., B. A. Cooksey, et al. (2002). "Steroid regulation of midgut cell death during Drosophila development." Dev Biol **250**(1): 101-111.

Lee, H. K., J. M. Lund, et al. (2007). "Autophagy-dependent viral recognition by plasmacytoid dendritic cells." Science **315**(5817): 1398-1401.

Lee, H. K., L. M. Mattei, et al. (2010). "In vivo requirement for Atg5 in antigen presentation by dendritic cells." Immunity **32**(2): 227-239.

Leenders, M. W., M. W. Nijkamp, et al. (2008). "Mouse models in liver cancer research: a review of current literature." World J Gastroenterol **14**(45): 6915-6923.

Legrand, N., A. Ploss, et al. (2009). "Humanized mice for modeling human infectious disease: challenges, progress, and outlook." Cell Host Microbe **6**(1): 5-9.

Levine, B. and J. Abrams (2008). "p53: The Janus of autophagy?" Nat Cell Biol **10**(6): 637-639.

Li, Y., L. X. Wang, et al. (2008). "Efficient cross-presentation depends on autophagy in tumor cells." Cancer Res **68**(17): 6889-6895.

Liang, C. and J. U. Jung (2010). "Autophagy genes as tumor suppressors." Curr Opin Cell Biol **22**(2): 226-233.

Liang, X. H., S. Jackson, et al. (1999). "Induction of autophagy and inhibition of tumorigenesis by beclin 1." Nature **402**(6762): 672-676.

Liu, H., S. Urbe, et al. (2012). "Selective protein degradation in cell signalling." Semin Cell Dev Biol **23**(5): 509-514.

Lobo, I. (2008). "Genetics and Statistical Analysis." Nature Education **1**(1).

Lorin, S., A. Borges, et al. (2009). "c-Jun NH2-terminal kinase activation is essential for DRAM-dependent induction of autophagy and apoptosis in 2-methoxyestradiol-treated Ewing sarcoma cells." Cancer Res **69**(17): 6924-6931.

Lorin, S., G. Pierron, et al. (2010). "Evidence for the interplay between JNK and p53-DRAM signalling pathways in the regulation of autophagy." Autophagy **6**(1): 153-154.

Madeo, F., N. Tavernarakis, et al. (2010). "Can autophagy promote longevity?" Nat Cell Biol **12**(9): 842-846.

Mah, L. Y., J. O'Prey, et al. (2012). "DRAM-1 encodes multiple isoforms that regulate autophagy." Autophagy **8**(1): 18-28.

Mah, L. Y. and K. M. Ryan (2012). "Autophagy and cancer." Cold Spring Harb Perspect Biol **4**(1): a008821.

Maiuri, M. C., S. A. Malik, et al. (2009). "Stimulation of autophagy by the p53 target gene Sestrin2." Cell Cycle **8**(10): 1571-1576.

Maiuri, M. C., E. Zalckvar, et al. (2007). "Self-eating and self-killing: crosstalk between autophagy and apoptosis." Nat Rev Mol Cell Biol **8**(9): 741-752.

Manfredi, J. J. (2010). "The Mdm2-p53 relationship evolves: Mdm2 swings both ways as an oncogene and a tumor suppressor." Genes Dev **24**(15): 1580-1589.

Mantovani, A., P. Allavena, et al. (2008). "Cancer-related inflammation." Nature **454**(7203): 436-444.

Marino, G., N. Salvador-Montoliu, et al. (2007). "Tissue-specific autophagy alterations and increased tumorigenesis in mice deficient in Atg4C/autophagin-3." J Biol Chem **282**(25): 18573-18583.

Mathew, R., C. M. Karp, et al. (2009). "Autophagy suppresses tumorigenesis through elimination of p62." Cell **137**(6): 1062-1075.

Matsunaga, K., T. Saitoh, et al. (2009). "Two Beclin 1-binding proteins, Atg14L and Rubicon, reciprocally regulate autophagy at different stages." Nat Cell Biol **11**(4): 385-396.

Meek, D. W. (2009). "Tumour suppression by p53: a role for the DNA damage response?" Nat Rev Cancer **9**(10): 714-723.

Melkus, M. W., J. D. Estes, et al. (2006). "Humanized mice mount specific adaptive and innate immune responses to EBV and TSST-1." Nat Med **12**(11): 1316-1322.

Mercer, C. A., A. Kaliappan, et al. (2009). "A novel, human Atg13 binding protein, Atg101, interacts with ULK1 and is essential for macroautophagy." Autophagy **5**(5): 649-662.

Merritt, A. J., T. D. Allen, et al. (1997). "Apoptosis in small intestinal epithelial from p53-null mice: evidence for a delayed, p53-independent G2/M-associated cell death after gamma-irradiation." Oncogene **14**(23): 2759-2766.

Michalak, E. M., E. S. Jansen, et al. (2009). "Puma and to a lesser extent Noxa are suppressors of Myc-induced lymphomagenesis." Cell Death Differ **16**(5): 684-696.

Michaud, M., I. Martins, et al. (2011). "Autophagy-dependent anticancer immune responses induced by chemotherapeutic agents in mice." Science **334**(6062): 1573-1577.

Mihara, M., S. Erster, et al. (2003). "p53 has a direct apoptogenic role at the mitochondria." Mol Cell **11**(3): 577-590.

Mizushima, N. (2007). "Autophagy: process and function." Genes Dev **21**(22): 2861-2873.

Mizushima, N. and B. Levine (2010). "Autophagy in mammalian development and differentiation." Nat Cell Biol **12**(9): 823-830.

Mizushima, N., B. Levine, et al. (2008). "Autophagy fights disease through cellular self-digestion." Nature **451**(7182): 1069-1075.

Mizushima, N. and T. Yoshimori (2007). "How to interpret LC3 immunoblotting." Autophagy **3**(6): 542-545.

Mizushima, N., T. Yoshimori, et al. (2010). "Methods in mammalian autophagy research." Cell **140**(3): 313-326.

Momand, J., D. Jung, et al. (1998). "The MDM2 gene amplification database." Nucleic Acids Res **26**(15): 3453-3459.

Momand, J., G. P. Zambetti, et al. (1992). "The mdm-2 oncogene product forms a complex with the p53 protein and inhibits p53-mediated transactivation." Cell **69**(7): 1237-1245.

Mortensen, M., D. J. Ferguson, et al. (2010). "Loss of autophagy in erythroid cells leads to defective removal of mitochondria and severe anemia in vivo." Proc Natl Acad Sci U S A **107**(2): 832-837.

Mortensen, M., E. J. Soilleux, et al. (2011). "The autophagy protein Atg7 is essential for hematopoietic stem cell maintenance." J Exp Med **208**(3): 455-467.

Mostowy, S. and P. Cossart (2012). "Bacterial autophagy: restriction or promotion of bacterial replication?" Trends Cell Biol.

Moussay, E., T. Kaoma, et al. (2011). "The acquisition of resistance to TNFalpha in breast cancer cells is associated with constitutive activation of autophagy as revealed by a transcriptome analysis using a custom microarray." Autophagy **7**(7): 760-770.

Munafo, D. B. and M. I. Colombo (2001). "A novel assay to study autophagy: regulation of autophagosome vacuole size by amino acid deprivation." J Cell Sci **114**(Pt 20): 3619-3629.

Munoz, J., D. E. Stange, et al. (2012). "The Lgr5 intestinal stem cell signature: robust expression of proposed quiescent '+4' cell markers." EMBO J **31**(14): 3079-3091.

Munoz-Gamez, J. A., J. M. Rodriguez-Vargas, et al. (2009). "PARP-1 is involved in autophagy induced by DNA damage." Autophagy **5**(1): 61-74.

Munz, C. (2006). "Autophagy and antigen presentation." Cell Microbiol **8**(6): 891-898.

Munz, C. (2010). "Antigen processing via autophagy--not only for MHC class II presentation anymore?" Curr Opin Immunol **22**(1): 89-93.

Munz, C. (2012). "Antigen Processing for MHC Class II Presentation via Autophagy." Front Immunol **3**: 9.

N'Diaye, E. N., K. K. Kajihara, et al. (2009). "PLIC proteins or ubiquilins regulate autophagy-dependent cell survival during nutrient starvation." EMBO Rep **10**(2): 173-179.

Neefjes, J., M. L. Jongsma, et al. (2011). "Towards a systems understanding of MHC class I and MHC class II antigen presentation." Nat Rev Immunol **11**(12): 823-836.

Nikitina, E. Y., J. I. Clark, et al. (2001). "Dendritic cells transduced with full-length wild-type p53 generate antitumor cytotoxic T lymphocytes from peripheral blood of cancer patients." Clin Cancer Res **7**(1): 127-135.

Nimmerjahn, F., S. Milosevic, et al. (2003). "Major histocompatibility complex class II-restricted presentation of a cytosolic antigen by autophagy." Eur J Immunol **33**(5): 1250-1259.

Nishida, Y., S. Arakawa, et al. (2009). "Discovery of Atg5/Atg7-independent alternative macroautophagy." Nature **461**(7264): 654-658.

Noda, A., Y. Ning, et al. (1994). "Cloning of senescent cell-derived inhibitors of DNA synthesis using an expression screen." Exp Cell Res **211**(1): 90-98.

Noguchi, T., T. Kato, et al. (2012). "Intracellular tumor-associated antigens represent effective targets for passive immunotherapy." Cancer Res **72**(7): 1672-1682.

Noursadeghi, M., J. Tsang, et al. (2009). "Genome-wide innate immune responses in HIV-1-infected macrophages are preserved despite attenuation of the NF-kappa B activation pathway." J Immunol **182**(1): 319-328.

Nysoeter, G., K. Erichsen, et al. (2007). "Effect of live Salmonella Ty21a in dextran sulfate sodium-induced colitis." Drug Target Insights **2**: 221-228.

O'Keefe, G. M., V. T. Nguyen, et al. (2002). "Regulation and function of class II major histocompatibility complex, CD40, and B7 expression in

macrophages and microglia: Implications in neurological diseases." J Neurovirol **8**(6): 496-512.

O'Prey, J., D. Crighton, et al. (2010). "p53-mediated induction of Noxa and p53AIP1 requires NFkappaB." Cell Cycle **9**(5): 947-952.

O'Prey, J., J. Skommer, et al. (2009). "Analysis of DRAM-related proteins reveals evolutionarily conserved and divergent roles in the control of autophagy." Cell Cycle **8**(14): 2260-2265.

O'Sullivan, G. A., M. Kneussel, et al. (2005). "GABARAP is not essential for GABA receptor targeting to the synapse." Eur J Neurosci **22**(10): 2644-2648.

Oda, K., Y. Nishimura, et al. (1991). "Bafilomycin A1 inhibits the targeting of lysosomal acid hydrolases in cultured hepatocytes." Biochem Biophys Res Commun **178**(1): 369-377.

Ogier-Denis, E. and P. Codogno (2003). "Autophagy: a barrier or an adaptive response to cancer." Biochim Biophys Acta **1603**(2): 113-128.

Oikawa, T., M. Okuda, et al. (2005). "Transcriptional control of BubR1 by p53 and suppression of centrosome amplification by BubR1." Mol Cell Biol **25**(10): 4046-4061.

Okayasu, I., S. Hatakeyama, et al. (1990). "A novel method in the induction of reliable experimental acute and chronic ulcerative colitis in mice." Gastroenterology **98**(3): 694-702.

Okuda, Y., M. Okuda, et al. (2003). "Regulatory role of p53 in experimental autoimmune encephalomyelitis." J Neuroimmunol **135**(1-2): 29-37.

Oliner, J. D., J. A. Pietenpol, et al. (1993). "Oncoprotein MDM2 conceals the activation domain of tumour suppressor p53." Nature **362**(6423): 857-860.

Orkin, S. H. and L. I. Zon (2008). "Hematopoiesis: an evolving paradigm for stem cell biology." Cell **132**(4): 631-644.

Orkin, S. H. and L. I. Zon (2008). "SnapShot: hematopoiesis." Cell **132**(4): 712.

Park, S. M., K. Kim, et al. (2009). "Reduced expression of DRAM2/TMEM77 in tumor cells interferes with cell death." Biochem Biophys Res Commun **390**(4): 1340-1344.

Pattingre, S., A. Tassa, et al. (2005). "Bcl-2 antiapoptotic proteins inhibit Beclin 1-dependent autophagy." Cell **122**(6): 927-939.

Periyasamy-Thandavan, S., M. Jiang, et al. (2008). "Autophagy is cytoprotective during cisplatin injury of renal proximal tubular cells." Kidney Int **74**(5): 631-640.

Phadwal, K., J. Alegre-Abarrategui, et al. (2012). "A novel method for autophagy detection in primary cells: impaired levels of macroautophagy in immunosenescent T cells." Autophagy **8**(4): 677-689.

Piao, Z. X., W. S. Wang, et al. (2004). "Autophagy of neuron axon during regeneration of rat sciatic nerves." Di Yi Jun Yi Da Xue Xue Bao **24**(4): 361-364.

Pierre, P., S. J. Turley, et al. (1997). "Developmental regulation of MHC class II transport in mouse dendritic cells." Nature **388**(6644): 787-792.

Polager, S., M. Ofir, et al. (2008). "E2F1 regulates autophagy and the transcription of autophagy genes." Oncogene **27**(35): 4860-4864.

Porter, E. M., C. L. Bevins, et al. (2002). "The multifaceted Paneth cell." Cell Mol Life Sci **59**(1): 156-170.

Potten, C. S. (1992). "The significance of spontaneous and induced apoptosis in the gastrointestinal tract of mice." Cancer Metastasis Rev **11**(2): 179-195.

Potten, C. S. (1998). "Stem cells in gastrointestinal epithelium: numbers, characteristics and death." Philos Trans R Soc Lond B Biol Sci **353**(1370): 821-830.

Potten, C. S., A. Merritt, et al. (1994). "Characterization of radiation-induced apoptosis in the small intestine and its biological implications." Int J Radiat Biol **65**(1): 71-78.

Pua, H. H., I. Dzhagalov, et al. (2007). "A critical role for the autophagy gene Atg5 in T cell survival and proliferation." J Exp Med **204**(1): 25-31.

Pua, H. H., J. Guo, et al. (2009). "Autophagy is essential for mitochondrial clearance in mature T lymphocytes." J Immunol **182**(7): 4046-4055.

Pyo, J. O., M. H. Jang, et al. (2005). "Essential roles of Atg5 and FADD in autophagic cell death: dissection of autophagic cell death into vacuole formation and cell death." J Biol Chem **280**(21): 20722-20729.

Qiao, L. and J. Zhang (2009). "Inhibition of lysosomal functions reduces proteasomal activity." Neurosci Lett **456**(1): 15-19.

Qu, X., J. Yu, et al. (2003). "Promotion of tumorigenesis by heterozygous disruption of the beclin 1 autophagy gene." J Clin Invest **112**(12): 1809-1820.

Quah, B. J., H. S. Warren, et al. (2007). "Monitoring lymphocyte proliferation in vitro and in vivo with the intracellular fluorescent dye carboxyfluorescein diacetate succinimidyl ester." Nat Protoc **2**(9): 2049-2056.

Quigley, D. A., M. D. To, et al. (2011). "Network analysis of skin tumor progression identifies a rewired genetic architecture affecting inflammation and tumor susceptibility." Genome Biol **12**(1): R5.

Quigley, D. A., M. D. To, et al. (2009). "Genetic architecture of mouse skin inflammation and tumour susceptibility." Nature **458**(7237): 505-508.

Rabb, H. (2002). "The T cell as a bridge between innate and adaptive immune systems: implications for the kidney." Kidney Int **61**(6): 1935-1946.

Reggiori, F., T. Shintani, et al. (2005). "Atg9 cycles between mitochondria and the pre-autophagosomal structure in yeasts." Autophagy **1**(2): 101-109.

Reggiori, F., K. A. Tucker, et al. (2004). "The Atg1-Atg13 complex regulates Atg9 and Atg23 retrieval transport from the pre-autophagosomal structure." Dev Cell **6**(1): 79-90.

Ridley, S. H., N. Ktistakis, et al. (2001). "FENS-1 and DFCP1 are FYVE domain-containing proteins with distinct functions in the endosomal and Golgi compartments." J Cell Sci **114**(Pt 22): 3991-4000.

Roberts, S. A. and C. S. Potten (1994). "Clonogen content of intestinal crypts: its deduction using a microcolony assay on whole mount preparations and its dependence on radiation dose." Int J Radiat Biol **65**(4): 477-481.

Roncucci, L., E. Mora, et al. (2008). "Myeloperoxidase-positive cell infiltration in colorectal carcinogenesis as indicator of colorectal cancer risk." Cancer Epidemiol Biomarkers Prev **17**(9): 2291-2297.

Rong, Y., C. K. McPhee, et al. (2011). "Spinster is required for autophagic lysosome reformation and mTOR reactivation following starvation." Proc Natl Acad Sci U S A **108**(19): 7826-7831.

Rosenfeldt, M., C. Nixon, et al. (2012). "Analysis of macroautophagy by immunohistochemistry." Autophagy **8**(6).

Rosenfeldt, M. T. and K. M. Ryan (2009). "The role of autophagy in tumour development and cancer therapy." Expert Rev Mol Med **11**: e36.

Rouschop, K. M., C. H. Ramaekers, et al. (2009). "Autophagy is required during cycling hypoxia to lower production of reactive oxygen species." Radiother Oncol **92**(3): 411-416.

Rovere, P., C. Vallinoto, et al. (1998). "Bystander apoptosis triggers dendritic cell maturation and antigen-presenting function." J Immunol **161**(9): 4467-4471.

Rowe, H. M., L. Lopes, et al. (2006). "Immunization with a lentiviral vector stimulates both CD4 and CD8 T cell responses to an ovalbumin transgene." Mol Ther **13**(2): 310-319.

Rozenknop, A., V. V. Rogov, et al. (2011). "Characterization of the interaction of GABARAPL-1 with the LIR motif of NBR1." J Mol Biol **410**(3): 477-487.

Ruck, A., J. Attonito, et al. (2011). "The Atg6/Vps30/Beclin 1 ortholog BEC-1 mediates endocytic retrograde transport in addition to autophagy in C. elegans." Autophagy **7**(4): 386-400.

Rusten, T. E., T. Vaccari, et al. (2007). "ESCRTs and Fab1 regulate distinct steps of autophagy." Curr Biol **17**(20): 1817-1825.

Ryan, K. M., M. K. Ernst, et al. (2000). "Role of NF-kappaB in p53-mediated programmed cell death." Nature **404**(6780): 892-897.

Saitoh, T., N. Fujita, et al. (2008). "Loss of the autophagy protein Atg16L1 enhances endotoxin-induced IL-1beta production." Nature **456**(7219): 264-268.

Sakai, Y., M. Oku, et al. (2006). "Pexophagy: autophagic degradation of peroxisomes." Biochim Biophys Acta **1763**(12): 1767-1775.

Sancho, E., E. Batlle, et al. (2004). "Signaling pathways in intestinal development and cancer." Annu Rev Cell Dev Biol **20**: 695-723.

Sansom, O. J. and A. R. Clarke (2000). "P53 null mice: damaging the hypothesis?" Mutat Res **452**(2): 149-162.

Santambrogio, L., I. Potolicchio, et al. (2005). "Involvement of caspase-cleaved and intact adaptor protein 1 complex in endosomal remodeling in maturing dendritic cells." Nat Immunol **6**(10): 1020-1028.

Santhanam, U., A. Ray, et al. (1991). "Repression of the interleukin 6 gene promoter by p53 and the retinoblastoma susceptibility gene product." Proc Natl Acad Sci U S A **88**(17): 7605-7609.

Sato, T., J. H. van Es, et al. (2011). "Paneth cells constitute the niche for Lgr5 stem cells in intestinal crypts." Nature **469**(7330): 415-418.

Scarlatti, F., R. Maffei, et al. (2008). "Non-canonical autophagy: an exception or an underestimated form of autophagy?" Autophagy **4**(8): 1083-1085.

Scherz-Shouval, R., E. Shvets, et al. (2007). "Reactive oxygen species are essential for autophagy and specifically regulate the activity of Atg4." EMBO J **26**(7): 1749-1760.

Sekito, T., T. Kawamata, et al. (2009). "Atg17 recruits Atg9 to organize the pre-autophagosomal structure." Genes Cells **14**(5): 525-538.

Shankarling, G. and K. W. Lynch (2010). "Living or dying by RNA processing: caspase expression in NSCLC." J Clin Invest **120**(11): 3798-3801.

Shi, C. S. and J. H. Kehrl (2008). "MyD88 and Trif target Beclin 1 to trigger autophagy in macrophages." J Biol Chem **283**(48): 33175-33182.

Shibue, T., S. Suzuki, et al. (2006). "Differential contribution of Puma and Noxa in dual regulation of p53-mediated apoptotic pathways." EMBO J **25**(20): 4952-4962.

Steidl, U., F. Rosenbauer, et al. (2006). "Essential role of Jun family transcription factors in PU.1 knockdown-induced leukemic stem cells." Nat Genet **38**(11): 1269-1277.

Steiger-Barraissoul, S. and A. Rami (2009). "Serum deprivation induced autophagy and predominantly an AIF-dependent apoptosis in hippocampal HT22 neurons." Apoptosis **14**(11): 1274-1288.

Sugrue, M. M., D. Y. Shin, et al. (1997). "Wild-type p53 triggers a rapid senescence program in human tumor cells lacking functional p53." Proc Natl Acad Sci U S A **94**(18): 9648-9653.

Sun, L. Z., S. Elsayed, et al. (2010). "Comparison between ovalbumin and ovalbumin peptide 323-339 responses in allergic mice: humoral and cellular aspects." Scand J Immunol **71**(5): 329-335.

Sun, Q., W. Fan, et al. (2008). "Identification of Barkor as a mammalian autophagy-specific factor for Beclin 1 and class III phosphatidylinositol 3-kinase." Proc Natl Acad Sci U S A **105**(49): 19211-19216.

Surani, A. and J. Tischler (2012). "Stem cells: a sporadic super state." Nature **487**(7405): 43-45.

Suzuki, K. and Y. Ohsumi (2007). "Molecular machinery of autophagosome formation in yeast, Saccharomyces cerevisiae." FEBS Lett **581**(11): 2156-2161.

Suzuki, S. W., J. Onodera, et al. (2011). "Starvation induced cell death in autophagy-defective yeast mutants is caused by mitochondria dysfunction." PLoS One **6**(2): e17412.

Svensson, M. and M. J. Wick (1999). "Classical MHC class I peptide presentation of a bacterial fusion protein by bone marrow-derived dendritic cells." Eur J Immunol **29**(1): 180-188.

Swanlund, J. M., K. C. Kregel, et al. (2008). "Autophagy following heat stress: the role of aging and protein nitration." Autophagy **4**(7): 936-939.

Tait, S. W. and D. R. Green (2008). "Caspase-independent cell death: leaving the set without the final cut." Oncogene **27**(50): 6452-6461.

Takahashi, M. and K. Wakabayashi (2004). "Gene mutations and altered gene expression in azoxymethane-induced colon carcinogenesis in rodents." Cancer Sci **95**(6): 475-480.

Takahashi, Y., D. Coppola, et al. (2007). "Bif-1 interacts with Beclin 1 through UVRAG and regulates autophagy and tumorigenesis." Nat Cell Biol **9**(10): 1142-1151.

Takamura, A., M. Komatsu, et al. (2011). "Autophagy-deficient mice develop multiple liver tumors." Genes Dev **25**(8): 795-800.

Tanida, I. (2011). "Autophagosome formation and molecular mechanism of autophagy." Antioxid Redox Signal **14**(11): 2201-2214.

Tasdemir, E., M. C. Maiuri, et al. (2008). "Regulation of autophagy by cytoplasmic p53." Nat Cell Biol **10**(6): 676-687.

Terzic, J., S. Grivennikov, et al. (2010). "Inflammation and colon cancer." Gastroenterology **138**(6): 2101-2114 e2105.

Tokunaga, N., T. Murakami, et al. (2005). "Human monocyte-derived dendritic cells pulsed with wild-type p53 protein efficiently induce CTLs against p53 overexpressing human cancer cells." Clin Cancer Res **11**(3): 1312-1318.

Tra, T., L. Gong, et al. (2011). "Autophagy in human embryonic stem cells." PLoS One **6**(11): e27485.

Tresse, E., C. Giusti, et al. (2008). "Autophagy and autophagic cell death in Dictyostelium." Methods Enzymol **451**: 343-358.

Tripathi, S., D. Bruch, et al. (2008). "Ginger extract inhibits LPS induced macrophage activation and function." BMC Complement Altern Med **8**: 1.

Tsubuki, S., Y. Saito, et al. (1996). "Differential inhibition of calpain and proteasome activities by peptidyl aldehydes of di-leucine and tri-leucine." J Biochem **119**(3): 572-576.

Tsuchihara, K., S. Fujii, et al. (2008). "Autophagy and cancer: Dynamism of the metabolism of tumor cells and tissues." Cancer Lett.

Tsukamoto, S., A. Kuma, et al. (2008). "Autophagy is essential for preimplantation development of mouse embryos." Science **321**(5885): 117-120.

Uhl, M., O. Kepp, et al. (2009). "Autophagy within the antigen donor cell facilitates efficient antigen cross-priming of virus-specific CD8+ T cells." Cell Death Differ **16**(7): 991-1005.

Unanue, E. R. (1984). "Antigen-presenting function of the macrophage." Annu Rev Immunol **2**: 395-428.

Vakifahmetoglu, H., M. Olsson, et al. (2008). "Death through a tragedy: mitotic catastrophe." Cell Death Differ **15**(7): 1153-1162.

Valbuena, A., S. Castro-Obregon, et al. (2011). "Downregulation of VRK1 by p53 in response to DNA damage is mediated by the autophagic pathway." PLoS One **6**(2): e17320.

Valentin-Vega, Y. A., H. Okano, et al. (2008). "The intestinal epithelium compensates for p53-mediated cell death and guarantees organismal survival." Cell Death Differ **15**(11): 1772-1781.

van der Flier, L. G., A. Haegebarth, et al. (2009). "OLFM4 is a robust marker for stem cells in human intestine and marks a subset of colorectal cancer cells." Gastroenterology **137**(1): 15-17.

van Kerkhof, P., C. M. Alves dos Santos, et al. (2001). "Proteasome inhibitors block a late step in lysosomal transport of selected membrane but not soluble proteins." Mol Biol Cell **12**(8): 2556-2566.

Vassilev, L. T. (2005). "p53 Activation by small molecules: application in oncology." J Med Chem **48**(14): 4491-4499.

Vassilev, L. T., B. T. Vu, et al. (2004). "In vivo activation of the p53 pathway by small-molecule antagonists of MDM2." Science **303**(5659): 844-848.

Vazquez-Martin, A., C. Oliveras-Ferraros, et al. (2009). "Autophagy facilitates the development of breast cancer resistance to the anti-HER2 monoclonal antibody trastuzumab." PLoS One **4**(7): e6251.

Vessoni, A. T., A. R. Muotri, et al. (2012). "Autophagy in stem cell maintenance and differentiation." Stem Cells Dev **21**(4): 513-520.

Vidalain, P. O., O. Azocar, et al. (2000). "CD40 signaling in human dendritic cells is initiated within membrane rafts." EMBO J **19**(13): 3304-3313.

Vooijs, M., J. Jonkers, et al. (2001). "A highly efficient ligand-regulated Cre recombinase mouse line shows that LoxP recombination is position dependent." EMBO Rep **2**(4): 292-297.

Vousden, K. H. and D. P. Lane (2007). "p53 in health and disease." Nat Rev Mol Cell Biol **8**(4): 275-283.

Wang, D., K. Peregrina, et al. (2011). "Paneth cell marker expression in intestinal villi and colon crypts characterizes dietary induced risk for mouse sporadic intestinal cancer." Proc Natl Acad Sci U S A **108**(25): 10272-10277.

Wang, E. T., R. Sandberg, et al. (2008). "Alternative isoform regulation in human tissue transcriptomes." Nature **456**(7221): 470-476.

Wang, Y., X. X. Dong, et al. (2009). "p53 induction contributes to excitotoxic neuronal death in rat striatum through apoptotic and autophagic mechanisms." Eur J Neurosci **30**(12): 2258-2270.

Webber, J. L. and S. A. Tooze (2010). "Coordinated regulation of autophagy by p38alpha MAPK through mAtg9 and p38IP." EMBO J **29**(1): 27-40.

Webber, J. L. and S. A. Tooze (2010). "New insights into the function of Atg9." FEBS Lett **584**(7): 1319-1326.

Weidberg, H., E. Shvets, et al. (2009). "Lipophagy: selective catabolism designed for lipids." Dev Cell **16**(5): 628-630.

Weidberg, H., E. Shvets, et al. (2010). "LC3 and GATE-16/GABARAP subfamilies are both essential yet act differently in autophagosome biogenesis." EMBO J **29**(11): 1792-1802.

Wilkinson, S., J. O'Prey, et al. (2009). "Hypoxia-selective macroautophagy and cell survival signaled by autocrine PDGFR activity." Genes Dev **23**(11): 1283-1288.

Wirtz, S., C. Neufert, et al. (2007). "Chemically induced mouse models of intestinal inflammation." Nat Protoc **2**(3): 541-546.

Xie, Z. and D. J. Klionsky (2007). "Autophagosome formation: core machinery and adaptations." Nat Cell Biol **9**(10): 1102-1109.

Xue, W., L. Zender, et al. (2007). "Senescence and tumour clearance is triggered by p53 restoration in murine liver carcinomas." Nature **445**(7128): 656-660.

Yamada, Y., S. Marshall, et al. (1992). "A comparative analysis of two models of colitis in rats." Gastroenterology **102**(5): 1524-1534.

Yamamoto, K., T. Kiyohara, et al. (2005). "Production of adiponectin, an anti-inflammatory protein, in mesenteric adipose tissue in Crohn's disease." Gut **54**(6): 789-796.

Yamanishi, Y., D. L. Boyle, et al. (2002). "Regulation of joint destruction and inflammation by p53 in collagen-induced arthritis." Am J Pathol **160**(1): 123-130.

Yee, K. S., S. Wilkinson, et al. (2009). "PUMA- and Bax-induced autophagy contributes to apoptosis." Cell Death Differ **16**(8): 1135-1145.

Yoon, J. H., S. Her, et al. (2012). "The expression of damage-regulated autophagy modulator 2 (DRAM2) contributes to autophagy induction." Mol Biol Rep **39**(2): 1087-1093.

You, R. I., Y. C. Chang, et al. (2008). "Apoptosis of dendritic cells induced by decoy receptor 3 (DcR3)." Blood **111**(3): 1480-1488.

Young, A. R., E. Y. Chan, et al. (2006). "Starvation and ULK1-dependent cycling of mammalian Atg9 between the TGN and endosomes." J Cell Sci **119**(Pt 18): 3888-3900.

Young, A. R., M. Narita, et al. (2009). "Autophagy mediates the mitotic senescence transition." Genes Dev **23**(7): 798-803.

Yousefi, S., R. Perozzo, et al. (2006). "Calpain-mediated cleavage of Atg5 switches autophagy to apoptosis." Nat Cell Biol **8**(10): 1124-1132.

Yu, L., C. K. McPhee, et al. (2010). "Termination of autophagy and reformation of lysosomes regulated by mTOR." Nature **465**(7300): 942-946.

Yue, Z., S. Jin, et al. (2003). "Beclin 1, an autophagy gene essential for early embryonic development, is a haploinsufficient tumor suppressor." Proc Natl Acad Sci U S A **100**(25): 15077-15082.

Zhang, S., M. Zheng, et al. (2011). "Trp53 negatively regulates autoimmunity via the STAT3-Th17 axis." FASEB J **25**(7): 2387-2398.

Zheng, S. J., S. E. Lamhamedi-Cherradi, et al. (2005). "Tumor suppressor p53 inhibits autoimmune inflammation and macrophage function." Diabetes **54**(5): 1423-1428.

Zhou, J., J. Yao, et al. (2002). "Attachment and tension in the spindle assembly checkpoint." J Cell Sci **115**(Pt 18): 3547-3555.

Zhu, B. S., C. G. Xing, et al. (2011). "Blocking NF-kappaB nuclear translocation leads to p53-related autophagy activation and cell apoptosis." World J Gastroenterol **17**(4): 478-487.

Zhu, K., J. Wang, et al. (1999). "p53 induces TAP1 and enhances the transport of MHC class I peptides." Oncogene **18**(54): 7740-7747.

Zilfou, J. T. and S. W. Lowe (2009). "Tumor suppressive functions of p53." Cold Spring Harb Perspect Biol **1**(5): a001883.

Zou, C. Y., K. D. Smith, et al. (2009). "Dual targeting of AKT and mammalian target of rapamycin: a potential therapeutic approach for malignant peripheral nerve sheath tumor." Mol Cancer Ther **8**(5): 1157-1168.